Addis Ababa University
Addis Ababa Institute of Technology
School of Civil and Environmental Engineering

Application of a Generalized Subgrade Model in the Analysis of Circular Plates on Elastic Foundations

By

Meron Alebachew

Advisor

Asrat Worku (Dr.-Ing)

A thesis submitted to the School of Graduate Studies of Addis Ababa University in Partial fulfillment of the Degree of Master of Science in Geotechnical Engineering.

June, 2018
Addis Ababa

Addis Ababa University

School of Graduate Studies

Application of a Generalized Subgrade Model in the Analysis of Circular Plates on Elastic Foundations

By:

Meron Alebachew

Approved by Board of Examiners

1.	Asrat Worku (Dr.-Ing)	_____	_____
	Advisor	Signature	Date
2.	Henok Fikre (Dr.-Ing)	_____	_____
	Examiner (Internal)	Signature	Date
3.	Bedilu Habte (Dr.-Ing)	_____	_____
	Examiner (External)	Signature	Date
4.	_____	_____	_____
	Chairperson	Signature	Date

UNDERTAKING

I, the undersigned, declare that the research work entitled "**Application of a Generalized Subgrade Model in the Analysis of Circular Plates on Elastic Foundations**" is my original work. The work has not been presented as a thesis elsewhere. And all sources of materials used, have been properly acknowledged.

Meron Alebachew _____ _____ _____

Researcher Signature Date

This is to certify that the above declaration made by the candidate is correct to the best of my knowledge.

Asrat Worku (Dr.-Ing) _____ _____

Advisor Signature Date

ABSTRACT

The solution to the problem of beams and plates on an elastic foundation has been attempted in the past using various subgrade models developed by many researchers, one of the pioneers being Winkler. Most recently, a new calibrated and more advanced multifaceted continuum foundation model has been presented by Worku without neglecting any stress, strain, or deformation component in the continuum unlike previously proposed models.

The study of interaction between a plate and an elastic medium has useful applications in geotechnical engineering. This research investigates the use of a generalized continuum subgrade model of Worku for analyzing circular plates resting on an elastic foundation. The approach employed is both analytical and numerical. In the analytical work, the governing differential equations of an axisymmetric circular plate on a homogeneous elastic foundation has been formulated that incorporates Winkler and Pasternak-type subgrade models. Closed form particular solutions have been presented for different loading conditions of small and large circular plates after obtaining a general solution of the differential equations. A math solving software (i.e. Mathematica) is used to compute the deflections and internal actions in a spreadsheet program due to the complexity of the functions. In the numerical study a FEM based software (i.e. PLAXIS 2D) is used to calibrate the analyzed circular plate using the presented models by seeking adequate agreements with the FE outputs. At last, numerical examples are solved using these models and compared with PLAXIS 2D for small and large radii circular plates of some loading conditions. From the plots of the outputs, it is observed that the generalized models of Worku are suitable and more appropriate than classical models to analyze circular plates on elastic foundations.

Keywords: Continuum subgrade model, Circular plate, FEM, Mathematica and PLAXIS software.

Dedicated to My Parents

ACKNOWLEDGEMENT

First and foremost, I would like to thank my advisor, Dr. Asrat Worku, for his support, inspiring ideas, and advices. I am truly indebted to him for being my advisor and for directing me to go through all the challenges of accomplishing this research. And without his backing, this work would have been far from complete.

I express my sincere gratitude to Dr. Tsegaye Gedif of Mathematics Department for guiding me in understanding the complex and advanced mathematical methods. My heartfelt appreciation also goes to Ato Yimer Degu for his motivation and continuous assistance in the different phases of the study. And I would also like to offer my special thanks to Ato Ameyu Temesgen for giving me a good start with vital suggestions and Ato Mikias Workneh for his help in PLAXIS software.

Special thanks is extended to Addis Ababa University Female Scholarship Program for making this study possible.

Last, but not least, my deepest gratitude goes to my family and friends for their consistent moral and unfailing support. The success is theirs just as much as it is mine.

TABLE OF CONTENTS

CHAPTER THREE

CHAPTER FOUR

LIST OF TABLES

LIST OF FIGURES

LIST OF SYMBOLS AND ABBREVIATIONS

a : Radius of the plate

D : Flexural rigidity of a plate

DE: Differential Equation

E_p : Modulous of elasticity of a plate

E_s : Modulous of elasticity of a soil

FEM: Finite Element Method

G : Shear modulous of an elastic medium

G_p : Pasternak's coefficient of the shear layer with a dimension force per unit length

G_k : Kerr's coefficient of the shear layer with a dimension force per unit length

H : Subgrade thickness

h_p : Thickness of a plate

k : Modulous of subgrade reaction of an elastic medium

k_{wc} : Horvath's equivalent modulous of subgrade reaction

k_s, k_w : Winkler's spring stiffness with a dimension force per length cubed

k_p : Pasternak's spring stiffness with a dimension force per length cubed

k_{ku} : Kerr's upper spring layer stiffness with a dimension force per length cubed

k_{kl} : Kerr's lower spring layer stiffness with a dimension force per length cubed

M_o : Applied concentrated edge moment

M_x, M_y : Bending moments in Cartesian coordinate system

M_r, M_θ : Bending moments in polar coordinate system

P, P_o : Applied vertical concentrated loads

p : Load intensity at an interface

Q_r : Shear force in polar coordinate system

q : Applied distributed transverse load

q_o : Applied concentrated edge load

SSI: Soil Structure interaction

ν_p : Poisson's ratio of a plate

ν_s : Poisson's ratio of a soil

w_o : Transverse surface deflection

w_1 : Deflection of the plate within the loaded region in Pasternak's model

w_2 : Deflection of the plate outside the loaded region in Pasternak's model

λ : Characteristics size of the circular plate

ε : Strain

τ : Shear stress

σ : Normal stress

∇ : Laplace operator

θ : Slope

ϕ : Diameter of the circular plate

Chapter One: INTRODUCTION

1.1 Background

Regular use of plates in civil or mechanical engineering works initiated the development of analytical methods to analyze the foundation and the underlying soil with soil structure interaction. The key issue in the analysis is modeling the contact between the plate and the soil bed which is a soil-structure interaction (SSI) problem.

Most static analysis software currently on the market use Winkler's subgrade model to account for SSI effect, which represents the subgrade using a mechanical assemblage of elastic spring elements (Worku, 2013). Since the 1950s, multiple-parameter mechanical foundation models have been introduced in the development of foundation modeling. The main intention of these models was to improve on the inherent lack of shear interaction among the individual springs of the long-enduring model of Winkler (1867).

Analytical subgrade modeling follows two approaches; i.e. elastic continuum and mechanical. The elastic continuum approach idealizes the subgrade as a layer overlying a rigid base characterized by the elastic parameters of elastic modulus and Poisson's ratio and the layer thickness. The mechanical modelling approach idealizes the subgrade as an assemblage of few mechanical elements like springs, plates in pure bending, plates in pure shear and similar other arrangements. To this effect, these models introduced additional mechanical elements of one type or another to interconnect the springs (Filonenko-Borodich, 1950; Hetenyi, 1950; Pasternak, 1954; Kerr, 1964).

However, the improved mechanical models with coupled springs and the continuum-based models make assumptions to simplify the mathematical work involved in the derivation of the model compromising the actual conditions in the subgrade. Synthesis of the two approaches has the advantage of using the strengths of both methods and provides a means of quantifying the mechanical model parameters in terms of the known parameters of the continuum model.

Recently, by introducing two functions for the horizontal to vertical stress ratio and the vertical shear stress with depth, Worku (2010) proposed a generalized continuum-based subgrade model.

This is without neglecting any stress, strain and displacement components, unlike the previous models. The proposed model has application in the analysis of beams and plates on elastic foundations. This thesis attempts to show its potential use in the analysis of circular plates.

1.2. Research Problem

Problem is encountered in the analysis of building foundations or geotechnical structures resting on an elastic foundation. This problem is typically a soil-structure interaction problem. The commonly used subgrade models such as Winkler's model fall short of ensuring shear interaction among the springs, whereas FEM based software analyses are uneconomical to solve routine problems.

For this and related other reasons, the use of generalized subgrade model of Worku has the potential to eliminate the drawbacks on both sides of the aisle. Moreover, it is important to note that the purpose of subgrade models is to strike a balance between accuracy and ease of use in routine geotechnical engineering practice when solving a particular soil-structure interaction problem. Hence, expressing mathematically a material model for the underlying soil and modeling the mechanical behavior of a circular plate with Worku's generalized subgrade model is a demanding task.

1.3. Objective

The main objective of this study is to demonstrate the potential use of the generalized continuum-based subgrade model of Worku in the analysis of circular plates on an elastic foundation. Furthermore, the work aims at using results of the FEM of analysis to calibrate the model of two levels; Winkler and Pasternak-type. The study uses the Mathematica software to compute the deflection and the internal actions of the plate due to the complicated nature of the mathematical formulas. Circular plates of large and small diameter subjected to selected loading conditions are studied.

1.4. Scope

The analysis is limited to thin circular plates modeled as an axisymmetric plate element i.e. with rotationally symmetric loads, symmetrical edge conditions and resting on a homogeneous strata.

The plate is also assumed to be flexible. The study is limited to solid circular plates. This work does not consider analysis of annular circular plates. Analysis of the plate on the Kerr-type subgrade model is not covered due to its complexity, and also because Worku (2014) showed that it can be replaced by an equivalent two-parameter Pasternak-type model.

1.5. Methodology Overview

The study starts by reviewing relevant subgrade models. This is made with respect to both mechanical-and continuum-based subgrade models that demand a closed form solution for the differential equations. In addition, pertinent theories and analysis methods of elastic plates is concisely presented. Having done this, the differential equations of the plate-soil system are formulated and solved using analytical techniques. Furthermore, a spreadsheet program with the aid of the Mathematica software is used to determine the deflections, and the internal actions (i.e. rotations, moments and shears). Calibration of the models was also conducted using the FEM based software PLAXIS2D. Consequently, the numerical results obtained for the circular plate are compared with those obtained from the analytical solutions using a generalized continuum-based subgrade models of Worku. Then the application of the models together with the closed- form solutions is illustrated on the basis of selected examples.

1.6. Research Overview

The second chapter deals with the review and compilation of existing subgrade models, both mechanical and continuum, and relevant sections of plate theories as well. The third chapter is dedicated to the analysis of circular plates on elastic foundations. It includes both the formulation and solution of the governing differential equations of the plate using single- and two-parameter subgrade models for different boundary conditions.

In the fourth chapter, comparisons and evaluations are made of the results obtained using Worku's generalized continuum-based subgrade models and the FEM outputs. Important conclusions are drawn, and future works are recommended in the last chapter.

Chapter Two: MODELS FOR ELASTIC FOUNDATIONS

2.1 Introduction

Subgrade models are primarily foundation engineering applications involving relatively flexible, plate-like structural elements such as mats (rafts) and base slabs of cut-and-cover tunnels and water/wastewater treatment tanks where it is desirable or even necessary to model the combined superstructure, foundation, and underlying ground (which is usually referred to as the subgrade in such problems) as a single system (Colasanti and Horvath 2010).

In addition, subgrade models have proven to be useful in relatively flexible structural elements in contact with or embedded in the ground such as slabs-on grade, rigid pavements, and deep foundations subjected to lateral and/or moment loading. Collectively, these myriad and diverse applications involving relatively flexible structural elements in direct contact with the ground are referred to as soil structure interaction (SSI) problems. They reflect situations where a reasonably accurate assessment of the overall structure-subgrade system requires satisfying not only static force and moment equilibrium but also a complementary and compatible displacement and deformation pattern for both the structure and subgrade along their interface(s).

Following these, different subgrade models were developed from both *mechanical* approach using assemblages of mechanical elements such as axial springs, tensioned membranes, shear layers, and flexural layers and other physical elements, and *simplified-continuum* approach that is based on the theory of a linear-elastic continuum in an attempt to account for the continuity of deformation. Due to the resulting complex mathematical problem, however, it is common to introduce simplifying assumptions (Horvath, 2002).

2.2 Mechanical Models

2.2.1 Single - Parameter Models

The simplest mechanical foundation model is the equivalent of Winkler's analytical model that consists of a single bed of uniformly spaced springs (Horvath, 2002; Worku, 2013), as shown in Figure.2.1.

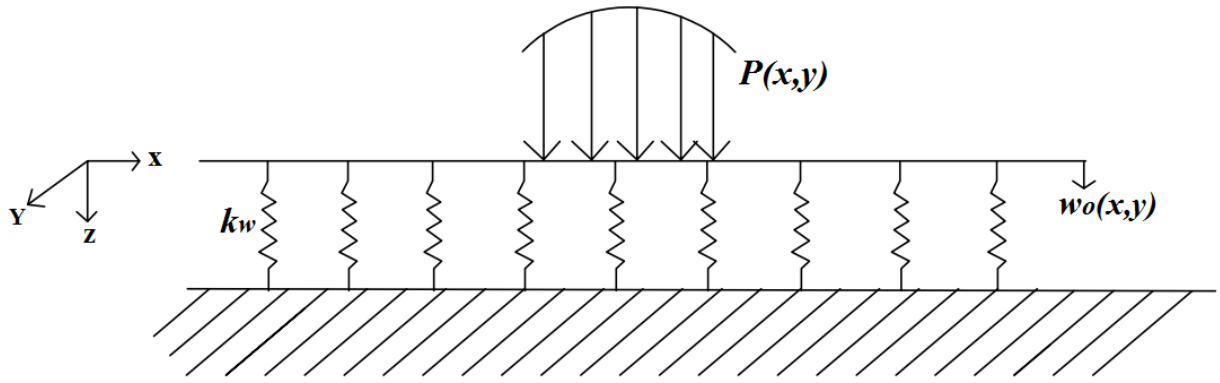

Figure 2.1 Mechanical equivalent of Winkler's model (Worku, 2013)

In its basic form, Winkler's Hypothesis assumes that the settlement, w_o, at an arbitrary point on the subgrade surface is caused only by the applied vertical normal stress, p, (subgrade reaction) at that point, and, each spring acts independent of the other and is responsible just for the normal stress within its tributary area. Furthermore, $p(x,y)$ and $w_o\ (x,y)$ are linearly related. Winkler (1867), mathematically expressed this as

$$p(x,y) = k_w w_o(x,y) \tag{2.1}$$

Where $p(x,y)$ = applied vertical normal stress or traction at the surface; w_o = vertical deformation at the same point; k_w= a constant commonly termed as the Winkler's coefficient of subgrade reaction with the dimension of force per length cubed; and the variables x and y= Cartesian coordinates defining the horizontal plane.

Note that Winkler's Hypothesis is a *single-parameter* subgrade model because only one parameter (the Winkler coefficient of subgrade reaction, k_w) is necessary to define its behavior. This parameter is often referred to as the "soil spring constant", because one physical interpretation of

the abstract behavior defined by Eq. (2.1) is a spring (not necessarily linear or elastic but usually assumed so) that is oriented perpendicular to the subgrade surface. Another physical interpretations of k_W is the unit weight (not density, as is often stated, to be dimensionally correct) of a liquid. For this reason, the model is also sometimes referred to as the dense-liquid model.

However, the spring analogy is by far the more common and enduring model. Since the springs act independently, there is no shear coupling or interaction among the springs, whereas there is a definite load spreading by vertical shear within an actual soil mass. Hence surface displacements outside any loaded region is considered to be zero. The portion beyond the edges of the foundation in most materials is also deformed due to inherent occurrence of load spreading (Horvath, 1979, 1983; Kerr, 1964). This is shown in Figure 2.2.

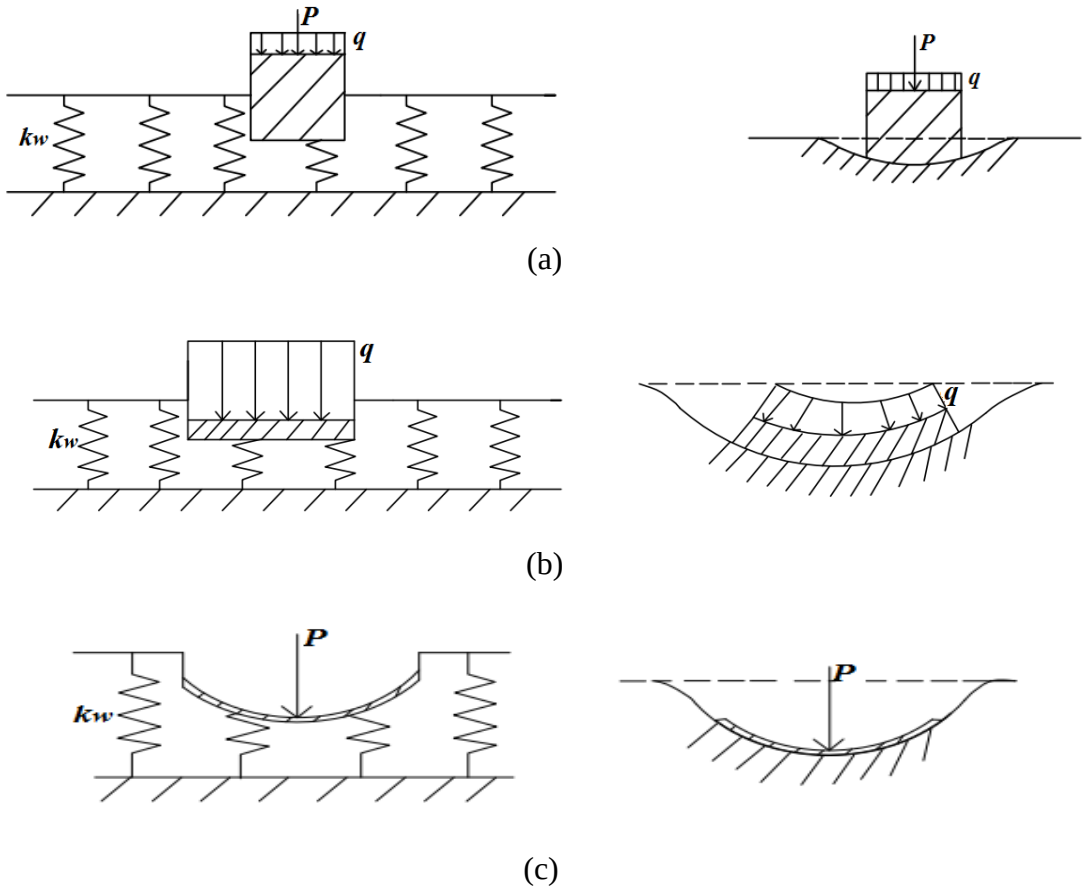

Figure 2.2 (a) surface deflection of a rigid foundation with uniform or concentrated load on Winkler's subgrade model and in the actual soil and (b) & (c) for non-rigid foundations.

In an attempt to develop a method for determining k_w, Vesic considered the bending of an infinitely long beam, loaded only by a point load and resting on a homogeneous, isotropic elastic half-space (Horvath, 1983). By equating the calculated value of the maximum bending moment in the beam with that of an identical beam resting on a Winkler subgrade, Vesic arrived at the relation:

$$k_w = 0.65\left(\frac{E_s}{1-\nu^2}\right)\sqrt[12]{\frac{E_s B^4}{EI}} \tag{2.2}$$

Where E and E_s are modulus of elasticity of the beam and soil respectively, ν is Poisson's ratio of the soil and I is moment of inertia of the beam.

There are a number of other relationships for k_w, proposed in the past.

2.2.2 Two - Parameter Models

Models of an order higher than Winkler's model were proposed by Filonenko-Borodich 1950; Hetenyi 1950; Pasternak 1954 to illustrate the continuous nature of real soils by introducing an additional element of their own to represent the shear interaction missing in Winkler's model. Pasternak's model uses a pure-shear layer to connect the springs at their heads, whereas the Filonenko-Borodich (FB) model uses a thin membrane under uniform tension T and Hetenyi's model employs a pure-flexural beam to bring about the missing shear interaction. These additional elements which account for the spring coupling effect bring a second parameter in addition to the coefficient of subgrade reaction (Horvath, 2002; Worku, 2013). Among these two-parameter models, Pasternak's model is presented briefly.

Pasternak's Model

Pasternak (1954), postulated the existence of shear forces between the springs of the Winkler model, with these forces producing the coupling effect. Kerr (1964), afterwards proposed a physical model to produce these shear forces. This physical model consists of an incompressible layer of unit thickness that deforms in transverse shear only connecting the top of Winkler springs as shown in Figure 2.3.

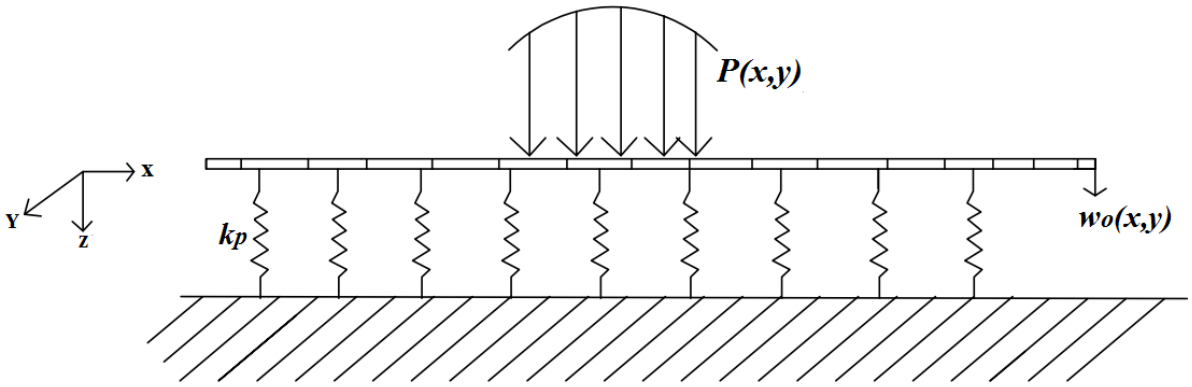

Figure 2.3 Pasternak's model (Worku, 2013)

The respective mathematical equation (Horvath, 1989; Worku, 2013), is given by

$$p(x,y) = k_p w_o(x,y) - G_p \nabla^2 w_o(x,y) \tag{2.3}$$

Where k_p = spring coefficient per unit area; G_p = coefficient of the shear element in Pasternak's model with the dimension of force per unit length and ∇^2 = Laplacian operator.

From this, it can be seen that Winkler's case can be obtained as the limiting case of G_p tending to zero.

2.2.3 Three - Parameter Models

The most widely known three-parameter model is Kerr's analytical model which introduces an additional spring bed in order to make the two-parameter models more representative (Kerr, 1964), as shown in Figure. 2.4.

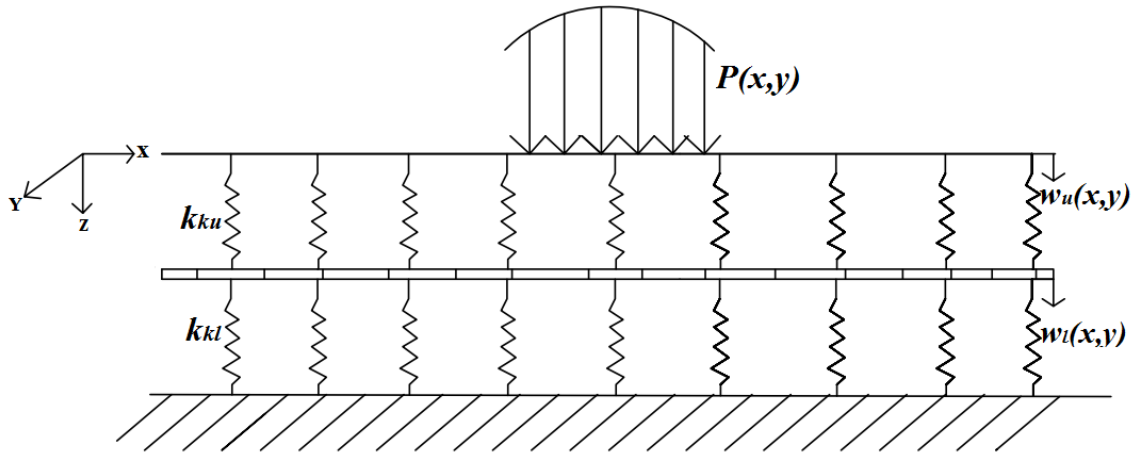

Figure 2.4 Kerr's model (Worku, 2013)

This additional element of the model accounts for the level of continuity of the vertical displacements at the boundaries between the loaded and the unloaded regions of the soil.

Kerr (1967), considers two linear elastic spring layers interconnected by a shear layer of a unit thickness. In its basic form, he assumes the plate deflection w is the sum of the upper and lower spring bed deflections. These parameters are back substituted into Eq. (2.1) and (2.3) and some mathematical steps are performed.

Then, the respective mathematical equation (Kerr, 1967), is obtained as

$$\left(1+\frac{k_{kl}}{k_{ku}}\right)p(x,y)-\frac{G_k}{k_{ku}}\nabla^2 p(x,y)=k_{kl}w(x,y)-G_k\nabla^2 w(x,y) \tag{2.4}$$

Where k_{ku} and k_{kl} = stiffness per unit area of the upper and lower spring beds, respectively; G_k = coefficient of the shear element in Kerr's model with the dimension of force per unit length and ∇^2 = Laplacian operator.

2.3 Continuum Models

2.3.1 Reissner's Model

Reissner (1958**),** pioneered a continuum subgrade model which is based on an isotopic elastic layer of thickness *H* and neglecting the in-plane stresses (in the x,y plane. i.e. σ_x, σ_y and τ_{xy} are assumed to be zero) in order to simplify the mathematical work (Figure. 2.5).

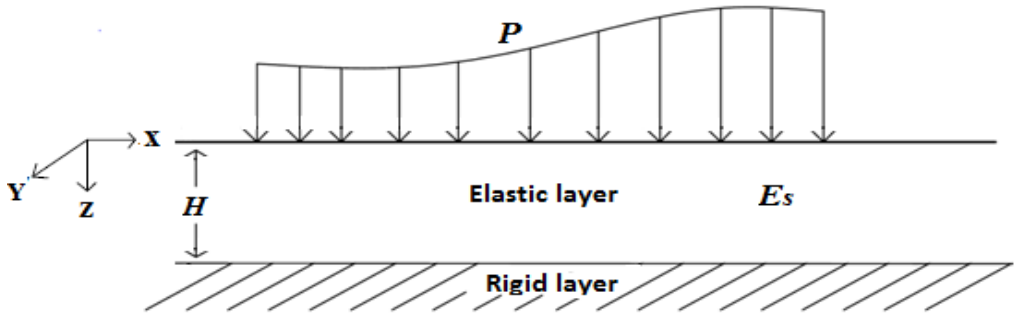

Figure 2.5 Simplified Elastic Continuum (Worku, 2010)

The remaining stress components satisfy the following system of equilibrium differential equations.

$$\frac{\partial \tau_{xz}}{\partial z} = 0, \quad \frac{\partial \tau_{yz}}{\partial z} = 0, \quad \frac{\partial \tau_{xz}}{\partial z} + \frac{\partial \tau_{yz}}{\partial z} + \frac{\partial \sigma_z}{\partial z} = 0 \tag{2.5}$$

Furthermore, stress-strain and the strain-displacement relations were engaged.

$$\frac{\partial w}{\partial z} = \frac{\sigma}{E_s}, \quad \frac{\partial u}{\partial z} + \frac{\partial w}{\partial x} = \frac{\tau_{xz}}{G}, \quad \frac{\partial v}{\partial z} + \frac{\partial w}{\partial y} = \frac{\tau_{yz}}{G} \tag{2.6}$$

The above two equations are solved by subjecting them to the appropriate boundary conditions at the surface and the base of the foundation respectively.

i. At $z = 0 : u = v = 0$ *and* $\sigma = -p$, and

ii. At $z = H : u = v = w = o$ (2.7)

Where *u* and *v* are displacements in the *x* and *y* direction.

The resulting partial differential equation is

$$p - \frac{GH^2}{12E_s}\nabla^2 p = \frac{E_s}{H}w - \frac{GH^2}{12E_s}\nabla^2 w \tag{2.8}$$

Where *G* is the shear modulus of the elastic continuum, *p* is the contact pressure at the interface and *H* is the subgrade thickness.

Horvath extended the concept proposed by Reissner to produce two simpler models that are called the *Winkler-Type Simplified Continuum* and *Pasternak- Type Simplified Continuum* models with two cases; Young's modulus varying with depth and the square root of depth for the finite thickness of Reissner's continuum (Horvath, 1979).

2.3.2 Horvath's Winkler-Type Model

A physical model similar to Reissner's was used, though with a further simplifying assumption that all stress and strain components except the vertical normal stress (σ_z) were equal to zero. The consequence of this highly simplifying assumption is that σ_z is constant with depth and equal to the magnitude *p*, and the vertical deflection *w* varies from w_o at the surface to zero at a depth equal to stratum thickness *H* (Horvath, 1983). Horvath solved the following cases of constant and variable elastic modulus with depth:

$$E_s = A \,(\text{Constant with depth}) \tag{2.9}$$

$$E_s = A + Bz \tag{2.10}$$

$$E_s = A + Bz^{0.5} \tag{2.11}$$

Where A= Young's modulus directly beneath the loaded area, B= the rate of change of Young's modulus with depth.

Horvath derived the following *Winkler-type simplified continuum* model for the case mentioned above by attempting to satisfy the various elasticity relationship:

$$p = \frac{A}{H}w = k_{wc}w \quad (\text{for } E_s = A) \tag{2.12}$$

Where k_{wc} = the equivalent modulus of subgrade reaction for a simplified continuum

$$k_{wc} = \frac{B}{\ln(A+BH) - \ln(A)} \quad (\text{for } E_s = A + Bz\ ) \tag{2.13}$$

$$k_{wc} = \frac{B^2}{2\left[\left(A+BH^{0.5}\right) - A\ln\left(A+BH^{0.5}\right) - A + A\ln(A)\right]} (\text{for } E_s = A + Bz^{0.5}) \tag{2.14}$$

This enables k_w to be evaluated from k_{wc} of elasticity theory, though based on a significantly simplified continuum model, from known soil parameters E_s, and H.

2.3.3 Horvath's Pasternak-Type Model

Further, Horvath assuming that all horizontal displacements are zero, he came up with another simplified as a special case of Reissner's model which itself is already simplified. For a constant Young's modulus, E_s, the model takes the form (Horvath, 1983).

$$p = \frac{E_s}{H} w - \frac{GH}{2} \nabla^2 w \tag{2.15}$$

Due to the equivalence of the above Equation and Eq. (2.3) of Pasternak's subgrade model this simplified model is referred to as the Pasternak-type simplified continuum Subgrade model.

2.3.4 Worku's Generalized Model

A more generalized continuum subgrade model has recently been presented based on a physical model of an isotropic elastic layer of finite thickness H overlying a rigid half space and without neglecting any stress, deformation, or strain components, which resulted in a mathematical model of the same order as that of Reissner, yet with significant improvements in the coefficients (Worku, 2010).

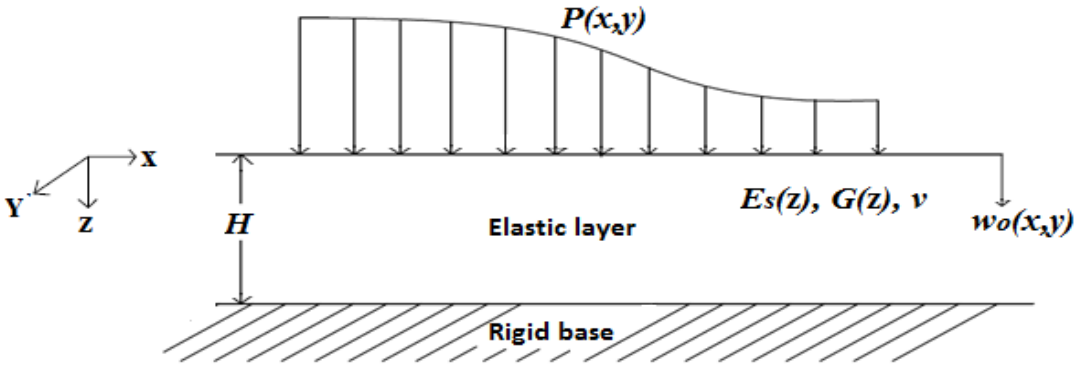

Figure 2.6 Elastic Continuum in the Generalized Model of Worku (Worku, 2010)

In this generalized formulation, he also took into account of the elasticity modulus, E_s, and the shear modulus, G, varying with depth, whereas the Poisson's ratio is kept constant with depth as his model is less sensitive to Poisson's ratio.

He expressed the lateral normal stresses components, σ_x and σ_y, in terms of the vertical normal stress, and the vertical shear stresses, τ_{xz} and τ_{yz} as products of a function of z and a function of x and y as given below:

$$\sigma_x(x,y,z) = g_x(z)\sigma_z(x,y,z);\quad \sigma_y(x,y,z) = g_y(z)\sigma_z(x,y,z) \tag{2.16}$$

$$\tau_{xz}(x,y,z) = I_{zx}(z)\bar{\tau}_{zx}(x,y);\quad \tau_{zy}(x,y,z) = I_{zy}(z)\bar{\tau}_{zy}(x,y) \tag{2.17}$$

Where g_x, g_y, I_{zx} and I_{zy} are functions of z, and $\bar{\tau}_{xz}$ and $\bar{\tau}_{zy}$ are functions of x and y. The pertinent equilibrium equation in the z-direction without body forces is given by

$$\sigma_{z,z} + \tau_{xz,x} + \tau_{zy,y} = 0 \tag{2.18}$$

The applicable stress-strain and strain-displacement relationships are

$$\frac{\partial w}{\partial z} = \frac{1}{E_s(z)}\left[\sigma_z - \nu(\sigma_x + \sigma_y)\right]$$
$$\frac{\partial u}{\partial z} + \frac{\partial w}{\partial x} = \frac{\tau_{zx}}{G};\quad \frac{\partial v}{\partial z} + \frac{\partial w}{\partial y} = \frac{\tau_{zy}}{G} \tag{2.19a, b}$$

And the prevailing and assumed boundary conditions are

$$\begin{aligned}
&\sigma_z(x,y,0) = -p \\
&u(x,y,0) = v(x,y,0) = 0;\ w(x,y,0) = w_0 \\
&u(x,y,H) = v(x,y,H) = w(x,y,H) = 0
\end{aligned} \tag{2.20}$$

For reasons of mathematical convenience, the following are also assumed

$$I_{zx}(z) = I_{zy}(z) = I_z(z) \tag{2.21}$$

This assumption means that the variation of the two vertical stress components, τ_{yz} and τ_{xz}, on the two perpendicular vertical planes of the stress cube with depth is similar, and is thus quite a reasonable assumption.

Then, he finally obtained the following relation between the vertical deflection and the contact stress at the surface:

$$p(x,y) - \frac{G}{E}\frac{1}{K_I}\left(L_{gI} - \frac{K_{gI}L_g}{K_g}\right)\nabla^2 p(x,y) = \frac{E}{K_g}w_o(x,y) - \frac{GL_{gI}}{K_g K_I}\nabla^2 w_o(x,y) \tag{2.22}$$

Where the terms in the coefficients are definite integrals given by

$$\begin{aligned}
&K_g = \int_0^H g\,dz;\ K_{gI} = \int_0^H g\,\bar{I}_z\,dz;\ K_I = \int_0^H I_z\,dz \\
&L_g = \int_0^H \left[\int g\,dz - \left(\int g\,dz\right)_{z=H}\right]\mathrm{dz}; \\
&L_{gI} = \int_0^H \left[\int g\,\bar{I}_z\,dz - \left(\int g\,\bar{I}_z\,dz\right)_{z=H}\right]\mathrm{dz} \\
&g(z) = 1 - \nu\left[g_x(z) + g_y(z)\right];\ \bar{I}(z) = \left(\int I_z dz\right)_{z=0} - \int I_z dz \\
&g_x(z) = \frac{\sigma_x(z)}{\sigma_z(z)};\ \ g_y(z) = \frac{\sigma_y(z)}{\sigma_z(z)} \\
&I_z(z) = \frac{\tau_{xz}(x,y,z)}{\bar{\tau}_{xz}(x,y)} = \frac{\tau_{yz}(x,y,z)}{\bar{\tau}_{yz}(x,y)}
\end{aligned} \tag{2.23a-f}$$

Equation (2.22) is the generalized mathematical model for the elastic subgrade. It is important to note that the maximum order of the governing differential equation of a (non-homogeneous) isotropic elastic subgrade is two occurring on the surface deformation, w_o, and the surface traction,

p. The coefficients in Eq. (2.22) are determined by evaluating the definite integrals in Eq. (2.23) with the aid of Eq. (2.16) and (2.17). Note that the soil moduli, E and *G* may generally vary with depth in the above formulation.

Worku (2010, 2013), Showed that this new model is a generalization of most existing continuum models; it reduces to the level of Reissner's (1958) model when the horizontal stress components in the continuum are dropped; to the level of Kerr and Rhines (1967) or Vlasov and Leont'ev (1966) if the horizontal deformation components alone are neglected. And it further reduces to other Kerr, Pasternak and Winkler-type simplified-continuum models as well which will be dealt with in the subsequent sections.

2.3.4.1 Winkler-Type Continuum Model

The generalized continuum model reduces to a Winkler-type model if the vertical shear stress components alone are neglected (Worku**,** 2010). i.e.

$$\tau_{xz} = \tau_{yz} = 0 \tag{2.24}$$

Because of this assumption, the equilibrium equation of (2.18) for the vertical direction reduces to

$$\sigma_{z,z} = 0 \tag{2.25}$$

Eq. (2.18) implies a constant vertical normal stress with depth, $\sigma_z(x,y) = -p(x,y)$. Introducing this relation into Eq. (2.19a) and applying the boundary conditions appropriately, the Winkler-type subgrade model is obtained as:

$$p = k_w w_o \tag{2.26}$$

Where, k_w =the coefficient of subgrade reaction with the dimension of force per length cubed in Winkler's model and given by

$$k_w = \frac{1}{\int_0^H \frac{g(z)}{E_s(z)}\,dz} \tag{2.27}$$

And where $g(z) = 1 - v\left[g_x(z) + g_y(z)\right]$ (2.28)

This result shows that disregarding the vertical shear stress components alone suffices to arrive at a Winkler-type subgrade model without the need to omit the lateral normal stresses unlike what was done by Horvath (1983).

Eq. (2.26) can also be obtained directly from Eq. (2.22) provided that L_{gI} and K_{gI} vanish which again require that I_z is zero. Thus, the type of model sought is obtained with k_w given by $1/K_g$. i.e.

$$k_w = \frac{E_s}{\int_0^H g dz} \tag{2.29}$$

2.3.4.2 Pasternak-Type Continuum Model

Pasternak-type continuum models are supposed to evolve from Eq. (2.22) when the second term on the left-hand side vanishes. Nevertheless, neither neglecting the horizontal normal stresses nor the lateral strains (k_o-at rest condition) succeeds to do so. Hence, Worku made the next logical simplifying assumption of zero horizontal deformations (Worku, 2010).

$$u = v = 0 \tag{2.30}$$

This assumption yields the following relationship between the horizontal and vertical normal stresses:

$$\sigma_x = \sigma_y = \frac{v}{1-v}\sigma_z = k_o \sigma_z \tag{2.31}$$

Where k_o = lateral earth-pressure coefficient for at-rest condition.

It has to be noted that the assumption of zero lateral displacement is not identical to assuming at-rest condition, because this assumption is not limited to merely mean $\varepsilon_{xx} = \varepsilon_{yy} = 0$, but also affects all the shear strain components as can be observed from Equations (2.19b).

The vertical shear stress components are represented as in Eq. (2.17). The pertinent combined stress-strain and strain-displacement relationships of Eq. (2.19) reduce to

$$\frac{\partial w}{\partial z} = \frac{\alpha_o}{E_s}\sigma_z, \quad \frac{\partial w}{\partial x} = \frac{\tau_{zx}}{G}, \quad \frac{\partial w}{\partial y} = \frac{\tau_{zy}}{G} \tag{2.32}$$

Where $\alpha_o = \dfrac{1-\nu-2\nu^2}{1-\nu}$ (2.33)

With these relationships and applying the boundary conditions, Worku came up with the model;

$$p = \frac{1}{L_E}\left(\frac{1}{\alpha_o} w_o + L_x w_{o,xx} + L_y w_{o,yy}\right) \tag{2.34}$$

Where

$$L_E = \int_0^H \frac{1}{E_s} dz;\ \mathrm{L}_x = \int_0^H \frac{\bar{I}_{zx} G}{E_s I_{zx}} dz,\ L_y = \int_0^H \frac{I_{zy} G}{E_s I_{zy}} dz$$
$$\bar{I}_{zx}(z) = \left(\int I_{zx} dz\right)_{z=0} - \int I_{zx} dz;\ \bar{I}_{zy}(z) = \left(\int I_{zy} dz\right)_{z=0} - \int I_{zy} dz \tag{2.35a-b}$$

Eq. (2.34) does not involve a second derivative of *p*. This shows that neglecting the lateral deformations alone suffices to arrive at this lower order DE.

Furthermore, with $I_{zx} = I_{zy} = I_z$, L_x and L_y in Eq. (2.35a) become identical and the model takes the form

$$p = \frac{1}{L_E}\left(\frac{1}{\alpha_0} w_o + L\nabla^2 w_o\right) \tag{2.36}$$

Where again,

$$L = L_x = L_y = \int_0^H \frac{\bar{I}_z G}{E_s I_z} dz \tag{2.37}$$

Eq. (2.36) is similar in form and order to Eq. (2.3), so that one may refer to it as the generalized Pasternak-type continuum model.

2.3.4.3 Kerr-Type Continuum Model

Equation (2.22) is the mathematical model for the elastic subgrade, in which no major simplifying assumptions are made a priori except Eq. (2.21). The differential equation (DE) with constant coefficients is similar in form and order to Kerr's mechanical model (Kerr, 1964). Thus the generalized continuum model is a Kerr-type model given by (Worku, 2010):

$$p-\frac{G}{EK_{kl}}\left(L_{gI}-\frac{K_{gI}L_g}{K_g}\right)\nabla^2 p=\frac{E}{K_g}w-\frac{GL_{gI}}{K_gK_I}\nabla^2 w \tag{2.38}$$

This formulation shows that the highest possible order of the DE is only two occurring with respect to both the surface deformation and the surface traction, unlike reported in some previous works, where derivatives of still higher order were used (Hetenyi 1950, Kerr and Rhines 1967). This model may thus be regarded as the generalization of continuum models from which the existing simplified continuum models and other new ones can be easily derived.

2.4 Synthesis of Mechanical and Continuum Models

From the existing direct mathematical analogy between corresponding mechanical and continuum models presented earlier, equivalence of coefficients of like terms can be sought so that the resulting equations yield the mechanical model parameters in terms of the definite integrals defined in Eq. (2.23), which, in turn, involve the continuum parameters *E*, *G*, and the layer thickness *H*. Thus, this synthesis is beneficial to exploit the strength of both approaches (Worku**,** 2013).

2.4.1 Winkler's Mechanical Model with the Winkler-Type Continuum Model

Comparing the coefficients in Eq. (2.1) of Winkler's mechanical model with Eq. (2.12) of Horvath's Winkler-type continuum model, the following equation for k_w is obtained (Worku**,** 2013);

$$k_w=\frac{E_s}{H} \tag{2.39}$$

Similar synthesis of Eq. (2.1) with the generalized Winkler-type continuum model of Worku Eq. (2.27), the resulting expression is;

$$k_w=\frac{E}{K_g} \tag{2.40}$$

This equation is a generalized form of expression in terms of the continuum parameter. The definite integrals involved in this expression and defined in Eq. (2.23) is evaluated once the functions $g_x(z)$ and $g_y(z)$ are specified.

Worku (2010, 2014), stated that the variation for the ratios of the lateral-to-vertical normal stress components with depth $\frac{\sigma_x}{\sigma_z}$ and $\frac{\sigma_y}{\sigma_z}$ under circular and rectangular regions subjected to uniformly distributed loads can be represented by an exponentially decaying function. Similarly, the distribution of the vertical shear stresses can be expressed using a bilinear function. Hence based on curve fitting to plot data, relations for g and I_z are obtained as;

$$\begin{aligned} g(z) &= 1 - v\left[g_x(z) + g_y(z) \right] = 1 - 1.6ve^{-(3.96z/H)} \\ I_z(z) &= \begin{Bmatrix} 5z/3H, 0 \le z/H \le 0.6 \\ 2.35 - 2.25z/\mathrm{H}, 0.6 \le \mathrm{z}/\mathrm{H} \le 1 \end{Bmatrix} \end{aligned} \tag{2.41}$$

Then substituting for g(z) from Eq. (2.41) into Eq. (2.23) and evaluating the definite integral, Eq.(2.40) will take the following form:

$$k_w = \frac{E}{(1-0.4v)H} \tag{2.42}$$

The layer thickness H in the above equation is eliminated by using the substitution $\chi_w = H/B$. And can be equivalently expressed as;

$$k_w = \frac{E}{(1-0.4v)\chi_w B} \tag{2.43}$$

Where B = width of the plate under consideration. And χ_w = the calibration factor for Winkler's model.

2.4.2 Pasternak's Mechanical Model with the Pasternak-Type Continuum Model

Comparing the coefficients in Eq. (2.3) of Pasternak's mechanical model with Eq. (2.15) of Horvath's Pasternak-type continuum model, the following expressions for k_p and G_p are obtained (Worku, 2013);

$$k_p = \frac{E_s}{H}, \quad G_p = \frac{GH}{2} \tag{2.44}$$

Worku (2014), pointed out that because of the neglected lateral deformations, the generalized Pasternak-type model is obviously less accurate than the generalized Kerr-type model. For this reason, better expressions for the Pasternak model parameters are presented in section 2.4.4.

2.4.3 Kerr's Mechanical Model with the Kerr-Type Continuum Model

Equating the corresponding terms in Eq. (2.4) and (2.38) one obtains the following expressions for Kerr's model parameters (Worku, 2014);

$$\begin{aligned} k_{ku} &= \frac{L_{gI}H}{\left(k_g L_{gI} - k_{gI} L_g\right)}\frac{E}{H}; \quad k_{kl} = \frac{L_{gI}H}{\left(k_{gI} L_g\right)}\frac{E}{H}; \\ G_k &= \frac{{L_{gI}}^2}{\left(k_I K_{gI} L_g H\right)} GH \end{aligned} \tag{2.45}$$

Similarly substituting Eq. (2.41) into Eq. (2.23) and evaluating the definite integrals, Eq. (2.45) takes the following form.

$$\begin{aligned} k_{ku} &= \frac{E}{(0.46 - 0.18\nu)H}; \quad k_{kl} = \frac{E}{(0.54 - 0.26\nu)H} \\ G_k &= \left(\frac{0.33 - 0.15\nu}{0.14 - 0.11\nu}\right) GH \end{aligned} \tag{2.46}$$

The layer thickness H in the above equation is once again replaced by $x = H / B$. Hence, Eq. (2.46) can be equivalently expressed as;

$$\begin{aligned} k_{ku} &= \frac{E}{(0.46 - 0.18\nu)\chi_k B}; \quad k_{kl} = \frac{E}{(0.54 - 0.26\nu)\chi_k B} \\ G_k &= \left(\frac{0.33 - 0.15\nu}{0.14 - 0.11\nu}\right) G\chi_k B \end{aligned} \tag{2.47}$$

Where B is as defined previously and χ_k = the calibration factor for Kerr's model.

2.4.4 The New Kerr-Equivalent Pasternak-Type Continuum Model

According to Worku (2014), the Kerr-equivalent Pasternak parameters are better established by seeking equivalence of performance to the Calibrated Kerr model parameters stated in Eq. (2.47).

For the two mechanical models shown in Figure. 2.7, with the corresponding relations in Eq. (2.3) and (2.4) to yield equivalent results, they have to exhibit identical shear interaction (i.e. G_k must be equal to G_p) and their surface deflection under the action of the same system of loading must be equal, i.e.

$$w_o = w_u + w_l \tag{2.48}$$

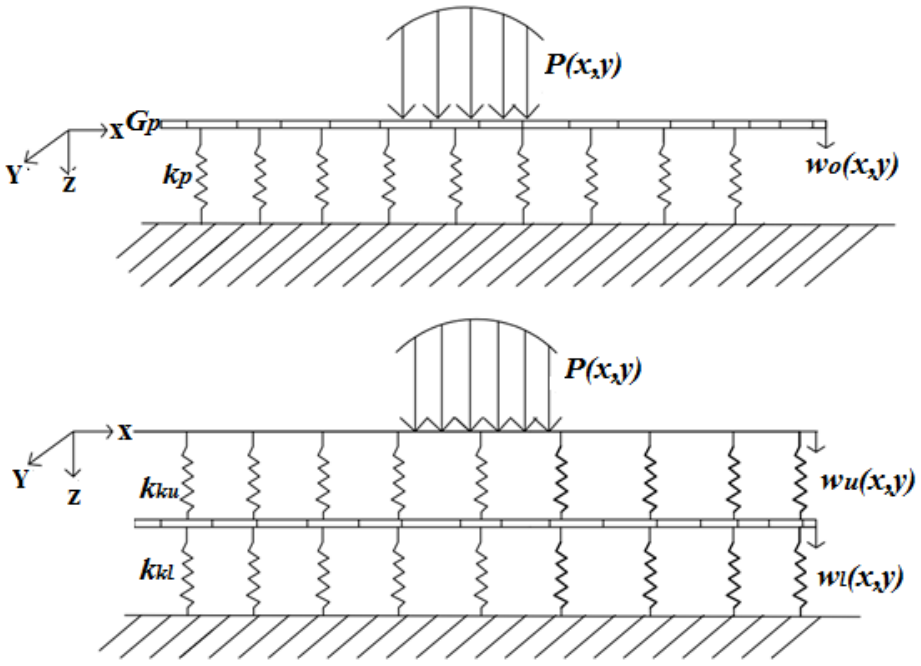

Figure 2.7 Pasternak's and Kerr's model (Worku, 2013)

Where w_o = is the surface deflection in both models, and w_u and w_l are the deflection in the upper and lower spring beds, respectively, of the Kerr model shown in Figure. 2.4.

The surface pressure in Eq. (2.3) can be expressed as:

$$p = p_p + p_{sl} \tag{2.49}$$

Where p_p = is the surface pressure shared by the Pasternak spring bed and p_{sl} is the pressure attributed to the shear layer as shown in Figure. (2.3).

Similarly, the pressure sharing in the Kerr model of Fig. (2.4) can be written as:

$$p = p_{sl} + p_l \tag{2.50}$$

Where p_{sl} = as defined above and p_l is the pressure carried by the lower spring bed of Kerr's model. Since the upper spring layer of Kerr's model directly transfers the entire contact pressure to the shear layer and the lower spring bed, the pressure shared by this layer is identical to p. i.e.

$$p_u = p \tag{2.51}$$

Substituting Eq. (2.49) and (2.50) into Eq. (2.48) together with the definition of a linear spring, the following expression is obtained:

$$\frac{p-p_{sl}}{k_p}=\frac{p}{k_u}+\frac{p-p_{sl}}{k_l} \tag{2.52}$$

Dividing Eq. (2.52) by p and rearranging, one obtains:

$$k_p=\frac{k_{ku}k_{kl}}{k_{ku}+\eta k_{kl}} \tag{2.53}$$

Where $\eta=\frac{1}{1-\left(p_{sl}/p\right)}$; for most actual cases the value of η is close to unity.

To obtain the normalized equivalent Pasternak spring coefficient, the expressions of k_u and k_l of Eq. (2.45) are inserted into Eq. (2.53) resulting in

$$\bar{k}_p=\frac{k_p}{\left(E/H\right)}=\frac{{L_{gI}}^2 H}{K_{gI}L_gL_{gI}+\eta(K_g{L_{gI}}^2-K_{gI}L_gL_{gI})} \tag{2.54}$$

For $\eta=1$ this equation simplifies to:

$$\bar{k}_p=\frac{k_p}{\left(E/H\right)}=\frac{H}{K_g} \tag{2.55}$$

Likewise, the normalized shear parameter for the replacement Pasternak model in Eq. (2.45) can be written as:

$$\bar{G}_p=\frac{G_p}{\left(GH\right)}=\frac{{L_{gI}}^2}{K_I K_{gI}L_gH} \tag{2.56}$$

Thus, the replacement Pasternak model is fully established with the two Pasternak parameters, k_p and G_p, found as in Eq. (2.55) and Eq. (2.56).

With the introduction of the evaluated definite integrals defined in Eq. (2.23) and additional observations, from the plots of the respective normalized forms, linear relationships are fitted. This, together with the introduction of the calibration factor, leads to the Kerr-equivalent Pasternak model parameters:

$$k_p = \frac{(0.4\nu + 0.67)E}{\chi_p B}$$
$$G_p = (1.36\nu + 2.28)G\chi_p B \qquad (2.57)$$

Thus, the syntheses made in this section shows that the various constants in the mechanical models can be determined from the soil properties of the corresponding simplified continuum models, the foundation size and a calibration factor, which is mainly dependent on the foundation-subgrade relative rigidity.

Chapter Three: PLATES ON ELASTIC FOUNDATIONS

3.1 The Classical Plate Theory

3.1.1 Introduction

A plate is a flat structural element with dimensions that are large compared to its thickness and is subjected to loads that cause bending deformation in addition to stretching. The thickness is usually constant but may be variable and is measured normal to the middle surface of the plate (Reddy, 2007; Szilard, 2004) (see Figure. 3.1).

In most cases, the thickness is no greater than one-tenth of the smallest in-plane dimension. Because of the small thickness, it is often not necessary to model them using 3D elasticity equations. Simple 2D plane stress theories can be developed to study the deformation and stresses in plate structures that are subjected only to in-plane loading.

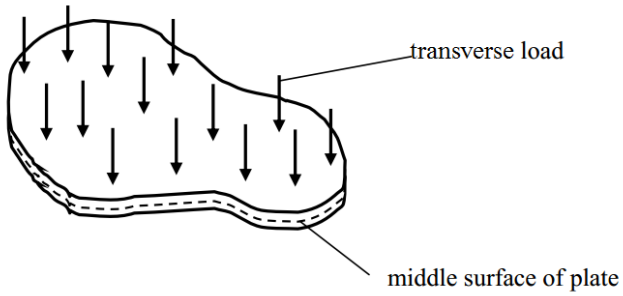

Figure 3.1 A plate subjected to a transverse loading (Szilard, 2004)

On the other hand, plate theory is concerned mainly with transverse loading. One of the differences between plane stress and plate theory is that in the plate theory the stress components are allowed to vary through the thickness of the plate, so that there can be bending moments, as shown in Figure. 3.2 (Charles, 2003; Kelly, 2007).

Figure 3.2 Stress distribution through the thickness of a plate and resultant bending moment (Charles, 2003; Kelly, 2007)

Geometrically, a plate is said to be *thin* if its *thickness to length and width ratio, h/B,* remains less than 1/20, otherwise, the plate is said to be *thick*. A thin plate is usually regarded as a body bounded by two surfaces of small or zero curvature and the distance between these surfaces, the thickness of the plate, being much smaller than the other dimensions.

3.1.2 Basic Assumptions of the Elastic Theory of Thin Plates

The classical plate theory is one in which the displacement field is based on the Poisson-Kirchhoff hypothesis for the flexure of thin plates. The following assumptions allow us to reduce the elasticity equations to one differential equation describing the plate-bending problem in the analysis section (Kelly, 2007; Reddy, 2007).

(i) The plate material is linear elastic and follows Hooke's law.

(ii) The plate material is homogeneous and isotropic. Its elastic deformation is characterized by Young's modulus E and Poisson's ratio ν .

(iii) The thickness of the plate is small compared to its lateral dimensions. The normal stress in the transverse direction can be neglected compared to the normal stresses in the plane of the plate.

(iv) **The mid-plane is a "neutral plane":** The middle plane of the plate remains free of in-plane stress/strain. Bending of the plate will cause material above and below this mid-plane to deform in-plane. The mid-plane plays the same role in plate theory as the neutral axis does in the beam theory.

(v) **Line elements remain normal to the mid-plane:** Straight lines perpendicular to the mid-surface (i.e., transverse normal) before deformation remain straight after deformation. Even if they rotate, they still remain perpendicular to the middle surface after deformation. This is similar to the Bernoulli's "plane sections remain plane" assumption of the beam theory (Kelly, 2007; Reddy, 2007) (see Figure 3.3).

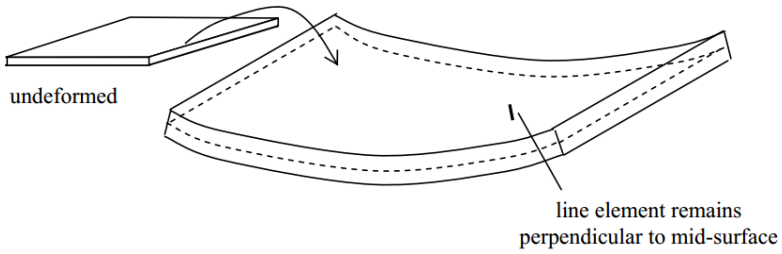

Figure 3.3 Assumptions of plate theory (Kelly, 2007; Reddy, 2007).

(vi) Vertical strain is ignored: Line elements lying perpendicular to the mid-surface (transverse normal) do not change length during deformation (i.e., they are inextensible), so that $\varepsilon_{zz} = \frac{\partial w}{\partial z} = 0$ throughout the plate. Again, this is similar to an assumption of the beam theory (Kelly, 2007; Reddy, 2007) (see Figure 3.4).

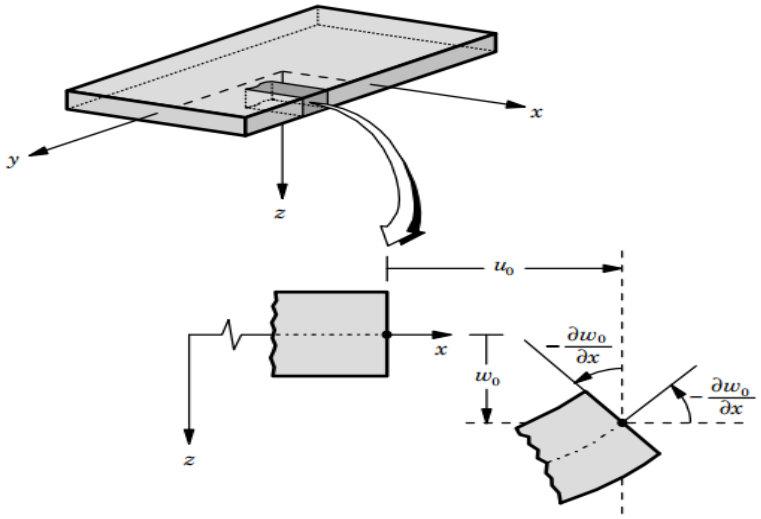

Figure 3.4 Undeformed and deformed geometries of the edge of a plate under Kirchhoff assumptions for rectangular plates (Kelly, 2007; Reddy, 2007).

(vii) The deflection *w* of the plate is small compared to the plate thickness. The curvature of the plate after deformation can then be approximated by the second derivative of the deflection *w*.

(viii) Loads are applied in a direction perpendicular to the center plane of the plate.

3.2 Governing Equations of Plates on Elastic Foundation

In this section the differential equation (DE) of a rectangular plate on an elastic foundation when subjected to a transverse load is concisely presented. Having done this, the derivation for the flexural rigidity of a plate *D* is formulated. Consequently, the moment-displacement and shear force-displacement relations are articulated.

The governing equations were derived using a semi-inverse method in which the form of the displacement field is assumed using the Kirchhoff hypothesis. The chosen displacement field contains, while satisfying the Kirchhoff hypothesis, three functions (u_o, v_o, w_o) that represent the displacements of a point on the mid plane of the plate in the three coordinate directions. Then the equations governing (u_o, v_o, w_o) are defined using the dynamic version of the principle of virtual displacements. And the plate is assumed to be made of an orthotropic material with principal material coordinates coinciding with the plate coordinates. (Reddy, 2007). In addition, the following derivations are solely taken from this book.

- For a laminated plate that are symmetrically disposed, the constitutive equations are given with the laminate stiffness coefficients A_{ij} and D_{ij} defined by

$$A_{ij} = \sum_{k=1}^{N} \overline{Q}_{ij}^{(k)} \left(z_{k+1} - z_k \right), \quad D_{ij} = \frac{1}{3} \sum_{k=1}^{N} \overline{Q}_{ij}^{(k)} \left(z^3{}_{k+1} - z^3{}_k \right) \tag{3.1}$$

- For a symmetrically laminated plate composed of multiple isotropic layers, the laminate stiffness coefficients are as defined in Eq. (3.1) with

$$\begin{aligned} \overline{Q}_{11}^{(k)} &= \overline{Q}_{22}^{(k)} = \frac{E^k}{1-\nu_k^2}, \quad \overline{Q}_{16}^{(k)} = \overline{Q}_{26}^{(k)} = 0 \\ \overline{Q}_{12}^{(k)} &= \frac{\nu_k E^k}{1-\nu_k^2}, \quad \overline{Q}_{44}^{(k)} = \overline{Q}_{55}^{(k)} = \overline{Q}_{66}^{(k)} = \frac{E^k}{2(1+\nu_k)} \end{aligned} \tag{3.2}$$

- For homogeneous plates (i.e. for plates with constant A_{ij} and D_{ij}), the equation of motion can be expressed in terms of displacements (u_o, v_o, w_o) as

$$A_{11}\left(\frac{\partial^2 u_o}{\partial x^2}+\frac{\partial^2 w_o}{\partial x}\frac{\partial^2 w_o}{\partial x^2}\right)+A_{12}\left(\frac{\partial^2 u_o}{\partial x\partial y}+\frac{\partial w_o}{\partial y}\frac{\partial^2 w_o}{\partial x\partial y}\right)$$
$$+A_{66}\left(\frac{\partial^2 u_o}{\partial y^2}+\frac{\partial^2 v_o}{\partial x\partial y}+\frac{\partial^2 w_o}{\partial x}\frac{\partial w_o}{\partial y}+\frac{\partial w_o}{\partial x}\frac{\partial^2 w_o}{\partial y^2}\right)-\left(\frac{\partial N^T{}_{xx}}{\partial x}+\frac{\partial N^T{}_{xy}}{\partial y}\right)=I_o\frac{\partial^2 u_o}{\partial t^2} \tag{3.3}$$

$$A_{66}\left(\frac{\partial^2 u_o}{\partial x\partial y}+\frac{\partial^2 v_o}{\partial x^2}+\frac{\partial^2 w_o}{\partial x^2}\frac{\partial w_o}{\partial y}+\frac{\partial w_o}{\partial x}\frac{\partial^2 w_o}{\partial x\partial y}\right)$$
$$+A_{12}\left(\frac{\partial^2 u_o}{\partial x\partial y}+\frac{\partial w_o}{\partial x}\frac{\partial^2 w_o}{\partial x\partial y}\right)+A_{22}\left(\frac{\partial^2 u_o}{\partial y^2}+\frac{\partial w_o}{\partial y}\frac{\partial^2 w_o}{\partial y^2}\right)-\left(\frac{\partial N^T{}_{xy}}{\partial x}+\frac{\partial N^T{}_{yy}}{\partial y}\right)=I_o\frac{\partial^2 u_o}{\partial t^2} \tag{3.4}$$

$$-D_{11}\frac{\partial^4 w_o}{\partial x^4}-2\left(D_{12}+2D_{66}\right)\frac{\partial^4 w_o}{\partial x^2\partial y^2}-D_{22}\frac{\partial^4 w_o}{\partial y^4}-p\left(x,\mathrm{y}\right)$$
$$-\left(\frac{\partial^2 M^T{}_x}{\partial x^2}+2\frac{\partial^2 M^T{}_{xy}}{\partial y\partial x}+\frac{\partial^2 M^T{}_y}{\partial y^2}\right)+\mathbb{N}\left(u_o,v_o,w_o\right)+q\left(x,y\right)=I_o\frac{\partial^2 w_0}{\partial t^2}-I_2\frac{\partial^2}{\partial t^2}\left(\frac{\partial^2 w_0}{\partial x^2}+\frac{\partial^2 w_0}{\partial y^2}\right) \tag{3.5}$$

Where N_{xx}, N_{xy}, N_{yy} are thickness integrated forces; t is time and I is moment of inertia

- For isotropic case, we have

$A_{11}=A_{22}=A,\ A_{12}=vA,\ 2A_{66}=\left(1-v\right)A,$ and $D_{11}=D_{22}=D,\ D_{12}=vD,\ 2D_{66}=\left(1-v\right)D$ with $A=E\big/\left(1-v^2\right)$ and $D=Ah_p{}^3\big/12$.

Then equations (3.3), (3.4) and (3.5) reduces to

$$A_{11}\frac{\partial^2 u_o}{\partial x^2}+A_{12}\frac{\partial^2 u_o}{\partial x\partial y}+A_{66}\left(\frac{\partial^2 u_o}{\partial y^2}+\frac{\partial^2 v_o}{\partial x\partial y}\right)-\left(\frac{\partial N^T{}_{xx}}{\partial x}+\frac{\partial N^T{}_{xy}}{\partial y}\right)=0 \tag{3.6}$$

$$A_{66}\left(\frac{\partial^2 u_o}{\partial x\partial y}+\frac{\partial^2 v_o}{\partial x^2}\right)+A_{12}\frac{\partial^2 u_o}{\partial x\partial y}+A_{22}\frac{\partial^2 u_o}{\partial y^2}-\left(\frac{\partial N^T{}_{xy}}{\partial x}+\frac{\partial N^T{}_{yy}}{\partial y}\right)=0 \tag{3.7}$$

$$D_{11}\frac{\partial^4 w_o}{\partial x^4}+2\left(D_{12}+2D_{66}\right)\frac{\partial^4 w_o}{\partial x^2\partial y^2}-D_{22}\frac{\partial^4 w_o}{\partial y^4}+p\left(x,\mathrm{y}\right)$$
$$=q\left(x,y\right)-\left(\frac{\partial^2 M^T{}_{xx}}{\partial x^2}+2\frac{\partial^2 M^T{}_{xy}}{\partial y\partial x}+\frac{\partial^2 M^T{}_{yy}}{\partial y^2}\right) \tag{3.8}$$

Finally, the equation of equilibrium governing the linear bending of isotropic plates on an elastic foundation experiencing small strains and small displacements (neglecting the thermal effects) will have the following form according to Reddy (2007):

$$D\left(\frac{\partial^4 w_o}{\partial x^4}+2\frac{\partial^4 w_o}{\partial x^2\partial y^2}+\frac{\partial^4 w_o}{\partial y^4}\right)+p(x,y)=q(x,y) \tag{3.9}$$

Using the Laplace operator ∇^2, Eq. (3.9) can be expressed as

$$D\nabla^4 w_o + p(x,y)=q(x,y) \tag{3.10}$$

Where $\nabla^4=\nabla^2\nabla^2$ is the biharmonic operator; $w_o=w_o(x,y)$ or $w_o(r,\theta)$= the transverse deflection; $q(x,y)$= the distributed transverse load; $p(x,y)$ is the reaction of the elastic foundation and D = the flexural rigidity of the plate (and the derivation for this follows).

For pure bending of plates of uniform thickness, if stresses $\sigma_x=\frac{E_p z}{R}$ (where R is the radius of curvature of the plate after bending) are distributed over the edges of the plate parallel to the y-axis (Figure 3.5), the curvature of which in planes parallel to the *xz*-plane is $1/R$ and in the perpendicular direction is $-\nu_p/R$ (Timoshenko, 1951).

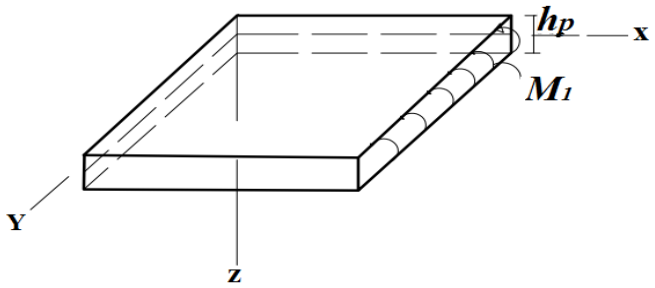

Figure 3.5 Bending moment in one perpendicular direction (Timoshenko, 1951).

If h_p denotes the thickness of the plate and M_1 the bending moment per unit length on the edges parallel to the y-axis, the moment of inertia per unit length I_y is given by

$$I_y=\frac{1*h_p^{\,3}}{12} \tag{3.11}$$

And the bending moment is given by the equation

$$M_1 = \int \sigma_x z \, dA = \int \frac{E_p z^2}{R} dA = \frac{E_p I_y}{R} \tag{3.12}$$

Then the relation between M_1 and R can be derived as

$$\frac{1}{R} = \frac{M_1}{E_p I_y} = \frac{12 M_1}{E_p h_p^{\,3}} \tag{3.13}$$

For two bending moments (M_1 and M_2 on the edges parallel to the y- and x- axes, resp.) in the perpendicular directions (Figure 3.6), the curvatures of the deflection surface are obtained by superposition.

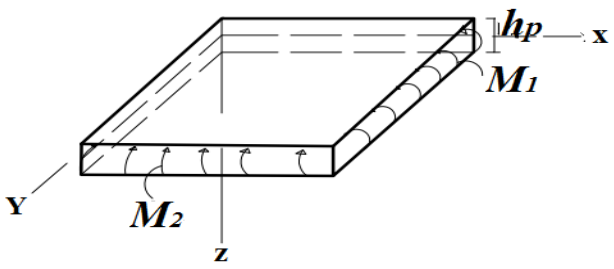

Figure 3.6 Bending moments in two perpendicular directions (Timoshenko, 1951).

The curvatures in planes, $1/R_1$ and $1/R_2$, parallel to the coordinate planes *zx* and *zy* respectively are

$$\begin{aligned} \frac{1}{R_1} &= \frac{12}{E_p h_p^{\,3}} \left(M_1 - \nu_p M_2 \right) \\ \frac{1}{R_2} &= \frac{12}{E_p h_p^{\,3}} \left(M_2 - \nu_p M_1 \right) \end{aligned} \tag{3.14}$$

Solving for M_1 and M_2, we find

$$\begin{aligned} M_1 &= \frac{E_p h_p^{\,3}}{12\left(1-\nu_p^{\,2}\right)} \left(\frac{1}{R_1} + \nu_p \frac{1}{R_2} \right) \\ M_2 &= \frac{E_p h_p^{\,3}}{12\left(1-\nu_p^{\,2}\right)} \left(\frac{1}{R_2} + \nu_p \frac{1}{R_1} \right) \end{aligned} \tag{3.15}$$

For small deflections the following approximation can be used for the curvatures as given as

$$\frac{1}{R_1} = -\frac{\partial^2 w_o}{\partial x^2}; \quad \frac{1}{R_2} = -\frac{\partial^2 w_o}{\partial y^2} \tag{3.16}$$

Then the flexural rigidity of the plate D is expressed as

$$D = \frac{E_p h_p{}^3}{12\left(1 - \nu_p{}^2\right)} \tag{3.17}$$

Where E_p is an elastic modulus of the plate and ν_p is Poisson's ratio of the plate

Hence, using Eq. (3.15) and (3.16), the moment-displacement relations for an isotropic homogeneous plate in the Cartesian rectangular coordinate system can be obtained as

$$M_x = -D\left(\frac{\partial^2 w_o}{\partial x^2} + \nu_p\left(\frac{\partial^2 w_o}{\partial y^2}\right)\right)$$
$$M_y = -D\left(\nu_p\left(\frac{\partial^2 w_o}{\partial x^2}\right) + \frac{\partial^2 w_o}{\partial y^2}\right) \tag{3.18a-b}$$

And the shear force-displacement relation is deduced from the general equations of equilibrium of stress components of a small rectangular element and compatibility conditions with valid approximations. Then after, the derivation follows from the Figure 3.7.

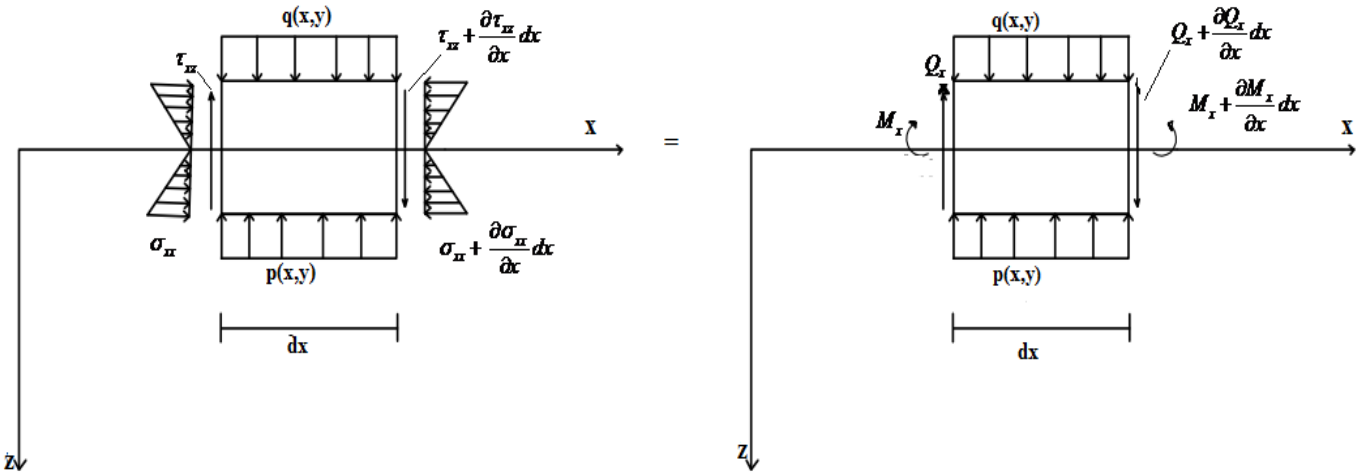

Figure 3.7 Stress, flexural moments and shearing forces acting on a plate element in the x-z plane. (Timoshenko, 1951; Selvadurai, 1979).

The twisting moment M_{xy} induced by the shear stresses τ_{xy} is given by

$$M_{xy} = -2\left(1-\nu_p\right) D \frac{\partial^2 w_o}{\partial x \partial y} \tag{3.19}$$

From the moment of equilibrium of the element about the y- axes we have (neglecting higher-order terms), we have

$$\frac{\partial M_{xy}}{\partial y} - \frac{\partial M_x}{\partial x} + Q_x = 0 \tag{3.20}$$

Then the shear force-displacement relation in reference to Eq. (3.18a), (3.19) and (3.20);

$$Q_x = -D\left(\frac{\partial^3 w_o}{\partial x^3} + 2\frac{\partial^3 w_o}{\partial x \partial y^2} \right) \tag{3.21}$$

3.3 Analysis of Thin Circular Plates on an Elastic Foundation

3.3.1 Introduction

Circular plates are found in manhole covers, closures of pressure vessels, pump diaphragms, clutches, and turbine disks, to name a few. In addition, circular raft foundations for cylindrical structures such as nuclear reactors, tower silos, cylindrical water reservoirs and storage tanks are often analysed as circular plates resting on an elastic half space (Reddy, 2007).

Nowadays, the theory of plates and shells on elastic foundations occupies a prominent place in contemporary structural mechanics. As a result, it is of interest to study the flexural behaviour of circular plates on elastic media. The state of rotational symmetry (or axisymmetry with respect to the z-axis, which is taken normal to the plane of the plate with the origin at the center of the plate) exists and the deformation is independent of the angular coordinate (i.e. all variables are only functions of the radial coordinate r and, u_θ, the angular displacement is identically zero.) only when the boundary conditions, material properties, and loading are also rotationally symmetric. Consequently, the problem is reduced to a one-dimensional one (Reddy, 2007; Szilard, 2004).

Therefore, the analysis of circular plates considering linear, static bending with axisymmetric loads and edge conditions is dealt with in this section.

3.3.2 Basic Governing Equations in Polar Coordinate

The equations governing circular plates is obtained using transformation relations between the polar coordinates (r,θ) and the rectangular Cartesian coordinates (x,y) (Reddy, 2007). To illustrate this, we consider the Poisson equation

$$\nabla^2 u = f \tag{3.22}$$

Where f is a specified function of position, u is a governing function in a two-dimensional domain with a source f and ∇^2 is 2D Laplace operator.

Using the translation relation, see Figure (3.8)

$$x = r\cos\theta,\ y = r\sin\theta \tag{3.23}$$

$$\frac{\partial}{\partial x} = \frac{\partial r}{\partial x}\frac{\partial}{\partial r} + \frac{\partial \theta}{\partial x}\frac{\partial}{\partial \theta},\quad \frac{\partial}{\partial y} = \frac{\partial r}{\partial y}\frac{\partial}{\partial r} + \frac{\partial \theta}{\partial y}\frac{\partial}{\partial \theta} \tag{3.24}$$

Where [from $r^2 = x^2 + y^2$ and Eq. (3.24)]

$$\frac{\partial r}{\partial x} = \frac{x}{r} = \cos\theta,\ \frac{\partial r}{\partial y} = \frac{y}{r} = \sin\theta,\ \frac{\partial \theta}{\partial x} = -\frac{\sin\theta}{r},\ \frac{\partial \theta}{\partial y} = \frac{\cos\theta}{r} \tag{3.25}$$

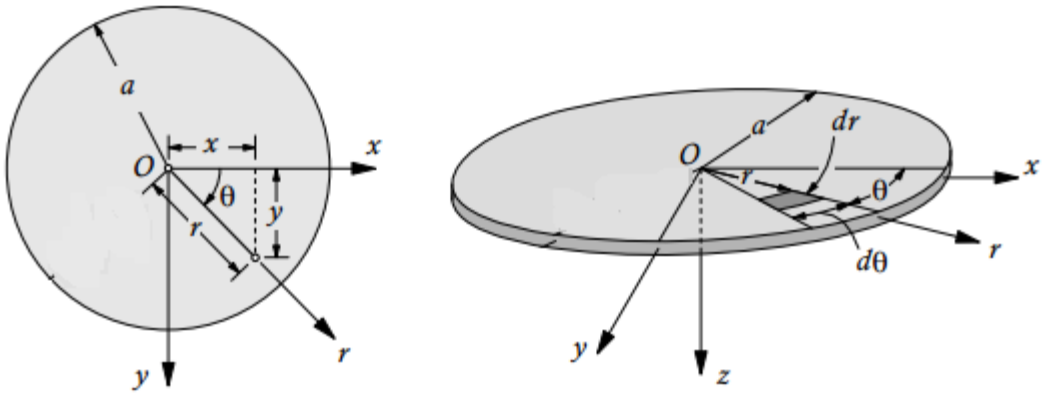

Figure 3.8 Transformation between rectangular and polar coordinate systems (Reddy, 2007).

Hence,

$$\frac{\partial}{\partial x} = \cos\theta\frac{\partial}{\partial r} - \frac{\sin\theta}{r}\frac{\partial}{\partial \theta},\quad \frac{\partial}{\partial y} = \sin\theta\frac{\partial}{\partial r} + \frac{\cos\theta}{r}\frac{\partial}{\partial \theta} \tag{3.26}$$

The second derivatives with respect to x and y are computed using the above relations and chain rule of differentiation as follows:

$$\frac{\partial^2}{\partial x^2} = \cos\theta \frac{\partial}{\partial r}\frac{\partial}{\partial x} - \frac{\sin\theta}{r}\frac{\partial}{\partial \theta}\left(\frac{\partial}{\partial x}\right)$$

$$= \cos^2\theta \frac{\partial^2}{\partial r^2} + \frac{\sin^2\theta}{r}\frac{\partial}{\partial r} - \frac{\sin 2\theta}{r}\frac{\partial^2}{\partial r \partial \theta} + \frac{\sin 2\theta}{r^2}\frac{\partial}{\partial \theta} + \frac{\sin^2\theta}{r^2}\frac{\partial^2}{\partial \theta^2} \tag{3.27}$$

$$\frac{\partial^2}{\partial y^2} = \sin^2\theta \frac{\partial^2}{\partial r^2} + \frac{\cos^2\theta}{r}\frac{\partial}{\partial r} + \frac{\sin 2\theta}{r}\frac{\partial^2}{\partial r \partial \theta} - \frac{\sin 2\theta}{r^2}\frac{\partial}{\partial \theta} + \frac{\cos^2\theta}{r^2}\frac{\partial^2}{\partial \theta^2} \tag{3.28}$$

Adding Eq. (3.27) and (3.28) in the polar coordinate system, we get

$$\nabla^2 = \nabla.\nabla = \frac{1}{r}\frac{\partial}{\partial r}\left(r\frac{\partial}{\partial r}\right) + \frac{1}{r^2}\frac{\partial^2}{\partial \theta^2} \tag{3.29}$$

Using this transformation relation of the Laplace operator, Eq. (3.9) becomes

$$D\left[\frac{1}{r}\frac{\partial}{\partial r}\left(r\frac{\partial}{\partial r}\right) + \frac{1}{r^2}\frac{\partial^2}{\partial \theta^2}\right]\left[\frac{1}{r}\frac{\partial}{\partial r}\left(r\frac{\partial w_o}{\partial r}\right) + \frac{1}{r^2}\frac{\partial^2 w_o}{\partial \theta^2}\right] + p(r,\theta) = q(r,\theta) \tag{3.30}$$

But for axisymmetric deformation, $w_o = w_o(r)$, and Eq. (3.30) reduces to

$$D\left[\frac{1}{r}\frac{d}{dr}\left(r\frac{d}{dr}\right)\right]\left[\frac{1}{r}\frac{d}{dr}\left(r\frac{dw_o}{dr}\right)\right] + p(r) = q(r) \tag{3.31}$$

This is the governing equation which can also be rewritten as

$$\frac{D}{r}\frac{d}{dr}\left\{r\frac{d}{dr}\left[\frac{1}{r}\frac{d}{dr}\left(r\frac{dw_o}{dr}\right)\right]\right\} + p(r) = q(r) \tag{3.32}$$

Again using the transformation relations and curvatures in the radial and tangential direction in reference to Eq. (3.16),

$$K_r = \frac{\partial^2 w_o}{\partial r^2}; \quad K_\theta = \frac{\partial^2 w_o}{\partial r^2} \tag{3.33}$$

Where $K_r = 1/R_1$ and $K_\theta = 1/R_2$

Eq. (3.18a-b) and (3.21) can be expressed in polar coordinate while noting to Eq. (3.27) and (3.28) as

$$M_r = -D\left(\frac{d^2 w_o}{dr^2} + v_p\left(\frac{1}{r}\frac{dw_o}{dr}\right)\right)$$
$$M_\theta = -D\left(v_p\frac{d^2 w_o}{dr^2} + \left(\frac{1}{r}\frac{dw_o}{dr}\right)\right) \qquad \text{(3.34a-c)}$$
$$Q_r = -D\frac{d}{dr}\left(\frac{1}{r}\frac{d}{dr}\left(r\frac{dw_o}{dr}\right)\right)$$

3.3.3 Formulation of the Differential Equations of the Circular Plate

In this section, the differential equation (DE) of a circular plates on an elastic subgrade is formulated for a single parameter and two parameter subgrade models. And the following procedures and formats of the subsections to formulate the differential equations and analytical solutions of the circular plate are taken from Degu (2008).

3.3.3.1 Single- Parameter (Winkler's) Subgrade Model

In this model, support is provided by a bed of uniformly spaced springs as shown in Figure 3.9. A plate supported along its entire length by such an elastic medium is considered to formulate the DE of the plate.

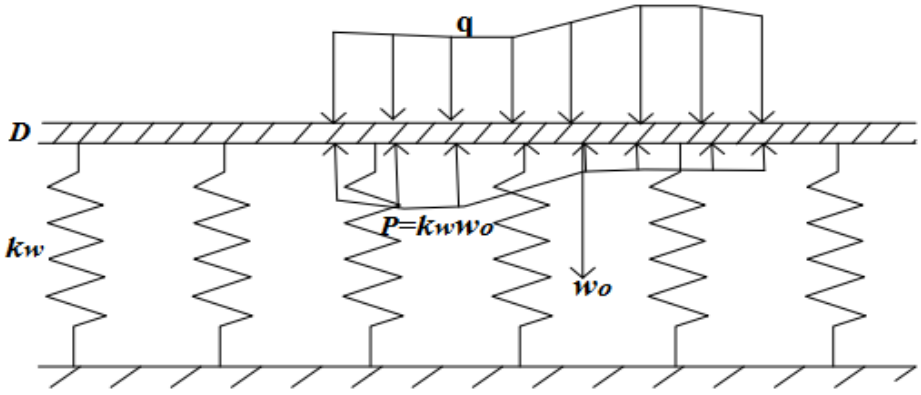

Figure 3.9 Winkler's mechanical model

The governing equation in Eq. (3.32) can be considered as the governing differential equation of Winkler's subgrade model with $p(r)=k_w w_o(r)$ (Reddy, 2007).

$$\frac{D}{r}\frac{d}{dr}\left\{r\frac{d}{dr}\left[\frac{1}{r}\frac{d}{dr}\left(r\frac{dw_o}{dr}\right)\right]\right\}+k_w w_o(r)=q(r) \tag{3.35}$$

3.3.3.2 Two- Parameter (Pasternak's) Subgrade Model

For this model a shear layer with parameter G_p, which represents the stiffness of the vertical shear interaction, is introduced to improve the shear interaction between spring elements (Figure 3.10).

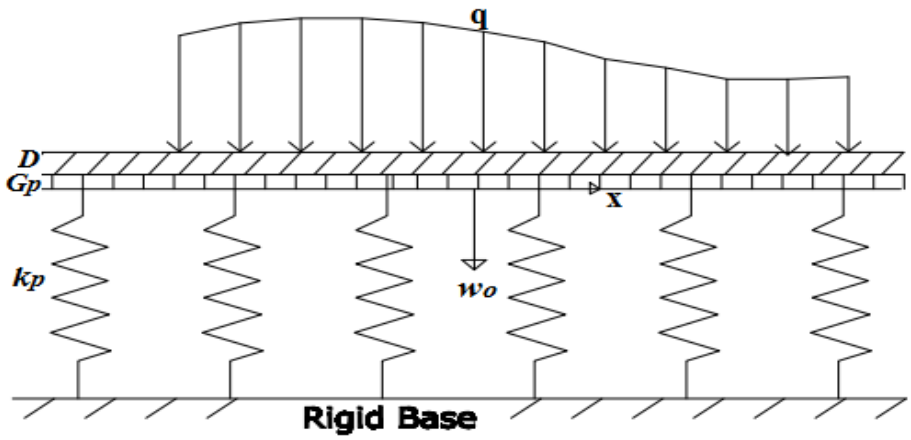

Figure 3.10 Pasternak's mechanical model

Transforming the reaction of the elastic foundation given in Eq. (2.3) into polar coordinate, we have

$$p(r)=k_p w_o(r)-G_p\nabla^2 w_o(r) \tag{3.36}$$

Substituting Eq. (3.36) into the expression (3.32) in place of $p(r)$ and taking note of Eq. (3.29), we obtain the governing DE for Pasternak's subgrade model as

$$\frac{D}{r}\frac{d}{dr}\left\{r\frac{d}{dr}\left[\frac{1}{r}\frac{d}{dr}\left(r\frac{dw_o}{dr}\right)\right]\right\}+k_p w_o(r)-\frac{G_p}{r}\frac{d}{dr}\left(r\frac{dw_o}{dr}\right)=q(r) \tag{3.37}$$

3.3.4 Analytical Solution to the Differential Equations of the Circular Plate

Fundamental solutions of Eq. (3.35) and (3.37) for different possible loading conditions are sought using Fourier and Hankel integral transforms in this section.

3.3.4.1 Plates on Winkler's Subgrade Model

The circular plate is assumed to be subjected to a loading distributed symmetrically with respect to the center *o*. It can be regarded as consisting of wedge shaped elements, each of which is deformed in the same manner (Hetenyi, 1979; Selvadurai, 1979).

- ✓ The deformation of the cross section is restrained on account of the continuity of the material in the circumferential direction.
- ✓ Thus, opposing moments act on the sides of each wedge element. (Figure 3.11)

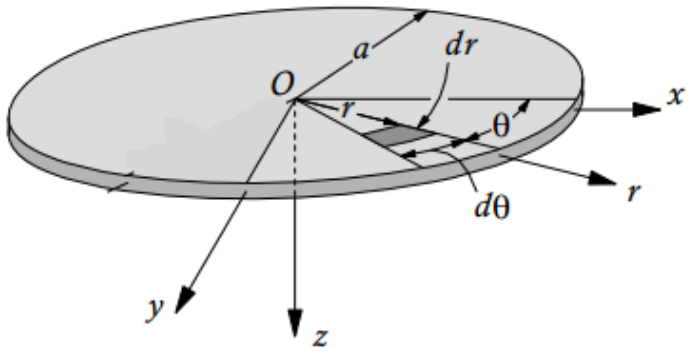

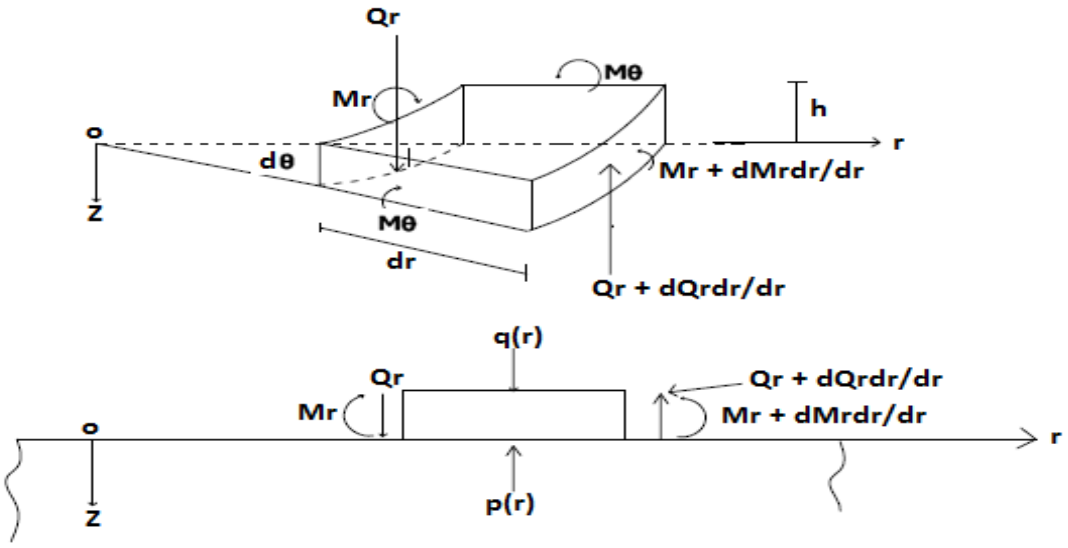

Figure 3.11 A circular plate showing an infinitesimal element and a figure showing flexural moments and shear forces subjected to an axisymmetric external load and supported by a contact stress $q(r)$ which is axisymmetric resp. (Selvadurai, 1979).

The infinitesimal element is acted upon, per unit length of its sides, by bending moments M_r and shearing forces Q_r in the radial and bending moments M_θ in the circumferential direction, while unit areas of its upper and lower surfaces will be subjected to a distributed loading q and a distributed reaction of the foundation p, respectively. Other force components vanish on account of the assumed symmetry of the loading (Hetenyi, 1979).

Equilibrium of the moments in the radial plane,

$$\sum M_r = 0, \quad \frac{dM_r}{dr} + \frac{M_r}{r} - \frac{M_\theta}{r} - Q_r = 0 \tag{3.38}$$

Equilibrium of the forces in the vertical direction,

$$\sum F_z = 0, \quad \frac{dQ_r}{dr} + \frac{Q_r}{r} + q - p = 0 \tag{3.39}$$

Substituting from equations (3.34 a-c) into expression (3.38), we get the shear force as

$$Q_r = -D\left(\frac{d^3 w_o}{dr^3} + \frac{1}{r}\frac{d^2 w_o}{dr^2} - \frac{1}{r^2}\frac{dw_o}{dr}\right) \tag{3.40}$$

And substituting Eq. (3.40) into (3.39), the DE of bending of the plate is obtained as

$$\frac{d^4 w_o}{dr^4} + \frac{2}{r}\frac{d^3 w_o}{dr^3} - \frac{1}{r^2}\frac{d^2 w_o}{dr^2} + \frac{1}{r^3}\frac{dw_o}{dr} = \frac{q-p}{D} \tag{3.41}$$

When the distributed loading q is eliminated by a change in the dependent variable because there is no distributed load applied on top of the plate, Eq. (3.41) becomes equivalent to scattered form of Eq. (3.35). (.i.e. undergoing the biharmonic operator, ∇^4 and dividing by D.)

$$\frac{d^4 w_o}{dr^4} + \frac{2}{r}\frac{d^3 w_o}{dr^3} - \frac{1}{r^2}\frac{d^2 w_o}{dr^2} + \frac{1}{r^3}\frac{dw_o}{dr} + \frac{k_w w_o}{D} = 0 \tag{3.42}$$

Introducing a differential operator,

$$\Delta_r = \frac{d^2}{dr^2} + \frac{1}{r}\frac{d}{dr} \tag{3.43}$$

Then Eq. (3.42) can be written as

$$\left(\frac{d^2}{dr^2} + \frac{1}{r}\frac{d}{dr}\right)\left(\frac{d^2 w_o}{dr^2} + \frac{1}{r}\frac{dw_o}{dr}\right) + \frac{k_w w_o}{D} = 0 \tag{3.44}$$

Letting $\lambda = \sqrt[4]{\frac{k_w}{D}}$, Eq. (3.44) reduces to

$$\Delta_r{}^2 w_o + \lambda^4 w_o = 0 \tag{3.45}$$

Where λ is the characteristic size of the circular plate-soil system, which with the use of Eq. (3.17) can be expressed as

$$\lambda = \sqrt[4]{\frac{12 k_w \left(1 - \nu_p{}^2\right)}{E_p h_p{}^3}} \tag{3.46}$$

Rigorous solutions of DE of this type can be derived in form of power series, which are expressible in terms of Bessel functions because these functions utilize problems presenting axial symmetry. The details to the solution of Eq. (3.45) is provided in Appendix B.

Thus, the general solution to Eq. (3.45) is

$$w_o = A_1 z_1(\lambda r) + A_2 z_2(\lambda r) + A_3 z_3(\lambda r) + A_4 z_4(\lambda r) \tag{3.47}$$

Where A_1 to A_4 are open constants and, $z_1(\lambda r)$, $z_2(\lambda r)$, $z_3(\lambda r)$ and $z_4(\lambda r)$ are four independent solutions of the governing equation for an argument λr. These functions are infinite series solutions of modified Bessel equations. Due to the lengthy nature of these functions, they are provided in appendices A and B.

Using the notations stated in Appendix A, Eq. (3.47) can also be expressed as:

$$w_o = a\,ber(\lambda r) + b\,bei(\lambda r) + c\,\ker(\lambda r) + d\,kei(\lambda r) \tag{3.48}$$

Where *a* to *d* are open constants and *ber*, *bei*, *ker* and *kei* are first and second kind solutions of modified Bessel equations, respectively.

With the aid of Eq. (3.34a-c) the corresponding internal actions are derived as

$$\begin{aligned}
M_r &= -D\lambda^2 \left[\begin{array}{l} A_1 z_2(\lambda r) - A_2 z_1(\lambda r) + A_3 z_4(\lambda r) - A_4 z_3(\lambda r) \\ -\dfrac{1}{r}(1-\nu_p)\left\{ A_1 z_1'(\lambda r) + A_2 z_2'(\lambda r) + A_3 z_3'(\lambda r) + A_4 z_4'(\lambda r) \right\} \end{array} \right] \\
M_\theta &= -D\lambda^2 \left[\begin{array}{l} \nu_p \left\{ A_1 z_2(\lambda r) - A_2 z_1(\lambda r) + A_3 z_4(\lambda r) - A_4 z_3(\lambda r) \right\} \\ +\dfrac{1}{r}(1-\nu_p)\left\{ A_1 z_1'(\lambda r) + A_2 z_2'(\lambda r) + A_3 z_3'(\lambda r) + A_4 z_4'(\lambda r) \right\} \end{array} \right] \\
Q_r &= -D\lambda^3 \left[A_1 z_2'(\lambda r) - A_2 z_1'(\lambda r) + A_3 z_4'(\lambda r) - A_4 z_3'(\lambda r) \right]
\end{aligned} \tag{3.49a-c}$$

The slope can also be obtained from the differentiation of the deflections as

$$\theta_r = \frac{dw_o}{dr} = \lambda \left[A_1 z_1'(\lambda r) + A_2 z_2'(\lambda r) + A_3 z_3'(\lambda r) + A_4 z_4'(\lambda r) \right] \tag{3.49d}$$

3.3.4.1.1 Large Plates

I. Circular Plate under Central Concentrated Load with Free End Condition

A sketch of such a plate is shown in Figure 3.12. The deformed subgrade is qualitatively given in Figure 3.13.

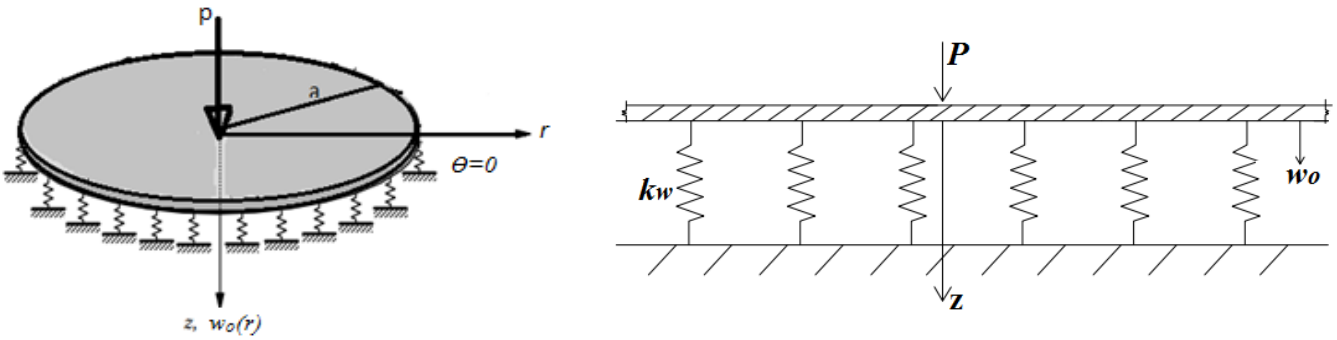

Figure 3.12 A circular plate on an elastic foundation and subjected to a central concentrated load (Reddy, 2007).

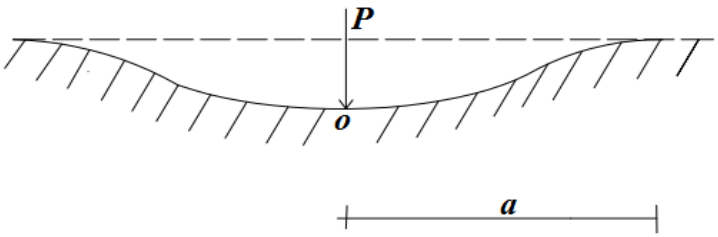

Figure 3.13 The actual deflection shape (Hetenyi, 1979).

The four constants, A_1 to A_4, in the general solution of Eq. (3.48) can be found by introducing the following boundary conditions for the solid circular plate as stated by Hetenyi (1979), Reddy (2007) and Timoshenko (1951).

i. For $r = \infty,\ w_o = 0$

ii. For $r = 0,\ w_o$ must be finite

iii. For $r = 0,\ \frac{dw_o}{dr} = 0$ (because w_o is maximum)

iv. For $r \to 0,\ Q_r = \frac{-P}{2\pi r}$

Now, in order to determine the integration constants in equation (3.47 or 3.48), the above boundary conditions are employed.

- ✓ Boundary condition (i) leads *a* or $A_1=0$ and *b* or $A_2=0$ because the asymptotic values of ber and bei are infinite as it can be seen from Eq. (A-23) and (A-24), Appendix A.
- ✓ Boundary condition (ii) requires *c* or A_4 to be zero because $\ker(0)$ is undefined or it becomes infinitely large at the origin referring to Eq. (A-29), Appendix A.

Hence the solution, Eq. (3.48) reduces to

$$w_o = d\,kei(\lambda r) \text{ or } w_o = A_3 z_3(\lambda r) \tag{3.50}$$

- ✓ Boundary condition (iii) gives

$$\lim_{r\to 0}\frac{dkei(\lambda r)}{dr} = -\left[\frac{2\left(\frac{\lambda r}{2}\right)}{1!1!\frac{2}{\lambda}}\ldots\right]\left[\log\left(\frac{\lambda r}{2}\right)+\gamma\right]-\left[\frac{\left(\frac{\lambda r}{2}\right)^2}{1!1!}\ldots\right]\left[\frac{1}{2\frac{r}{\lambda}}\right]$$

$$-\frac{\pi}{4}\left[\frac{-4\left(\frac{\lambda r}{2}\right)^3}{1!1!\frac{2}{\lambda}}\ldots\right]+\frac{2\left(\frac{\lambda r}{2}\right)}{1!1!\frac{2}{\lambda}}\ldots = 0$$

Thus, boundary condition (iii) is satisfied.

- ✓ Boundary condition (iv) is applied to find the last constant *d* or A_3.

Referring to Q_r from Eq. (3.34c)

$$Q_r = -D\left(\frac{d^3w_o}{dr^3}+\frac{1}{r}\frac{d^2w_o}{dr^2}-\frac{1}{r^2}\frac{dw_o}{dr}\right)=\frac{-P}{2\pi r}$$

$$= -D\frac{d}{dr}\left(\frac{d^2w_o}{dr^2}+\frac{1}{r}\frac{dw_o}{dr}\right)=\frac{-P}{2\pi r}$$

In reference to Eq. (A-26, A-27 and A-28), $kei(\lambda r)$ is derived as (when limited to the first terms i.e. with A_2 coefficient.)

$$kei(\lambda r) = -bei(\lambda r)\left[\log\left(\frac{\lambda r}{2}\right)+\gamma\right]-\frac{\pi}{4}ber(\lambda r)$$

$$ber(\lambda r) = 1-\frac{\left(\frac{\lambda r}{2}\right)^4}{2!2!} \text{ and } bei(\lambda r) = \frac{\left(\frac{\lambda r}{2}\right)^2}{1!1!}$$

Hence, $\frac{d}{dr}\left(\frac{d^2 w_o}{dr^2}+\frac{1}{r}\frac{dw_o}{dr}\right)=\frac{-\lambda^2}{r}$ in a similar manner done for boundary condition (iii) .i.e. applying the limit of differentiation.

Equating the value of boundary condition (iii) with this one for any r, $Q_r = \frac{-P}{2\pi r} = d\frac{D\lambda^2}{r}$, we get the constant as:

$$d = \frac{-P}{2\pi D\lambda^2} \tag{3.51}$$

Substituting $kei(\lambda r)$ into Eq. (3.50), we have;

$$w_o = \frac{-P}{2\pi D\lambda^2}\left[-bei(\lambda r)\left[\log\left(\frac{\lambda r}{2}\right)+\gamma\right]-\frac{\pi}{4}ber(\lambda r)\right] \tag{3.52}$$

Equivalently,

$$w_o = \frac{P}{2\pi D\lambda^2} z_3(\lambda r) \tag{3.53}$$

Where

$$z_3(\lambda r) = z_1(\lambda r)+\frac{i\left[N_o\left(\lambda r\sqrt{i}\right)-N_o\left(\lambda r\sqrt{-i}\right)\right]}{2} = -\frac{2}{\pi}kei(\lambda r) \tag{3.54}$$

The deflection at the origin (*r=0*) is obtained by substituting the power series for *ber* and *bei* functions provided in (A-21) and (A-22),

$$w_{\max} = \frac{P}{8D\lambda^2} \tag{3.55}$$

Where, D and λ are as defined in Eq. (3.17) and Eq. (3.46) respectively.

The corresponding slope, radial and tangential moments, and shear forces applying Eq. (3.34a-c);

$$\theta_r = \frac{dw_o}{dr} = z_3'(\lambda r)$$
$$M_r = -\frac{P}{2\pi\lambda^2}\left[z_3''(\lambda r) + \frac{\nu_p}{r} z_3'(\lambda r)\right]$$
$$M_\theta = -\frac{P}{2\pi\lambda^2}\left[\frac{1}{r} z_3'(\lambda r) + \nu_p z_3''(\lambda r)\right] \qquad (3.56)$$
$$Q_r = -\frac{P}{2\pi\lambda^2}\left[z_3'''(\lambda r) + \frac{1}{r} z_3''(\lambda r) - \frac{1}{r^2} z_3'(\lambda r)\right]$$

II. Circular Plate under Uniformly Distributed Load with Free End Condition

Adopting the method of Hetenyi (1979), the effect of this loading at arbitrary point is dealt with as follows considering three cases.

a) When point c is under the loading

The solution for this case can be obtained by integrating the solution obtained above for a central concentrated load (see Figure 3.14).

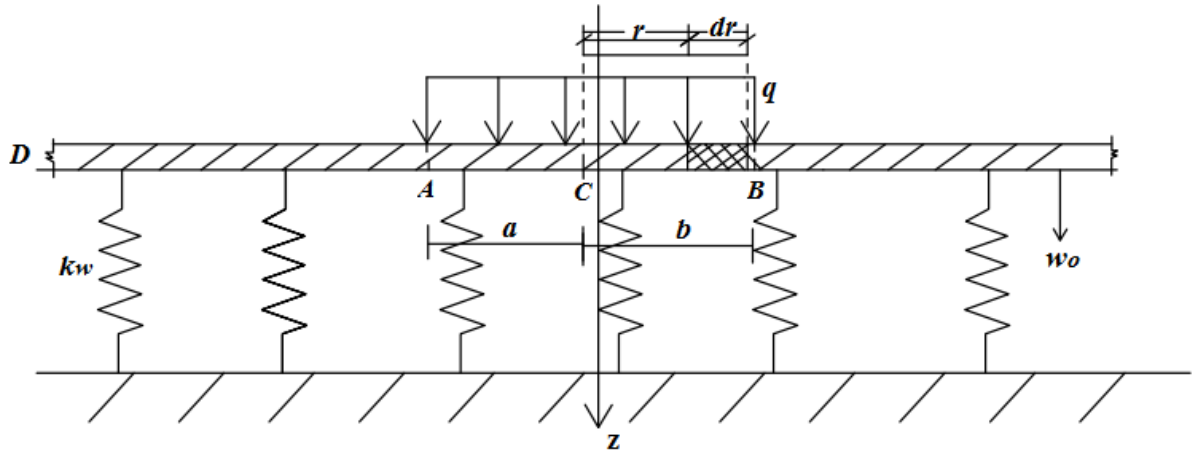

Figure 3.14 An axisymmetric circular plate under uniformly distributed load when point c is under the loading

$$w_c = \frac{q}{2\pi D\lambda^2}\left[\int_0^a z_3(\lambda r)\,dr + \int_0^b z_3(\lambda r)\,dr\right]$$
$$w_c \cong \frac{q}{4\pi D\lambda^3}\left[J_1(\lambda a) + J_1(\lambda b)\right] \tag{3.57}$$

Where J_1 is Bessel function of first kind (with an order of one) expressed as:

$$J_1(\lambda r) = \sum_{n=0}^{\infty} \frac{(-1)^n \left(\frac{\lambda r}{2}\right)^{2n+1}}{n!\Gamma(n+2)} \tag{3.58}$$

Referring to appendix A; (A-33, A-34 and A-35), the slope and internal actions are obtained as

$$\theta_c = \frac{dw_c}{dr} = \frac{q}{4\pi D\lambda^3}\left[\left(\lambda J_o(\lambda a) - \frac{1}{r}J_1(\lambda a)\right) + \left(\lambda J_o(\lambda b) - \frac{1}{r}J_1(\lambda b)\right)\right]$$

$$M_{r_c} = \frac{q}{4\pi\lambda^3}\left[\begin{array}{l} \frac{-\lambda}{r}(1-\nu_p)J_o(\lambda a) + \frac{-\lambda^2 r^2 + r + 1 - \nu_p}{r^2}J_1(\lambda a) \\ -\frac{\lambda}{r}(1-\nu_p)J_o(\lambda b) + \frac{-\lambda^2 r^2 + r + 1 - \nu_p}{r^2}J_1(\lambda b) \end{array}\right]$$

$$M_{\theta_c} = \frac{q}{4\pi\lambda^3}\left[\begin{array}{l} \frac{-\lambda}{r}(\nu_p - 1)J_o(\lambda a) + \frac{(-\lambda^2 r^2 + r + 1)\nu_p - 1}{r^2}J_1(\lambda a) \\ -\frac{\lambda}{r}(\nu_p - 1)J_o(\lambda b) + \frac{(-\lambda^2 r^2 + r + 1)\nu_p - 1}{r^2}J_1(\lambda b) \end{array}\right] \tag{3.59}$$

$$Q_{r_c} = \frac{q}{4\pi\lambda^3}\left[\begin{array}{l} \frac{-\lambda(\lambda^2 r - 1)}{r}J_o(\lambda a) + \frac{(\lambda^2 - 1)}{r^2}J_1(\lambda a) - \frac{\lambda(\lambda^2 r - 1)}{r}J_o(\lambda b) \\ + \frac{(\lambda^2 - 1)}{r^2}J_1(\lambda b) \end{array}\right]$$

Where J_o is Bessel function of first kind (with an order of zero) expressed as

$$J_o(r) = \sum_{n=0}^{\infty} \frac{(-1)^n \left(\frac{r}{2}\right)^{2n}}{n!^2} \tag{3.60}$$

b) When point c is to the left of the loading

The solution for this case proceeds in a similar manner (see Figure 3.15) and is obtained as

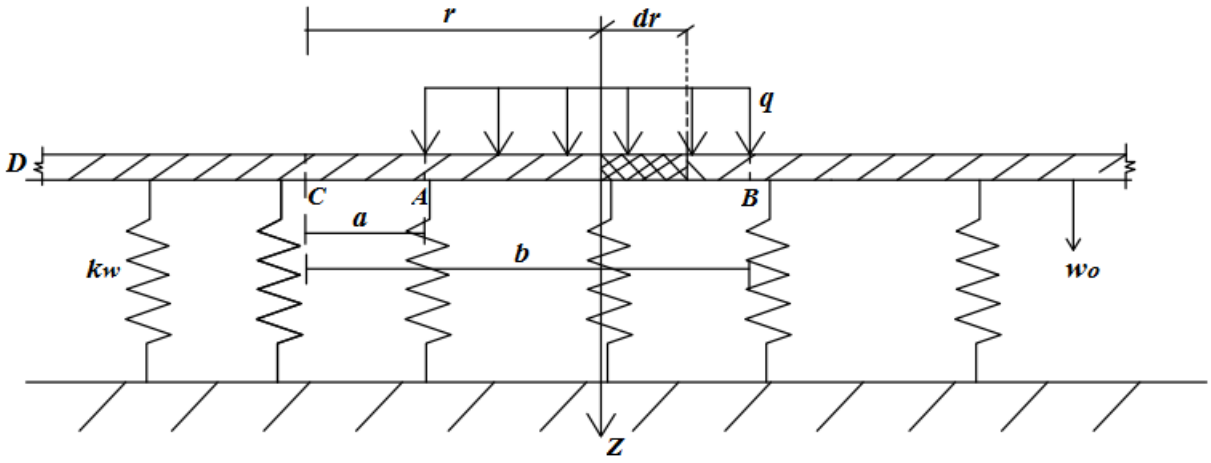

Figure 3.15 An axisymmetric circular plate under uniformly distributed load when point c is to the left of the loading.

$$w_c = \frac{q}{2\pi D\lambda^2}\left[\int_0^b z_3(\lambda r)\,dr - \int_0^a z_3(\lambda r)\,dr\right]$$
$$w_c \cong \frac{q}{4\pi D\lambda^3}\left[J_1(\lambda b) - J_1(\lambda a)\right] \qquad (3.61)$$

The slope and internal actions,

$$\theta_c = \frac{q}{4\pi D\lambda^3}\left[\left(\lambda J_o(\lambda b) - \frac{1}{r}J_1(\lambda b)\right) - \left(\lambda J_o(\lambda a) - \frac{1}{r}J_1(\lambda a)\right)\right]$$

$$M_{r_c} = \frac{-q}{4\pi\lambda^3}\left[\begin{array}{l}\dfrac{-\lambda}{r}(1-\nu_p)J_o(\lambda b) + \dfrac{-\lambda^2 r^2 + r + 1 - \nu_p}{r^2}J_1(\lambda b) \\ +\dfrac{\lambda}{r}(1-\nu_p)J_o(\lambda a) + \dfrac{\lambda^2 r^2 - r - 1 + \nu_p}{r^2}J_1(\lambda a)\end{array}\right]$$

$$M_{\theta_c} = \frac{-q}{4\pi\lambda^3}\left[\begin{array}{l}\dfrac{-\lambda}{r}(\nu_p - 1)J_o(\lambda b) + \dfrac{(-\lambda^2 r^2 + r + 1)\nu_p - 1}{r^2}J_1(\lambda b) \\ -\dfrac{\lambda}{r}(\nu_p - 1)J_o(\lambda a) + \dfrac{(\lambda^2 r^2 - r - 1)\nu_p - 1}{r^2}J_1(\lambda a)\end{array}\right] \qquad (3.62)$$

$$Q_{r_c} = \frac{q}{4\pi\lambda^3}\left[\begin{array}{l}\dfrac{-\lambda(\lambda^2 r^2 - 1)}{r^2}J_o(\lambda b) + \dfrac{2r^2\lambda^2 - \lambda r^2 - 1}{r^3}J_1(\lambda b) \\ +\dfrac{\lambda(\lambda^2 r^2 + 1)}{r^2}J_o(\lambda a) + \dfrac{r^2\lambda^2 - 3}{r^3}J_1(\lambda a)\end{array}\right]$$

c) When point c is to the right of the loading

The solution is obtained similarly as (Figure 3.16)

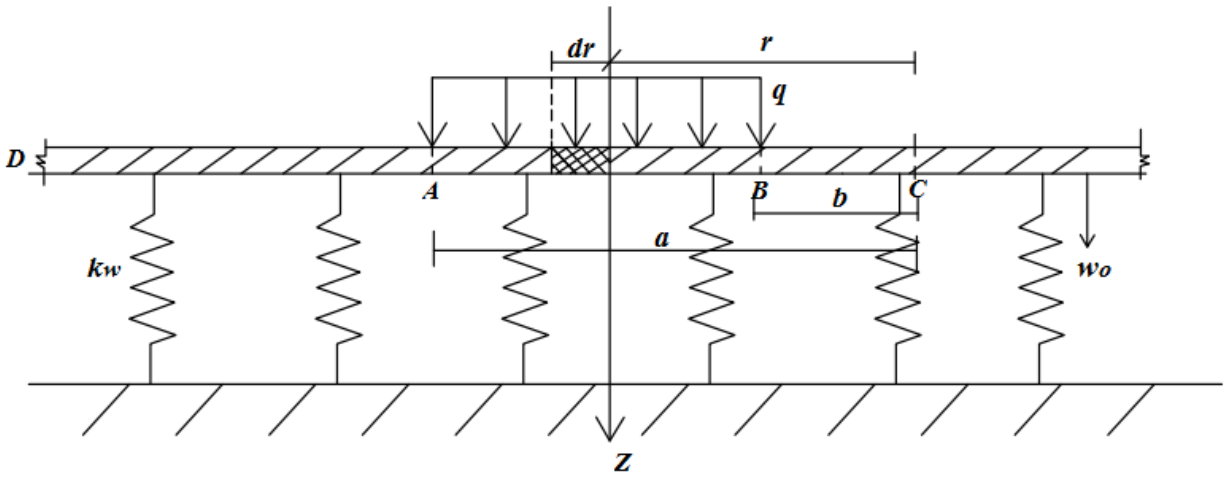

Figure 3.16 An axisymmetric circular plate under uniformly distributed load when point c is to the right of the loading

$$w_c = \frac{q}{2\pi D\lambda^2}\left[\int_0^a z_3(\lambda r)\,dr - \int_0^b z_3(\lambda r)\,dr\right]$$
$$w_c \cong \frac{-q}{4\pi D\lambda^3}\left[J_1(\lambda a) - J_1(\lambda b)\right] \tag{3.63}$$

The corresponding slope and internal actions;

$$\theta_c = \frac{q}{4\pi D\lambda^3}\left[\left(\lambda J_o(\lambda a) - \frac{1}{r}J_1(\lambda a)\right) - \left(\lambda J_o(\lambda b) - \frac{1}{r}J_1(\lambda b)\right)\right]$$
$$M_{r_c} = \frac{q}{4\pi\lambda^3}\left[\begin{array}{l}\dfrac{-\lambda}{r}(1-\nu_p)J_o(\lambda a) + \dfrac{-\lambda^2 r^2 + r + 1 - \nu_p}{r^2}J_1(\lambda a) \\ +\dfrac{\lambda}{r}(1-\nu_p)J_o(\lambda b) + \dfrac{\lambda^2 r^2 - r - 1 + \nu_p}{r^2}J_1(\lambda b)\end{array}\right]$$
$$M_{\theta_c} = \frac{q}{4\pi\lambda^3}\left[\begin{array}{l}\dfrac{-\lambda}{r}(\nu_p - 1)J_o(\lambda a) + \dfrac{(-\lambda^2 r^2 + r + 1)\nu_p - 1}{r^2}J_1(\lambda a) \\ -\dfrac{\lambda}{r}(\nu_p - 1)J_o(\lambda b) + \dfrac{(\lambda^2 r^2 - r - 1)\nu_p - 1}{r^2}J_1(\lambda b)\end{array}\right] \tag{3.64}$$
$$Q_{r_c} = \frac{q}{4\pi\lambda^3}\left[\begin{array}{l}\dfrac{-\lambda(\lambda^2 r^2 - 1)}{r^2}J_o(\lambda a) + \dfrac{2r^2\lambda^2 - \lambda r^2 - 1}{r^3}J_1(\lambda a) \\ +\dfrac{\lambda(\lambda^2 r^2 + 1)}{r^2}J_o(\lambda b) + \dfrac{r^2\lambda^2 - 3}{r^3}J_1(\lambda b)\end{array}\right]$$

3.3.4.1.2 Small Plates

In this section the general method of solution by superposition proposed by Hetenyi (1979) has been applied to solve the problem of a small circular plate when subjected to the following different loading conditions.

I. Circular Plate under a Central Concentrated Load with Free End Condition

A circular plate subjected to a concentrated central load (see Figure 3.17).

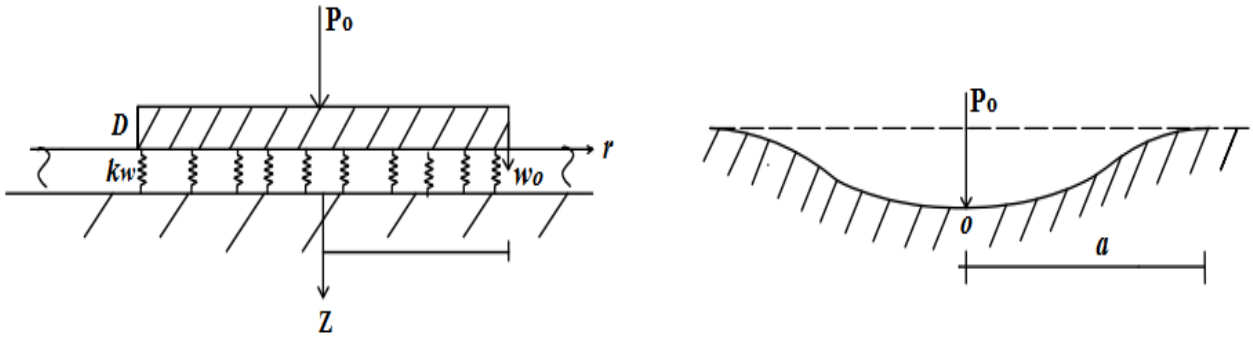

(a) (b)

Figure 3.17 (a) and (b) axisymmetric loading of a small circular plate subjected to a concentrated load at center and the actual deflection curve of the circular plate resp. (Selvadurai, 1979).

Where P_o = concentrated vertical load.

According to Hetenyi (1979) and Selvadurai (1979), the following boundary conditions are stated:

i. For $r = 0$, w_o must be finite

ii. For $r = a$, $M_r = 0$

iii. For $r = a$, $Q_r = 0$

iv. For $r = 0$, $\lim_{r \to 0} 2\pi r Q_r + P_o = 0$

✓ Boundary condition (i) requires A_4 to be zero because $Ker(0)$ is undefined for small values of λr.

Hence, the general solution of deflection reduces to

$$w_o = A_1 z_1(\lambda r) + A_2 z_2(\lambda r) + A_3 z_3(\lambda r) \qquad (3.65)$$

✓ Applying boundary condition (ii), (iii) and (iv) into the expression Eq. (3.34a and c), and solving for A_1, A_2 and A_3, we get

$$A_3 = \frac{P_o \lambda^2}{4k}$$

$$A_1 = A_3 \left\{ \frac{\left[z_1'(\lambda a) z_4(\lambda a) - z_4'(\lambda a) z_1(\lambda a) - \left(\frac{1-\nu_p}{\lambda a} \right) \left[z_4'(\lambda a) z_2'(\lambda a) + z_1'(\lambda a) z_3'(\lambda a) \right] \right]}{z_1(\lambda a) z_2'(\lambda a) - z_1'(\lambda a) z_2(\lambda a) + \left(\frac{1-\nu_p}{\lambda a} \right) \left[(z_1'(\lambda a))^2 + (z_2'(\lambda a))^2 \right]} \right\}$$

$$A_2 = A_3 \left\{ \frac{\left[z_{22}'(\lambda a) z_4(\lambda a) - z_4'(\lambda a) z_2(\lambda a) + \left(\frac{1-\nu_p}{\lambda a} \right) \left[z_4'(\lambda a) z_1'(\lambda a) - z_2'(\lambda a) z_3'(\lambda a) \right] \right]}{z_1(\lambda a) z_2'(\lambda a) - z_1'(\lambda a) z_2(\lambda a) + \left(\frac{1-\nu_p}{\lambda a} \right) \left[(z_1'(\lambda a))^2 + (z_2'(\lambda a))^2 \right]} \right\}$$

(3.66)

Where $z_1'(\lambda a)$, $z_2'(\lambda a)$, $z_3'(\lambda a)$ *and* $z_4'(\lambda a)$ are first derivatives of the functions defined in Appendix B, (B-23a-d).

The deflection for different *r* will be evaluated using an Excel sheet, the slope and corresponding internal actions;

$$\begin{aligned}
\theta_r &= \lambda \left[A_1 z_1'(\lambda r) + A_2 z_2'(\lambda r) + A_3 z_3'(\lambda r) \right] \\
M_r &= -D\lambda^2 \left[\begin{array}{l} A_1 z_2(\lambda r) - A_2 z_1(\lambda r) + A_3 z_4(\lambda r) \\ -\frac{1}{r}(1-\nu_p) \left\{ A_1 z_1'(\lambda r) + A_2 z_2'(\lambda r) + A_3 z_3'(\lambda r) \right\} \end{array} \right] \\
M_\theta &= -D\lambda^2 \left[\begin{array}{l} \nu_p \left\{ A_1 z_2(\lambda r) - A_2 z_1(\lambda r) + A_3 z_4(\lambda r) \right\} \\ +\frac{1}{r}(1-\nu_p) \left\{ A_1 z_1'(\lambda r) + A_2 z_2'(\lambda r) + A_3 z_3'(\lambda r) \right\} \end{array} \right] \\
Q_r &= -D\lambda^3 \left[A_1 z_2'(\lambda r) - A_2 z_1'(\lambda r) + A_3 z_4'(\lambda r) \right]
\end{aligned} \tag{3.67}$$

II. Circular Plate under a Concentrated Edge Load with Free End Condition

A circumferential load of q_o that is uniformly distributed per unit run along the edge is considered (see Figure 3.18)

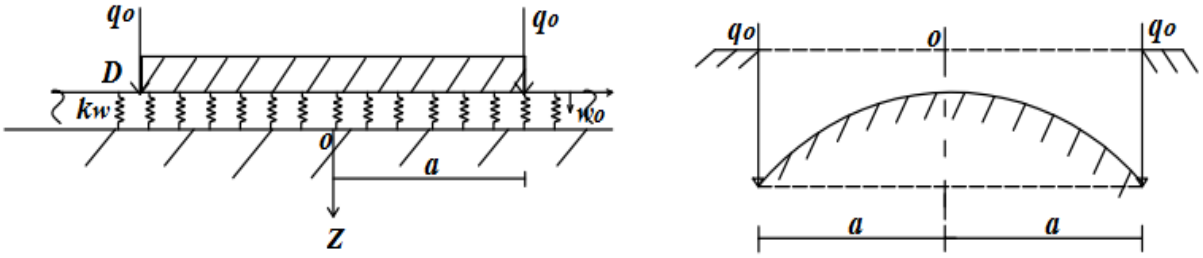

(a) (b)

Figure 3.18 (a) and (b) axisymmetric loading of a small circular plate subjected to a concentrated edge load and the actual deflection curve of the circular plate resp. (Selavdurai, 1979).

According to Hetenyi (1979), Reddy (2007), Timoshenko (1951) and Selvadurai (1979), the following boundary conditions can be stated.

i. For $r = 0,\ \dfrac{dw_o}{dr} = 0$

ii. For $r = 0,\ Q_r = 0$

iii. For $r = a,\ M_r = 0$

iv. For $r = a,\ Q_r = -q_o$

✓ Boundary condition (i) is similar with boundary condition (iii) for a concentrated loading and the same procedure is followed that necessitate, A_4 or c = 0 to be satisfied.

$$\lim_{r\to 0} c\ker(\lambda r) = -\left[0 - \frac{4\left(\frac{\lambda r}{2}\right)^3}{2!2!\frac{2}{\lambda}} \ldots\right]\left[\log\left(\frac{\lambda r}{2}\right) + \gamma\right] + \left[\frac{\left(\frac{\lambda r}{2}\right)^4}{2!2!}\right]\left[\frac{1}{2\frac{r}{\lambda}}\right]$$

$$+\frac{\pi}{4}\left[\frac{2\left(\frac{\lambda r}{2}\right)^3}{1!1!\frac{2}{\lambda}} \ldots\right] + \frac{4\left(\frac{\lambda r}{2}\right)^3}{2!2!\frac{2}{\lambda}} \ldots = 0$$

Thus, boundary condition (i) is satisfied.

✓ Boundary condition (ii) requires d or A_3 = 0 because $kei(0)$ is undefined for Eq. (A-26) from Appendix A.

Hence, the general solution of the deflection reduces to

$$w_o = A_1 z_1(\lambda r) + A_2 z_2(\lambda r) \tag{3.68}$$

✓ Applying boundary condition (iii) and (iv) into the expression Eq. (3.34 a and c), we have;

$$0 = -\frac{E_p h^3}{12\left(1-\nu_p{}^2\right)}\left(\lambda^2 A_1 z_1{}''(\lambda a) + \lambda^2 A_2 z_1{}''(\lambda a) + \frac{\nu_p}{a}\left(\lambda A_1 z_1{}'(\lambda a) + \lambda A_2 z_2{}'(\lambda a)\right)\right) \tag{3.69a}$$

Similarly,

$$-q_o = -\frac{E_p h^3}{12\left(1-\nu_p{}^2\right)}\left(\lambda^3 A_1 z_1{}'''(\lambda a) + \lambda^3 A_2 z_2{}'''(\lambda a) + \frac{1}{a}\left(\lambda^2 A_1 z_1{}''(\lambda a) + \lambda^2 A_2 z_2{}''(\lambda a)\right)\right) - \frac{1}{a^2}\left(\lambda A_1 z_1{}'(\lambda a) + \lambda A_2 z_2{}'(\lambda a)\right) \tag{3.69b}$$

From (3.69a) and (3.69b) for integration constants, we get

$$A_1 = \frac{-q_o \lambda}{k}\frac{z_1(\lambda a) + \frac{1-\nu_p}{\lambda a} z_2{}'(\lambda a)}{z_1(\lambda a) z_2{}'(\lambda a) - z_1{}'(\lambda a) z_2(\lambda a) + \frac{1-\nu_p}{\lambda a}\left[\left(z_1{}'\right)^2(\lambda a) + \left(z_2{}'\right)^2(\lambda a)\right]}$$

$$A_2 = \frac{-q_o \lambda}{k}\frac{z_2(\lambda a) + \frac{1-\nu_p}{\lambda a} z_1{}'(\lambda a)}{z_1(\lambda a) z_2{}'(\lambda a) - z_1{}'(\lambda a) z_2(\lambda a) + \frac{1-\nu_p}{\lambda a}\left[\left(z_1{}'\right)^2(\lambda a) + \left(z_2{}'\right)^2(\lambda a)\right]} \tag{3.70}$$

The deflection for different *r* will be evaluated using a spread sheet program, the slope and corresponding internal actions;

$$\begin{aligned}
\theta_r &= \lambda\left[A_1 z_1{}'(\lambda r) + A_2 z_2{}'(\lambda r)\right] \\
M_r &= -D\lambda^2\left[A_1 z_2(\lambda r) - A_2 z_1(\lambda r) - \frac{1}{r}(1-\nu_p)\left\{A_1 z_1{}'(\lambda r) + A_2 z_2{}'(\lambda r)\right\}\right] \\
M_\theta &= -D\lambda^2\left[\nu_p\left\{A_1 z_2(\lambda r) - A_2 z_1(\lambda r)\right\} + \frac{1}{r}(1-\nu_p)\left\{A_1 z_1{}'(\lambda r) + A_2 z_2{}'(\lambda r)\right\}\right] \\
Q_r &= -D\lambda^3\left[A_1 z_2{}'(\lambda r) - A_2 z_1{}'(\lambda r)\right]
\end{aligned} \tag{3.71}$$

III. Circular Plate under a Concentrated Edge Moment with Free End Condition

A circumferential moment of M_o that is uniformly distributed per unit length along the edge is considered (see Figure 3.19).

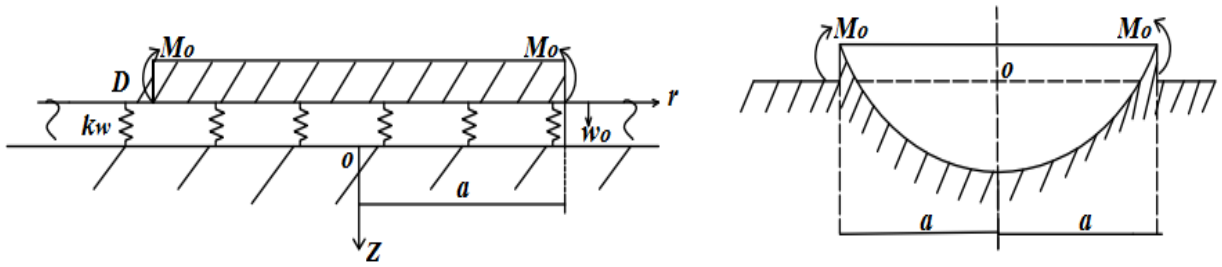

(a) (b)

Figure 3.19 (a) and (b) axisymmetric loading of a small circular plate subjected to a concentrated edge moment and the actual deflection curve of the circular plate resp. (Selavdurai, 1979).

The boundary conditions stated by Hetenyi (1979) and Selvadurai (1979) are:

i. For $r = 0,\ \dfrac{dw_o}{dr} = 0$

ii. For $r = 0,\ Q_r = 0$

iii. For $r = a,\ \mathrm{M}_r = M_o$

iv. For $r = a,\ \mathrm{Q}_r = 0$

✓ Since boundary condition (i) and (ii) are the same with the previous case. The general solution will have the same form:

$$w_o = A_1 z_1(\lambda r) + A_2 z_2(\lambda r) \tag{3.72}$$

✓ Applying boundary condition (iii) and (iv) into the expression Eq.(3.22 a and c) and solving for A_1 and A_2, we get

$$A_1 = \frac{M_o \lambda^2}{k} \frac{z_1'(\lambda a)}{z_1(\lambda a) z_2'(\lambda a) - z_1'(\lambda a) z_2(\lambda a) + \dfrac{1-\nu_p}{\lambda a}\left[(z_1')^2(\lambda a) + (z_2')^2(\lambda a)\right]}$$

$$A_2 = \frac{M_o \lambda^2}{k} \frac{z_2'(\lambda a)}{z_1(\lambda a) z_2'(\lambda a) - z_1'(\lambda a) z_2(\lambda a) + \dfrac{1-\nu_p}{\lambda a}\left[(z_1')^2(\lambda a) + (z_2')^2(\lambda a)\right]} \tag{3.73}$$

Likewise, the deflection for different r will be evaluated using an Excel sheet and the corresponding internal actions i.e. radial and tangential moments, and shear forces have the same form with that of the previous loading condition.

3.3.4.2 Plates on Pasternak's Subgrade Model

As in Winkler's model, the circular plate is assumed to be subjected to a loading distributed symmetrically with respect to the center.

The formulated governing differential equation (3.37) can be rewritten as

$$\left[\frac{d^4w_o}{dr^4}+\frac{2}{r}\frac{d^3w_o}{dr^3}-\frac{1}{r^2}\frac{d^2w_o}{dr^2}+\frac{1}{r^3}\frac{dw_o}{dr}\right]-\frac{G_p}{D}\left[\frac{d^2w_o}{dr^2}+\frac{1}{r}\frac{dw_o}{dr}\right]+\frac{k_p}{D}w_o(r)=q(r) \tag{3.74}$$

With the use of a differential operator, $\Delta_r=\frac{d^2}{dr^2}+\frac{1}{r}\frac{d}{dr}$, Eq. (3.74) can also be written as

$$\left(\frac{d^2}{dr^2}+\frac{1}{r}\frac{d}{dr}\right)\left(\frac{d^2w_o}{dr^2}+\frac{1}{r}\frac{dw_o}{dr}\right)-\frac{G_p}{D}\left[\frac{d^2w_o}{dr^2}+\frac{1}{r}\frac{dw_o}{dr}\right]+\frac{k_p}{D}w_o=\frac{q}{D} \tag{3.75}$$

Recall, we deduced the following expressions in Eq. (3.34)

- The radial moment per unit length in the plate

$$M_r=-D\left(\frac{d^2w_o}{dr^2}+\frac{v_p}{r}\frac{dw_o}{dr}\right)$$

- The tangential moment in the circumferential direction in the plate

$$M_\theta=-D\left(v_p\frac{d^2w_o}{dr^2}+\frac{1}{r}\frac{dw_o}{dr}\right)$$

- The radial shear force per unit length in the plate

$$Q_r=-D\frac{d}{dr}\left(\frac{d^2w_o}{dr^2}+\frac{1}{r}\frac{dw_o}{dr}\right)$$

The homogeneous form of Eq. (3.75) with the use of a differential operator, Δ_r, can be expressed as

$$\Delta_r{}^4w_o(r)-\frac{G_p}{D}\Delta_r{}^2w_o(r)+\frac{k_p}{D}w_o(r)=0 \tag{3.76}$$

The roots of equation (3.76) will give the argument of the modified Bessel functions.

$$d^4 - \frac{G_p}{D} d^2 + \frac{k_p}{D} = 0 \tag{3.77}$$

Substituting $d^2 = n$, a quadratic equation with the following format is obtained.

$$n^2 - \frac{G_p}{D} n + \frac{k_p}{D} = 0$$

Thus, the roots are given by

$$d_{1,2,3,4} = \pm \sqrt{\frac{1}{2}\left[\frac{G_p}{D} \pm \sqrt{\left(\frac{G_p}{D} \right)^2 - \frac{4k_p}{D}} \right]} \tag{3.78}$$

There are three possible cases of the general solution of equation (3.77) depending on whether $G_p^{\,2} > 4k_pD \text{ or } T > 1$, $G_p^{\,2} = 4k_pD \text{ or } T = 1$ or $G_p^{\,2} < 4k_pD \text{ or } T < 1$. The details to this problem is dealt within Appendix C.

Where *T* is a parameter which depends both on the parameters of the subgrade and the flexural rigidity of the plate. And it is expressed as

$$T = \sqrt{G_p^{\,2} \big/ 4k_pD} \tag{3.79}$$

Letting $\frac{k_p}{D} = \frac{1}{l^4}$ where $\frac{1}{l} = \lambda$, Eq. (3.75) becomes

$$\left(\frac{d^2}{dr^2} + \frac{1}{r}\frac{d}{dr} \right)\left(\frac{d^2 w_o}{dr^2} + \frac{1}{r}\frac{dw_o}{dr} \right) - \frac{G_p}{D}\left[\frac{d^2 w_o}{dr^2} + \frac{1}{r}\frac{dw_o}{dr} \right] + \frac{w_o}{l^4} = \frac{q}{D} \tag{3.80}$$

Case I

i. $G_p^{\,2} < 4k_pD \text{ or } T < 1$

The term $\sqrt{\left(\frac{G_p}{D} \right)^2 - \frac{4k_p}{D}}$ is a complex number, so Eq. (3.78) can be re-written as

$$d_{1,2,3,4} = \pm\sqrt{\frac{1}{2}\left(\frac{G_p}{D} \pm i\left(\frac{4k_p}{D} - \left(\frac{G_p}{D}\right)^2\right)\right)}$$

Hence, the complementary solution is given as

$$w_o(r) = \mathrm{B}_1 u_o(r/l) + \mathrm{B}_2 v_o(r/l) + B_3 f_o(r/l) + B_4 g_o(r/l) \tag{3.81}$$

Where

$$\begin{aligned}
u_o(r/l) &= \mathrm{Re}\, J_o\left(\sqrt{d}r/l\right) = \frac{1}{2}\left[J_o\left(\sqrt{d}r/l\right) + J_o\left(\sqrt{\overline{d}}r/l\right)\right] \\
v_o(r/l) &= \mathrm{Im}\, J_o\left(\sqrt{\overline{d}}r/l\right) = \frac{1}{2i}\left[J_o\left(\sqrt{d}r/l\right) - J_o\left(\sqrt{\overline{d}}r/l\right)\right] \\
f_o(r/l) &= \mathrm{Re}\, H_o^{(1)}\left(\sqrt{d}r/l\right) = \frac{1}{2}\left[H_o^{(1)}\left(\sqrt{d}r/l\right) + H_o^{(2)}\left(\sqrt{\overline{d}}r/l\right)\right] \\
g_o(r/l) &= \mathrm{Im}\, H_o^{(2)}\left(\sqrt{\overline{d}}r/l\right) = \frac{1}{2i}\left[H_o^{(1)}\left(\sqrt{d}r/l\right) - H_o^{(2)}\left(\sqrt{\overline{d}}r/l\right)\right]
\end{aligned} \tag{3.82a-d}$$

Where d and $\overline{d}$ are introduced constants for the root**.** $H_o^{(1)}$ and $H_o^{(2)}$ are conjugate complex functions of Hankel's functions.

From Eq. (3.81) the slope, bending moments and shearing forces can be obtained applying the expressions of Eq. (3.34a-c).

The following can be deduced from recurrence relation by Hildebrand (1962) as presented in Appendix A, Eq. (A-33);

$$\theta_r = -\frac{1}{l}\left[B_1 u_o'(r/l) + B_2 v_o'(r/l) + B_3 f_o'(r/l) + B_4 g_o'(r/l)\right]$$

$$M_r = -\frac{D}{l^2}\left\{\begin{array}{l}\left[B_1 v_o(r/l) - B_2 u_o(r/l) + B_3 g_o(r/l) - B_4 f_o(r/l)\right] \\ -\frac{l}{r}(1-v_p)\left[B_1 u_o'(r/l) + B_2 v_o'(r/l) + B_3 g_o'(r/l) + B_4 f_o'(r/l)\right]\end{array}\right\}$$

$$M_\theta = -\frac{D}{l^2}\left\{\begin{array}{l}v_p\left[B_1 v_o(r/l) - B_2 u_o(r/l) + B_3 g_o(r/l) - B_4 f_o(r/l)\right] \\ +\frac{l}{r}(1-v_p)\left[B_1 u_o'(r/l) + B_2 v_o'(r/l) + B_3 g_o'(r/l) + B_4 f_o'(r/l)\right]\end{array}\right\}$$

$$Q_r = -\frac{D}{l^3}\left\{B_1 v_o'(r/l) - B_2 u_o'(r/l) + B_3 g_o'(r/l) - B_4 f_o'(r/l)\right\}$$

Collecting similar terms for each function derivatives;

$$\theta_r = -\frac{1}{l}\begin{bmatrix} B_1\left[u_1(r/l)\cos\delta - v_1(r/l)\sin\delta\right] + B_2\left[u_1(r/l)\sin\delta + v_1(r/l)\cos\delta\right] + \\ B_3\left[f_1(r/l)\cos\delta - g_1(r/l)\sin\delta\right] + B_4\left[f_1(r/l)\sin\delta + g_1(r/l)\cos\delta\right] \end{bmatrix}$$

$$M_r = -\frac{D}{l^2}\begin{Bmatrix} B_1\left[\left(u_o(r/l)\cos 2\delta - v_o(r/l)\sin 2\delta\right) - \frac{l}{r}(1-\nu_p)\left(u_1(r/l)\cos\delta - v_1(r/l)\sin\delta\right)\right] \\ +B_2\left[\left(u_o(r/l)\sin 2\delta + v_o(r/l)\cos 2\delta\right) - \frac{l}{r}(1-\nu_p)\left(u_1(r/l)\sin\delta + v_1(r/l)\cos\delta\right)\right] \\ +B_3\left[\left(f_o(r/l)\cos 2\delta - v_o(r/l)\sin 2\delta\right) - \frac{l}{r}(1-\nu_p)\left(f_1(r/l)\cos\delta - g_1(r/l)\sin\delta\right)\right] \\ +B_4\left[\left(f_o(r/l)\sin 2\delta + g_o(r/l)\cos 2\delta\right) - \frac{l}{r}(1-\nu_p)\left(f_1(r/l)\sin\delta + g_1(r/l)\cos\delta\right)\right] \end{Bmatrix}$$

$$M_\theta = -\frac{D}{l^2}\begin{Bmatrix} B_1\left[\nu_p\left(u_o(r/l)\cos 2\delta - v_o(r/l)\sin 2\delta\right) + \frac{l}{r}(1-\nu_p)\left(u_1(r/l)\cos\delta - v_1(r/l)\sin\delta\right)\right] \\ +B_2\left[\nu_p\left(u_o(r/l)\sin 2\delta + v_o(r/l)\cos 2\delta\right) + \frac{l}{r}(1-\nu_p)\left(u_1(r/l)\sin\delta + v_1(r/l)\cos\delta\right)\right] \\ +B_3\left[\nu_p\left(f_o(r/l)\cos 2\delta - v_o(r/l)\sin 2\delta\right) + \frac{l}{r}(1-\nu_p)\left(f_1(r/l)\cos\delta - g_1(r/l)\sin\delta\right)\right] \\ +B_4\left[\nu_p\left(f_o(r/l)\sin 2\delta + g_o(r/l)\cos 2\delta\right) + \frac{l}{r}(1-\nu_p)\left(f_1(r/l)\sin\delta + g_1(r/l)\cos\delta\right)\right] \end{Bmatrix}$$

$$Q_r = -\frac{D}{l^3}\begin{Bmatrix} B_1\left[u_1(r/l)\cos 3\delta - v_1(r/l)\sin 3\delta\right] + B_2\left[u_1(r/l)\sin 3\delta + v_1(r/l)\cos 3\delta\right] \\ +B_3\left[f_1(r/l)\cos 3\delta - g_1(r/l)\sin 3\delta\right] + B_4\left[f_1(r/l)\sin 3\delta + g_1(r/l)\cos 3\delta\right] \end{Bmatrix}$$

(3.83a-d)

Where

$$\delta = \frac{1}{2}\cos^{-1}\left(-\frac{G_p}{\sqrt{4k_p D}}\right)$$

<u>Case II</u>

ii. $G_p{}^2 = 4k_p D$ or $T = 1$

Substituting $G_p{}^2 = 4k_pD$ in the homogeneous form of Eq. (3.80), the root becomes

$$d_{1,2,3,4} = 1$$

Then the complementary solution is given by

$$w_o(r) = \mathrm{A}_1 J_o(r/l) + A_2 H_o^{(1)}(r/l) + A_3 J_o(r/l) + A_4 H_o^{(2)}(r/l) \tag{3.84}$$

From Eq. (3.84) the slope, bending moments and shearing forces can be obtained applying the expressions of Eq. (3.34 a-c).

The following can be deduced from recurrence relation by Hildebrand (1962) as presented in Appendix A, Eq. (A-33);

$$\theta_r = A_1 J_o'(r/l) + A_2 H_o^{(1)'}(r/l) + A_3 J_o'(r/l) + A_4 H_o^{(2)'}(r/l)$$

$$M_r = -\frac{D}{l^2}\left\{\begin{array}{l}\left[A_1 J_o(r/l) - A_2 H_o^{(1)}(r/l) + A_3 J_o(r/l) - A_4 H_o^{(2)}(r/l)\right] \\ -\frac{l}{r}(1-\nu_p)\left[A_1 J_o'(r/l) + A_2 H_o^{(1)}(r/l) + A_3 J_o'(r/l) + A_4 H_o^{(2)'}(r/l)\right]\end{array}\right\}$$

$$M_\theta = -\frac{D}{l^2}\left\{\begin{array}{l}\nu_p\left[A_1 J_o(r/l) - A_2 H_o^{(1)}(r/l) + A_3 J_o(r/l) - A_4 H_o^{(2)}(r/l)\right] \\ +\frac{l}{r}(1-\nu_p)\left[A_1 J_o'(r/l) + A_2 H_o^{(1)}(r/l) + A_3 J_o'(r/l) + A_4 H_o^{(2)'}(r/l)\right]\end{array}\right\}$$

$$Q_r = -\frac{D}{l^3}\left\{A_1 J_o'(r/l) - A_2 H_o^{(1)'}(r/l) + A_3 J_o'(r/l) - A_4 H_o^{(2)'}(r/l)\right\}$$

Collecting similar terms for each function derivatives;

$$\theta_r = -\frac{1}{l}\left[A_1 J_1(r/l) + A_2 H_1^{(1)}(r/l) + A_3 J_1(r/l) + A_4 H_1^{(2)}(r/l)\right]$$

$$M_r = -\frac{D}{l^2}\left\{\begin{array}{l}A_1\left[J_o(r/l) - \frac{l}{r}(1-\nu_p)\left(J_1(r/l)\right)\right] + A_2\left[H_o^{(1)}(r/l) - \frac{l}{r}(1-\nu_p)\left(H_1^{(1)}(r/l)\right)\right] \\ +A_3\left[J_o(r/l) - \frac{l}{r}(1-\nu_p)\left(J_1(r/l)\right)\right] + A_4\left[H_o^{(2)}(r/l) - \frac{l}{r}(1-\nu_p)\left(H_1^{(2)}(r/l)\right)\right]\end{array}\right\}$$

$$M_\theta = -\frac{D}{l^2}\left\{\begin{aligned}&A_1\left[v_p J_o(r/l)+\frac{l}{r}(1-v_p)\left(J_1(r/l)\right)\right]+A_2\left[v_p H_o^{(1)}(r/l)+\frac{l}{r}(1-v_p)\left(H_1^{(1)}(r/l)\right)\right]\\&+A_3\left[v_p J_o(r/l)+\frac{l}{r}(1-v_p)\left(J_1(r/l)\right)\right]+A_4\left[v_p H_o^{(2)}(r/l)+\frac{l}{r}(1-v_p)\left(H_1^{(2)}(r/l)\right)\right]\end{aligned}\right\}$$

$$Q_r = -\frac{D}{l^3}\left\{A_1 J_1(r/l)+A_2 H_o^{(1)}(r/l)+A_3 J_1(r/l)+A_4 H_1^{(2)}(r/l)\right\}$$

(3.85a-d)

Case III

iii. $G_p^{\,2} > 4k_pD$ or $T > 1$

Since $G_p^{\,2} > 4k_pD$, all the roots are real.

The roots,

$$d_{1,2,3,4} = \pm\sqrt{\frac{1}{2}\left[\frac{G_p}{D}\pm\sqrt{\left(\frac{G_p}{D}\right)^2-\frac{4k_p}{D}}\right]}$$

And then introducing constants $\boldsymbol{d}$ and $\bar{\boldsymbol{d}}$, the complementary solution for the homogeneous equation is given by

$$w_o(r) = \mathrm{A}_1 J_o\left(\sqrt{d}r/l\right)+A_2 H_o^{(1)}\left(\sqrt{d}r/l\right)+A_3 J_o\left(\sqrt{\bar{d}}r/l\right)+A_4 H_o^{(2)}\left(\sqrt{\bar{d}}r/l\right) \qquad (3.86)$$

From Eq. (3.86) the slope, bending moments and shearing forces can be obtained applying the expressions of Eq. (3.34 a-c).

The following can be deduced from recurrence relation by Hildebrand (1962) as presented in Appendix A, Eq. (A-33);

$$\theta_r = A_1 J_o^{'}\left(\sqrt{d}r/l\right)+A_2 H_o^{(1)'}\left(\sqrt{d}r/l\right)+A_3 J_o^{'}\left(\sqrt{\bar{d}}r/l\right)+A_4 H_o^{(2)'}\left(\sqrt{\bar{d}}r/l\right)$$

$$M_r = -\frac{D}{l^2}\left\{\begin{aligned}&\left[A_1 J_o\left(\sqrt{d}r/l\right)-A_2 H_o^{(1)}\left(\sqrt{d}r/l\right)+A_3 J_o\left(\sqrt{\bar{d}}r/l\right)-A_4 H_o^{(2)}\left(\sqrt{\bar{d}}r/l\right)\right]\\&-\frac{l}{r}(1-v_p)\left[A_1 J_o^{'}\left(\sqrt{d}r/l\right)+A_2 H_o^{(1)}\left(\sqrt{d}r/l\right)+A_3 J_o^{'}\left(\sqrt{\bar{d}}r/l\right)+A_4 H_o^{(2)'}\left(\sqrt{\bar{d}}r/l\right)\right]\end{aligned}\right\}$$

$$M_\theta = -\frac{D}{l^2}\left\{\begin{array}{l} v_p\left[A_1 J_o\left(\sqrt{d}r/l\right) - A_2 H_o^{(1)}\left(\sqrt{d}r/l\right) + A_3 J_o\left(\sqrt{\bar{d}}r/l\right) - A_4 H_o^{(2)}\left(\sqrt{\bar{d}}r/l\right)\right] \\ +\frac{l}{r}\left(1-v_p\right)\left[A_1 J_o'\left(\sqrt{d}r/l\right) + A_2 H_o^{(1)}\left(\sqrt{d}r/l\right) + A_3 J_o'\left(\sqrt{\bar{d}}r/l\right) + A_4 H_o^{(2)'}\left(\sqrt{\bar{d}}r/l\right)\right] \end{array}\right\}$$

$$Q_r = -\frac{D}{l^3}\left\{A_1 J_o'\left(\sqrt{d}r/l\right) - A_2 H_o^{(1)'}\left(\sqrt{d}r/l\right) + A_3 J_o'\left(\sqrt{\bar{d}}r/l\right) - A_4 H_o^{(2)'}\left(\sqrt{\bar{d}}r/l\right)\right\}$$

Collecting similar terms for each function derivatives;

$$\theta_r = -\frac{1}{l}\left[\begin{array}{l} A_1 J_1\left(\sqrt{d}r/l\right)\cos\delta + A_2 H_1^{(1)}\left(\sqrt{d}r/l\right)\cos\delta \\ +A_3 J_1\left(\sqrt{\bar{d}}r/l\right)\cos\delta + A_4 H_1^{(2)}\left(\sqrt{\bar{d}}r/l\right)\sin\delta \end{array}\right]$$

$$M_r = -\frac{D}{l^2}\left\{\begin{array}{l} A_1\left[J_o\left(\sqrt{d}r/l\right)\cos 2\delta - \frac{l}{r}\left(1-v_p\right)\left(J_1\left(\sqrt{d}r/l\right)\cos\delta\right)\right] \\ +A_2\left[H_o^{(1)}\left(\sqrt{d}r/l\right)\cos 2\delta - \frac{l}{r}\left(1-v_p\right)\left(H_1^{(1)}\left(\sqrt{d}r/l\right)\cos\delta\right)\right] \\ +A_3\left[J_o\left(\sqrt{\bar{d}}r/l\right)\cos 2\delta - \frac{l}{r}\left(1-v_p\right)\left(J_1\left(\sqrt{\bar{d}}r/l\right)\cos\delta\right)\right] \\ +A_4\left[H_o^{(2)}\left(\sqrt{\bar{d}}r/l\right)\sin 2\delta - \frac{l}{r}\left(1-v_p\right)H_1^{(2)}\left(\sqrt{\bar{d}}r/l\right)\sin\delta\right] \end{array}\right\}$$

$$M_\theta = -\frac{D}{l^2}\left\{\begin{array}{l} A_1\left[v_p J_o\left(\sqrt{d}r/l\right)\cos 2\delta + \frac{l}{r}\left(1-v_p\right)\left(J_1\left(\sqrt{d}r/l\right)\cos\delta\right)\right] \\ +A_2\left[v_p H_o^{(1)}\left(\sqrt{d}r/l\right)\cos 2\delta + \frac{l}{r}\left(1-v_p\right)\left(H_1^{(1)}\left(\sqrt{d}r/l\right)\cos\delta\right)\right] \\ +A_3\left[v_p J_o\left(\sqrt{\bar{d}}r/l\right)\cos 2\delta + \frac{l}{r}\left(1-v_p\right)\left(J_1\left(\sqrt{\bar{d}}r/l\right)\cos\delta\right)\right] \\ +A_4\left[v_p H_o^{(2)}\left(\sqrt{\bar{d}}r/l\right)\sin 2\delta + \frac{l}{r}\left(1-v_p\right)\left(H_1^{(2)}\left(\sqrt{\bar{d}}r/l\right)\sin\delta\right)\right] \end{array}\right\} \qquad \text{(3.87a-d)}$$

$$Q_r = -\frac{D}{l^3}\left\{\begin{array}{l} A_1 J_1\left(\sqrt{d}r/l\right)\cos 3\delta + A_2 H_o^{(1)}\left(\sqrt{d}r/l\right)\cos 3\delta \\ +A_3 J_1\left(\sqrt{\bar{d}}r/l\right)\cos 3\delta + A_4 H_1^{(2)}\left(\sqrt{\bar{d}}r/l\right)\sin 3\delta \end{array}\right\}$$

3.3.4.2.1 Large Plates

I. Circular Plate under a Central Concentrated Load with Free End Condition

A sketch of such a plate on Pasternak's subgrade model is shown in Figure 3.20.

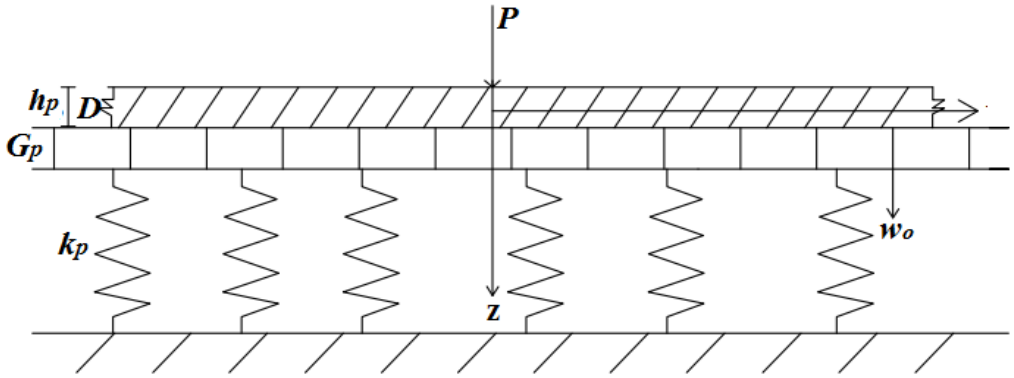

Figure 3.20 A circular plate on an elastic foundation and subjected to a concentrated load at center.

Where P = concentrated load over the circular area

r = the distance to the origin of the polar coordinate

The pertinent boundary conditions for the solid circular plate are

i. For $r = \infty,\ w_o = 0$

ii. For $r = 0,\ w_0$ must be finite

iii. For $r = 0,\ \dfrac{dw_o}{dr} = 0$

iv. For $r \to 0,\ Q_r = \dfrac{-P}{2\pi rD}$

Case I ($G_p^{\,2} < 4k_pD$ or $T < 1$)

The general solution is as given in Eq. (3.59)

$$w_o(r) = \mathrm{B}_1 u_o(r/l) + \mathrm{B}_2 v_o(r/l) + B_3 f_o(r/l) + B_4 g_o(r/l)$$

- ✓ Boundary condition (i) leads B_1 and B_2 to be zero because the Bessel functions present in $u_o(r/l)$ and $v_o(r/l)$ tend to infinity as $r \to \infty$ (refer Appendix A, Eq. (A-9)).
- ✓ Boundary condition (ii) requires B_4 to be zero since $g_o(r/l)$ has a resemblance to $H_o^{(2)}\left(\sqrt{\bar{d}r/l}\right)$ and is undefined. (refer to Appendix A, Eq. (A-17)).

Hence, $w_o(r)$ reduces to

$$w_o(r) = B_3 f_o(r/l) \qquad (3.88)$$

- ✓ Boundary condition (iii) is satisfied only if B_4=0. (refer to Appendix A, Eq.(A-8)).
- ✓ Boundary condition (iv)

$$Q_r = -D\begin{bmatrix} \frac{\sqrt{d^3}}{l^3}J_1\left(\sqrt{d}r/l\right)+\frac{d}{l^2r}J_0\left(\sqrt{d}r/l\right)-\frac{1}{r}J_1\left(\sqrt{d}r/l\right) \\ +i\frac{\sqrt{d^3}}{l^3}N_1\left(\sqrt{d}r/l\right)+i\frac{d}{l^2r}J_0\left(\sqrt{d}r/l\right)-i\frac{1}{r}J_1\left(\sqrt{d}r/l\right) \\ -\frac{d}{l^2r^2}J_0\left(\sqrt{d}r/l\right)+\frac{\sqrt{d}}{lr^2}J_1\left(\sqrt{d}r/l\right)-\frac{d}{l^2r^2}N_0\left(\sqrt{d}r/l\right)+i\frac{\sqrt{d}}{lr^2}N_1\left(\sqrt{d}r/l\right) \\ +\frac{\sqrt{d}}{lr^2}J_1\left(\sqrt{d}r/l\right)+i\frac{\sqrt{d}}{lr^2}N_1\left(\sqrt{d}r/l\right) \end{bmatrix} = -\frac{P}{2\pi rD}$$

Evaluating each argument with

$$B_3 = \frac{P}{4\sqrt{k_pD}\sin 2\delta} \tag{3.89}$$

Then, the general solution of the deflection becomes

$$w_o(r) = \frac{P}{4\sqrt{k_pD}\sin 2\delta}f_o(r/l) \tag{3.90}$$

The corresponding slope and internal actions applying Eq. (3.83 a-d);

$$\begin{aligned}
\theta_r &= \frac{P}{4\sqrt{kD}\sin 2\delta}\left[-\frac{\sqrt{d}}{l}\left(J_1\left(\sqrt{d}r/l\right)+iN_1\left(r/l\right)\right)\right] \\
M_r &= \frac{P}{4\sin 2\delta}\begin{bmatrix} f_o(r/l)\cos 2\delta - g_o(r/l)\sin 2\delta \\ -\left(1-\nu_p\right)\left(\frac{1}{r/l}\left\{f_1(r/l)\cos\delta - g_1(r/l)\sin\delta\right\}\right) \end{bmatrix} \\
M_\theta &= \frac{P}{4\sin 2\delta}\begin{bmatrix} \nu_p\left(f_o(r/l)\cos 2\delta - g_o(r/l)\sin 2\delta\right) \\ +\left(1-\nu_p\right)\left(\frac{1}{r/l}\left\{f_1(r/l)\cos\delta - g_1(r/l)\sin\delta\right\}\right) \end{bmatrix} \\
Q_r &= \frac{-P}{4l\sin 2\delta}\left[f_1(r/l)\cos 3\delta - g_1(r/l)\sin 3\delta\right]
\end{aligned} \tag{3.91}$$

Case II ($G_p^{\,2} = 4k_pD$ or $T = 1$)

The general solution is

$$w_o(r) = \mathrm{A}_1 J_o(r/l) + A_2 H_o^{(1)}(r/l) + A_3 J_o(r/l) + A_4 H_o^{(2)}(r/l)$$

- ✓ Boundary condition (i) leads A_1 and A_3 to be zero.
- ✓ Boundary condition (ii) requires A_4 to be zero.

The reduced deflection would be

$$w_o(r) = A_2 H_o^{(1)}(r/l) \tag{3.92}$$

- ✓ Boundary condition (iii) will be satisfied like the case in Winkler's subgrade model.
- ✓ Boundary condition (iv) gives the same constant with Winkler's subgrade model for concentrated load.

$$A_2 = \frac{P}{4\sqrt{k_pD}\sin 2\delta} \tag{3.93}$$

Thus,

$$w_o(r) = \frac{P}{4\sqrt{k_pD}\sin 2\delta} H_o^{(1)}(r/l) \tag{3.94}$$

The corresponding slope and internal actions;

$$\theta_r = \frac{P}{4\sqrt{kD}\sin 2\delta}\left[\frac{-1}{l}H_1^{(1)}(r/l)\right]$$

$$M_r = \frac{P}{4\sin 2\delta}\left[\begin{array}{l} H_0^{(1)}(r/l)\cos 2\delta - H_0^{(2)}(r/l)\sin 2\delta \\ -(1-\nu_p)\left(\frac{1}{r/l}\left\{H_1^{(1)}(r/l)\cos\delta - H_1^{(2)}(r/l)\sin\delta\right\}\right)\end{array}\right]$$

$$M_\theta = \frac{P}{4\sin 2\delta}\left[\begin{array}{l} \nu_p\left(H_0^{(1)}(r/l)\cos 2\delta - H_0^{(2)}(r/l)\sin 2\delta\right) \\ +(1-\nu_p)\left(\frac{1}{r/l}\left\{H_1^{(1)}(r/l)\cos\delta - H_1^{(2)}(r/l)\sin\delta\right\}\right)\end{array}\right] \qquad (3.95)$$

$$Q_r = \frac{-P}{4l\sin 2\delta}\left[H_1^{(1)}(r/l)\cos 3\delta - H_1^{(2)}(r/l)\sin 3\delta\right]$$

Case III ($G_p^{\,2} > 4k_pD$ or $T > 1$)

The general solution is as given in Eq. (3.86)

$$w_o(r) = \mathrm{A}_1 J_o\left(\sqrt{d}r/l\right) + A_2 H_o^{(1)}\left(\sqrt{d}r/l\right) + A_3 J_o\left(\sqrt{\bar{d}}r/l\right) + A_4 H_o^{(2)}\left(\sqrt{\bar{d}}r/l\right)$$

- ✓ Boundary condition (i) leads A_1 and A_3 to be zero.
- ✓ Boundary condition (ii) requires A_4 to be zero.

The reduced deflection would be,

$$w_o(r) = A_2 H_o^{(1)}\left(\sqrt{d}r/l\right) \qquad (3.96)$$

- ✓ Like the previous cases, boundary condition (iii) is satisfied.
- ✓ Likewise boundary condition (iv) gives,

$$A_2 = \frac{P}{4\sqrt{k_pD}\sin 2\delta} \qquad (3.97)$$

Then,

$$w_o(r) = \frac{P}{4\sqrt{k_pD}\sin 2\delta}H_o^{(1)}\left(\sqrt{d}r/l\right) \qquad (3.98)$$

The corresponding slope and internal actions are;

$$\theta_r = \frac{P}{4\sqrt{kD}\sin 2\delta}\left[\frac{-\sqrt{d}}{l}H_1^{(1)}\left(\sqrt{d}r/l\right)\right]$$

$$M_r = \frac{P}{4\sin 2\delta}\left[\begin{array}{l} H_0^{(1)}\left(\sqrt{d}r/l\right)\cos 2\delta - H_0^{(2)}\left(\sqrt{d}r/l\right)\sin 2\delta \\ -\left(1-\nu_p\right)\left(\frac{1}{\sqrt{d}r/l}\left\{H_1^{(1)}\left(\sqrt{d}r/l\right)\cos\delta - H_1^{(2)}\left(\sqrt{d}r/l\right)\sin\delta\right\}\right)\end{array}\right] \qquad (3.99)$$

$$M_\theta = \frac{P}{4\sin 2\delta}\left[\begin{array}{l} \nu_p\left(H_0^{(1)}\left(\sqrt{d}r/l\right)\cos 2\delta - H_0^{(2)}\left(\sqrt{d}r/l\right)\sin 2\delta\right) \\ +\left(1-\nu_p\right)\left(\frac{1}{\sqrt{d}r/l}\left\{H_1^{(1)}\left(\sqrt{d}r/l\right)\cos\delta - H_1^{(2)}\left(\sqrt{d}r/l\right)\sin\delta\right\}\right)\end{array}\right]$$

$$Q_r = \frac{-P}{4l\sin 2\delta}\left[H_1^{(1)}\left(\sqrt{d}r/l\right)\cos 3\delta - H_1^{(2)}\left(\sqrt{d}r/l\right)\sin 3\delta\right]$$

II. Circular Plate under a Uniformly Distributed Load with Free End Condition

A circular plate subjected to a uniformly distributed load (see Figure 3.21).

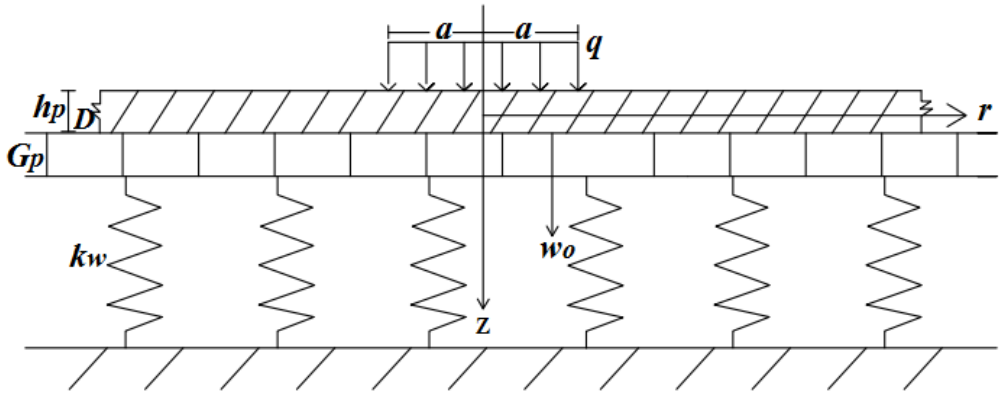

Figure 3.21 A circular plate on an elastic foundation and subjected to uniformly distributed load.

Where q = uniformly distributed load over the circular area with radius a

Note: Adopting the method used by Hetenyi(1979) to derive the general expression for the deflection of the plate would be difficult, in most cases, to evaluate the integrals involved. So, a different approach will be implemented here in.

Case I ($G_p{}^2 < 4k_pD$ or $T < 1$)

In order to find the solution of the differential equation, a Fourier-Bessel Integral called Hankel's Integral will be used.

The pair of intergrals represented by a Fourier-Bessel Integral (Hankel's transfrom) is as

$$f(r) = \int_0^\infty m J_o(mr) F(m)$$

Where

$F_m = \int_0^\infty r J_o(mr)\, f(r)\, dr = H_o\{f(r)\}$ zero order finite Hankel transform (Lokenath and Dambaru, 2007).

- For $r < a,\ f(r) = P,$ p = q (for our case)
- For $r > a,\ f(r) = 0$

$$F(m) = P\int_0^a r J_o(mr)\, dr + 0\int_0^\infty r J_o(mr)\, dr$$

$$F(m) = Pa\,\frac{J_1(ma)}{m}$$

$$\therefore f(r) = Pa\int_0^\infty J_o(mr)\, J_1(ma)\, dm$$

Similarly we can express the load as

$$q(r) = \frac{qa}{l}\int_0^\infty J_0\left(\sqrt{d}r/l\right) J_1\left(\sqrt{\bar{d}}r/l\right) dr = q, \text{ for } |r| < a \qquad (3.100a)$$

$$q(r) = \frac{qa}{l}\int_0^\infty J_0\left(\sqrt{d}r/l\right) J_1\left(\sqrt{\bar{d}}r/l\right) dr = 0, \text{ for } |r| > a \qquad (3.100b)$$

The deflection (w_o) in a similar manner to satisfy the equilibrium equation according to VanCauwelaert (2003), Piessens (2000) and Hankel Transform (2007);

$$w_o = \frac{2q}{\pi}\int_0^\infty A(r) J_o\left(\sqrt{d}r/l\right) J_1\left(\sqrt{\bar{d}}r/l\right) dr \qquad (3.101)$$

Where $A(r)$ is a function of the integration variable

Introducing Eq. (3.100a) and (3.101) into Eq. (3.75) derives;

$$w_o = \frac{qa}{l^2 k_p} \int_0^\infty \frac{J_o\left(\sqrt{d}\, r/l\right) J_1\left(\sqrt{d}\, r/l\right)}{\left(r^4 + 2\frac{G_p}{D} r^2 + 1\right)} dr \tag{3.102}$$

Since it is very difficult to express the solution as a real expression, it will be computed numerically by varying r and G_p so as the internal actions.

Case II ($G_p{}^2 = 4k_p D$ or $T = 1$)

Similarly the load for this case is expressed as

$$q(r) = \frac{qa}{l} \int_0^\infty J_0\left(r/l\right) J_1\left(r/l\right) dr = q, \text{ for } |r| < a \tag{3.103a}$$

$$q(r) = \frac{qa}{l} \int_0^\infty J_0\left(r/l\right) J_1\left(r/l\right) dr = 0, \text{ for } |r| > a \tag{3.103b}$$

The deflection (w_o) in a similar manner to satisfy the equilibrium equation,

$$w_o = \frac{2q}{\pi} \int_0^\infty A(r) J_o\left(r/l\right) J_1\left(r/l\right) dr \tag{3.104}$$

Where $A(r)$ is a function of the integration variable

Introducing Eq. (3.103a) and (3.104) into Eq. (3.75) derives;

$$w_o = \frac{qa}{l^2 k_p} \int_0^\infty \frac{J_o\left(r/l\right) J_1\left(a/l\right)}{\left(r^4 + 2\frac{G_p}{D} r^2 + 1\right)} dr \tag{3.105}$$

Then, w_o will be computed numerically by varying r and G_p so as the internal actions.

Case III ($G_p{}^2 > 4k_p D$ or $T > 1$)

The load for this case is expressed as

$$q(r)=\frac{qa}{l}\int_0^{\infty} J_0\left(\sqrt{d}r/l\right)J_1\left(\sqrt{d}r/l\right)dr=q,\ \text{for}\ |r|<a \tag{3.106a}$$

$$q(r)=\frac{qa}{l}\int_0^{\infty} J_0\left(\sqrt{d}r/l\right)J_1\left(\sqrt{d}r/l\right)dr=0\,,\ \text{for}|r|>a \tag{3.106b}$$

The deflection (w_o) in a similar manner to satisfy the equilibrium equation,

$$w_o=\frac{2q}{\pi}\int_0^{\infty} A(r)\,J_o\left(\sqrt{d}r/l\right)J_1\left(\sqrt{d}r/l\right)dr \tag{3.107}$$

Where $A(r)$ is a function of the integration variable

Introducing Eq. (3.106a) and (3.107) into Eq. (3.75) derives;

$$w_o=\frac{qa}{l^2k}\int_0^{\infty}\frac{J_o\left(\sqrt{d}r/l\right)J_1\left(\sqrt{d}a/l\right)}{\left(r^4+2\frac{G_p}{D}r^2+1\right)}dr \tag{3.108}$$

Then, w_o will be computed numerically by varying r and G_p so as the internal actions.

3.3.4.2.2 Small Plates

In order to analyse the circular plate subjected to the different external loading conditions, the loaded and unloaded regions of the plate are examined separately. (See Figure 3.22)

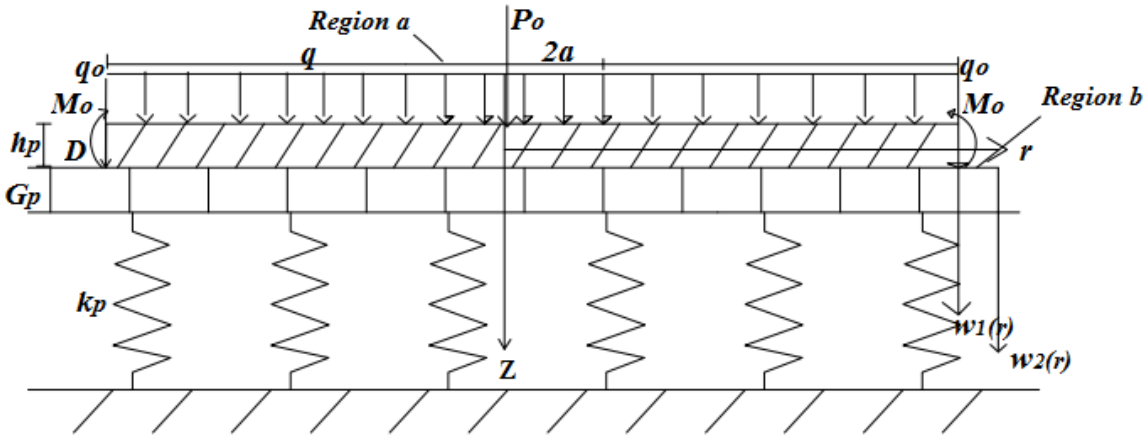

Figure 3.22 Free edged small circular plate under different loading conditions

Considering these two regions :

The DE necessary to express the boundary conditions of the plate itself and the foundation under the plate (i.e.the loaded region, region a) is the deflection $w_1(r)$ governed by a fourth order DE.

$$D\nabla^4 w_1(r) - G_p \nabla^2 w_1(r) + k w_1(r) = q, \quad \text{For } 0 \le r \le a$$

Which can also be rewritten as;

$$\left(\frac{d^2}{dr^2} + \frac{1}{r}\frac{d}{dr}\right)\left(\frac{d^2 w_1}{dr^2} + \frac{1}{r}\frac{dw_1}{dr}\right) - \frac{G_p}{D}\left[\frac{d^2 w_1}{dr^2} + \frac{1}{r}\frac{dw_1}{dr}\right] + \frac{k_p}{D} w_1 = 0 \qquad (3.109)$$

Since the spring bed in the unloaded region (region b) undergoes no deformation, the DE required to express the boundary conditions for the deflection outside the plate $w_2(r)$ is of second order. This specifically means a plate terminated by a free edge which reflects a soil subjected to horizontal shear forces.

$$-G_p \nabla^2 w_2(r) - k w_2(r) = 0, \text{ for } \; a \le r \le \infty \qquad (3.110)$$

Which can be rewritten as;

$$-G_p\left(\frac{d^2 w_2}{dr^2} + \frac{1}{r}\frac{dw_2}{dr}\right) + k_p w_2 = 0 \qquad (3.111)$$

Hence, the solution to Eq. (3.109) will be the homogeneous solutions, Eq. (3.81), (3.84) and (3.86). Similarly, the solution to Eq. (3.111) is given by modified zero order Bessel functions of first kind and second kind (I_o and K_o) respectively. These functions are selected because I_o's value is finite at the origin and asymptotic value of K_o tends to zero.

$$w_2(r) = B_5 I_o(\alpha r) + B_6 K_o(\alpha r) \qquad (3.112)$$

Where

$$\alpha = \sqrt{\frac{k_p}{G_p}}$$

$I_o(r)$ & $K_o(r)$ are as defined previously in Appendix A Eq. (A-19 and A-20).

I. Circular Plate under a Central Concentrated Load with Free End Condition

Such a plate subjected to a concentrated load is shown in Figure 3.23.

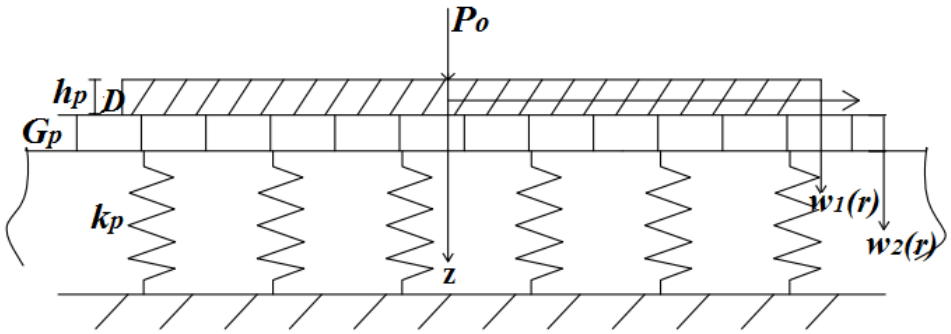

Figure 3.23 Axisymmetric loading of a small circular plate subjected to a concentrated load at center.

Where P_o = concentrated vertical load.

The pertinent boundary conditions are;

i. For $r = 0,\ \dfrac{dw_1}{dr} = 0$

ii. For $r \to 0,\ Q_{r1} = \dfrac{-P_o}{2\pi r D}$

iii. For $r = \infty,\ w_2 = 0$

iv. For $r = a,\ w_1 = w_2$

v. For $r = a,\ M_{r1} = 0$

vi. $r = a,\ Q_{r1} = G_p\left(\dfrac{dw_2}{dr} - \dfrac{dw_1}{dr}\right)$

Case I ($G_p^{\,2} < 4k_pD$ or $T < 1$)

The general expression for the displacement of the plate itself and outside (beyond the edge of the plate) are as given by (3.81) and (3.112).

- ✓ Condition (i) & (ii) necessitate B_3 and B_4 to be zero because the Hankel functions present on $f_o(r/l)$ and $g_o(r/l)$ are undefined for r=0. (refer Appendix A Eq.(A-17))

Hence, the general solution of plate deflection reduces to

$$w_1(r) = \mathrm{B}_1 u_o(r/l) + \mathrm{B}_2 v_o(r/l) \tag{3.113}$$

- ✓ Condition (iii) requires B_5 to be zero because I_o tend to be infinite for infinite value of r. (refer to Appendix A, Eq. (A-19)).

So, the general solution of the deflection beyond the edge of the plate reduces to

$$w_2(r) = B_6 K_o(\alpha r) \tag{3.114}$$

- ✓ Applying boundary condition (iv);

$$B_1 u_o(\mathrm{a}/l) + B_2 v_o(\mathrm{a}/l) = B_6 k_o(\alpha a) \tag{3.115}$$

From this,

$$B_6 = \frac{B_1 u_o(a/l) + B_2 v_o(a/l)}{k_o(\alpha a)} \tag{3.116}$$

- ✓ Applying boundary condition (v);

$$M_{r1} = -\frac{D}{l^2}\left\{\left[B_1 v_o(r/l) - B_2 u_o(r/l)\right] - \frac{l}{r}(1-v_p)\left[B_1 u_o'(r/l) + B_2 v_o'(r/l)\right]\right\}$$

$$M_{r1} = -\frac{D}{l^2}\left\{\begin{array}{l} B_1\left[u_o(r/l)\cos 2\delta - v_o(r/l)\sin 2\delta\right] - \frac{l}{r}(1-v_p)\left[u_1(r/l)\cos\delta + v_1(r/l)\sin\delta\right] \\ +B_2\left[u_o(r/l)\sin 2\delta + v_o(r/l)\cos 2\delta\right] - \frac{l}{r}(1-v_p)\left[u_1(r/l)\sin\delta + v_1(r/l)\cos\delta\right] \end{array}\right\}$$

$$M_{r1}(a) = 0 = -\frac{D}{l^2}\left\{\begin{array}{l} B_1\left[u_o(\mathrm{a}/l)\cos 2\delta - v_o(\mathrm{a}/l)\sin 2\delta\right] - \frac{l}{a}(1-v_p)\left[u_1(\mathrm{a}/l)\cos\delta + v_1(\mathrm{a}/l)\sin\delta\right] \\ +B_2\left[u_o(\mathrm{a}/l)\sin 2\delta + v_o(\mathrm{a}/l)\cos 2\delta\right] - \frac{l}{a}(1-v_p)\left[u_1(\mathrm{a}/l)\sin\delta + v_1(\mathrm{a}/l)\cos\delta\right] \end{array}\right\} \tag{3.117}$$

- ✓ Boundary condition (vi),

$$Q_{r1} = -\frac{D}{l^3}\left\{B_1 v_o'(r/l) - B_2 u_o'(r/l)\right\}$$

$$Q_{r1} = -\frac{D}{l^3}\left\{B_1\left[u_1(r/l)\cos 3\delta - v_1(r/l)\sin 3\delta\right] + B_2\left[u_1(r/l)\sin 3\delta + v_1(r/l)\cos 3\delta\right]\right\}$$

$$Q_{r1}(a) = -\frac{D}{l^3}\left\{B_1\left[u_1(\mathrm{a}/l)\cos 3\delta - v_1(\mathrm{a}/l)\sin 3\delta\right] + B_2\left[u_1(\mathrm{a}/l)\sin 3\delta + v_1(\mathrm{a}/l)\cos 3\delta\right]\right\} \quad (3.118a)$$

$$G_p\left[\frac{dw_2}{dr} - \frac{dw_1}{dr}\right] = G_p\left[-\alpha B_6 k_1(\alpha a) + \frac{1}{l}\left[\begin{matrix} B_1\left(u_1(a/l)\cos\delta - v_1(a/l)\sin\delta\right) \\ +B_2\left(u_1(a/l)\sin\delta + v_1(a/l)\cos\delta\right)\end{matrix}\right]\right] \quad (3.118b)$$

Equating these two equations (3.118a) and (3.118b), we will have

$$\begin{aligned} &-\frac{D}{l^3}\left\{B_1\left[u_1(\mathrm{a}/l)\cos 3\delta - v_1(\mathrm{a}/l)\sin 3\delta\right] + B_2\left[u_1(\mathrm{a}/l)\sin 3\delta + v_1(\mathrm{a}/l)\cos 3\delta\right]\right\} \\ &= G_p\left[-\alpha B_6 k_1(\alpha a) + \frac{1}{l}\left[\begin{matrix} B_1\left(u_1(a/l)\cos\delta - v_1(a/l)\sin\delta\right) \\ +B_2\left(u_1(a/l)\sin\delta + v_1(a/l)\cos\delta\right)\end{matrix}\right]\right] \end{aligned} \quad (3.119)$$

Substituting B_6 into Eq. (3.119), we get an equation with constants B_1 and B_2 only. Then solving this equation simultaneously with Eq. (3.118) which also have the same constants, we obtain;

$$B_1 = \frac{p\left[\left[u_o(\mathrm{a}/l)\sin 2\delta + v_o(\mathrm{a}/l)\cos 2\delta\right] - \frac{l}{a}(1-\nu_p)\left[u_1(\mathrm{a}/l)\sin\delta + v_1(\mathrm{a}/l)\cos\delta\right]\right]}{k_p l\left\{\begin{matrix} \left[\left(u_o(\mathrm{a}/l)\cos 2\delta - v_o(\mathrm{a}/l)\sin 2\delta\right) - \frac{l}{a}(1-\nu_p)\left(u_1(\mathrm{a}/l)\cos\delta - v_1(\mathrm{a}/l)\sin\delta\right)\right]\times \\ \left[u_1(\mathrm{a}/l)\sin 3\delta + v_1(\mathrm{a}/l)\cos 3\delta + \frac{u_1(a/l)\sin\delta + v_1(a/l)\cos\delta}{\frac{k_p l^2}{G_p}} - v_o(a/l)\frac{K_1(\alpha_o a/l)}{\alpha_o K_0(\alpha_o a/l)}\right] - \\ \left[\left(u_o(\mathrm{a}/l)\sin 2\delta + v_o(\mathrm{a}/l)\cos 2\delta\right) - \frac{l}{a}(1-\nu_p)\left(u_1(\mathrm{a}/l)\sin\delta + v_1(\mathrm{a}/l)\cos\delta\right)\right]\times \\ \left[u_1(\mathrm{a}/l)\cos 3\delta - v_1(\mathrm{a}/l)\sin 3\delta + \frac{u_1(a/l)\cos\delta - v_1(a/l)\sin\delta}{\frac{k_p l^2}{G_p}} - u_o(a/l)\frac{K_1(\alpha_o a/l)}{\alpha_o K_0(\alpha_o a/l)}\right] \end{matrix}\right\}$$

$$B_2 = -\frac{p\left[\left[u_o\left(\mathrm{a}/l\right)\cos 2\delta - v_o\left(\mathrm{a}/l\right)\sin 2\delta\right] - \frac{l}{a}\left(1-v_p\right)\left[u_1\left(\mathrm{a}/l\right)\cos\delta - v_1\left(\mathrm{a}/l\right)\sin\delta\right]\right]}{k_p l\left\{\begin{array}{l}\left[\left(u_o\left(\mathrm{a}/l\right)\cos 2\delta - v_o\left(\mathrm{a}/l\right)\sin 2\delta\right) - \frac{l}{a}\left(1-v_p\right)\left(u_1\left(\mathrm{a}/l\right)\cos\delta - v_1\left(\mathrm{a}/l\right)\sin\delta\right)\right]\times \\ \left[u_1\left(\mathrm{a}/l\right)\sin 3\delta + v_1\left(\mathrm{a}/l\right)\cos 3\delta + \frac{u_1\left(a/l\right)\sin\delta + v_1\left(a/l\right)\cos\delta}{\frac{k_p l^2}{G_p}} - v_o\left(a/l\right)\frac{K_1\left(\alpha_o a/l\right)}{\alpha_o K_0\left(\alpha_o a/l\right)}\right] - \\ \left[\left(u_o\left(\mathrm{a}/l\right)\sin 2\delta + v_o\left(\mathrm{a}/l\right)\cos 2\delta\right) - \frac{l}{a}\left(1-v_p\right)\left(u_1\left(\mathrm{a}/l\right)\sin\delta + v_1\left(\mathrm{a}/l\right)\cos\delta\right)\right]\times \\ \left[u_1\left(\mathrm{a}/l\right)\cos 3\delta - v_1\left(\mathrm{a}/l\right)\sin 3\delta + \frac{u_1\left(a/l\right)\cos\delta - v_1\left(a/l\right)\sin\delta}{\frac{k_p l^2}{G_p}} - u_o\left(a/l\right)\frac{K_1\left(\alpha_o a/l\right)}{\alpha_o K_0\left(\alpha_o a/l\right)}\right]\end{array}\right\}}$$

$$B_6 = \frac{B_1 u_o\left(\mathrm{a}/l\right) + B_2 v_o\left(a/l\right)}{K_o\left(\alpha_o a/l\right)} \tag{3.120}$$

The deflection for different values of *r* will be evaluated using a spreadsheet program, the slope and corresponding internal actions in a similar manner like in Eq. (3.83 a-d):

$$\theta_r = -\frac{1}{l}\left\{B_1\left[u_1\left(r/l\right)\cos\delta - v_1\left(r/l\right)\sin\delta\right] + B_2\left[u_1\left(r/l\right)\sin\delta + v_1\left(r/l\right)\cos\delta\right]\right\}$$

$$M_r = -\frac{D}{l^2}\left\{\begin{array}{l}B_1\left[\left(u_o\left(r/l\right)\cos 2\delta - v_o\left(r/l\right)\sin 2\delta\right) - \frac{l}{r}\left(1-v_p\right)\left(u_1\left(r/l\right)\cos\delta - v_1\left(r/l\right)\sin\delta\right)\right] \\ +B_2\left[\left(u_o\left(r/l\right)\sin 2\delta + v_o\left(r/l\right)\cos 2\delta\right) - \frac{l}{r}\left(1-v_p\right)\left(u_1\left(r/l\right)\sin\delta + v_1\left(r/l\right)\cos\delta\right)\right]\end{array}\right\}$$

$$M_\theta = -\frac{D}{l^2}\left\{\begin{array}{l}B_1\left[v_p\left(u_o\left(r/l\right)\cos 2\delta - v_o\left(r/l\right)\sin 2\delta\right) + \frac{l}{r}\left(1-v_p\right)\left(u_1\left(r/l\right)\cos\delta - v_1\left(r/l\right)\sin\delta\right)\right] \\ +B_2\left[v_p\left(u_o\left(r/l\right)\sin 2\delta + v_o\left(r/l\right)\cos 2\delta\right) + \frac{l}{r}\left(1-v_p\right)\left(u_1\left(r/l\right)\sin\delta + v_1\left(r/l\right)\cos\delta\right)\right]\end{array}\right\}$$

$$Q_r = -\frac{D}{l^3}\left\{B_1\left[u_1\left(r/l\right)\cos 3\delta - v_1\left(r/l\right)\sin 3\delta\right] + B_2\left[u_1\left(r/l\right)\sin 3\delta + v_1\left(r/l\right)\cos 3\delta\right]\right\}$$

(3.121)

Case II ($G_p^{\,2} = 4k_pD$ or $T = 1$)

The general expression for the displacement of the plate itself and outside (beyond the edge of the plate) are as given by (3.84 and 3.112).

- ✓ Condition (i) & (ii) necessitate A_2 and A_4 to be zero.

Hence, the general solution of plate deflection reduces to

$$w_1(r) = A_1 J_o(r/l) + A_3 J_o(r/l) \tag{3.122}$$

- ✓ Condition (iii) applies for $w_2(r)$ which is the same as case I.
- ✓ Applying boundary condition (iv) gives,

$$A_1 J_o(\mathrm{a}/l) + A_3 J_o(\mathrm{a}/l) = B_6 K_o(\alpha a) \tag{3.123}$$

From this,

$$B_6 = \frac{A_1 J_o(\mathrm{a}/l) + A_3 J_o(\mathrm{a}/l)}{K_o(\alpha a)} \tag{3.124}$$

- ✓ Applying boundary condition (v) stated in case one,

$$M_{r1}(a) = 0 = -\frac{D}{l^2}\left\{\begin{array}{l} A_1\left[J_o(a/l)\cos 2\delta - \dfrac{l}{a}(1-\nu_p)\left(J_1(a/l)\cos\delta\right)\right] \\ +A_3\left[J_o(a/l)\cos 2\delta - \dfrac{l}{a}(1-\nu_p)\left(J_1(a/l)\cos\delta\right)\right] \end{array}\right\} \tag{3.125}$$

- ✓ Boundary condition (vi),

$$\begin{aligned} &-\frac{D}{l^3}\left\{A_1 J_1(a/l)\cos 3\delta + A_3 J_1(a/l)\cos 3\delta\right\} = \\ &G_p\left[-\alpha B_6 k_1(\alpha a) + \frac{1}{l}\left[A_1 J_1(a/l)\cos\delta + A_3 J_1(a/l)\cos\delta\right]\right] \end{aligned} \tag{3.126}$$

Substituting B_6 into Eq. (3.126), we get an equation with constants A_1 and A_2 only. Then solving this equation simultaneously with Eq. (3.125) which also have the same constants, we obtain;

$$A_1 = \frac{p\left[J_o\left(\mathrm{a}/l\right)\cos 2\delta - \frac{l}{a}\left(1-\nu_p\right)\left(J_1\left(\mathrm{a}/l\right)\cos\delta\right)\right]}{k_p l\left\{\begin{array}{l}\left[J_o\left(\mathrm{a}/l\right)\cos 2\delta - \frac{l}{a}\left(1-\nu_p\right)\left(J_1\left(\mathrm{a}/l\right)\cos\delta\right)\right]\times \\ \left[J_1\left(\mathrm{a}/l\right)\cos 3\delta + \frac{J_1\left(\mathrm{a}/l\right)\cos\delta}{\frac{k_p l^2}{G_p}} - J_o\left(\mathrm{a}/l\right)\frac{K_1\left(\alpha_o a/l\right)}{\alpha_o K_0\left(\alpha_o a/l\right)}\right] \\ - \\ \left[J_o\left(\mathrm{a}/l\right)\cos 2\delta - \frac{l}{a}\left(1-\nu_p\right)\left(J_1\left(\mathrm{a}/l\right)\cos\delta\right)\right]\times \\ \left[J_1\left(\mathrm{a}/l\right)\cos 3\delta + \frac{J_1\left(\mathrm{a}/l\right)\cos\delta}{\frac{k_p l^2}{G_p}} - J_o\left(\mathrm{a}/l\right)\frac{K_1\left(\alpha_o a/l\right)}{\alpha_o K_0\left(\alpha_o a/l\right)}\right]\end{array}\right\}}$$

$$A_3 = -\frac{p\left[J_o\left(\mathrm{a}/l\right)\cos 2\delta - \frac{l}{a}\left(1-\nu_p\right)\left(J_1\left(\mathrm{a}/l\right)\cos\delta\right)\right]}{k_p l\left\{\begin{array}{l}\left[J_o\left(\mathrm{a}/l\right)\cos 2\delta - \frac{l}{a}\left(1-\nu_p\right)\left(J_1\left(\mathrm{a}/l\right)\cos\delta\right)\right]\times \\ \left[J_1\left(\mathrm{a}/l\right)\cos 3\delta + \frac{J_1\left(\mathrm{a}/l\right)\cos\delta}{\frac{k_p l^2}{G_p}} - J_o\left(\mathrm{a}/l\right)\frac{K_1\left(\alpha_o a/l\right)}{\alpha_o K_0\left(\alpha_o a/l\right)}\right] \\ - \\ \left[J_o\left(\mathrm{a}/l\right)\cos 2\delta - \frac{l}{a}\left(1-\nu_p\right)\left(J_1\left(\mathrm{a}/l\right)\cos\delta\right)\right]\times \\ \left[J_1\left(\mathrm{a}/l\right)\cos 3\delta + \frac{J_1\left(\mathrm{a}/l\right)\cos\delta}{\frac{k_p l^2}{G_p}} - J_o\left(\mathrm{a}/l\right)\frac{K_1\left(\alpha_o a/l\right)}{\alpha_o K_0\left(\alpha_o a/l\right)}\right]\end{array}\right\}}$$

$$B_6 = \frac{A_1 J_o\left(\mathrm{a}/l\right) + A_3 J_o\left(a/l\right)}{K_o\left(\alpha_o a/l\right)} \tag{3.127}$$

The deflection for different values of *r* will be evaluated using a spreadsheet program, the slope and corresponding internal actions in a similar manner like in Eq. (3.85a-d):

$$\begin{aligned}
\theta_r &= -\frac{1}{l}\left\{A_1 J_1\left(\sqrt{d}r/l\right)\cos\delta + A_3 J_1\left(\sqrt{\bar{d}}r/l\right)\cos\delta\right\} \\
M_r &= -\frac{D}{l^2}\left\{\begin{aligned}&A_1\left[J_o\left(\sqrt{d}r/l\right)\cos 2\delta - \frac{l}{r}\left(1-\nu_p\right)\left(J_1\left(\sqrt{d}r/l\right)\cos\delta\right)\right] \\ &+A_3\left[J_o\left(\sqrt{\bar{d}}r/l\right)\cos 2\delta - \frac{l}{r}\left(1-\nu_p\right)\left(J_1\left(\sqrt{\bar{d}}r/l\right)\cos\delta\right)\right]\end{aligned}\right\} \\
M_\theta &= -\frac{D}{l^2}\left\{\begin{aligned}&A_1\left[\nu_p J_o\left(\sqrt{d}r/l\right)\cos 2\delta + \frac{l}{r}\left(1-\nu_p\right)J_1\left(\sqrt{d}r/l\right)\cos\delta\right] \\ &+A_3\left[\nu_p J_o\left(\sqrt{\bar{d}}r/l\right)\cos 2\delta + \frac{l}{r}\left(1-\nu_p\right)J_1\left(\sqrt{\bar{d}}r/l\right)\cos\delta\right]\end{aligned}\right\} \\
Q_r &= -\frac{D}{l^3}\left\{A_1 J_1\left(\sqrt{d}r/l\right)\cos 3\delta + A_3 J_1\left(\sqrt{\bar{d}}r/l\right)\cos 3\delta\right\}
\end{aligned} \tag{3.128}$$

<u>Case III</u> ($G_p^{\,2} > 4k_pD$ or $T > 1$)

The general expression for the displacement of the plate itself and outside (beyond the edge of the plate) are as given by Eq. (3.86) and (3.112).

- ✓ Condition (i) & (ii) necessitate A_2 and A_4 to be zero because Hankel functions are undefined for $r = 0$.

Hence, the general solution of plate deflection reduces to

$$w_1(r) = A_1 J_o\left(\sqrt{d}r/l\right) + A_3 J_o\left(\sqrt{\bar{d}}r/l\right) \tag{3.129}$$

- ✓ Condition (iii) applies for $w_2(r)$ which is the same as case I.
- ✓ Boundary Condition (iv) gives

$$A_1 J_o\left(\sqrt{d}\,\mathrm{a}/l\right) + A_3 J_o\left(\sqrt{\bar{d}}\,\mathrm{a}/l\right) = B_6 K_o(\alpha a) \tag{3.130}$$

From this,

$$B_6 = \frac{A_1 J_o\left(\sqrt{d}\ \mathrm{a}/l\right) + A_3 J_o\left(\sqrt{\bar{d}}\ \mathrm{a}/l\right)}{K_o(\alpha a)} \tag{3.131}$$

✓ Applying boundary condition (v) stated in case one,

$$M_{r1}(a) = 0 = -\frac{D}{l^2}\left\{\begin{aligned} &A_1\left[J_o\left(\sqrt{d}a/l\right)\cos 2\delta - \frac{l}{a}(1-\nu_p)\left(J_1\left(\sqrt{d}a/l\right)\cos\delta\right)\right] \\ &+A_3\left[J_o\left(\sqrt{\bar{d}}a/l\right)\cos 2\delta - \frac{l}{a}(1-\nu_p)\left(J_1\left(\sqrt{\bar{d}}a/l\right)\cos\delta\right)\right]\end{aligned}\right\} \tag{3.132}$$

✓ Boundary condition (vi),

$$\begin{aligned} &-\frac{D}{l^3}\left\{A_1 J_1\left(\sqrt{d}a/l\right)\cos 3\delta + A_3 J_1\left(\sqrt{\bar{d}}a/l\right)\cos 3\delta\right\} = \\ &G_p\left[-\alpha B_6 k_1(\alpha a) + \frac{1}{l}\left[A_1 J_1\left(\sqrt{d}a/l\right)\cos\delta + A_3 J_1\left(\sqrt{\bar{d}}a/l\right)\cos\delta\right]\right] \end{aligned} \tag{3.133}$$

Substituting B_6 into Eq. (3.133), we get an equation with constants A_1 and A_2 only. Then solving this equation simultaneously with Eq. (3.132) which also have the same constants, we obtain;

$$A_1 = \frac{p\left[J_o\left(\sqrt{\bar{d}}\ \mathrm{a}/l\right)\cos 2\delta - \frac{l}{a}(1-\nu_p)\left(J_1\left(\sqrt{\bar{d}}\ \mathrm{a}/l\right)\cos\delta\right)\right]}{k_p l\left\{\begin{aligned} &\left[J_o\left(\sqrt{d}\ \mathrm{a}/l\right)\cos 2\delta - \frac{l}{a}(1-\nu_p)\left(J_1\left(\sqrt{d}\ \mathrm{a}/l\right)\cos\delta\right)\right]\times \\ &\left[J_1\left(\sqrt{\bar{d}}\ \mathrm{a}/l\right)\cos 3\delta + \frac{J_1\left(\sqrt{\bar{d}}\ \mathrm{a}/l\right)\cos\delta}{\frac{k_p l^2}{G_p}} - J_o\left(\sqrt{\bar{d}}\ \mathrm{a}/l\right)\frac{K_1(\alpha_o a/l)}{\alpha_o K_0(\alpha_o a/l)}\right] \\ &- \\ &\left[J_o\left(\sqrt{\bar{d}}\ \mathrm{a}/l\right)\cos 2\delta - \frac{l}{a}(1-\nu_p)\left(J_1\left(\sqrt{\bar{d}}\ \mathrm{a}/l\right)\cos\delta\right)\right]\times \\ &\left[J_1\left(\sqrt{d}\ \mathrm{a}/l\right)\cos 3\delta + \frac{J_1\left(\sqrt{d}\ \mathrm{a}/l\right)\cos\delta}{\frac{k_p l^2}{G_p}} - J_o\left(\sqrt{d}\ \mathrm{a}/l\right)\frac{K_1(\alpha_o a/l)}{\alpha_o K_0(\alpha_o a/l)}\right]\end{aligned}\right\}$$

$$A_3 = -\frac{p\left[J_o\left(\sqrt{d}\,\mathrm{a}/l\right)\cos 2\delta - \frac{l}{a}\left(1-\nu_p\right)\left(J_1\left(\sqrt{d}\,\mathrm{a}/l\right)\cos\delta\right)\right]}{k_p l\left\{\begin{array}{l}\left[J_o\left(\sqrt{d}\,\mathrm{a}/l\right)\cos 2\delta - \frac{l}{a}\left(1-\nu_p\right)\left(J_1\left(\sqrt{d}\,\mathrm{a}/l\right)\cos\delta\right)\right]\times \\ \left[J_1\left(\sqrt{d}\,\mathrm{a}/l\right)\cos 3\delta + \frac{J_1\left(\sqrt{d}\,\mathrm{a}/l\right)\cos\delta}{\frac{k_p l^2}{G_p}} - J_o\left(\sqrt{d}\,\mathrm{a}/l\right)\frac{K_1\left(\alpha_o a/l\right)}{\alpha_o K_0\left(\alpha_o a/l\right)}\right] \\ - \\ \left[J_o\left(\sqrt{\bar{d}}\,\mathrm{a}/l\right)\cos 2\delta - \frac{l}{a}\left(1-\nu_p\right)\left(J_1\left(\sqrt{\bar{d}}\,\mathrm{a}/l\right)\cos\delta\right)\right]\times \\ \left[J_1\left(\sqrt{d}\,\mathrm{a}/l\right)\cos 3\delta + \frac{J_1\left(\sqrt{d}\,\mathrm{a}/l\right)\cos\delta}{\frac{k_p l^2}{G_p}} - J_o\left(\sqrt{d}\,\mathrm{a}/l\right)\frac{K_1\left(\alpha_o a/l\right)}{\alpha_o K_0\left(\alpha_o a/l\right)}\right]\end{array}\right\}}$$

$$B_6 = \frac{A_1 J_o\left(\sqrt{d}\,\mathrm{a}/l\right) + A_3 J_o\left(\sqrt{\bar{d}}\,a/l\right)}{K_o\left(\alpha_o a/l\right)} \tag{3.134}$$

The deflection for different values of *r* will be evaluated using a spreadsheet program, the slope and the corresponding internal actions in a similar manner like in Eq. (3.87 a-d):

$$\begin{aligned}
\theta_r &= -\frac{1}{l}\left\{A_1 J_1\left(\sqrt{d}\,r/l\right)\cos\delta + A_3 J_1\left(\sqrt{\bar{d}}\,r/l\right)\cos\delta\right\} \\
M_r &= -\frac{D}{l^2}\left\{\begin{array}{l}A_1\left[J_o\left(\sqrt{d}\,r/l\right)\cos 2\delta - \frac{l}{r}\left(1-\nu_p\right)\left(J_1\left(\sqrt{d}\,r/l\right)\cos\delta\right)\right] \\ +A_3\left[J_o\left(\sqrt{\bar{d}}\,r/l\right)\cos 2\delta - \frac{l}{r}\left(1-\nu_p\right)\left(J_1\left(\sqrt{\bar{d}}\,r/l\right)\cos\delta\right)\right]\end{array}\right\} \\
M_\theta &= -\frac{D}{l^2}\left\{\begin{array}{l}A_1\left[\nu_p J_o\left(\sqrt{d}\,r/l\right)\cos 2\delta + \frac{l}{r}\left(1-\nu_p\right)J_1\left(\sqrt{d}\,r/l\right)\cos\delta\right] \\ +A_3\left[\nu_p J_o\left(\sqrt{\bar{d}}\,r/l\right)\cos 2\delta + \frac{l}{r}\left(1-\nu_p\right)J_1\left(\sqrt{\bar{d}}\,r/l\right)\cos\delta\right]\end{array}\right\} \\
Q_r &= -\frac{D}{l^3}\left\{A_1 J_1\left(\sqrt{d}\,r/l\right)\cos 3\delta + A_3 J_1\left(\sqrt{\bar{d}}\,r/l\right)\cos 3\delta\right\}
\end{aligned} \tag{3.135}$$

II. Circular Plate under a Concentrated Edge Load with Free End Condition

A circumferential load of q_o that is uniformly distributed per unit run along the edge is considered (see Figure 3.24).

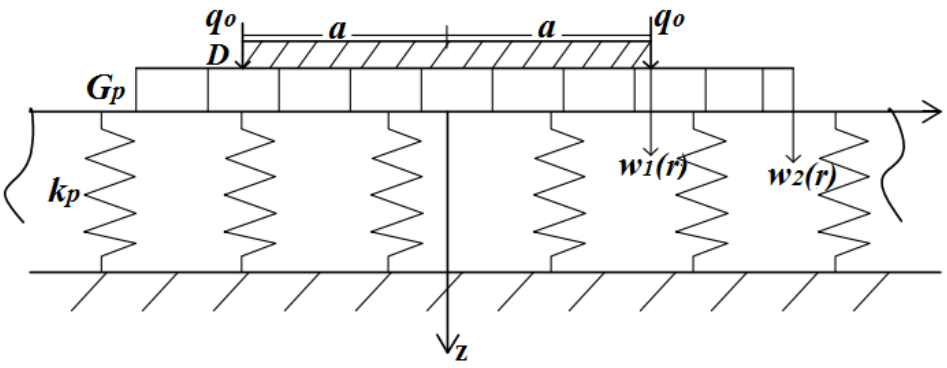

Figure 3.24 Axisymmetric loading of a small circular plate subjected to a concentrated edge load.

The following boundary conditions can be stated according to VanCauwelaert (2003) and Selvadurai (1979);

i. For $r = 0,\ \dfrac{dw_1}{dr} = 0$

ii. For $r = 0,\ Q_{r1} = 0$

iii. For $r = \infty,\ w_2 = 0$

<u>Case I</u> ($G_p{}^2 < 4kD$ or $T < 1$)

The general expression for the displacement of the plate itself and outside (beyond the edge of the plate) are as given by Eq. (3.81) and (3.112).

- ✓ Condition (i) & (ii) necessitate B_3 and B_4 to be zero because the Hankel functions present on $f_o(r/l)$ and $g_o(r/l)$ are undefined for $r = 0$. (refer Appendix A Eq.(A-17))

Hence, the general solution of plate deflection reduces to

$$w_1(r) = \mathrm{B}_1 u_o(r/l) + \mathrm{B}_2 v_o(r/l) \tag{3.136}$$

- ✓ Condition (iii) requires B_5 to be zero because I_o tend to be infinite for infinite value of r. (refer to Appendix A, Eq. (A-19)).

So, the general solution of the deflection beyond the edge of the plate reduces to

$$w_2(r) = B_6 K_o(\alpha r) \tag{3.137}$$

Again the following boundary conditions are stated to determine the constants.

iv. For $r = a,\ M_{r1} = 0$, M_{r1}-bending moment obtained from $w_1(r)$

v. For $r = a,\ Q_{r1} = G\left[\frac{dw_2}{dr} - \frac{dw_1}{dr}\right] + q_o$, Q_{r1}-shear force obtained from $w_1(r)$

vi. For $r = a,\ w_1 = w_2$

- ✓ Boundary condition (iv)

$$M_{r1} = -\frac{D}{l^2}\left\{\left[B_1 v_o(r/l) - B_2 u_o(r/l)\right] - \frac{l}{r}(1-\nu_p)\left[B_1 u_o'(r/l) + B_2 v_o'(r/l)\right]\right\}$$

$$M_{r1} = -\frac{D}{l^2}\left\{\begin{aligned} &B_1\left[u_o(r/l)\cos 2\delta - v_o(r/l)\sin 2\delta\right] - \frac{l}{r}(1-\nu_p)\left[u_1(r/l)\cos\delta + v_1(r/l)\sin\delta\right] \\ &+B_2\left[u_o(r/l)\sin 2\delta + v_o(r/l)\cos 2\delta\right] - \frac{l}{r}(1-\nu_p)\left[u_1(r/l)\sin\delta + v_1(r/l)\cos\delta\right] \end{aligned}\right\}$$

$$M_{r1}(a) = 0 = -\frac{D}{l^2}\left\{\begin{aligned} &B_1\left[u_o(\mathrm{a}/l)\cos 2\delta - v_o(\mathrm{a}/l)\sin 2\delta\right] - \frac{l}{a}(1-\nu_p)\left[u_1(\mathrm{a}/l)\cos\delta + v_1(\mathrm{a}/l)\sin\delta\right] \\ &+B_2\left[u_o(\mathrm{a}/l)\sin 2\delta + v_o(\mathrm{a}/l)\cos 2\delta\right] - \frac{l}{a}(1-\nu_p)\left[u_1(\mathrm{a}/l)\sin\delta + v_1(\mathrm{a}/l)\cos\delta\right] \end{aligned}\right\}$$

(3.138)

- ✓ Boundary condition (v),

$$Q_{r1} = -\frac{D}{l^3}\left\{B_1 v_o'(r/l) - B_2 u_o'(r/l)\right\}$$

$$Q_{r1} = -\frac{D}{l^3}\left\{B_1\left[u_1(r/l)\cos 3\delta - v_1(r/l)\sin 3\delta\right] + B_2\left[u_1(r/l)\sin 3\delta + v_1(r/l)\cos 3\delta\right]\right\}$$

$$Q_{r1}(a) = -\frac{D}{l^3}\left\{B_1\left[u_1(\mathrm{a}/l)\cos 3\delta - v_1(\mathrm{a}/l)\sin 3\delta\right] + B_2\left[u_1(\mathrm{a}/l)\sin 3\delta + v_1(\mathrm{a}/l)\cos 3\delta\right]\right\}$$

(3.139a)

$$G_p\left[\frac{dw_2}{dr}-\frac{dw_1}{dr}\right]+q_o=G_p\left[-\alpha B_6 k_1(\alpha a)+\frac{1}{l}\begin{bmatrix}B_1\left(u_1(a/l)\cos\delta-v_1(a/l)\sin\delta\right)\\+B_2\left(u_1(a/l)\sin\delta+v_1(a/l)\cos\delta\right)\end{bmatrix}\right]+q_o \quad (3.139b)$$

Equating these two equations (3.139a and 3.139b), we will have

$$\begin{aligned}&-\frac{D}{l^3}\left\{B_1\left[u_1(\mathrm{a}/l)\cos 3\delta-v_1(\mathrm{a}/l)\sin 3\delta\right]+B_2\left[u_1(\mathrm{a}/l)\sin 3\delta+v_1(\mathrm{a}/l)\cos 3\delta\right]\right\}\\&=G\left[-\alpha B_6 k_1(\alpha a)+\frac{1}{l}\begin{bmatrix}B_1\left(u_1(a/l)\cos\delta-v_1(a/l)\sin\delta\right)\\+B_2\left(u_1(a/l)\sin\delta+v_1(a/l)\cos\delta\right)\end{bmatrix}\right]+q_o\end{aligned} \quad (3.140)$$

- ✓ Boundary condition(vi) gives,

$$\mathrm{B}_1 u_o(\mathrm{a}/l)+\mathrm{B}_2 v_o(\mathrm{a}/l)=B_6 K_o(\alpha a) \quad (3.141)$$

From this,

$$B_6=\frac{\mathrm{B}_1 u_o(\mathrm{a}/l)+\mathrm{B}_2 v_o(\mathrm{a}/l)}{K_o(\alpha a)} \quad (3.142)$$

Substituting B_6 into Eq. (3.140), we get an equation with constants B_1 and B_2 only. Then solving this equation simultaneously with Eq. (3.138) which also have the same constants, we obtain;

$$B_1 = \frac{q_o\left[\left[u_o(\mathrm{a}/l)\sin 2\delta + v_o(\mathrm{a}/l)\cos 2\delta\right] - \frac{l}{a}(1-\nu_p)\left[u_1(\mathrm{a}/l)\sin\delta + v_1(\mathrm{a}/l)\cos\delta\right]\right]}{k_p l\left\{\begin{array}{l}\left[\left(u_o(\mathrm{a}/l)\cos 2\delta - v_o(\mathrm{a}/l)\sin 2\delta\right) - \frac{l}{a}(1-\nu_p)\left(u_1(\mathrm{a}/l)\cos\delta - v_1(\mathrm{a}/l)\sin\delta\right)\right]\times \\ \left[u_1(\mathrm{a}/l)\sin 3\delta + v_1(\mathrm{a}/l)\cos 3\delta + \frac{u_1(a/l)\sin\delta + v_1(a/l)\cos\delta}{\frac{k_p l^2}{G_p}} - v_o(a/l)\frac{K_1(\alpha_o a/l)}{\alpha_o K_0(\alpha_o a/l)}\right] - \\ \left[\left(u_o(\mathrm{a}/l)\sin 2\delta + v_o(\mathrm{a}/l)\cos 2\delta\right) - \frac{l}{a}(1-\nu_p)\left(u_1(\mathrm{a}/l)\sin\delta + v_1(\mathrm{a}/l)\cos\delta\right)\right]\times \\ \left[u_1(\mathrm{a}/l)\cos 3\delta - v_1(\mathrm{a}/l)\sin 3\delta + \frac{u_1(a/l)\cos\delta - v_1(a/l)\sin\delta}{\frac{k_p l^2}{G_p}} - u_o(a/l)\frac{K_1(\alpha_o a/l)}{\alpha_o K_0(\alpha_o a/l)}\right]\end{array}\right\}}$$

$$B_2 = -\frac{q_o\left[\left[u_o(\mathrm{a}/l)\cos 2\delta - v_o(\mathrm{a}/l)\sin 2\delta\right] - \frac{l}{a}(1-\nu_p)\left[u_1(\mathrm{a}/l)\cos\delta - v_1(\mathrm{a}/l)\sin\delta\right]\right]}{k_p l\left\{\begin{array}{l}\left[\left(u_o(\mathrm{a}/l)\cos 2\delta - v_o(\mathrm{a}/l)\sin 2\delta\right) - \frac{l}{a}(1-\nu_p)\left(u_1(\mathrm{a}/l)\cos\delta - v_1(\mathrm{a}/l)\sin\delta\right)\right]\times \\ \left[u_1(\mathrm{a}/l)\sin 3\delta + v_1(\mathrm{a}/l)\cos 3\delta + \frac{u_1(a/l)\sin\delta + v_1(a/l)\cos\delta}{\frac{k_p l^2}{G_p}} - v_o(a/l)\frac{K_1(\alpha_o a/l)}{\alpha_o K_0(\alpha_o a/l)}\right] - \\ \left[\left(u_o(\mathrm{a}/l)\sin 2\delta + v_o(\mathrm{a}/l)\cos 2\delta\right) - \frac{l}{a}(1-\nu_p)\left(u_1(\mathrm{a}/l)\sin\delta + v_1(\mathrm{a}/l)\cos\delta\right)\right]\times \\ \left[u_1(\mathrm{a}/l)\cos 3\delta - v_1(\mathrm{a}/l)\sin 3\delta + \frac{u_1(a/l)\cos\delta - v_1(a/l)\sin\delta}{\frac{k_p l^2}{G_p}} - u_o(a/l)\frac{K_1(\alpha_o a/l)}{\alpha_o K_0(\alpha_o a/l)}\right]\end{array}\right\}}$$

$$B_6 = \frac{B_1 u_o(\mathrm{a}/l) + B_2 v_o(a/l)}{K_o(\alpha_o a/l)} \qquad (3.143)$$

The deflection for different values of *r* will be evaluated using an excel sheet and the corresponding internal actions in a similar manner like in Eq. (3.83 a-d):

$$\theta_r = -\frac{1}{l}\left\{B_1\left[u_1(r/l)\cos\delta - v_1(r/l)\sin\delta\right] + B_2\left[u_1(r/l)\sin\delta + v_1(r/l)\cos\delta\right]\right\}$$

$$M_r = -\frac{D}{l^2}\left\{\begin{array}{l} B_1\left[\left(u_o(r/l)\cos 2\delta - v_o(r/l)\sin 2\delta\right) - \frac{l}{r}(1-\nu_p)\left(u_1(r/l)\cos\delta - v_1(r/l)\sin\delta\right)\right] \\ +B_2\left[\left(u_o(r/l)\sin 2\delta + v_o(r/l)\cos 2\delta\right) - \frac{l}{r}(1-\nu_p)\left(u_1(r/l)\sin\delta + v_1(r/l)\cos\delta\right)\right] \end{array}\right\}$$

$$M_\theta = -\frac{D}{l^2}\left\{\begin{array}{l} B_1\left[\nu_p\left(u_o(r/l)\cos 2\delta - v_o(r/l)\sin 2\delta\right) + \frac{l}{r}(1-\nu_p)\left(u_1(r/l)\cos\delta - v_1(r/l)\sin\delta\right)\right] \\ +B_2\left[\nu_p\left(u_o(r/l)\sin 2\delta + v_o(r/l)\cos 2\delta\right) + \frac{l}{r}(1-\nu_p)\left(u_1(r/l)\sin\delta + v_1(r/l)\cos\delta\right)\right] \end{array}\right\}$$

$$Q_r = -\frac{D}{l^3}\left\{B_1\left[u_1(r/l)\cos 3\delta - v_1(r/l)\sin 3\delta\right] + B_2\left[u_1(r/l)\sin 3\delta + v_1(r/l)\cos 3\delta\right]\right\}$$

(3.144)

<u>Case II</u> ($G_p^{\,2} = 4k_pD$ or $T = 1$)

The general expression for the displacement of the plate itself and outside (beyond the edge of the plate) are as given by Eq. (3.84) and (3.112).

- ✓ Condition (i) & (ii) necessitate A_2 and A_4 to be zero.

Hence, the general solution of plate deflection reduces to

$$w_1(r) = A_1 J_o(r/l) + A_3 J_o(r/l) \tag{3.145}$$

- ✓ Condition (iii) applies for $w_2(r)$ which is the same as case I.
- ✓ Applying boundary condition (iv) stated in case one,

$$M_{r1}(a) = 0 = -\frac{D}{l^2}\left\{A_1\left[J_o(a/l) - \frac{l}{a}(1-\nu_p)\left(J_1(a/l)\right)\right] + A_3\left[J_o(a/l) - \frac{l}{a}(1-\nu_p)\left(J_1(a/l)\right)\right]\right\}$$

(3.146)

- ✓ Boundary condition (v),

$$Q_{r1}(a) = -\frac{D}{l^3}\left\{A_1 J_1(a/l) + A_3 J_1(a/l)\right\} = G_p\left[-\alpha B_6 k_1(\alpha a) + \frac{1}{l}\left[A_1 J_1(a/l) + A_3 J_1(a/l)\right]\right] + q_o \tag{3.147}$$

✓ Boundary condition (vi) gives,

$$A_1 J_o(\mathrm{a}/l) + A_3 J_o(\mathrm{a}/l) = B_6 K_o(\alpha a) \tag{3.148}$$

From this,

$$B_6 = \frac{A_1 J_o(\mathrm{a}/l) + A_3 J_o(\mathrm{a}/l)}{K_o(\alpha a)} \tag{3.149}$$

Substituting B_6 into Eq. (3.147), we get an equation with constants A_1 and A_2 only. Then solving this equation simultaneously with Eq. (3.146) which also have the same constants, we obtain;

$$A_1 = \frac{q_o\left[J_o(\mathrm{a}/l) - \frac{l}{a}(1-\nu_p)\left(J_1(\mathrm{a}/l)\right)\right]}{k_p l\left\{\begin{array}{l}\left[J_o(\mathrm{a}/l) - \frac{l}{a}(1-\nu_p)\left(J_1(\mathrm{a}/l)\right)\right]\times\left[J_1(\mathrm{a}/l) + \frac{J_1(a/l)}{\frac{k_p l^2}{G_p}} - J_o(a/l)\frac{K_1(\alpha_o a/l)}{\alpha_o K_0(\alpha_o a/l)}\right] \\ - \\ \left[J_o(\mathrm{a}/l) - \frac{l}{a}(1-\nu_p)\left(J_1(\mathrm{a}/l)\right)\right]\times\left[J_1(\mathrm{a}/l) + J_1(\mathrm{a}/l) + \frac{J_1(a/l)}{\frac{k_p l^2}{G_p}} - J_o(a/l)\frac{K_1(\alpha_o a/l)}{\alpha_o K_0(\alpha_o a/l)}\right]\end{array}\right\}}$$

$$A_3 = -\frac{q_o\left[J_o(\mathrm{a}/l)-\frac{l}{a}(1-\nu_p)\left(J_1(\mathrm{a}/l)\right)\right]}{k_p l\left\{\begin{array}{l}\left[J_o(\mathrm{a}/l)-\frac{l}{a}(1-\nu_p)\left(J_1(\mathrm{a}/l)\right)\right]\times\left[J_1(\mathrm{a}/l)+\frac{J_1(a/l)}{\frac{k_p l^2}{G_p}}-J_o(a/l)\frac{K_1(\alpha_o a/l)}{\alpha_o K_0(\alpha_o a/l)}\right] \\ - \\ \left[J_o(\mathrm{a}/l)-\frac{l}{a}(1-\nu_p)\left(J_1(\mathrm{a}/l)\right)\right]\times\left[J_1(\mathrm{a}/l)+J_1(\mathrm{a}/l)+\frac{J_1(a/l)}{\frac{k_p l^2}{G_p}}-J_o(a/l)\frac{K_1(\alpha_o a/l)}{\alpha_o K_0(\alpha_o a/l)}\right]\end{array}\right\}}$$

$$B_6 = \frac{A_1 J_o(\mathrm{a}/l)+A_3 J_o(a/l)}{K_o(\alpha_o a/l)} \tag{3.150}$$

The deflection for different values of *r* will be evaluated using an excel sheet, the slope and the corresponding internal actions in a similar manner like in Eq. (3.85 a-d):

$$\begin{aligned}
\theta_r &= -\frac{1}{l}\left\{A_1 J_1(r/l)+A_3 J_1(r/l)\right\} \\
M_r &= -\frac{D}{l^2}\left\{A_1\left[J_o(r/l)-\frac{l}{r}(1-\nu_p)\left(J_1(r/l)\right)\right]+A_3\left[J_o(r/l)-\frac{l}{r}(1-\nu_p)\left(J_1(r/l)\right)\right]\right\} \\
M_\theta &= -\frac{D}{l^2}\left\{A_1\left[\nu_p J_o(r/l)+\frac{l}{r}(1-\nu_p)J_1(r/l)\right]+A_3\left[\nu_p J_o(r/l)+\frac{l}{r}(1-\nu_p)J_1(r/l)\right]\right\} \\
Q_r &= -\frac{D}{l^3}\left\{A_1 J_1(r/l)+A_3 J_1(r/l)\right\}
\end{aligned} \tag{3.151}$$

Case III ($G_p{}^2 > 4k_p D$ or $T > 1$)

The general expression for the displacement of the plate itself and outside (beyond the edge of the plate) are as given by Eq. (3.86) and (3.112).

- ✓ Condition (i) & (ii) necessitate A_2 and A_4 to be zero.

Hence, the general solution of plate deflection reduces to

$$w_1(r) = A_1 J_o\left(\sqrt{d}\,r/l\right)+A_3 J_o\left(\sqrt{d}\,r/l\right) \tag{3.152}$$

- ✓ Condition (iii) applies for $w_2(r)$ which is the same as case I.
- ✓ Applying boundary condition (iv) stated in case one,

$$M_{r1}(a)=0=-\frac{D}{l^2}\left\{\begin{array}{l}A_1\left[J_o\left(\sqrt{d}a/l\right)\cos 2\delta-\frac{l}{a}\left(1-\nu_p\right)\left(J_1\left(\sqrt{d}a/l\right)\cos\delta\right)\right]\\+A_3\left[J_o\left(\sqrt{\bar{d}}a/l\right)\cos 2\delta-\frac{l}{a}\left(1-\nu_p\right)\left(J_1\left(\sqrt{\bar{d}}a/l\right)\cos\delta\right)\right]\end{array}\right\} \tag{3.153}$$

- ✓ Boundary condition (v),

$$\begin{aligned}&-\frac{D}{l^3}\left\{A_1J_1\left(\sqrt{d}a/l\right)\cos 3\delta+A_3J_1\left(\sqrt{\bar{d}}a/l\right)\cos 3\delta\right\}=\\&G_p\left[-\alpha B_6k_1(\alpha a)+\frac{1}{l}\left[A_1J_1\left(\sqrt{d}a/l\right)\cos\delta+A_3J_1\left(\sqrt{\bar{d}}a/l\right)\cos\delta\right]\right]+q_o\end{aligned} \tag{3.154}$$

- ✓ Boundary condition (vi) gives,

$$A_1J_o\left(\sqrt{d}\ \mathrm{a}/l\right)+A_3J_o\left(\sqrt{\bar{d}}\ \mathrm{a}/l\right)=B_6K_o(\alpha a) \tag{3.155}$$

From this,

$$B_6=\frac{A_1J_o\left(\sqrt{d}\ \mathrm{a}/l\right)+A_3J_o\left(\sqrt{\bar{d}}\ \mathrm{a}/l\right)}{K_o(\alpha a)} \tag{3.156}$$

Substituting B_6 into Eq. (3.154), we get an equation with constants A_1 and A_2 only. Then solving this equation simultaneously with Eq. (3.153) which also have the same constants, we obtain;

$$A_1 = \frac{q_o\left[J_o\left(\sqrt{\bar{d}}\,\mathrm{a}/l\right)\cos 2\delta - \frac{l}{a}\left(1-\nu_p\right)\left(J_1\left(\sqrt{\bar{d}}\,\mathrm{a}/l\right)\cos\delta\right)\right]}{k_p l\left\{\begin{array}{l}\left[J_o\left(\sqrt{\bar{d}}\,\mathrm{a}/l\right)\cos 2\delta - \frac{l}{a}\left(1-\nu_p\right)\left(J_1\left(\sqrt{\bar{d}}\,\mathrm{a}/l\right)\cos\delta\right)\right]\times \\ \left[J_1\left(\sqrt{\bar{d}}\,\mathrm{a}/l\right)\cos 3\delta + \frac{J_1\left(\sqrt{\bar{d}}\,\mathrm{a}/l\right)\cos\delta}{\frac{k_p l^2}{G_p}} - J_o\left(\sqrt{\bar{d}}\,\mathrm{a}/l\right)\frac{K_1\left(\alpha_o a/l\right)}{\alpha_o K_0\left(\alpha_o a/l\right)}\right] \\ - \\ \left[J_o\left(\sqrt{\bar{d}}\,\mathrm{a}/l\right)\cos 2\delta - \frac{l}{a}\left(1-\nu_p\right)\left(J_1\left(\sqrt{\bar{d}}\,\mathrm{a}/l\right)\cos\delta\right)\right]\times \\ \left[J_1\left(\sqrt{d}\,\mathrm{a}/l\right)\cos 3\delta + \frac{J_1\left(\sqrt{d}\,\mathrm{a}/l\right)\cos\delta}{\frac{k_p l^2}{G_p}} - J_o\left(\sqrt{d}\,\mathrm{a}/l\right)\frac{K_1\left(\alpha_o a/l\right)}{\alpha_o K_0\left(\alpha_o a/l\right)}\right]\end{array}\right\}}$$

$$A_3 = -\frac{q_o\left[J_o\left(\sqrt{d}\,\mathrm{a}/l\right)\cos 2\delta - \frac{l}{a}\left(1-\nu_p\right)\left(J_1\left(\sqrt{d}\,\mathrm{a}/l\right)\cos\delta\right)\right]}{k_p l\left\{\begin{array}{l}\left[J_o\left(\sqrt{d}\,\mathrm{a}/l\right)\cos 2\delta - \frac{l}{a}\left(1-\nu_p\right)\left(J_1\left(\sqrt{d}\,\mathrm{a}/l\right)\cos\delta\right)\right]\times \\ \left[J_1\left(\sqrt{\bar{d}}\,\mathrm{a}/l\right)\cos 3\delta + \frac{J_1\left(\sqrt{\bar{d}}\,\mathrm{a}/l\right)\cos\delta}{\frac{k_p l^2}{G_p}} - J_o\left(\sqrt{\bar{d}}\,\mathrm{a}/l\right)\frac{K_1\left(\alpha_o a/l\right)}{\alpha_o K_0\left(\alpha_o a/l\right)}\right] \\ - \\ \left[J_o\left(\sqrt{\bar{d}}\,\mathrm{a}/l\right)\cos 2\delta - \frac{l}{a}\left(1-\nu_p\right)\left(J_1\left(\sqrt{\bar{d}}\,\mathrm{a}/l\right)\cos\delta\right)\right]\times \\ \left[J_1\left(\sqrt{d}\,\mathrm{a}/l\right)\cos 3\delta + \frac{J_1\left(\sqrt{d}\,\mathrm{a}/l\right)\cos\delta}{\frac{k_p l^2}{G_p}} - J_o\left(\sqrt{d}\,\mathrm{a}/l\right)\frac{K_1\left(\alpha_o a/l\right)}{\alpha_o K_0\left(\alpha_o a/l\right)}\right]\end{array}\right\}}$$

$$B_6 = \frac{A_1 J_o\left(\sqrt{d}\,\mathrm{a}/l\right) + A_3 J_o\left(\sqrt{\bar{d}}\,a/l\right)}{K_o\left(\alpha_o a/l\right)} \qquad (3.157)$$

The deflection for different values of r will be evaluated using an excel sheet, the slope and the corresponding internal actions in a similar manner like in Eq. (3.87 a-d):

$$\begin{aligned}
\theta_r &= -\frac{1}{l}\left\{A_1 J_1\left(\sqrt{d}r/l\right)\cos\delta + A_3 J_1\left(\sqrt{\bar{d}}r/l\right)\cos\delta\right\} \\
M_r &= -\frac{D}{l^2}\left\{\begin{aligned}&A_1\left[J_o\left(\sqrt{d}r/l\right)\cos 2\delta - \frac{l}{r}\left(1-\nu_p\right)\left(J_1\left(\sqrt{d}r/l\right)\cos\delta\right)\right] \\ &+A_3\left[J_o\left(\sqrt{\bar{d}}r/l\right)\cos 2\delta - \frac{l}{r}\left(1-\nu_p\right)\left(J_1\left(\sqrt{\bar{d}}r/l\right)\cos\delta\right)\right]\end{aligned}\right\} \\
M_\theta &= -\frac{D}{l^2}\left\{\begin{aligned}&A_1\left[\nu_p J_o\left(\sqrt{d}r/l\right)\cos 2\delta + \frac{l}{r}\left(1-\nu_p\right)J_1\left(\sqrt{d}r/l\right)\cos\delta\right] \\ &+A_3\left[\nu_p J_o\left(\sqrt{\bar{d}}r/l\right)\cos 2\delta + \frac{l}{r}\left(1-\nu_p\right)J_1\left(\sqrt{\bar{d}}r/l\right)\cos\delta\right]\end{aligned}\right\} \\
Q_r &= -\frac{D}{l^3}\left\{A_1 J_1\left(\sqrt{d}r/l\right)\cos 3\delta + A_3 J_1\left(\sqrt{\bar{d}}r/l\right)\cos 3\delta\right\}
\end{aligned} \tag{3.158}$$

III. Circular Plate under Concentrated Edge Moment with Free End Condition

A circumferential moment of M_o that is uniformly distributed per unit length along the edge is considered (see Figure 3.25).

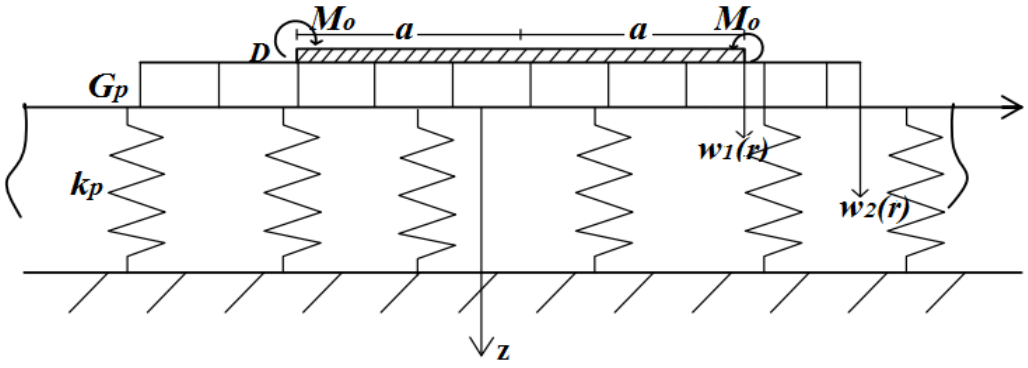

Figure 3.25 Axisymmetric loading of a small circular plate subjected to a concentrated edge moment

The prevailing boundary conditions to determine the constants in reference to Selvadurai (1979) are;

i. For $r = a,\ M_{r1} = M_o$

ii. For $r = a,\ Q_{r1} = G_p\left[\frac{dw_2}{dr} - \frac{dw_1}{dr}\right]$

iii. For $r = a,\ w_1 = w_2$

Case I ($G_p{}^2 < 4k_pD$ or $T < 1$)

The general solution obtained i.e. Eq. (3.81) and (3.112) for the deflection of the plate itself and outside the plate holds true for this loading condition too.

- ✓ Boundary condition (i), is similar to loading (II) using boundary condition (iv) but equal to M_o.

$$M_{r1}(a) = -\frac{D}{l^2}\left\{\begin{array}{l} B_1\left[u_o(\mathrm{a}/l)\cos 2\delta - v_o(\mathrm{a}/l)\sin 2\delta\right] - \frac{l}{a}(1-v_p)\left[u_1(\mathrm{a}/l)\cos\delta + v_1(\mathrm{a}/l)\sin\delta\right] \\ +B_2\left[u_o(\mathrm{a}/l)\sin 2\delta + v_o(\mathrm{a}/l)\cos 2\delta\right] - \frac{l}{a}(1-v_p)\left[u_1(\mathrm{a}/l)\sin\delta + v_1(\mathrm{a}/l)\cos\delta\right] \end{array}\right\} = M_o \tag{3.159}$$

- ✓ Boundary condition (ii), which is similar to boundary condition (v) of loading (II);

$$\begin{aligned} &-\frac{D}{l^3}\left\{B_1\left[u_1(\mathrm{a}/l)\cos 3\delta - v_1(\mathrm{a}/l)\sin 3\delta\right] + B_2\left[u_1(\mathrm{a}/l)\sin 3\delta + v_1(\mathrm{a}/l)\cos 3\delta\right]\right\} \\ &= G_p\left[-\alpha B_6 k_1(\alpha a) + \frac{1}{l}\left[\begin{array}{l} B_1\left(u_1(a/l)\cos\delta - v_1(a/l)\sin\delta\right) \\ +B_2\left(u_1(a/l)\sin\delta + v_1(a/l)\cos\delta\right) \end{array}\right]\right] \end{aligned} \tag{3.160}$$

- ✓ Boundary condition (iii) likewise; boundary condition (vi) of loading (II) gives the same expression for B_6. Then solving for B_1 and B_2.

$$B_1 = \frac{-M_o\left[\left[u_1(\mathrm{a}/l)\sin 3\delta + v_1(\mathrm{a}/l)\cos 3\delta\right] + \dfrac{u_1(\mathrm{a}/l)\sin\delta + v_1(\mathrm{a}/l)\cos\delta}{\dfrac{k_p l^2}{G_p}} - v_o(a/l)\dfrac{K_1(\alpha_o a/l)}{\alpha_o K_0(\alpha_o a/l)}\right]}{k_p l^2\left\{\begin{array}{l}\left[\left(u_o(\mathrm{a}/l)\cos 2\delta - v_o(\mathrm{a}/l)\sin 2\delta\right) - \dfrac{l}{a}(1-\nu_p)\left(u_1(\mathrm{a}/l)\cos\delta - v_1(\mathrm{a}/l)\sin\delta\right)\right]\times \\ \left[u_1(\mathrm{a}/l)\sin 3\delta + v_1(\mathrm{a}/l)\cos 3\delta + \dfrac{u_1(a/l)\sin\delta + v_1(a/l)\cos\delta}{\dfrac{k_p l^2}{G_p}} - v_o(a/l)\dfrac{K_1(\alpha_o a/l)}{\alpha_o K_0(\alpha_o a/l)}\right] - \\ \left[\left(u_o(\mathrm{a}/l)\sin 2\delta + v_o(\mathrm{a}/l)\cos 2\delta\right) - \dfrac{l}{a}(1-\nu_p)\left(u_1(\mathrm{a}/l)\sin\delta + v_1(\mathrm{a}/l)\cos\delta\right)\right]\times \\ \left[u_1(\mathrm{a}/l)\cos 3\delta - v_1(\mathrm{a}/l)\sin 3\delta + \dfrac{u_1(a/l)\cos\delta - v_1(a/l)\sin\delta}{\dfrac{k_p l^2}{G_p}} - u_o(a/l)\dfrac{K_1(\alpha_o a/l)}{\alpha_o K_0(\alpha_o a/l)}\right]\end{array}\right\}}$$

$$B_2 = \frac{M_o\left[\left[u_1(\mathrm{a}/l)\cos 3\delta - v_1(\mathrm{a}/l)\cos 3\delta\right] + \dfrac{u_1(\mathrm{a}/l)\cos\delta - v_1(\mathrm{a}/l)\sin\delta}{\dfrac{k_p l^2}{G_p}} - u_o(a/l)\dfrac{K_1(\alpha_o a/l)}{\alpha_o K_0(\alpha_o a/l)}\right]}{k_p l^2\left\{\begin{array}{l}\left[\left(u_o(\mathrm{a}/l)\cos 2\delta - v_o(\mathrm{a}/l)\sin 2\delta\right) - \dfrac{l}{a}(1-\nu_p)\left(u_1(\mathrm{a}/l)\cos\delta - v_1(\mathrm{a}/l)\sin\delta\right)\right]\times \\ \left[u_1(\mathrm{a}/l)\sin 3\delta + v_1(\mathrm{a}/l)\cos 3\delta + \dfrac{u_1(a/l)\sin\delta + v_1(a/l)\cos\delta}{\dfrac{k_p l^2}{G_p}} - v_o(a/l)\dfrac{K_1(\alpha_o a/l)}{\alpha_o K_0(\alpha_o a/l)}\right] - \\ \left[\left(u_o(\mathrm{a}/l)\sin 2\delta + v_o(\mathrm{a}/l)\cos 2\delta\right) - \dfrac{l}{a}(1-\nu_p)\left(u_1(\mathrm{a}/l)\sin\delta + v_1(\mathrm{a}/l)\cos\delta\right)\right]\times \\ \left[u_1(\mathrm{a}/l)\cos 3\delta - v_1(\mathrm{a}/l)\sin 3\delta + \dfrac{u_1(a/l)\cos\delta - v_1(a/l)\sin\delta}{\dfrac{k_p l^2}{G_p}} - u_o(a/l)\dfrac{K_1(\alpha_o a/l)}{\alpha_o K_0(\alpha_o a/l)}\right]\end{array}\right\}}$$

(3.161)

Therefore, the slope and corresponding internal actions are similarly evaluated using Eq. (3.83).

Case II ($G_p{}^2 = 4k_pD$ or $T = 1$)

The general expression for the displacement of the plate itself and outside (beyond the edge of the plate) are as given by Eq. (3.84) and (3.112).

- ✓ Applying boundary condition (i),

$$M_{r1}(a) = -\frac{D}{l^2}\left\{\begin{array}{l} A_1\left[J_o(\mathrm{a}/l) - \frac{l}{a}(1-\nu_p)\left(J_1(\mathrm{a}/l)\right)\right] \\ +A_3\left[J_o(\mathrm{a}/l) - \frac{l}{a}(1-\nu_p)\left(J_1(\mathrm{a}/l)\right)\right] \end{array}\right\} = M_o \tag{3.162}$$

- ✓ Boundary condition (ii),

$$-\frac{D}{l^3}\left\{A_1J_1(\mathrm{a}/l) + A_3J_1(\mathrm{a}/l)\right\} = G_p\left[-\alpha B_6 k_1(\alpha a) + \frac{1}{l}\left[A_1J_1(\mathrm{a}/l) + A_3J_1(\mathrm{a}/l)\right]\right] \tag{3.163}$$

- ✓ Boundary condition (iii) likewise; boundary condition (vi) of loading (II) gives the same expression for B_6. Then solving for A_1 and A_3.

$$A_1 = \frac{-M_o\left[\left(J_1(\mathrm{a}/l) + \frac{J_1(\mathrm{a}/l)}{\frac{k_pl^2}{G_p}}\right) - J_0(\mathrm{a}/l)\frac{K_1(\alpha_o a/l)}{\alpha_o K_0(\alpha_o a/l)}\right]}{k_pl^2\left\{\begin{array}{l} \left[J_0(\mathrm{a}/l) - \frac{l}{a}(1-\nu_p)\left(J_1(\mathrm{a}/l)\right)\right]\times\left[J_1(\mathrm{a}/l) + J_1(\mathrm{a}/l) - J_0(\mathrm{a}/l)\frac{K_1(\alpha_o a/l)}{\alpha_o K_0(\alpha_o a/l)}\right] \\ - \\ \left[J_0(\mathrm{a}/l) - \frac{l}{a}(1-\nu_p)\left(J_1(\mathrm{a}/l)\right)\right]\times\left[J_1(\mathrm{a}/l) + \frac{J_1(\mathrm{a}/l)}{\frac{k_pl^2}{G_p}} - J_0(\mathrm{a}/l)\frac{K_1(\alpha_o a/l)}{\alpha_o K_0(\alpha_o a/l)}\right] \end{array}\right\}}$$

$$A_3 = \frac{M_o\left[\left(J_1(\mathrm{a}/l)+\frac{J_1(\mathrm{a}/l)}{\frac{k_p l^2}{G_p}}\right)-J_0(\mathrm{a}/l)\frac{K_1(\alpha_o a/l)}{\alpha_o K_0(\alpha_o a/l)}\right]}{k_p l^2\left\{\begin{array}{l}\left[J_0(\mathrm{a}/l)-\frac{l}{a}(1-\nu_p)(J_1(\mathrm{a}/l))\right]\times\left[J_1(\mathrm{a}/l)+J_1(\mathrm{a}/l)-J_0(\mathrm{a}/l)\frac{K_1(\alpha_o a/l)}{\alpha_o K_0(\alpha_o a/l)}\right] \\ - \\ \left[J_0(\mathrm{a}/l)-\frac{l}{a}(1-\nu_p)(J_1(\mathrm{a}/l))\right]\times\left[J_1(\mathrm{a}/l)+\frac{J_1(\mathrm{a}/l)}{\frac{k_p l^2}{G_p}}-J_0(\mathrm{a}/l)\frac{K_1(\alpha_o a/l)}{\alpha_o K_0(\alpha_o a/l)}\right]\end{array}\right\}} \tag{3.164}$$

Therefore, the slope and corresponding internal actions are similarly evaluated using Eq. (3.85).

Case III ($G_p^{\,2} > 4k_pD$ or $T > 1$)

The general expression for the displacement of the plate itself and outside (beyond the edge of the plate) are as given by Eq. (3.86) and (3.112).

- ✓ Applying boundary condition (i),

$$M_{r1}(a) = -\frac{D}{l^2}\left\{\begin{array}{l}A_1\left[J_o\left(\sqrt{d}\,\mathrm{a}/l\right)\cos 2\delta-\frac{l}{a}(1-\nu_p)\left(J_1\left(\sqrt{d}\,\mathrm{a}/l\right)\cos\delta\right)\right] \\ +A_3\left[J_o\left(\sqrt{\bar{d}}\,\mathrm{a}/l\right)\cos 2\delta-\frac{l}{a}(1-\nu_p)\left(J_1\left(\sqrt{\bar{d}}\,\mathrm{a}/l\right)\cos\delta\right)\right]\end{array}\right\} = M_o \tag{3.165}$$

- ✓ Boundary condition (ii),

$$\begin{aligned}&-\frac{D}{l^3}\left\{A_1J_1\left(\sqrt{d}\,\mathrm{a}/l\right)\cos 3\delta + A_3J_1\left(\sqrt{\bar{d}}\,\mathrm{a}/l\right)\cos 3\delta\right\} = \\ &G_p\left[-\alpha B_6k_1(\alpha a)+\frac{1}{l}\left[A_1J_1\left(\sqrt{d}\,\mathrm{a}/l\right)\cos\delta + A_3J_1\left(\sqrt{\bar{d}}\,\mathrm{a}/l\right)\cos\delta\right]\right]\end{aligned} \tag{3.166}$$

- ✓ Boundary condition (iii) likewise; boundary condition (vi) of loading (II) gives the same expression for B_6. Then solving for A_1 and A_3.

$$A_1 = \frac{-M_o\left[\left(J_1\left(\sqrt{\bar{d}}\,\mathrm{a}/l\right)\cos 3\delta + \dfrac{J_1\left(\sqrt{\bar{d}}\,\mathrm{a}/l\right)\cos\delta}{\dfrac{k_p l^2}{G_p}}\right) - J_0\left(\sqrt{\bar{d}}\,\mathrm{a}/l\right)\dfrac{K_1(\alpha_o a/l)}{\alpha_o K_0(\alpha_o a/l)}\right]}{k_p l^2\left\{\begin{array}{l}\left[J_0\left(\sqrt{d}\,\mathrm{a}/l\right)\cos 2\delta - \dfrac{l}{a}(1-\nu_p)\left(J_1\left(\sqrt{d}\,\mathrm{a}/l\right)\cos\delta\right)\right]\times \\ \left[J_1\left(\sqrt{\bar{d}}\,\mathrm{a}/l\right)\cos 3\delta + \dfrac{J_1\left(\sqrt{\bar{d}}\,\mathrm{a}/l\right)\cos\delta}{\dfrac{k_p l^2}{G_p}} - J_0\left(\sqrt{\bar{d}}\,\mathrm{a}/l\right)\dfrac{K_1(\alpha_o a/l)}{\alpha_o K_0(\alpha_o a/l)}\right] \\ - \\ \left[J_0\left(\sqrt{\bar{d}}\,\mathrm{a}/l\right)\cos 2\delta - \dfrac{l}{a}(1-\nu_p)\left(J_1\left(\sqrt{\bar{d}}\,\mathrm{a}/l\right)\cos\delta\right)\right]\times \\ \left[J_1\left(\sqrt{d}\,\mathrm{a}/l\right)\cos 3\delta + \dfrac{J_1\left(\sqrt{d}\,\mathrm{a}/l\right)\cos\delta}{\dfrac{k_p l^2}{G_p}} - J_0\left(\sqrt{d}\,\mathrm{a}/l\right)\dfrac{K_1(\alpha_o a/l)}{\alpha_o K_0(\alpha_o a/l)}\right]\end{array}\right\}}$$

$$A_3 = \frac{M_o\left[\left(J_1\left(\sqrt{d}\,\mathrm{a}/l\right)\cos 3\delta + \dfrac{J_1\left(\sqrt{d}\,\mathrm{a}/l\right)\cos\delta}{\dfrac{k_p l^2}{G_p}}\right) - J_0\left(\sqrt{d}\,\mathrm{a}/l\right)\dfrac{K_1(\alpha_o a/l)}{\alpha_o K_0(\alpha_o a/l)}\right]}{k_p l^2\left\{\begin{array}{l}\left[J_0\left(\sqrt{d}\,\mathrm{a}/l\right)\cos 2\delta - \dfrac{l}{a}(1-\nu_p)\left(J_1\left(\sqrt{d}\,\mathrm{a}/l\right)\cos\delta\right)\right]\times \\ \left[J_1\left(\sqrt{\bar{d}}\,\mathrm{a}/l\right)\cos 3\delta + \dfrac{J_1\left(\sqrt{\bar{d}}\,\mathrm{a}/l\right)\cos\delta}{\dfrac{k_p l^2}{G_p}} - J_0\left(\sqrt{\bar{d}}\,\mathrm{a}/l\right)\dfrac{K_1(\alpha_o a/l)}{\alpha_o K_0(\alpha_o a/l)}\right] \\ - \\ \left[J_0\left(\sqrt{\bar{d}}\,\mathrm{a}/l\right)\cos 2\delta - \dfrac{l}{a}(1-\nu_p)\left(J_1\left(\sqrt{\bar{d}}\,\mathrm{a}/l\right)\cos\delta\right)\right]\times \\ \left[J_1\left(\sqrt{d}\,\mathrm{a}/l\right)\cos 3\delta + \dfrac{J_1\left(\sqrt{d}\,\mathrm{a}/l\right)\cos\delta}{\dfrac{k_p l^2}{G_p}} - J_0\left(\sqrt{d}\,\mathrm{a}/l\right)\dfrac{K_1(\alpha_o a/l)}{\alpha_o K_0(\alpha_o a/l)}\right]\end{array}\right\}} \qquad (3.167)$$

Therefore, the corresponding slope and internal actions are similarly evaluated using Eq. (3.87 a-d).

Chapter Four: NUMERICAL ANALYSIS

4.1 Introduction

In this chapter, numerical studies and evaluations of circular plates are made for Winkler and Pasternak-type subgrade models derived using Worku's generalized approach. The results obtained are compared with FEM (PLAXIS 2D) model outputs as applied to circular plates of large and small radii subjected to the loading conditions treated in the previous chapter. The procedures and formats of this chapter are similar to those of Degu (2008) established for analysis of beams.

The solutions for different loadings supported by Pasternak's foundation are expressed in terms of the coefficients of the elastic spring stiffness, K_p, and stiffness of the shear layer, G_p. As these coefficients are dependent on the plate and soil parameters, various solutions of the deflection with the loading types are obtained. Hence the case to be considered for practical applications should be selected.

4.2 Identification of the Different Solution Cases for the Two-Parameter Subgrade Model

Among the different solution cases that ascended in the previous chapter under the circular plates on a two parameter subgrade, the case which represents most or all real cases should be chosen. This observation can be made by plotting the parameter, *T*, against another selected parameter combining all factors influencing *T* for selected values of thickness of the stratum, *H*. *T* is a function of G_p, E_p, h, ν_p, G and H. The following dimensionless stiffness factor or relative rigidity of the soil-plate system as suggested by Rajapakse and Selvadurai (1991) can be used to see the effect of these parameters.

$$K_r = \frac{E_p * \left(\frac{h_p}{a}\right)^3}{G} \tag{4.1}$$

Where a is the radius of the plate.

This relation is introduced because it is best to observe the effect of the above listed factors on the parameter *T* for various relative values of stratum thickness, rather than the characteristic of the plate-soil system.

Then combining Eq. (4.1) with the relationship for *T* in Eq. (3.79), one obtains

$$T = \frac{G_p}{\sqrt{4K_r D}} \tag{4.2}$$

The soil and plate properties taken to identify the case, and for illustration purpose of all the examples are as shown in the following table. (Table 4.1)

Table 4.1 Soil and Plate Properties (Bowles, 1997; Das, 2007 and EBCS-2, 1995).

Soil parameters			Plate Property	
	E_s(KN/m^2)	μ_s	Plate type	RC
Soft Clay	15,000	0.4	E_p (Gpa)	25
Medium Stiff Clay	30,000	0.3	ν_p	0.2
Stiff Clay	80,000	0.25	h_p(m)	0.15
Loose sand	20,000	0.3	ϕ (m)	20
Medium Dense Sand	40,000	0.25		
Dense Sand	81,000	0.2		

Taking these values the effect of relative rigidity on *T* can be observed with the help of an excel sheet. And the plot of *T* against K_r for various relative values of stratum thickness with respect to the radius of the plate are shown in Figure 4.1.

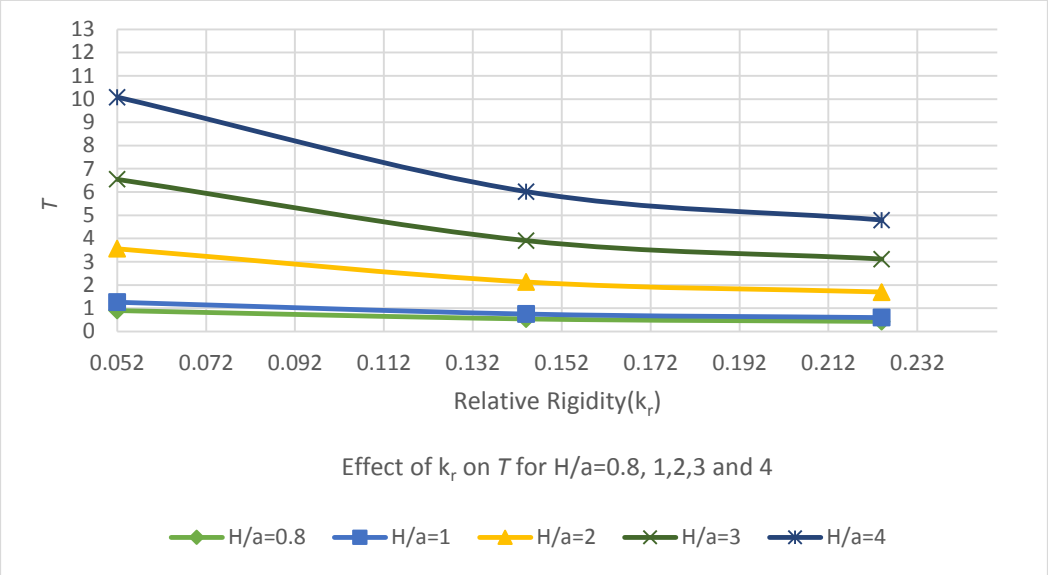

Figure 4.1 Effects of K_r and H on T

From the above plot of T against K_r for four relative stratum thicknesses on different soil types, it can be concluded that it is suitable to consider case three .i.e. $T > 1$ for almost all practical purposes. For the reason that, the occurrence of T less than the limiting value 0.8 is pronounced in a very soft soils which are unfit to bear the load of any foundation. And also the likelihood of the other two cases to take place is less as compared to the case three. Hence, the solutions developed for this case are used for the illustration of Pasternak's model.

4.3 Determination of the Calibration Factor for Winkler-Type and Pasternak-Type Subgrade Models

It is stated previously that Winkler and Pasternak type of models of Worku are sensitive to the stratum thickness, H as do all other simplified continuum models. Hence, it is vital to calibrate them with respect to this parameter in order to avoid their dependence on the soil thickness with the aid of FE-based (PLAXIS 2D) software.

In order to calibrate these two models the first thing to do is to obtain the optimum mesh size of the PLAXIS so that a sufficiently accurate result is achieved. This is attained by plotting the average mesh size against the maximum deflection and taking the average mesh size which gives approximately a constant deflection as shown in Figure 4.2. And Figure 4.3 shows PLAXIS plot of the mesh with fine global coarseness of the grid for the chosen geometry, with two clusters.

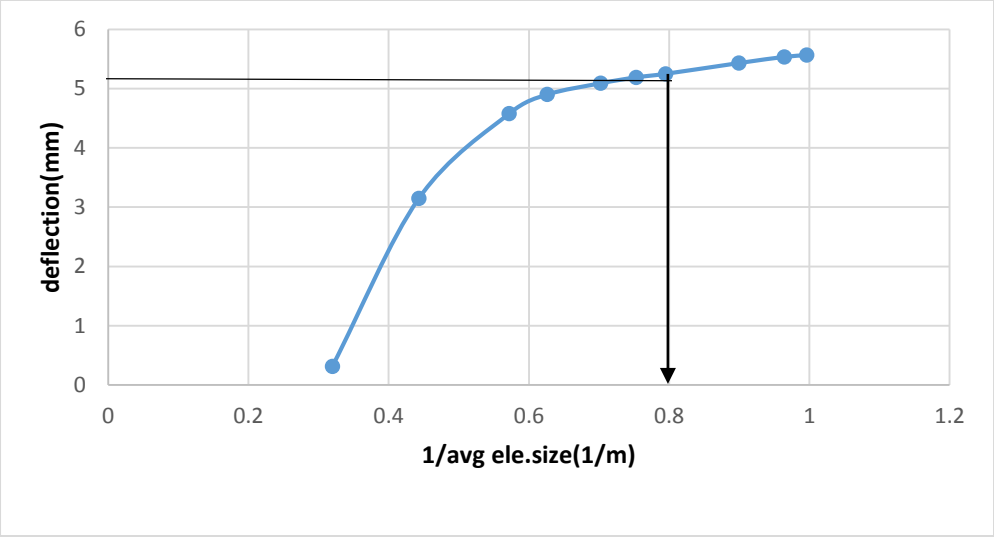

Figure 4.2 Effect of mesh size on deflection

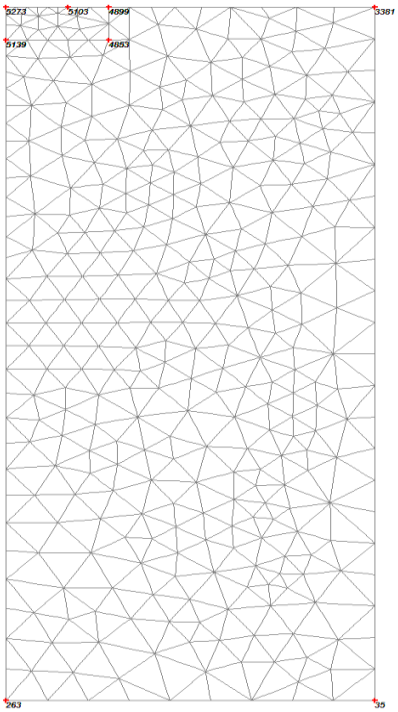

Figure 4.3 Plot of the mesh with significant nodes

It can be seen that the average element size which results in a more or less constant deflection is about 1.25m.

The next step will be calibrating the Winkler and Pasternak type models considering the loading conditions used to analyze the plate in the previous chapter. For the illustration purpose, typical graphs are presented for large and small circular plates separately when subjected to concentrated central and edge loads, and uniformly distributed loadings. To undertake the calibration, a selected soil type is taken for various relative thickness of stratum, $\chi = H / \phi$, where ϕ is the diameter of the circular plate. Note that in the above expression ϕ is taken instead of B since the reference parameter for circular plates is its diameter.

Then the maximum deflection is plotted against χ and the value of χ that gives a deflection in agreement with the PLAXIS output is identified for both models. Note that these values are selected corresponding to the intersection point of the asymptotic line drawn to the PLAXIS plot and the graphs of the models to be calibrated. This is illustrated in Figure 4.3 and 4.4 for a large circular plate on a typical soil under a central concentrated and distributed loadings, and for a small circular plate, under a concentrated central and edge loading cases, respectively.

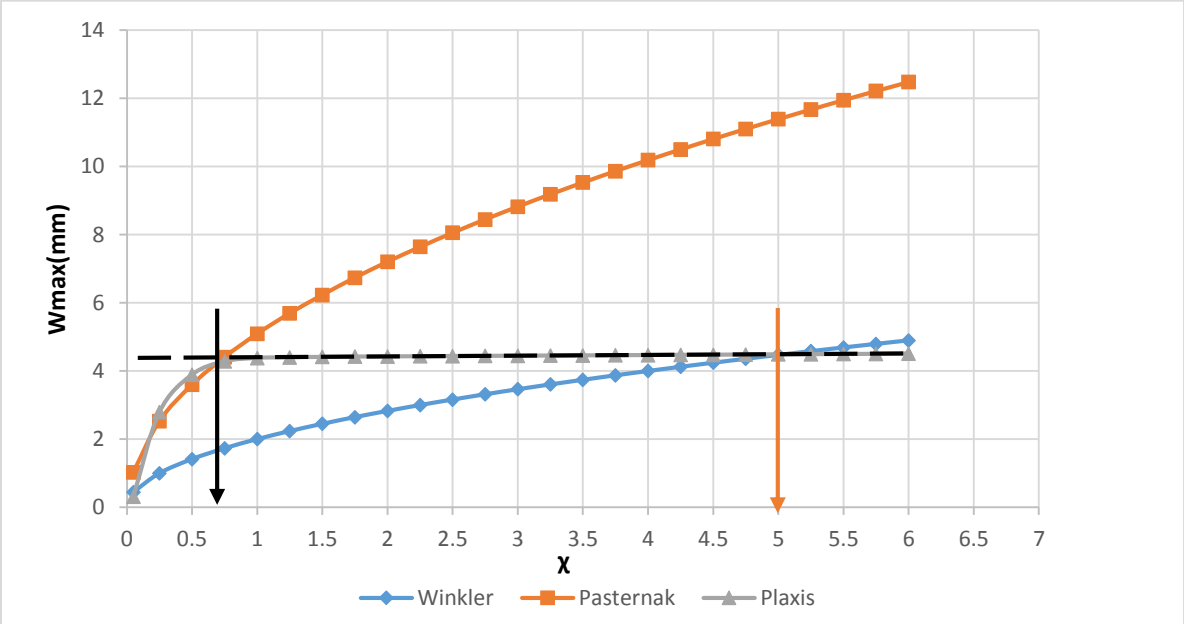

(a)

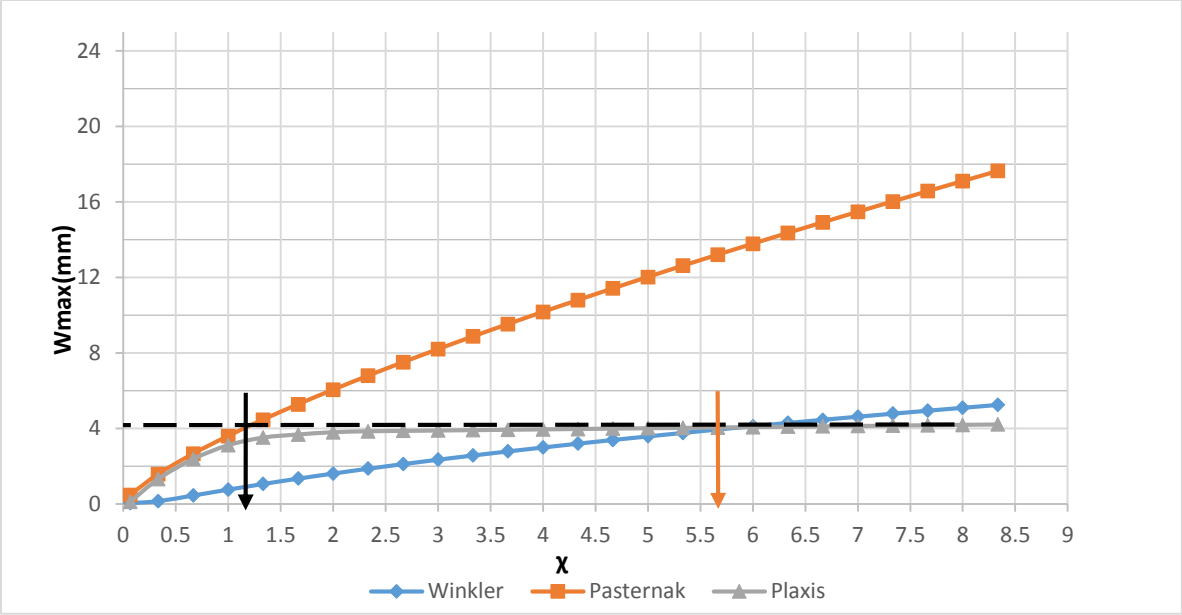

(b)

Figure 4.4 Determination of χ using (a) central concentrated load and (b) uniformly distributed load for large circular plates.

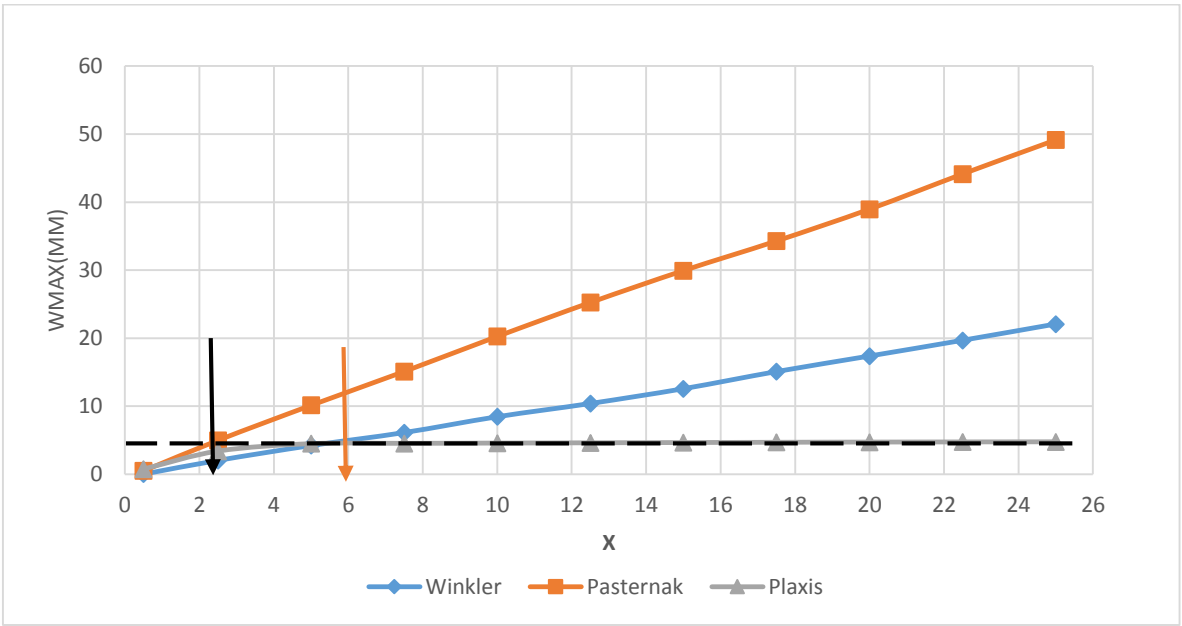

(a)

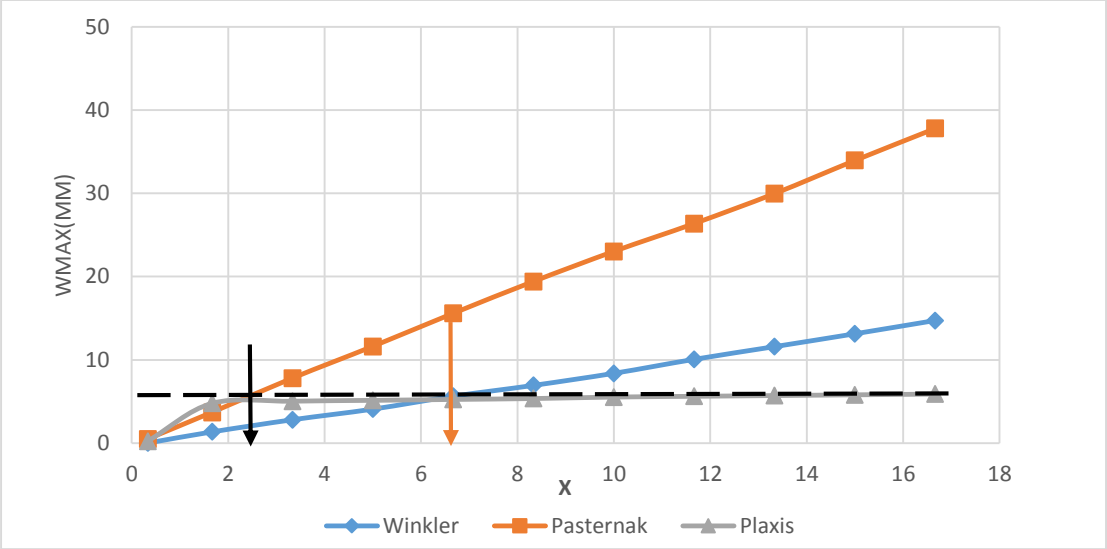

(b)

Figure 4.5 Determination of χ using (a) central concentrated load and (b) concentrated edge load for small circular plates.

And this whole process is repeated for numerous values of relative rigidity desired to cover any possible practical range for the four loading conditions stated. Finally, the best fitting trend is established (for both models) between χ and the characteristic size of the circular plate – soil system, $\tilde{\lambda}$, on different soil types for the ranges of values observed from the above graphs. These plots are presented in Figures 4.6 to 4.13.

4.3.1 Best Curve fittings for χ Determination

4.3.1.1 Winkler's Model

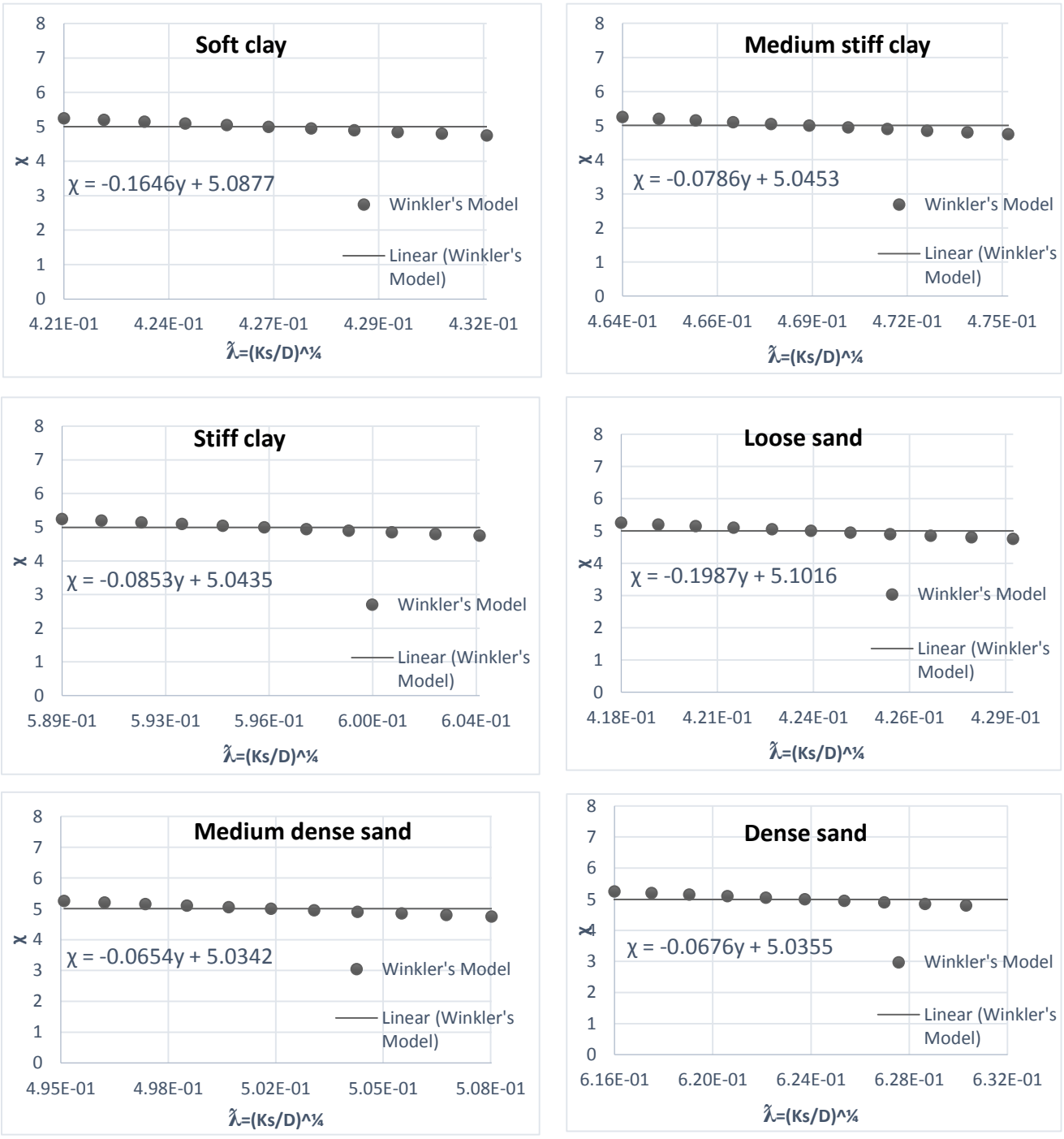

Figure 4.6 Calibration of Winkler's model for a central concentrated loading on large circular plates for weak to strong soils.

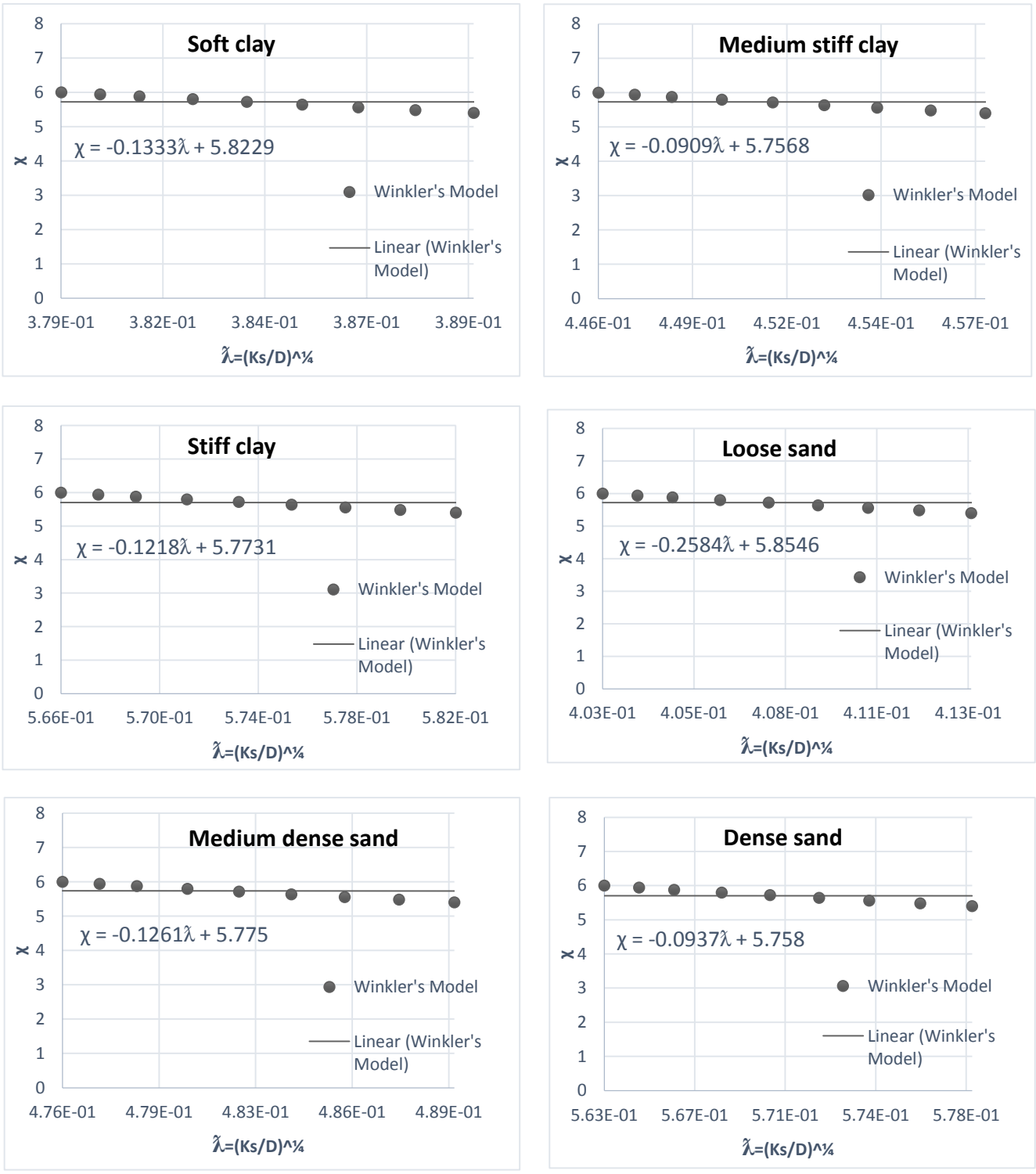

Figure 4.7 Calibration of Winkler's model for uniformly distributed loading on large circular plates for weak to strong soils.

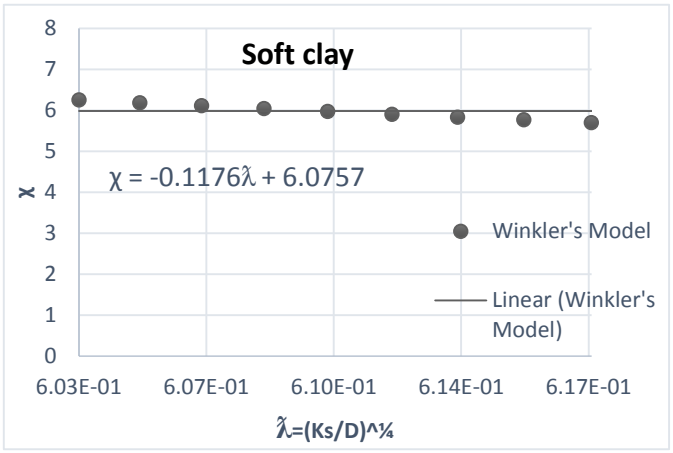

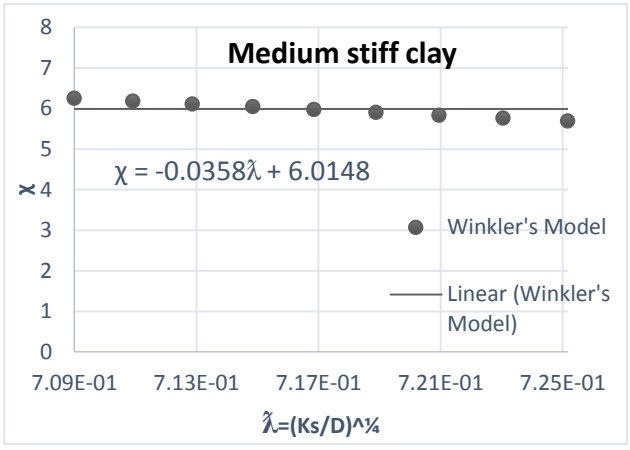

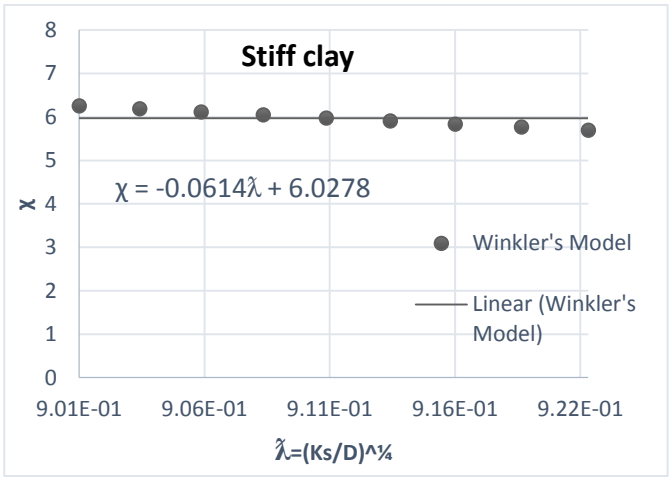

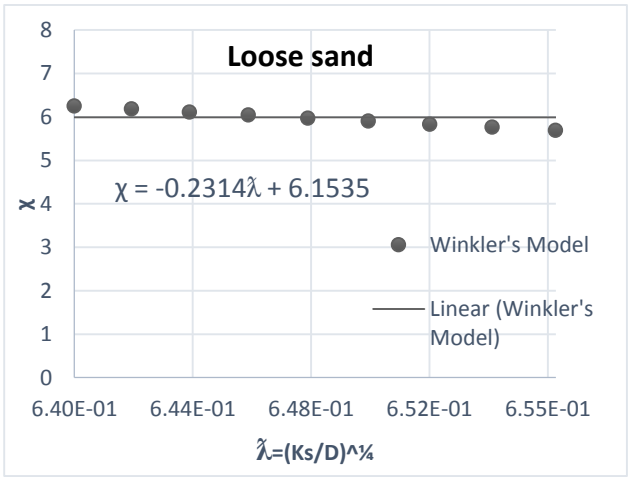

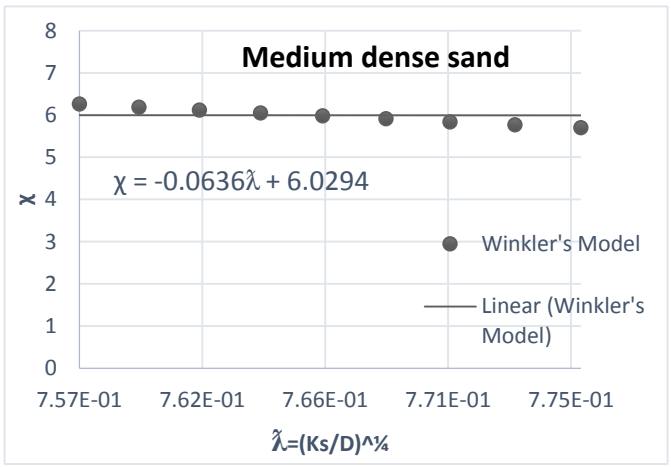

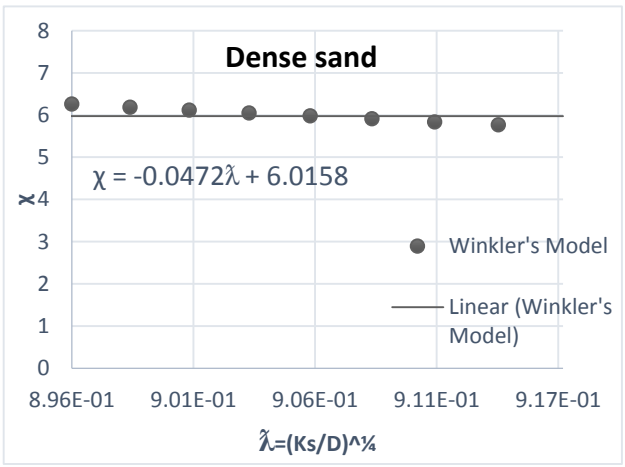

Figure 4.8 Calibration of Winkler's model for a central concentrated loading on small circular plates for weak to strong soils.

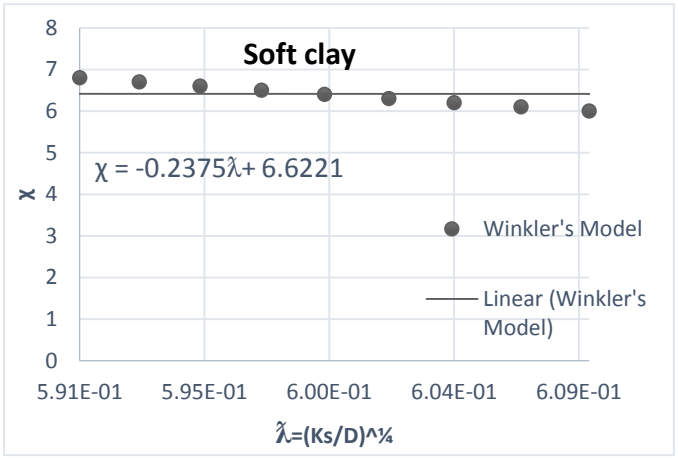

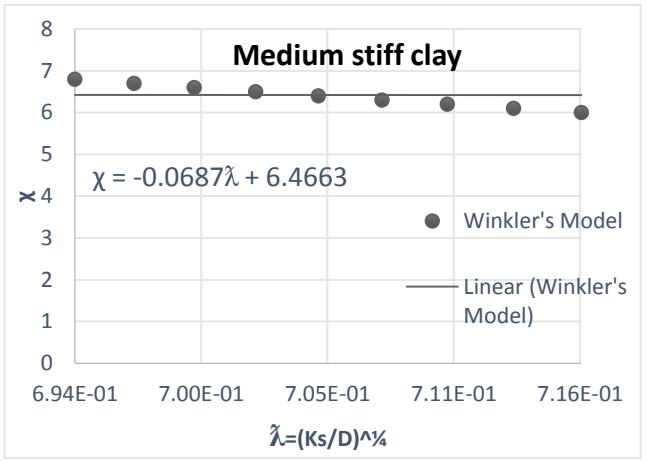

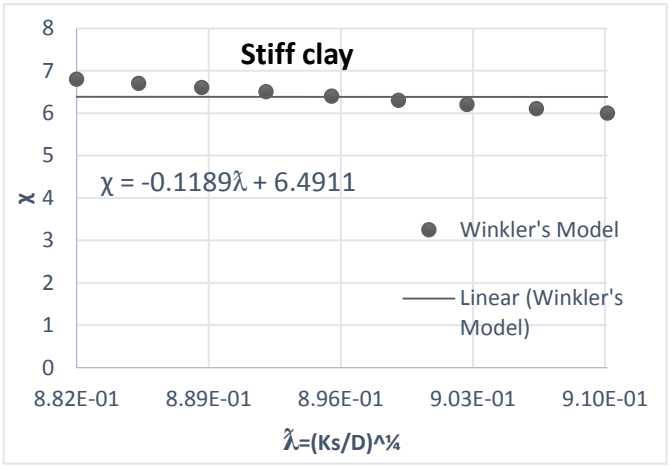

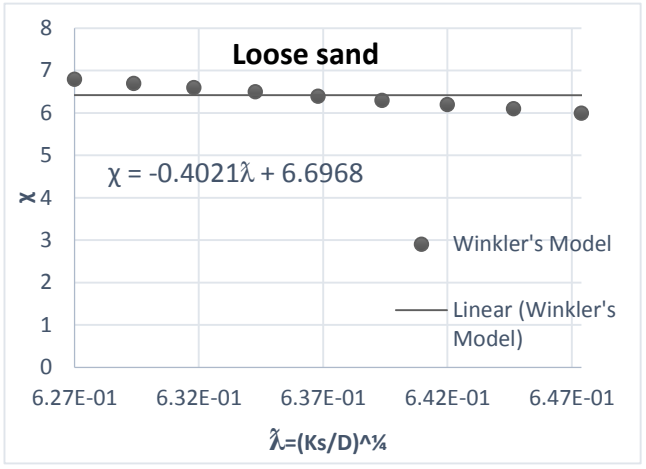

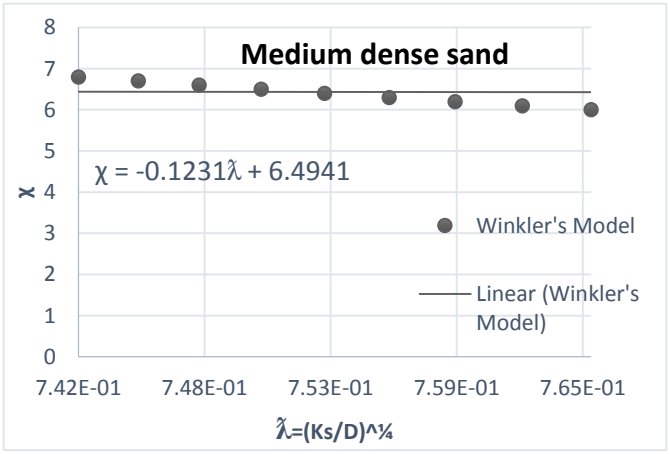

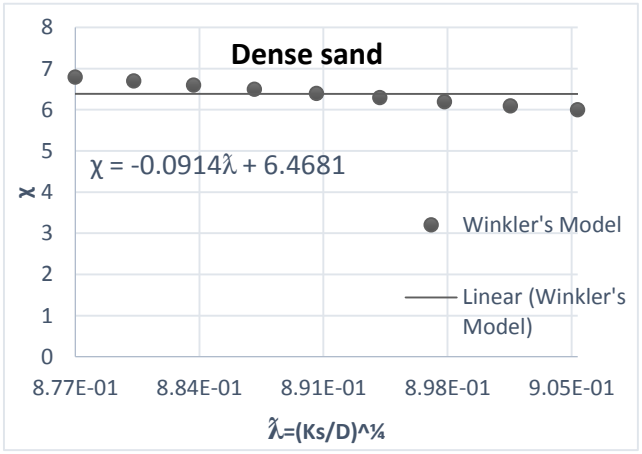

Figure 4.9 Calibration of Winkler's model for a concentrated edge loading on small circular plates for weak to strong soils.

4.3.1.2 Pasternak's Model

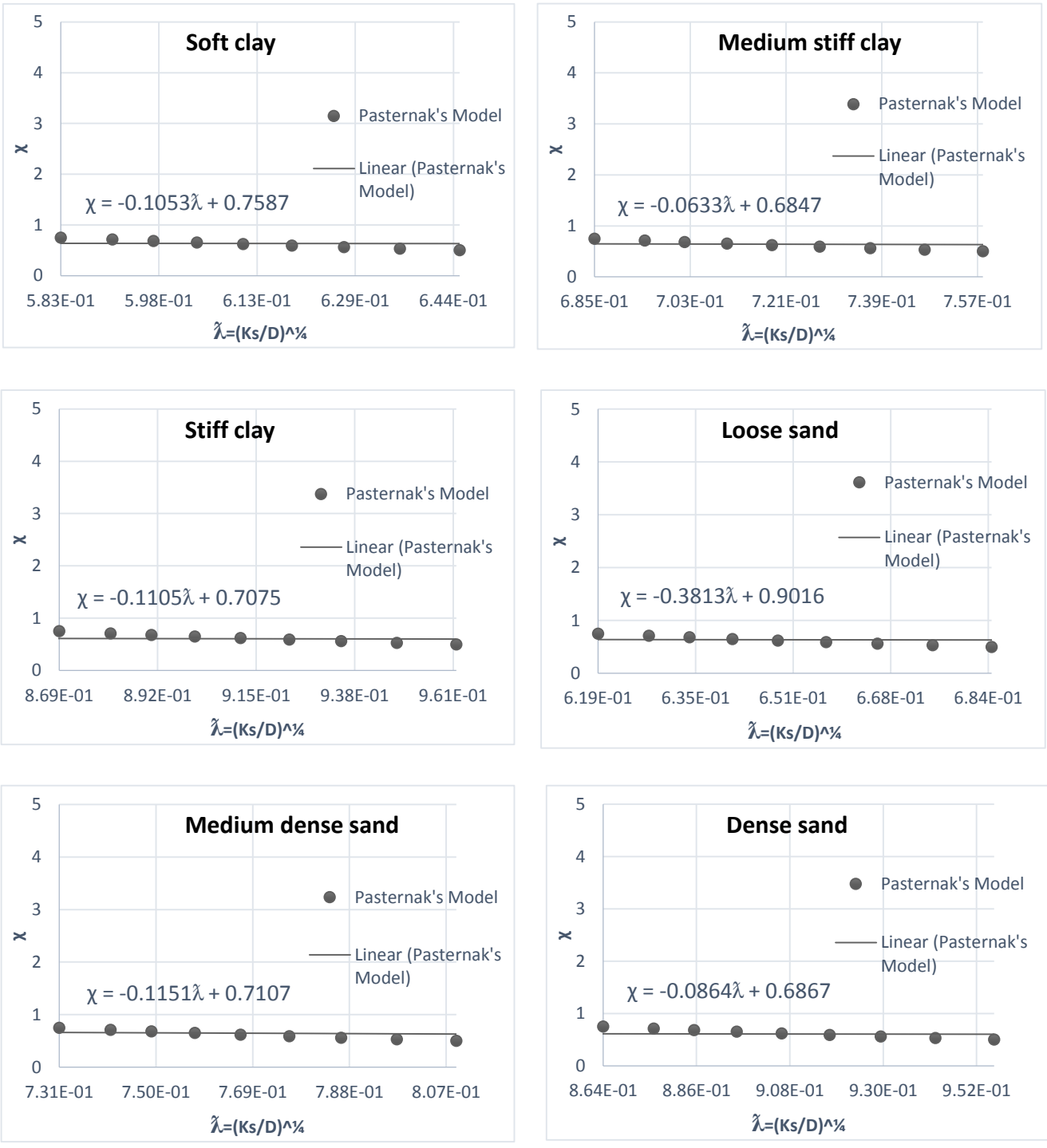

Figure 4.10 Calibration of Pasternak's model for a central concentrated loading on large circular plates for weak to strong soils.

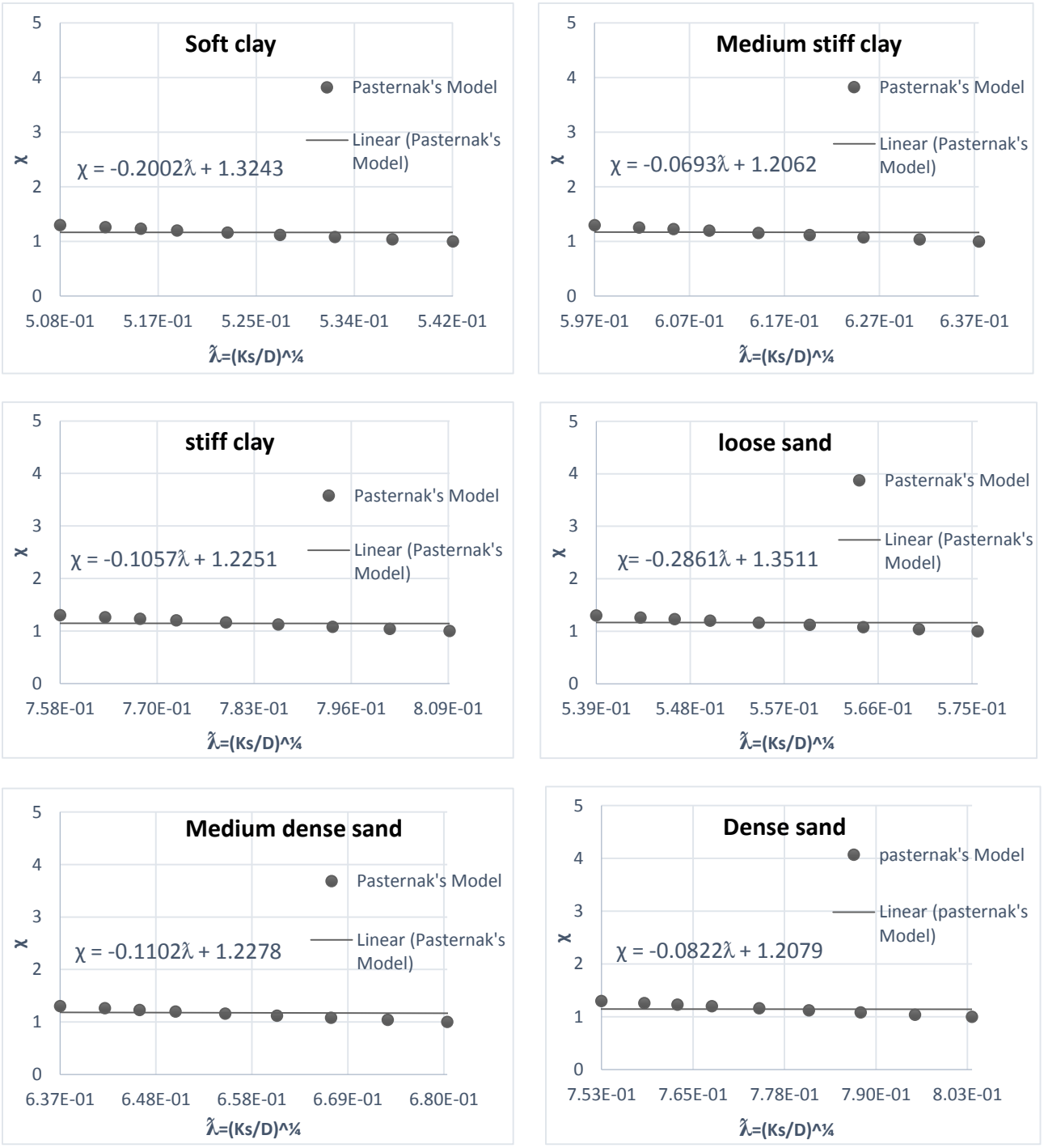

Figure 4.11 Calibration of Pasternak's model for uniformly distributed loading on large circular plates for weak to strong soils.

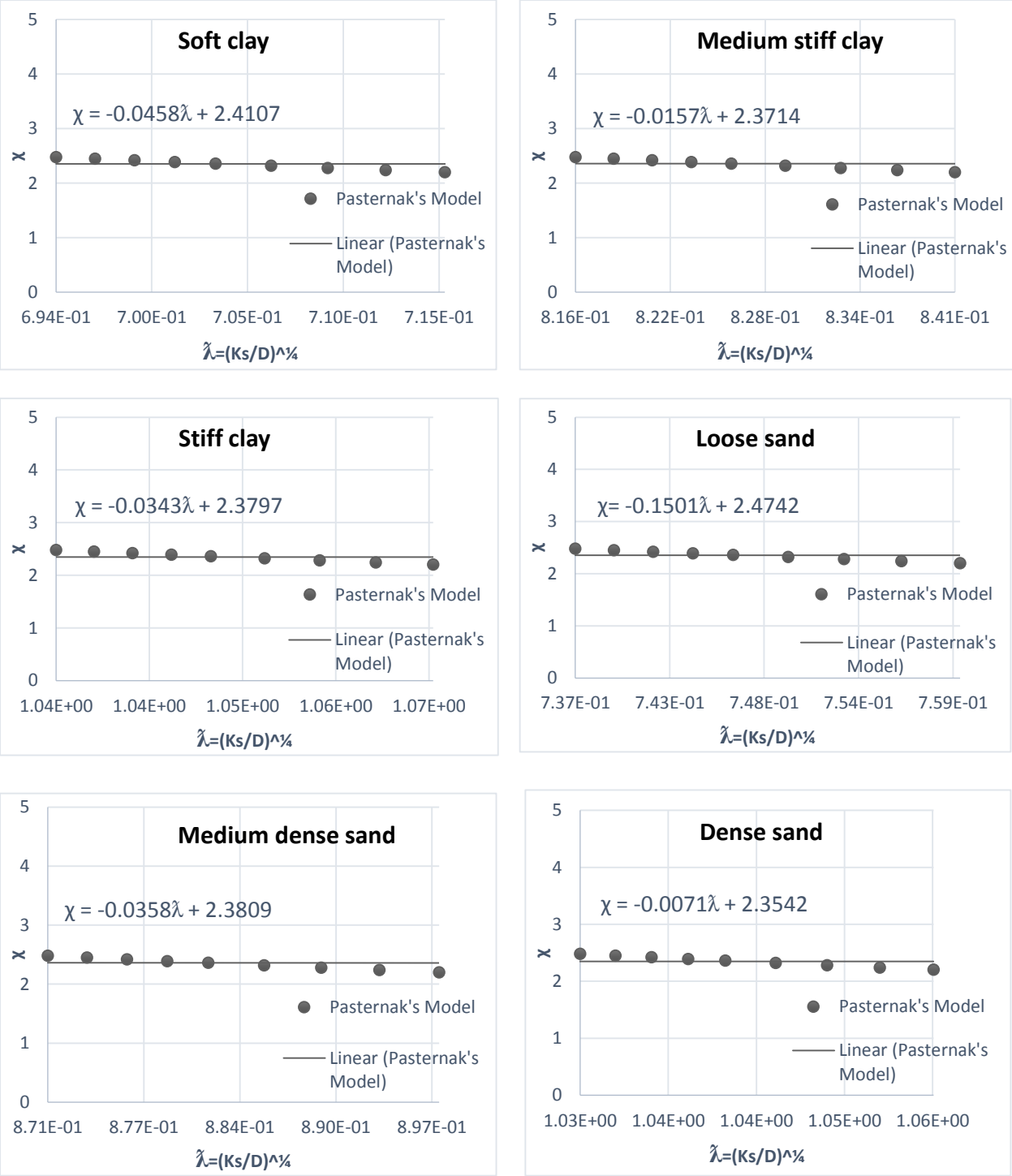

Figure 4.12 Calibration of Pasternak's model for a central concentrated loading on small circular plates for weak to strong soils.

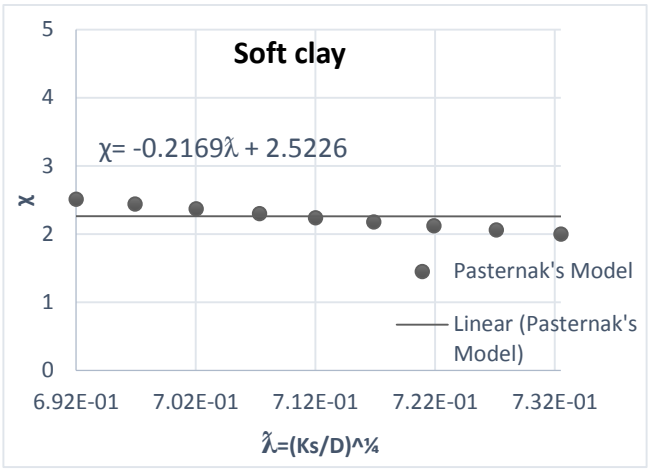

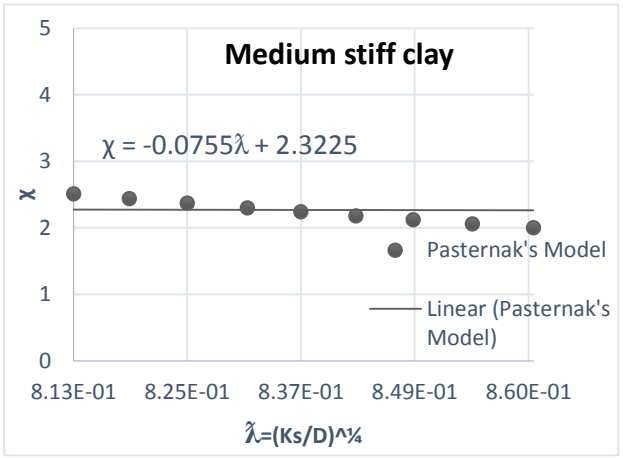

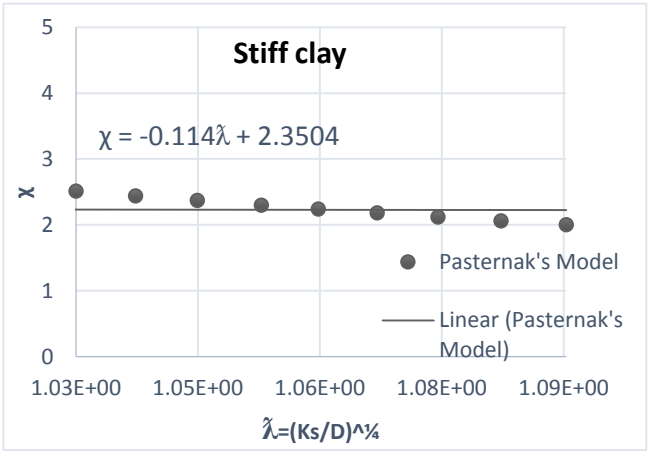

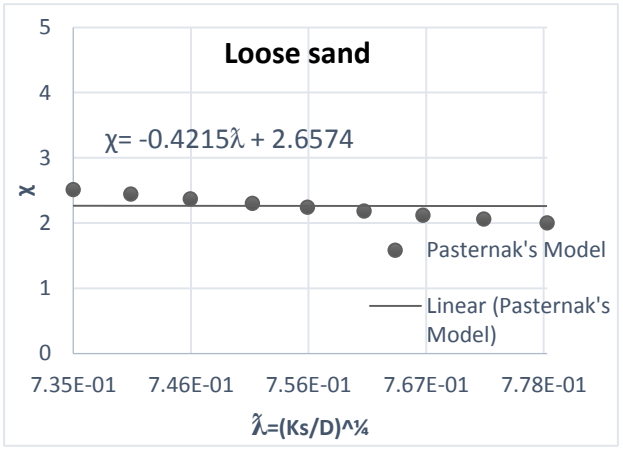

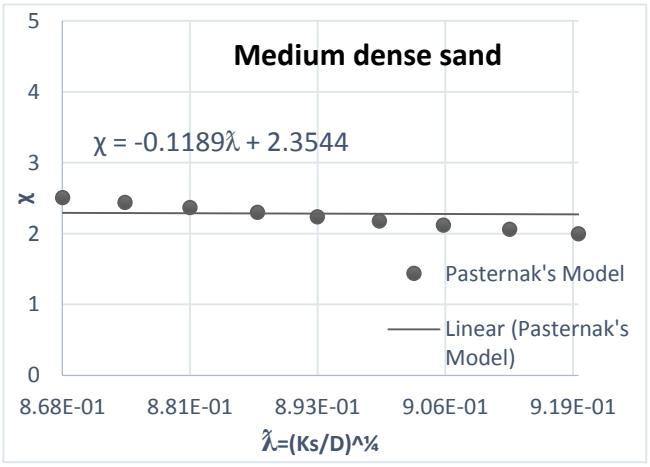

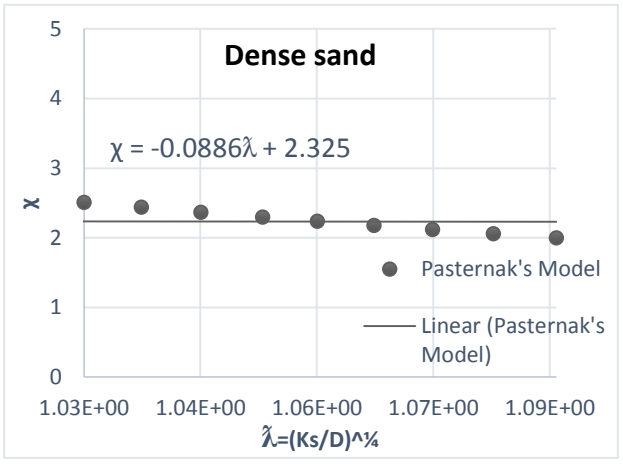

Figure 4.13 Calibration of Pasternak's model for a concentrated edge loading on small circular plates for weak to strong soils.

From the above curves of χ versus the characteristic size of the circular plate-soil system (λ), it can be seen clearly that:

- Almost all points lie on a horizontal band and the plots of both models show consistent trend irrespective of the loading type.
- Pasternak's model exhibits much lower values of χ compared to Winkler's model.
- From the slopes we can conclude that both models are less sensitive to the variation of the characteristic size of the circular plate-soil system λ.

The recommended values of χ for large and small circular plates subjected to different loading conditions on weak to strong soils are summarized in Table, 4.2 and 4.3.

Table 4.2 Recommended values of χ for large circular plates

Recommended values of χ for large circular plates on different soil types for the respective loading conditions				
Soil Type	**Central Concentrated Load**		**Uniformly Distributed Load**	
	Winkler's Model (χ_w)	Pasternak's Model (χ_p)	Winkler's Model (χ_w)	Pasternak's Model (χ_p)
Soft Clay	5.03	0.69	5.77	1.22
Medium Stiff Clay	5.01	0.64	5.72	1.16
Stiff Clay	4.99	0.61	5.7	1.14
Loose Sand	5.02	0.67	5.75	1.19
Medium Dense Sand	5	0.63	5.71	1.15
Dense Sand	4.99	0.61	5.7	1.14

Table 4.3 Recommended values of χ for small circular plates

Recommended values of χ for small circular plates on different soil types for the respective loading conditions				
Soil Type	**Central Concentrated Load**		**Concentrated Edge Load**	
	Winkler's Model (χ_w)	Pasternak's Model (χ_p)	Winkler's Model (χ_w)	Pasternak's Model (χ_p)
Soft Clay	6.02	2.38	6.48	2.37
Medium Stiff Clay	5.99	2.36	6.42	2.26
Stiff Clay	5.97	2.34	6.38	2.23
Loose Sand	6	2.36	6.45	2.35
Medium Dense Sand	5.98	2.35	6.4	2.25
Dense Sand	5.97	2.34	6.38	2.23

As the Figures 4.3 and 4.4 show, the models suggested by Worku are sensitive to thickness of the stratum. Hence, for an actual stratum with $H > \chi\phi$, it is recommended to take the calibration factors given in Table 4.2 and 4.3. However, the actual depth can be taken as it is for smaller thicknesses.

4.4 Calibration of Model Parameters

As stated above, the calibrating parameter takes the form

$$H = \chi\phi \tag{4.3}$$

Where H is the thickness of the stratum, ϕ is the diameter of the circular plate and χ is established from the calibration of both models as recommended in Table, 4.2 and 4.3.

a) Winkler's subgrade model

With the insertion of Eq. (4.3) into the Winkler –type continuum model of Worku, Eq. (2.43) and with the recommended χ values for this model, we have;

$$k_w = \frac{E_s}{(1-0.4\nu)\chi_w\phi} \tag{4.4}$$

b) Pasternak's subgrade model

With the insertion of Eq. (4.3) into the Kerr equivalent Pasternak–type continuum model of Worku, Eq. (2.57) and with the recommended χ values for this model, one obtains

$$k_p = \frac{(0.4\nu + 0.67)E_s}{\chi_p\phi},\ G_p = (1.36\nu + 2.28)G\chi_p\phi \tag{4.5}$$

4.5 Illustrative Examples

In this section, Winkler and Pasternak type models will be compared with the FE-based PLAXIS 2D results for selected loading conditions and for circular plates of large and small radii. The plate is classified by adopting the classification of beams proposed by Hetenyi (1946) with some adjustments.

i. Small circular plates: $\lambda\phi < \pi/4$, λ is the characteristics size of the circular plate
ii. Intermediate circular plates: $\pi/4 < \lambda\phi < \pi$
iii. Large circular plates: $\lambda\phi > \pi$

Circular plates which satisfy the requirements of class II can be classified as small plates according to Selvadurai (1979). Hence, in this work, small circular plates are treated under this class.

4.5.1 Large Plates

The numerical examples for large plates are carried out for different types of soils subjected to loads concentrated at center and uniformly distributed. The soil is represented by the models presented above and by PLAXIS 2D. The comparisons are conducted graphically in terms of deflection, moment and shear. These plots are presented in Figure 4.15 to 4.26 for the soil

parameters presented in Table 4.1, plate properties shown in Table 4.4 and the recommended χ values in Table 4.2. In advance to these plots, modeling of the circular plate in PLAXIS 2D with the calculation cases given Table 4.4 is presented in Table 4.5 with a typical input and output formats. And also outputs of the deformed mesh and the effective mean stresses are presented in Figure 4.14 for a typical loading.

Table 4.4 Calculation cases for large plates

<table>
<tr><th colspan="2">Plate Dimensions and Properties</th><th>Soil Thickness (H)</th><th colspan="2">Loading</th></tr>
<tr><td>Modulus of elasticity, E_p</td><td>25(GPa)</td><td rowspan="4">120(m)</td><td>Vertical concentrated, p</td><td>100(KN)</td></tr>
<tr><td>Poisson's ratio, υ_p</td><td>0.2</td><td>Uniformly distributed, q</td><td>40 (KN/m^2)</td></tr>
<tr><td>Thickness, h_p</td><td>0.15 (m)</td><td rowspan="2">Radius of loaded region, a</td><td rowspan="2">5(m)</td></tr>
<tr><td>Plate diameter, ϕ</td><td>20(m)</td></tr>
</table>

The plate rests on a very thick soil deposit and large thickness of this soil is used in the PLAXIS 2D software for such larger plates, so as to compare the two models together with the PLAXIS itself. And as it could be observed from Figure 4.4 (a) and (b), Winkler type model gives a deflection in agreement with the PLAXIS for greater χ values, i.e., at larger thickness of the soil.

Table 4.5 Modelling of a circular plate in PLAXIS 2D

PLAXIS MODELLING FOR ANALYIS OF CIRCULAR PLATE PROBLEMS						
INPUTS						
Model Dimensions						
(X_{min}, Y_{min})	(0,0)		(X_{max}, Y_{max})		(60,120)	
Soil and Plate Data Sets Parameter						
Soil Data Sets Parameter			**Plate Data Sets Parameter**			
Element	15-nodded		Material model		Axisymmetric	
Material model	Linear elastic		Material type		Elastic	
E_s (KN/m^2)	80000.00		EA (KN/m)		3.75E6	
υ_s	0.2		EI (KNm^2/m)		7031.00	
H (m)	120		υ_p		0.2	
			r (m)		10	
Plate Loading						
Load system	Point load A		Vertical force (KN/m)		100	
Load system	Distributed loads A		Vertical force (KNm^2/m)		40	
OUTPUTS (at certain radii)						
For Central Concentrated Load						
***r* (m)**	0	2	4	6	8	10
Deflection (mm), u_y	-5.591	-1.755	-1.109	-0.918	-0.775	-0.641
Moment (KNm/m), M	75.064	-5.453	-0.354	-0.094	0.015	0.055
Shear (KN/m), Q	1389.252	-1.565	-0.455	-0.0445	-0.0425	0.216
For Uniformly Distributed Load						
***r* (m)**	0	2	4	6	8	10
Deflection (mm), u_y	-4.8	-4.7	-4.0	-2.6	-1.9	-1.7
Moment (KNm/m), M	-0.742	-0.912	-2.254	1.326	0.345	0
Shear (KN/m), Q	0.002	-0.31	-0.833	-0.453	-0.21	-0.134

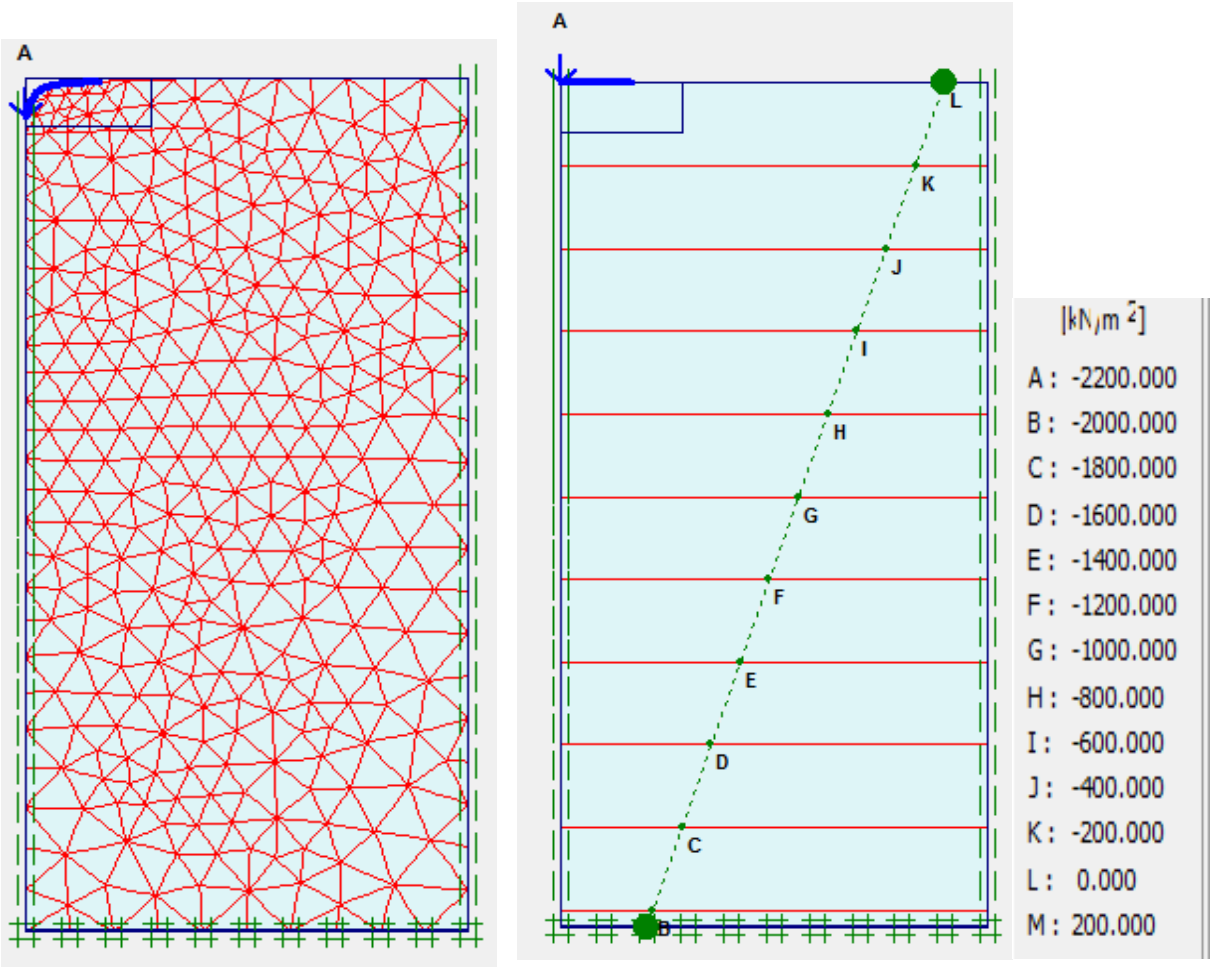

Figure 4.14 Overview of the deformed mesh and contour line representation of the effective mean stresses

4.5.1.1 Central Concentrated Load

Since the problem is axisymmetric, for all loading conditions, only the right half section of the loaded plate is considered to present the deflection and internal actions.

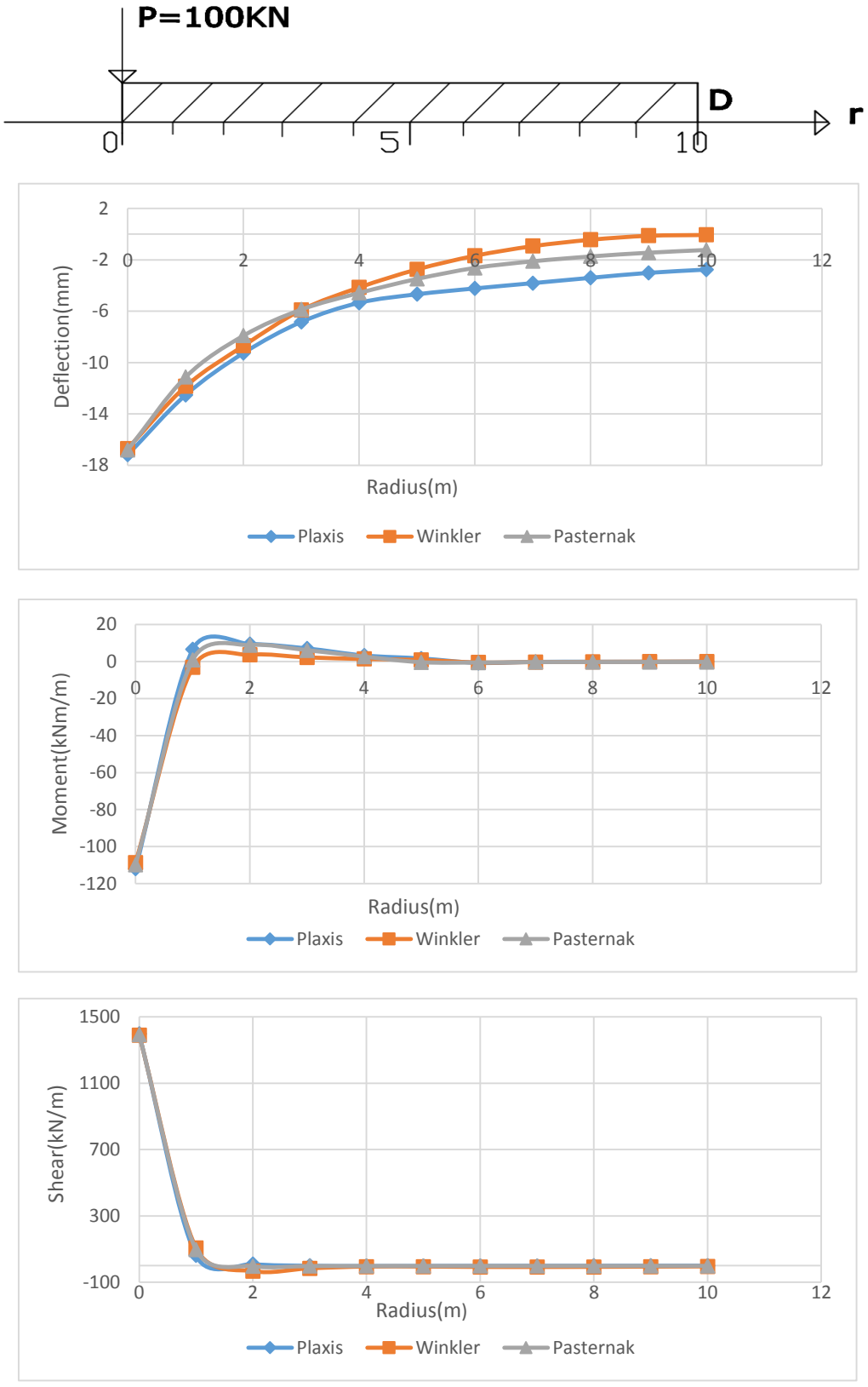

Figure 4.15 Response of a large circular plate on soft clay subjected to central concentrated load

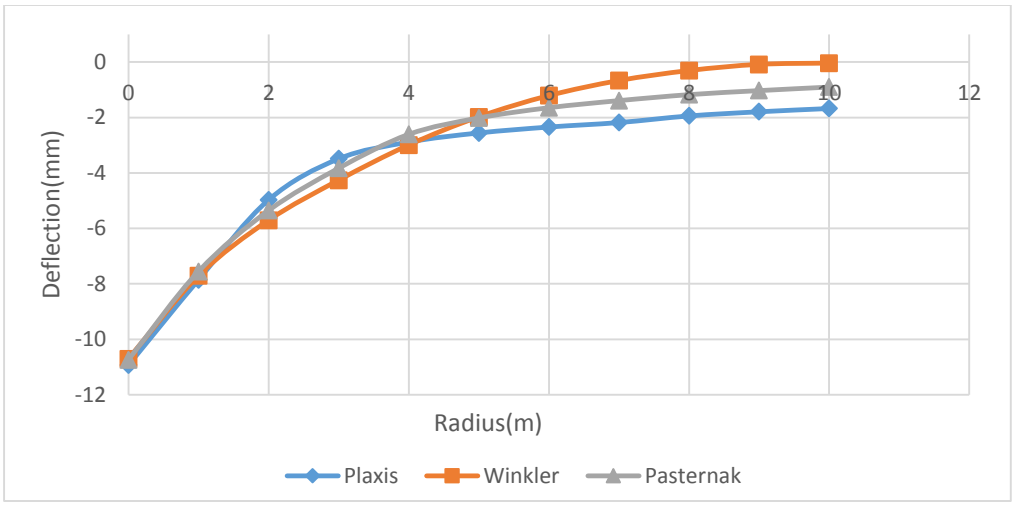

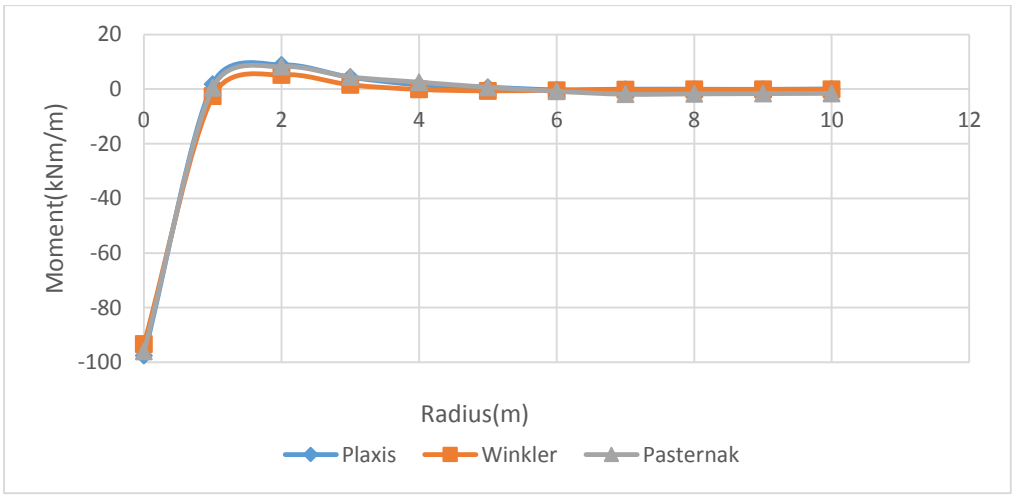

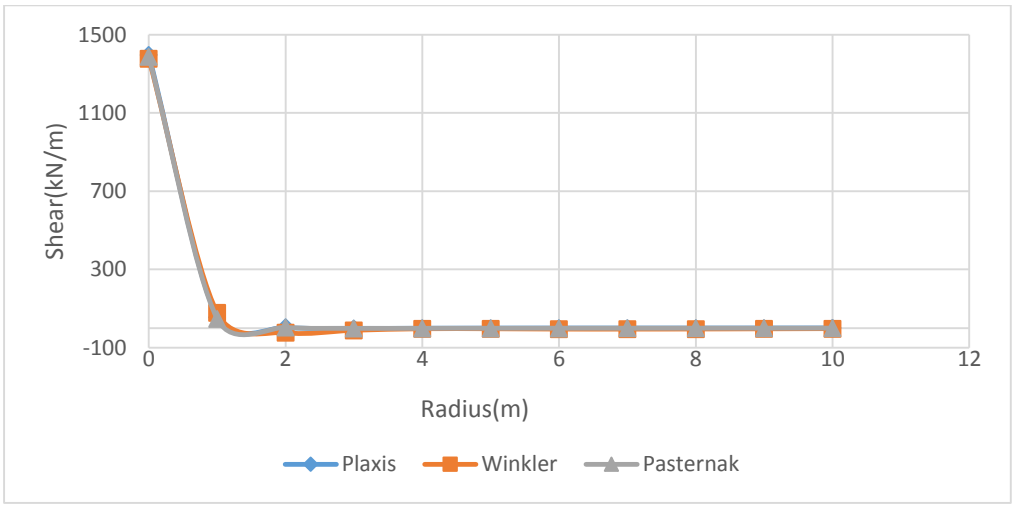

Figure 4.16 Response of a large circular plate on medium stiff clay subjected to central concentrated load

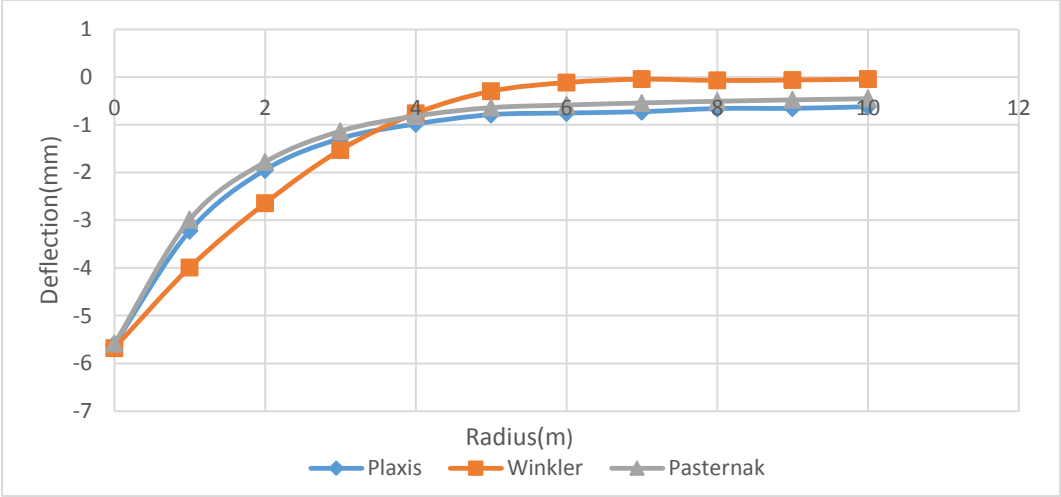

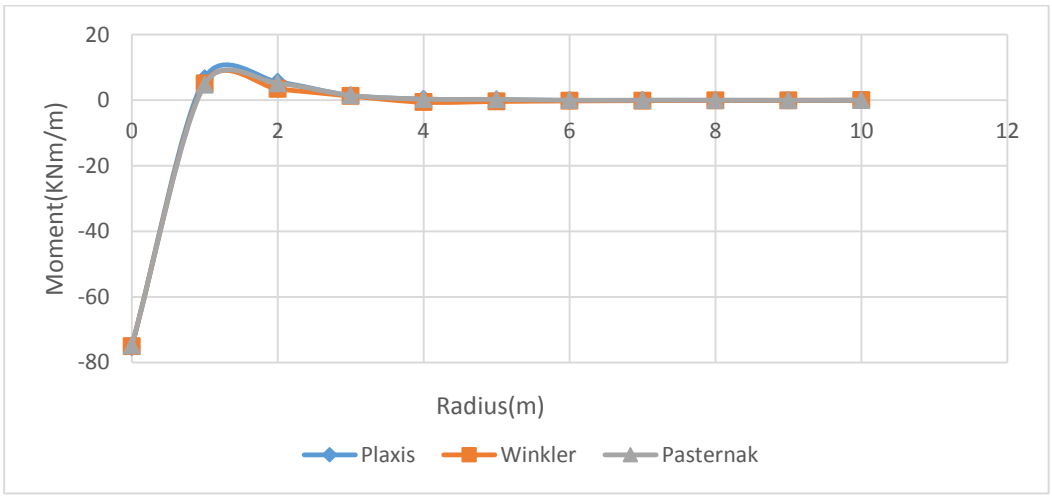

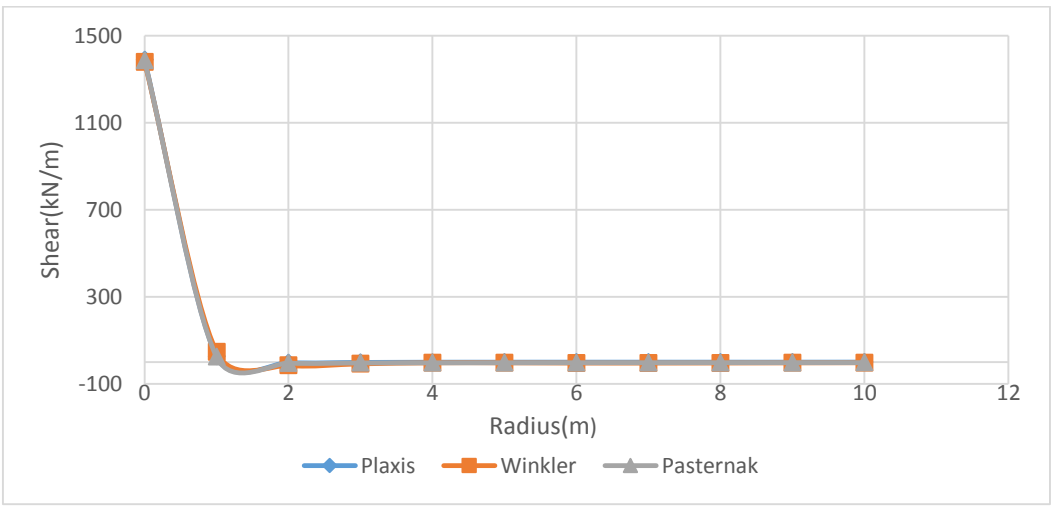

Figure 4.17 Response of a large circular plate on stiff clay subjected to central concentrated load

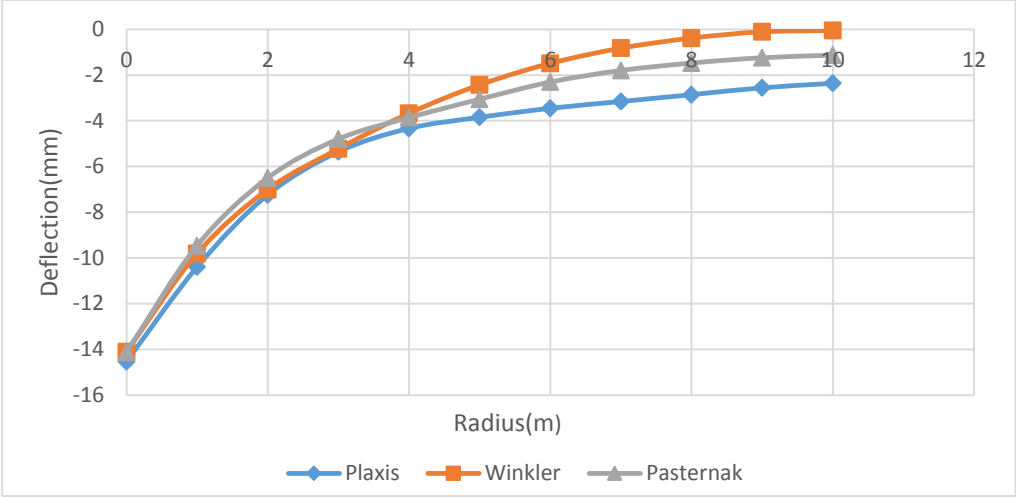

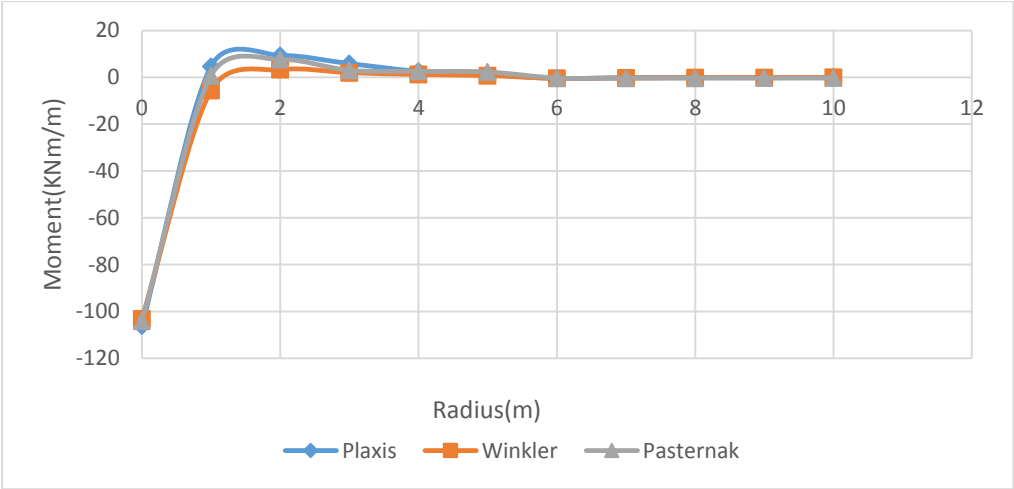

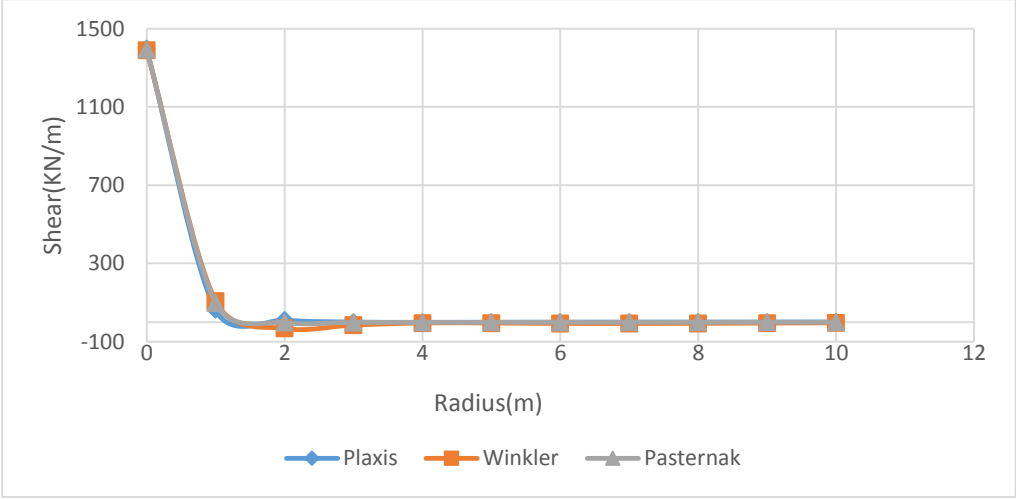

Figure 4.18 Response of a large circular plate on loose sand subjected to central concentrated load

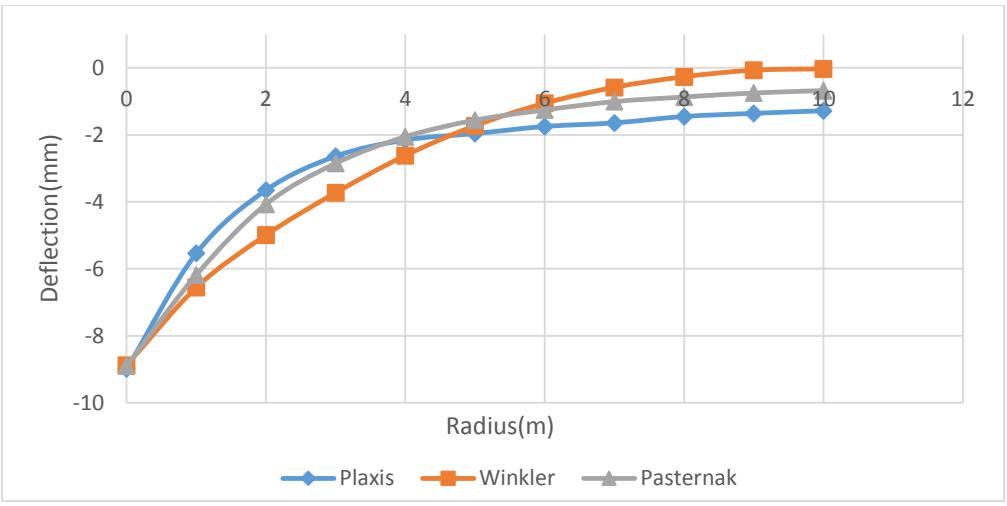

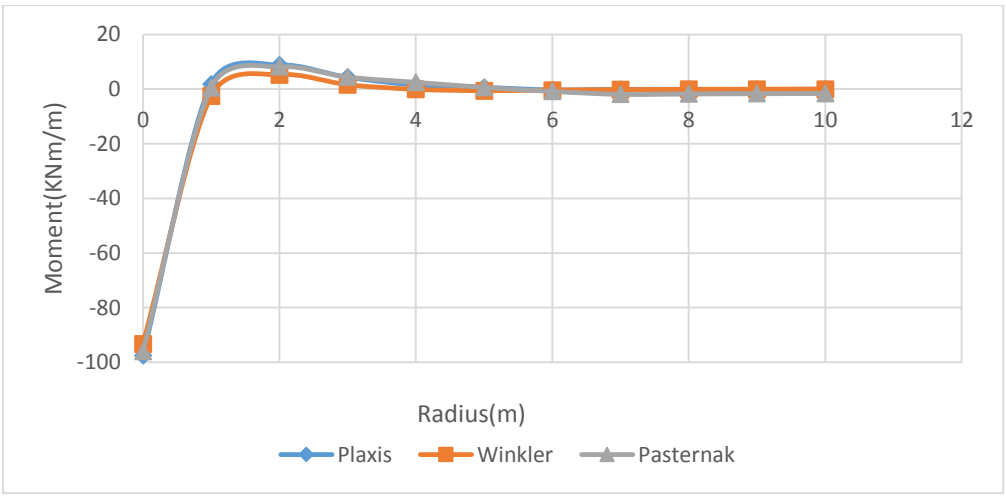

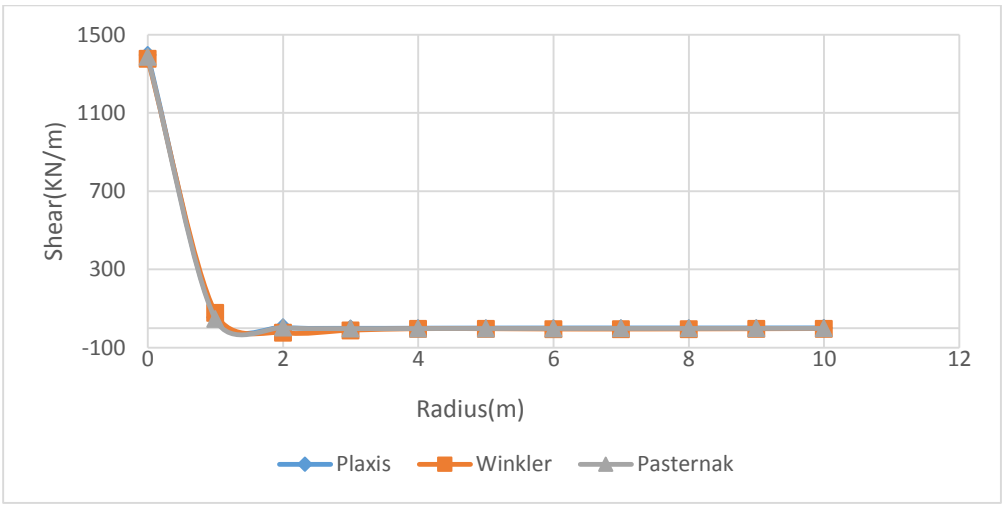

Figure 4.19 Response of a large circular plate on medium dense sand subjected to central concentrated load

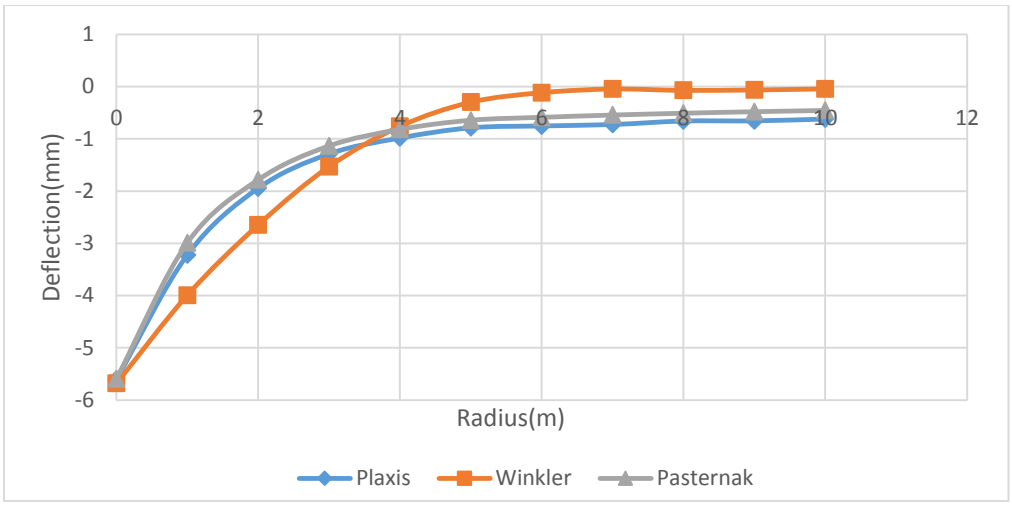

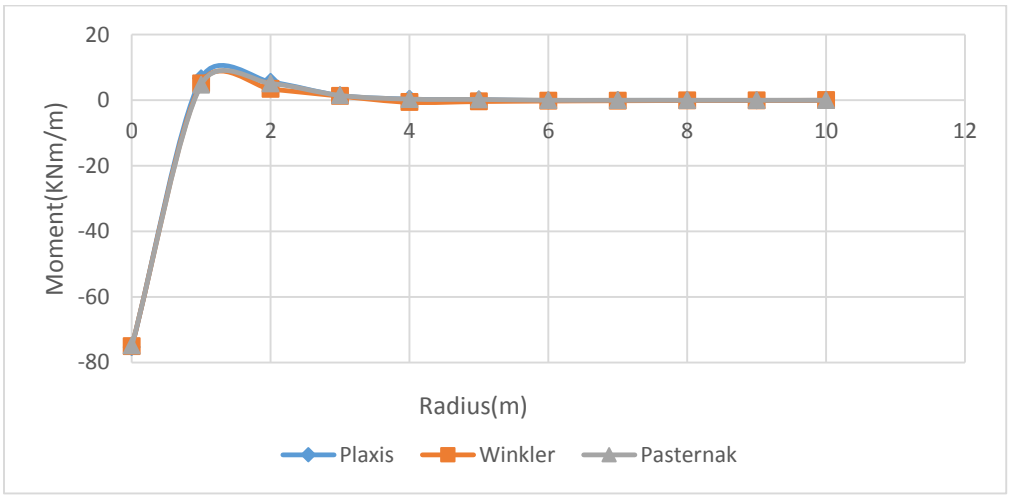

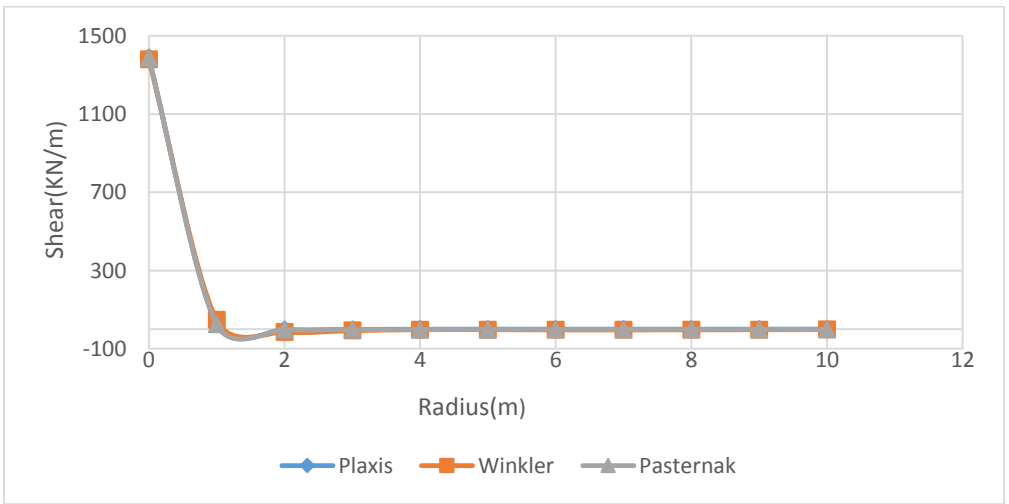

Figure 4.20 Response of a large circular plate on dense sand subjected to central concentrated load

4.5.1.2 Uniformly Distributed Load

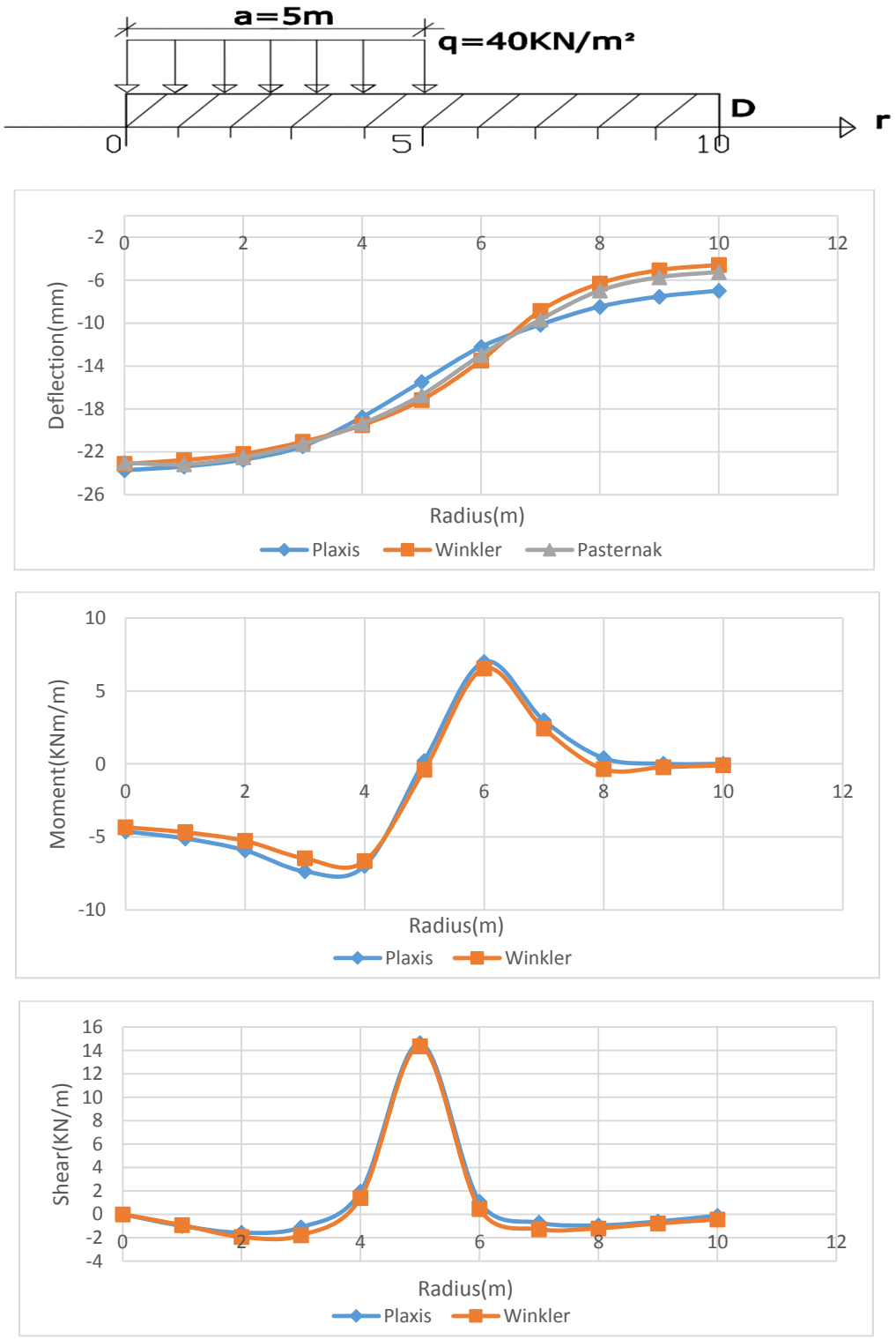

Figure 4.21 Response of a large circular plate on soft clay subjected to uniformly distributed load

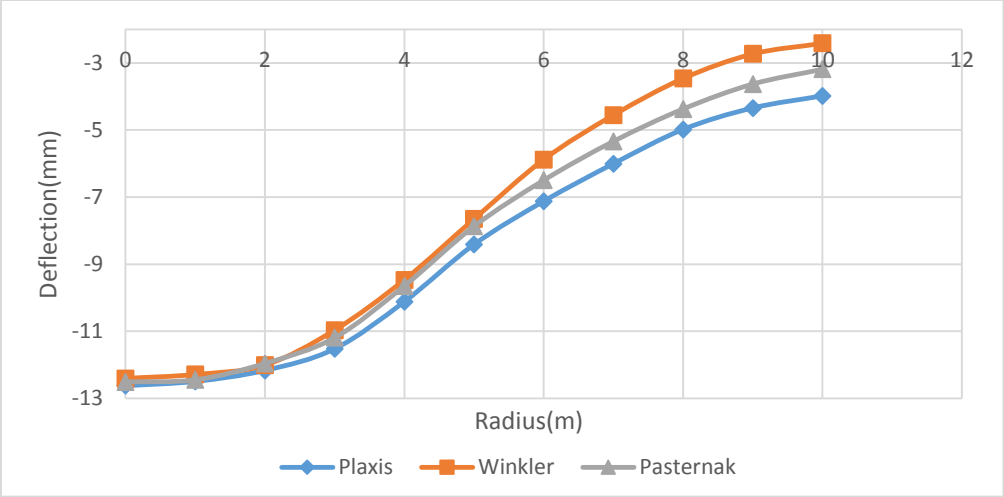

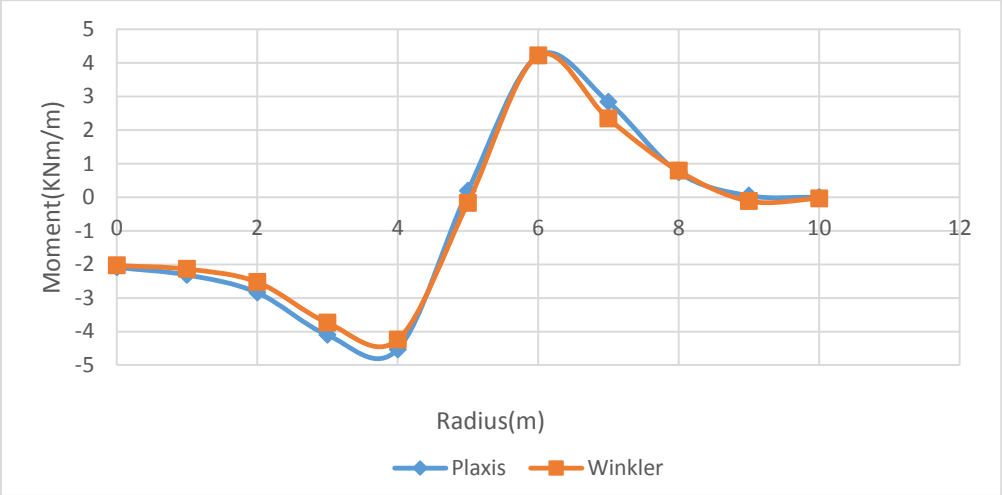

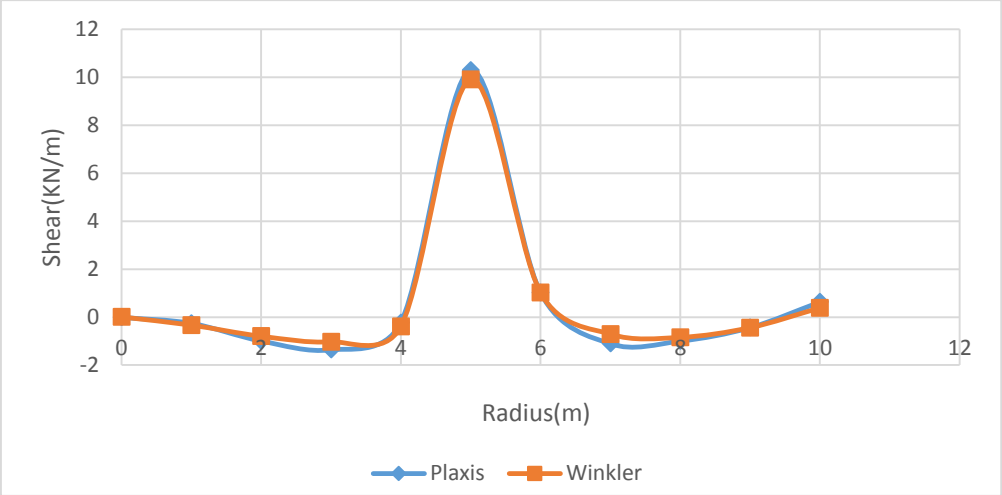

Figure 4.22 Response of a large circular plate on medium stiff clay subjected to uniformly distributed load

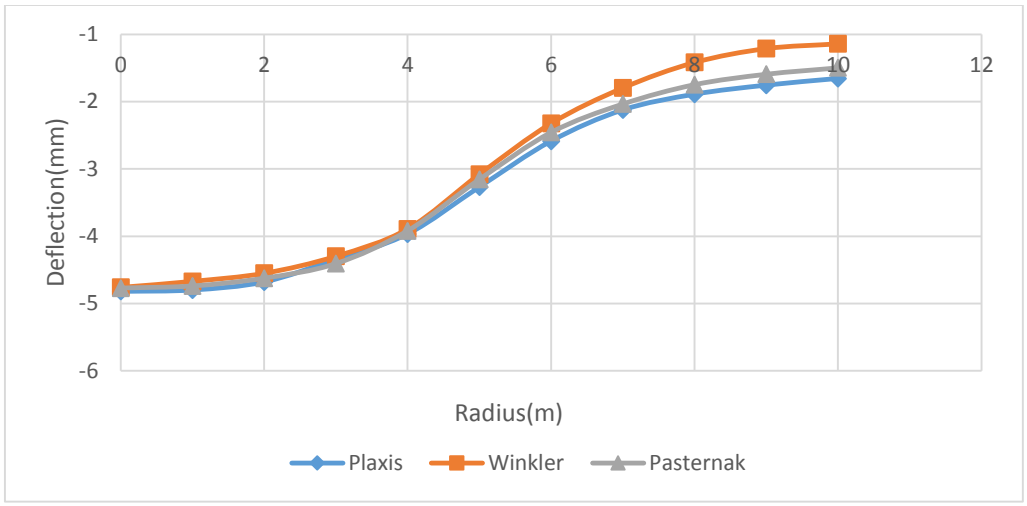

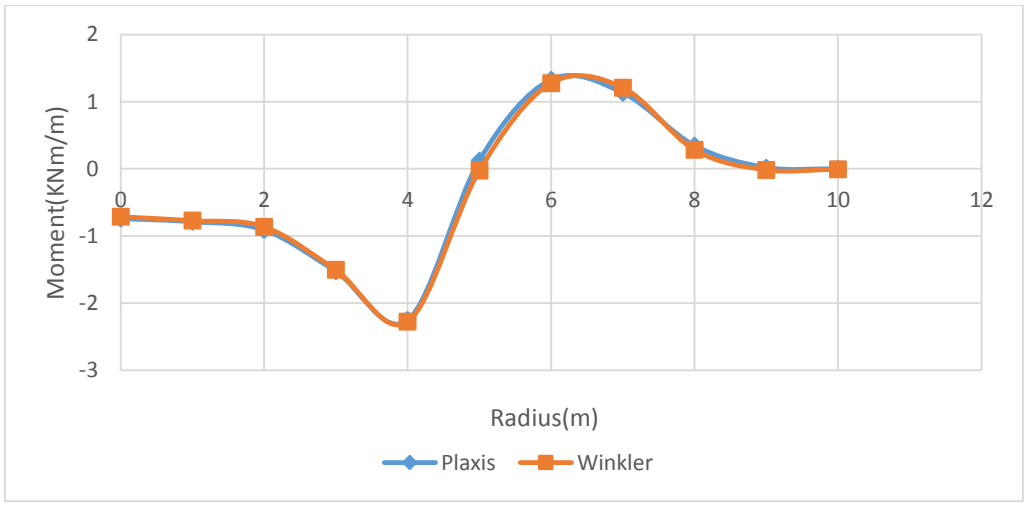

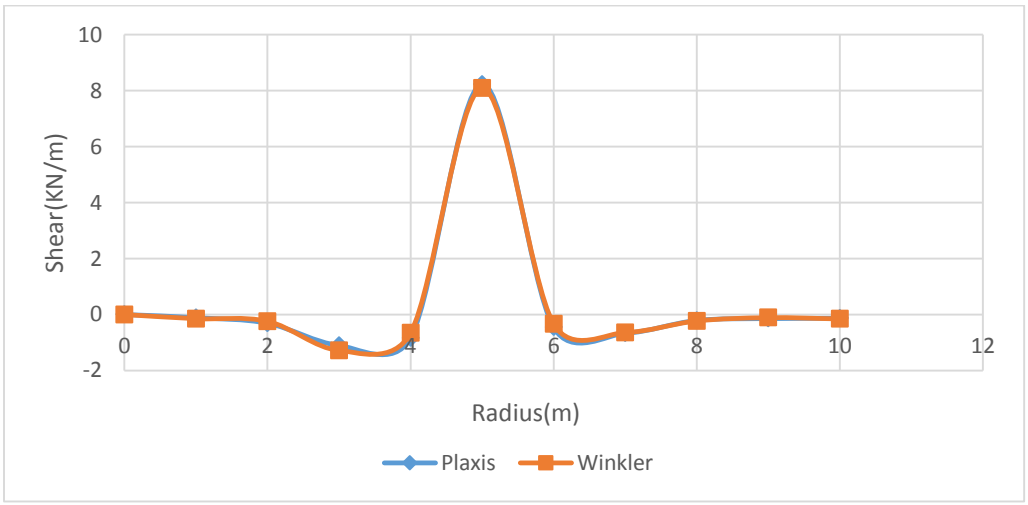

Figure 4.23 Response of a large circular plate on stiff clay subjected to uniformly distributed load

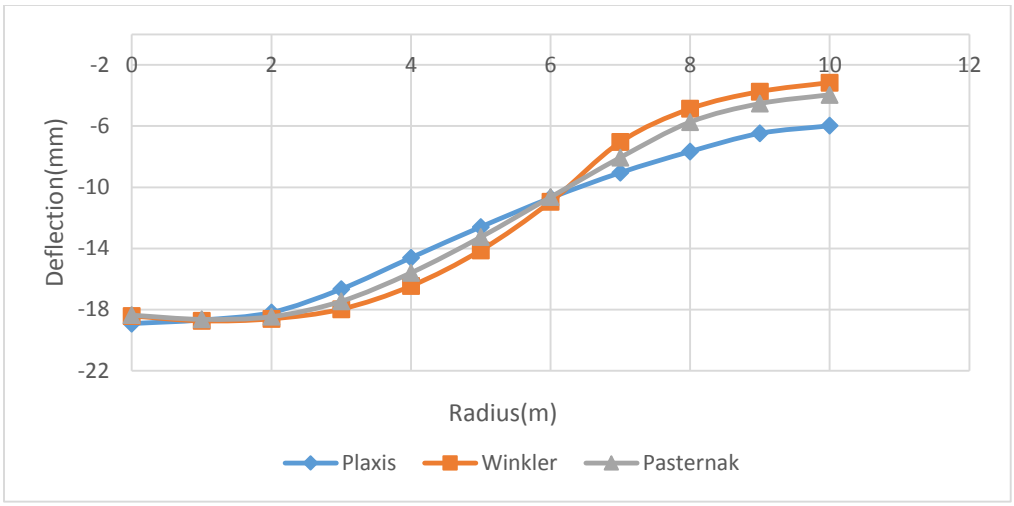

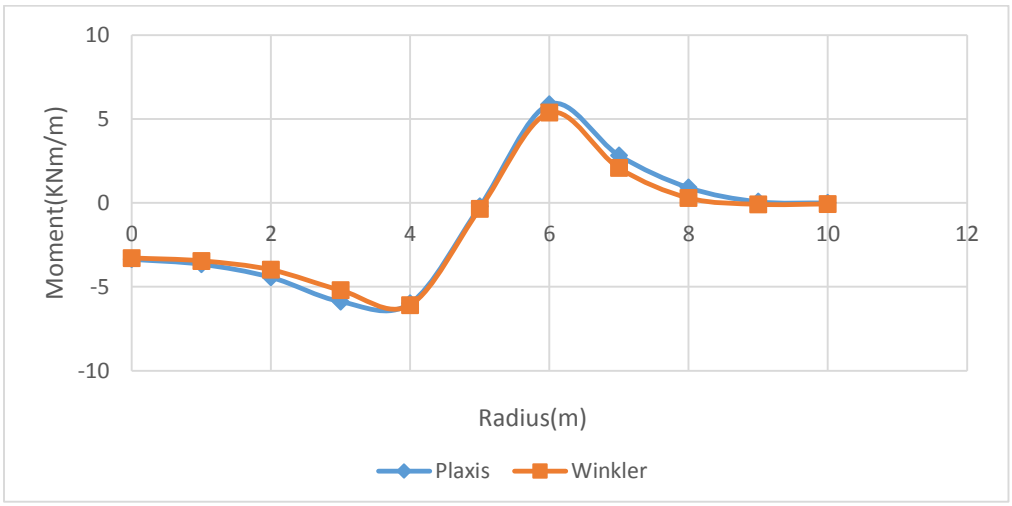

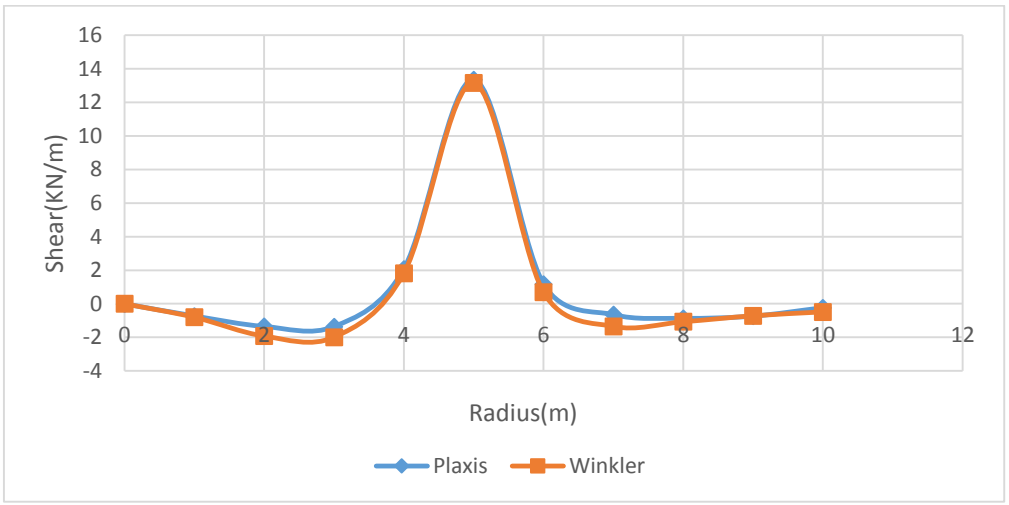

Figure 4.24 Response of a large circular plate on loose sand subjected to uniformly distributed load

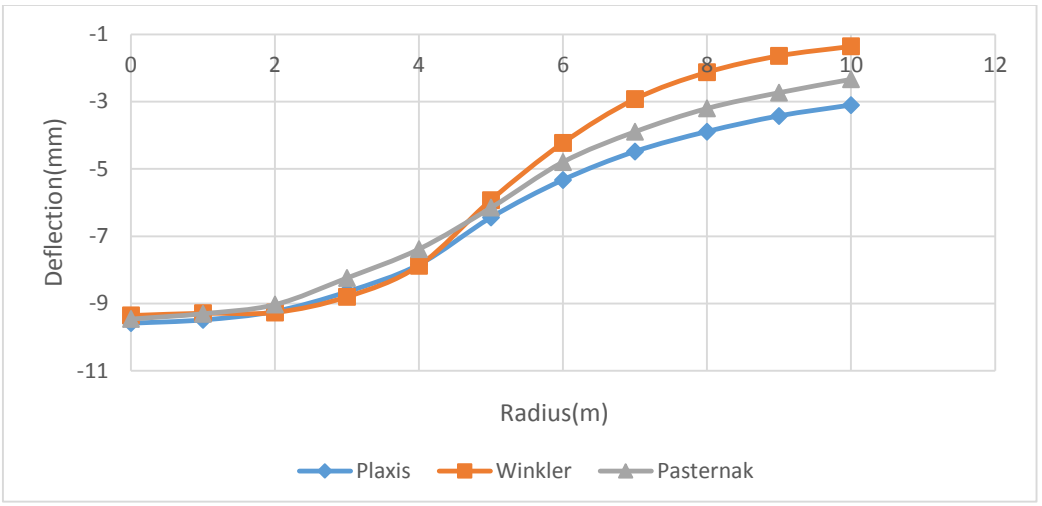

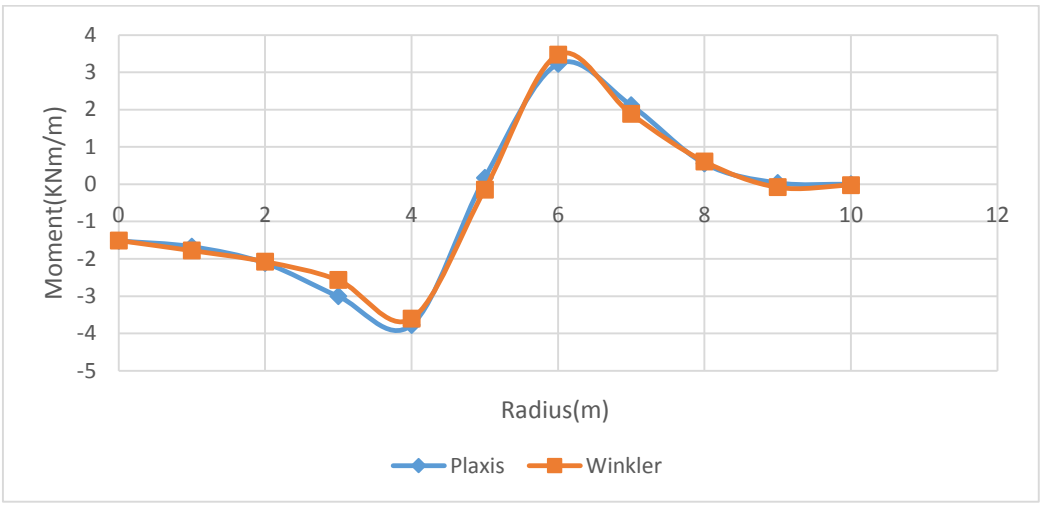

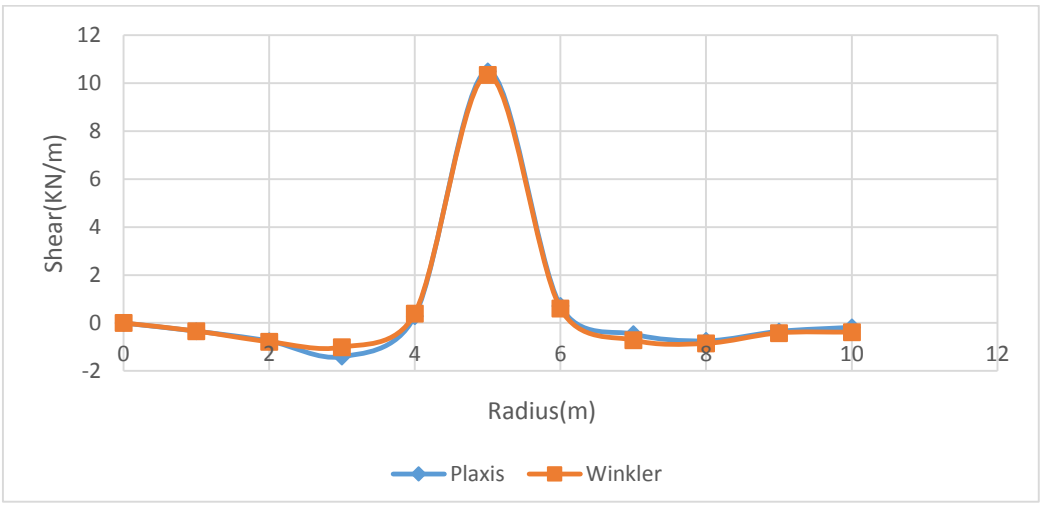

Figure 4.25 Response of a large circular plate on medium dense sand subjected to uniformly distributed load

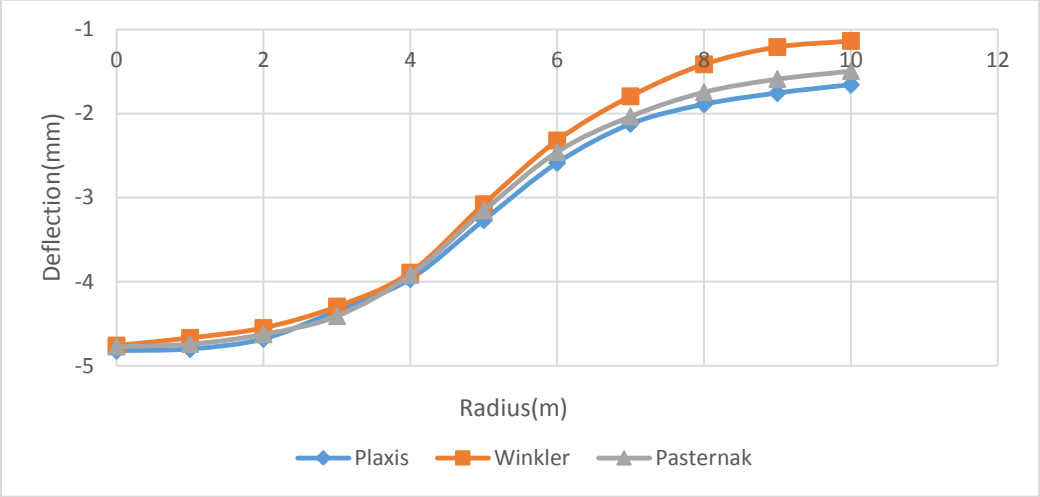

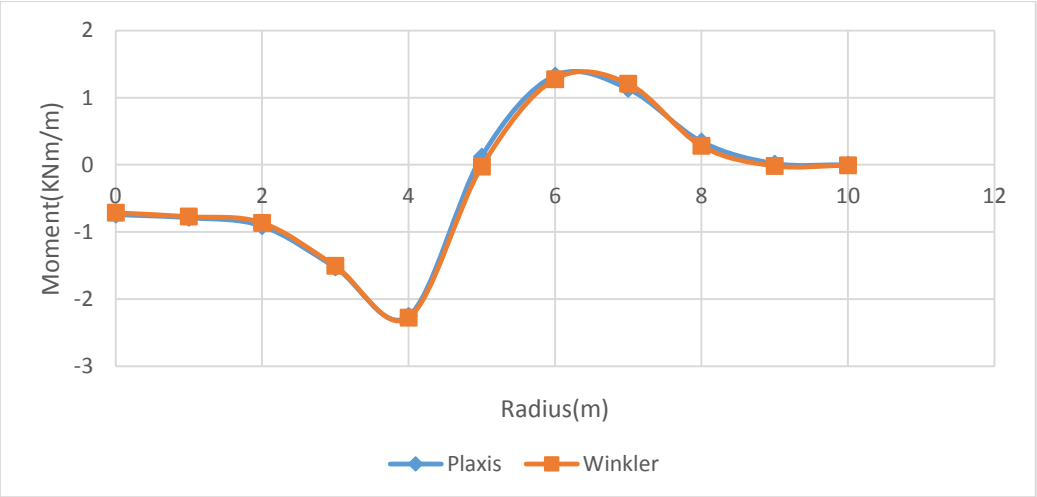

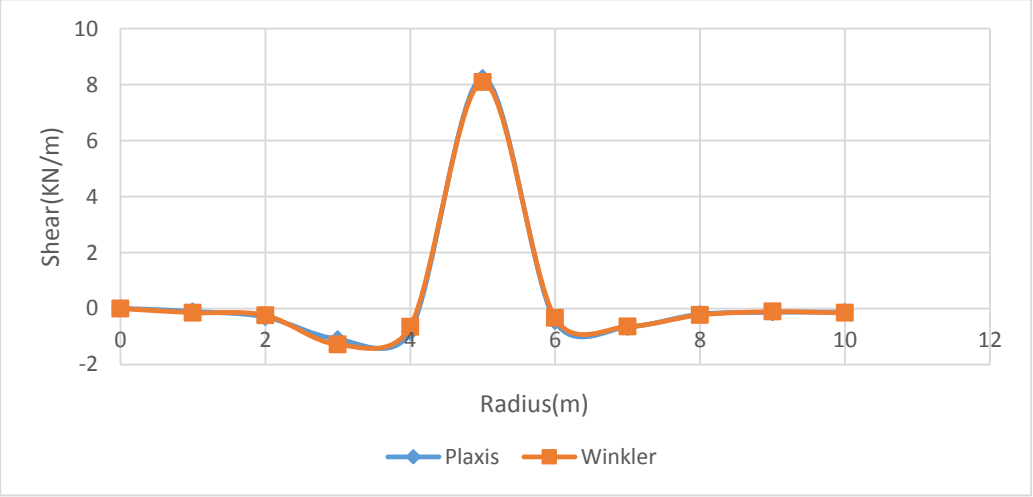

Figure 4.26 Response of a large circular plate on dense sand subjected to uniformly distributed load

As the figures 4.15 to 4.26 show, usage of the recommended calibration factors for the respective loading conditions gave similar maximum deflections for both models with that of the FE method of solution. Although in the case of relatively weak soils for a central concentrated load, both Winkler's and Pasternak's models underestimated the maximum deflection slightly by an amount of 4% and 1.7% respectively.

And there is a different condition in the case of medium dense and dense soil types where there is small deviation in the magnitudes of deflection between Winkler's model and PLAXIS results. These discrepancies are pronounced when moving from center to some ranges of radiuses. This may be attributed to the calibration factor which is obtained based on only the maximum deflection.

Noteworthy is also to observe that variations in the magnitudes of deflection in Winkler's model around the edges decrease as the stiffness of the soil increases as compared with the Pasternak's model and the PLAXIS itself.

In all cases of the internal actions, Pasternak's model shows a close convergence to the FE based analysis than Winkler's model. This can be noticed in the case of weaker soils where the bending moments show a little discrepancy for a small range of radius in Winkler's model. However, in all the cases, the shear force diagrams of both models are in good agreement with the finite element result.

For uniformly distributed type of loading, the deviations in the maximum deflection for Winkler's model may amount up to 5% while it is insignificant for Pasternak's model in the case of weak soils. Unlike the central concentrated load the deviations encountered in the deflection under the loaded region for both models becomes negligible as the soil stiffness increases.

As far as the bending moments are considered, there is a very little divergence with the FE results whereas the shear values are practically equal with the FE for Winkler's model. The bending moment and shear force diagrams of Pasternak's model for this type of loading are not included due to the difficulty of deriving the mathematical solutions. However, one can expect even a much better agreement.

The reason why the deflection is not approaching zero around the edges like all large plates is that, a large thickness of the soil is considered as compared to the plate radius to be classified as large. This discussion holds true for the case of central concentrated loading too.

In summary, it is apparent from all the plots, Winkler's model exhibits underestimation of the deflection with increasing distance from the center. This is the result of the missing shear interaction in the soil. And this variations can result to an unsafe design. However Pasternak's model fares excellently giving results almost identical to those of PLAXIS 2D as the stiffness of the soil increases.

4.5.2 Small Plates

Plots of deflection, moment and shear force for small plates subjected to a concentrated load at center and at edge are presented in this section for different types of soils. The comparisons are made for Pasternak -type model, Winkler -type model and PLAXIS 2D. These plots are presented in Figure 4.27 to 4.38. The soil parameters and the recommended χ values presented in Table 4.1 and 4.3 are used respectively. Though the radius of the plate and loaded region is different and it is given in Table 4.6.

Table 4.6 Calculation cases for small plates

Plate Dimensions and Properties		**Soil Thickness (*H*)**	**Loading**	
Modulous of elasticity, E_p	(25) GPa	21(m)	Vertical concentrated, p_o	100 (KN)
Poisson's ratio, υ_p	0.2		Edge load, q_o	100 (KN/m)
Thickness, h_p	0.15 (m)			
Plate diameter, ϕ	3(m)			

Unlike the large plate problem, a smaller thickness of the soil is used in the PLAXIS 2D software. This is because of the smaller diameter of the plate.

4.5.2.1 Central Concentrated Load

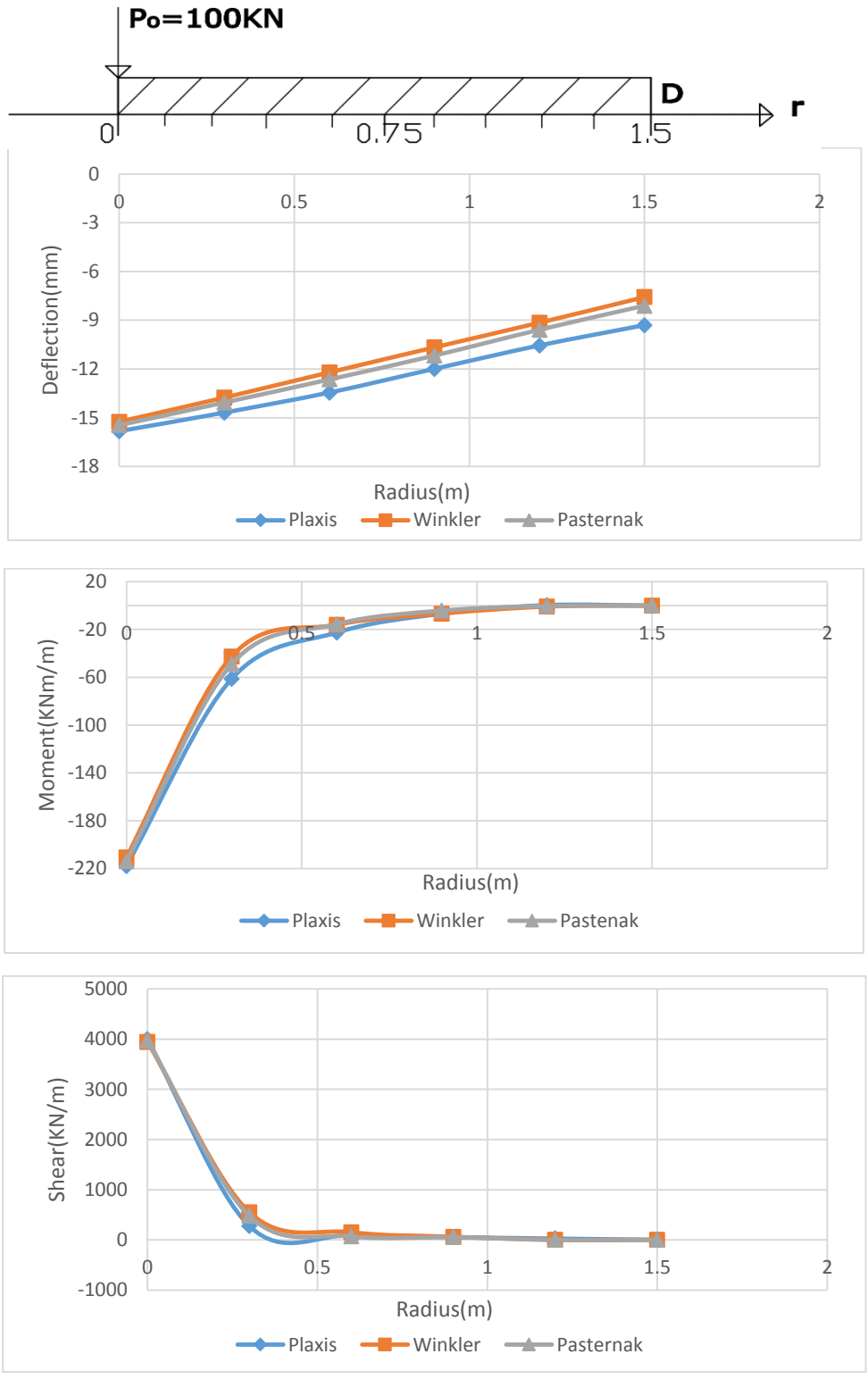

Figure 4.27 Response of a small circular plate on soft clay subjected to central concentrated load

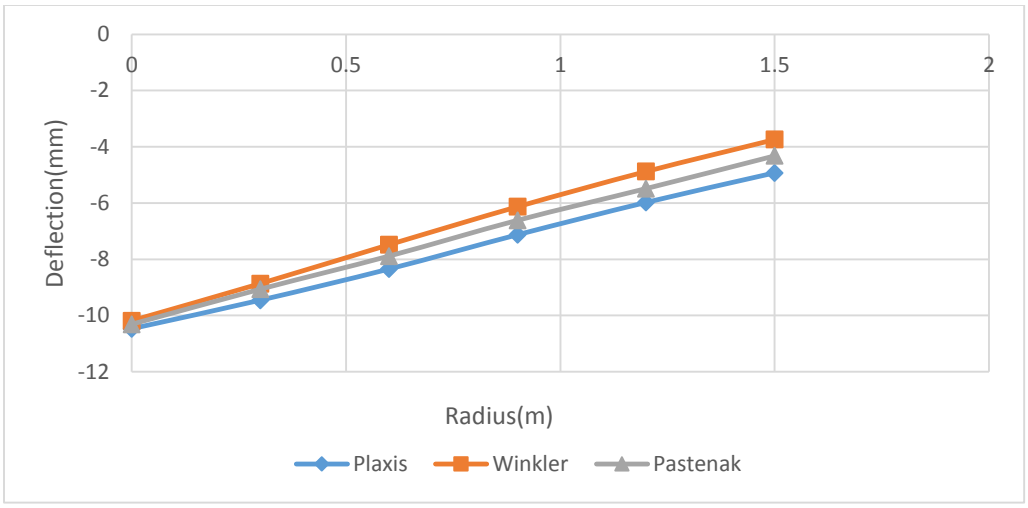

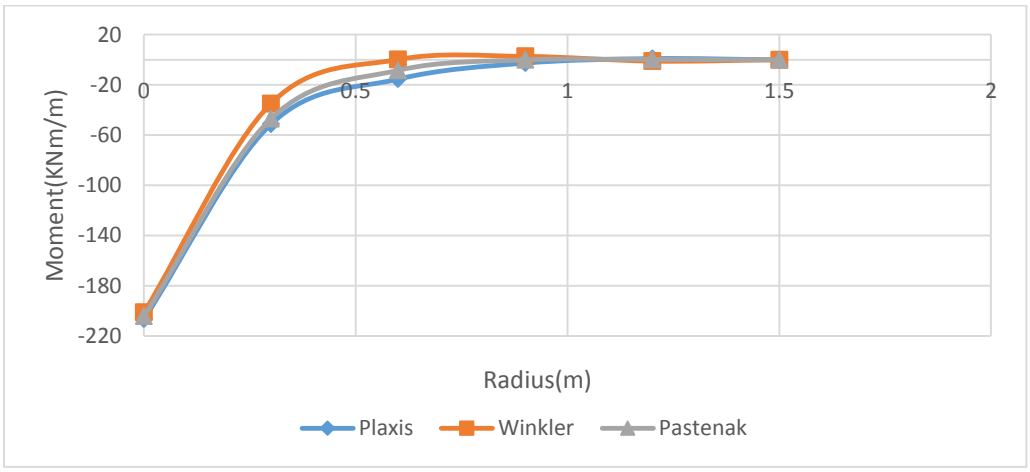

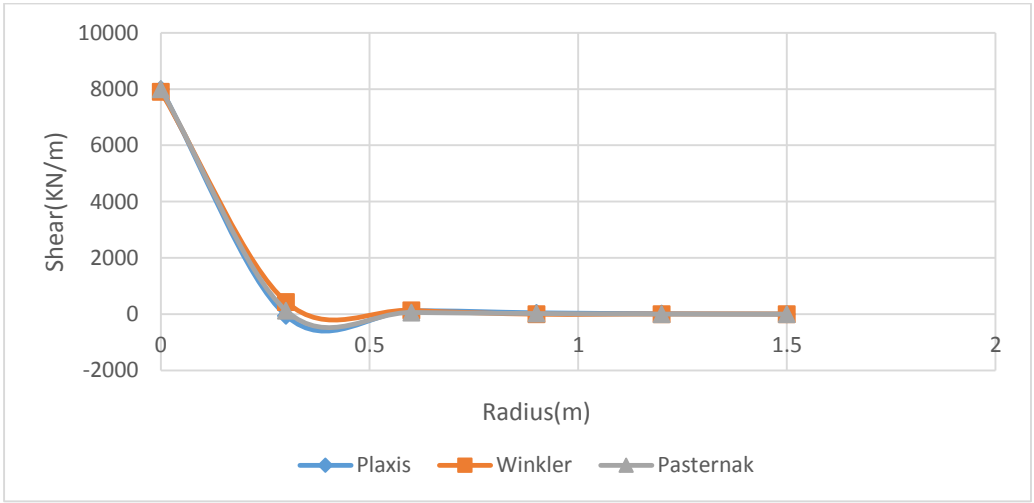

Figure 4.28 Response of a small circular plate on medium stiff clay subjected to central concentrated load

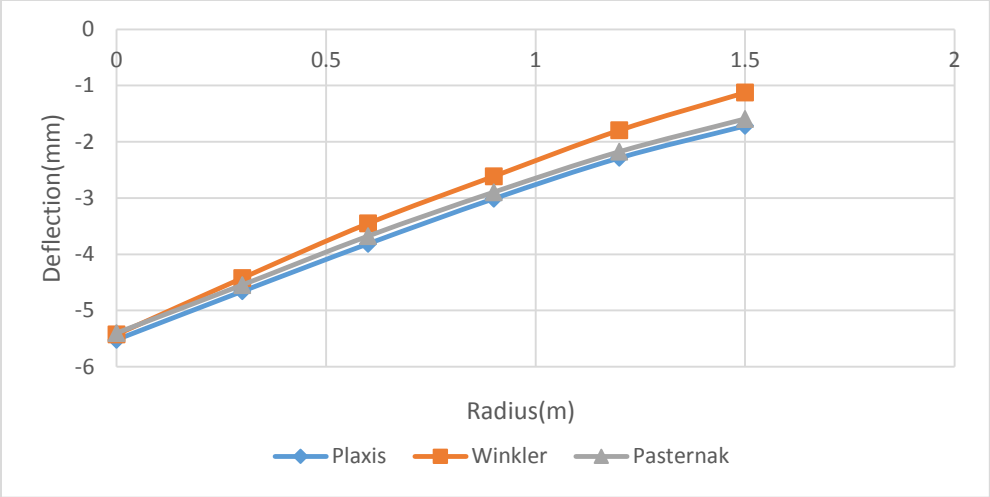

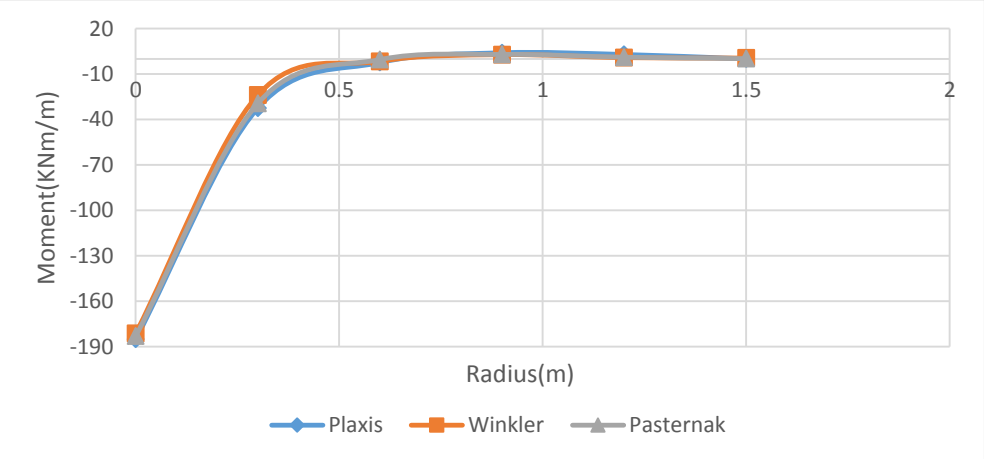

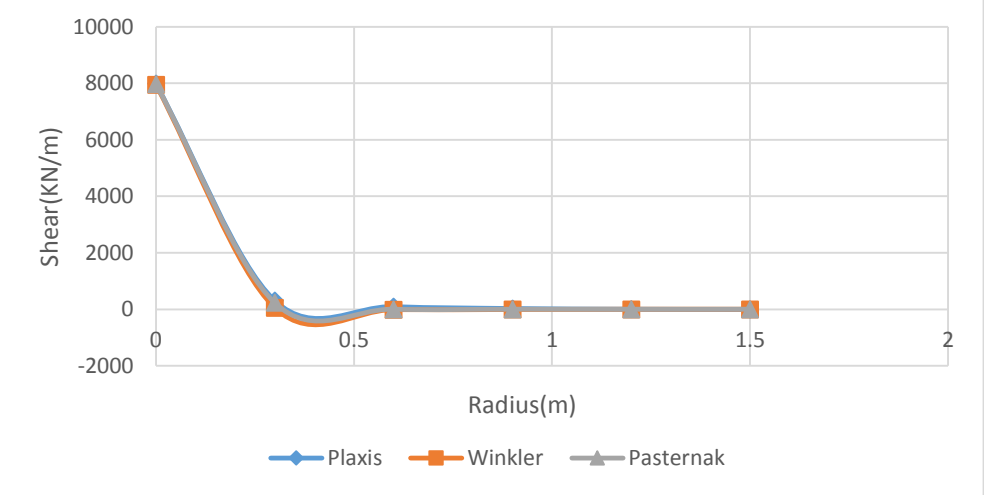

Figure 4.29 Response of a small circular plate on stiff clay subjected to central concentrated load

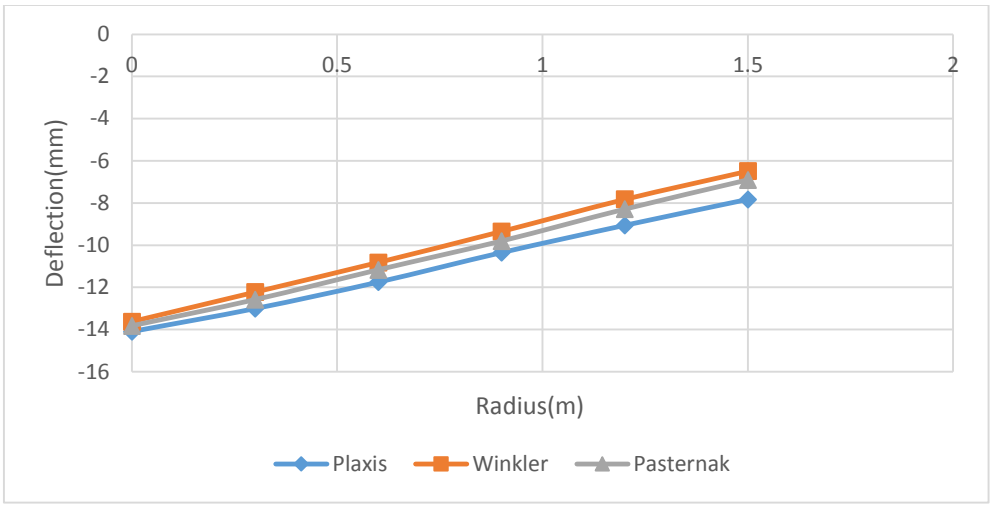

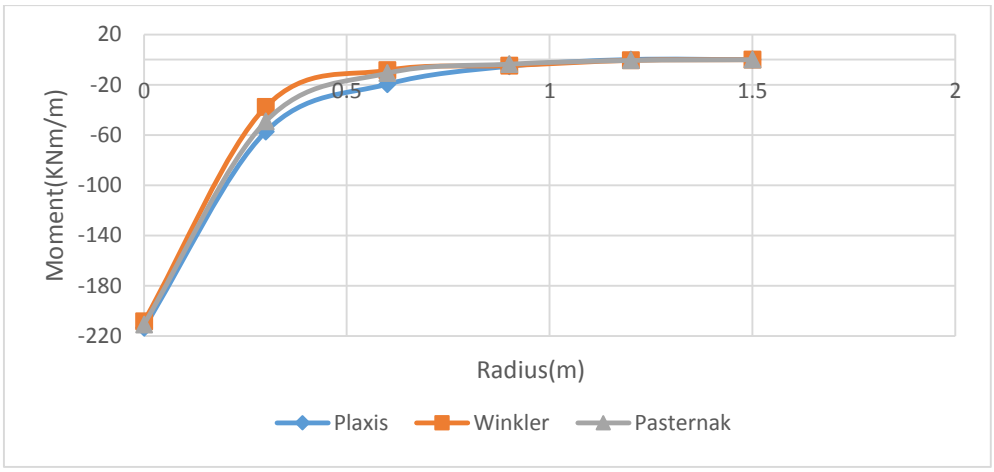

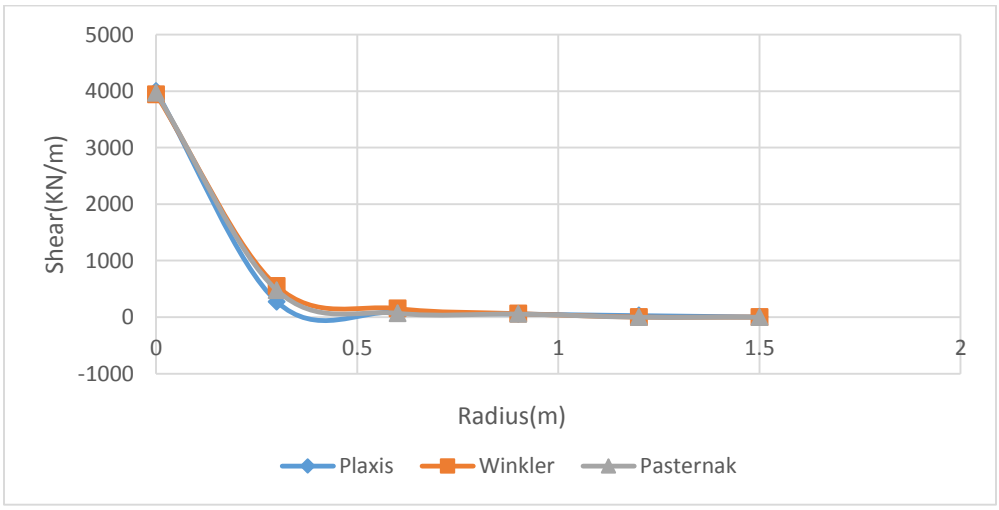

Figure 4.30 Response of a small circular plate on loose sand subjected to central concentrated load

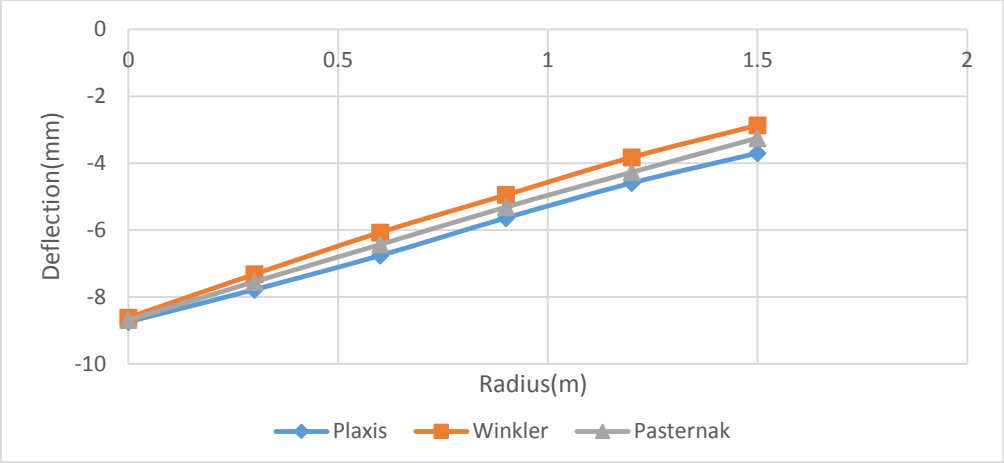

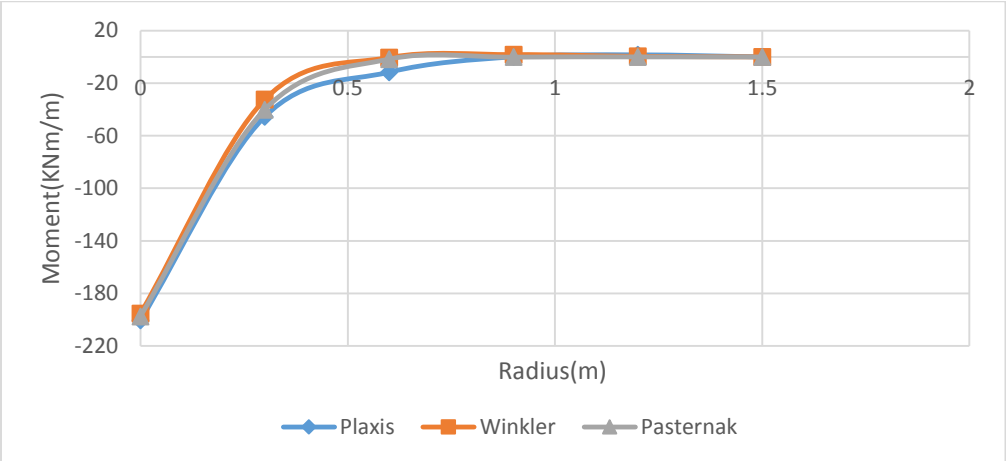

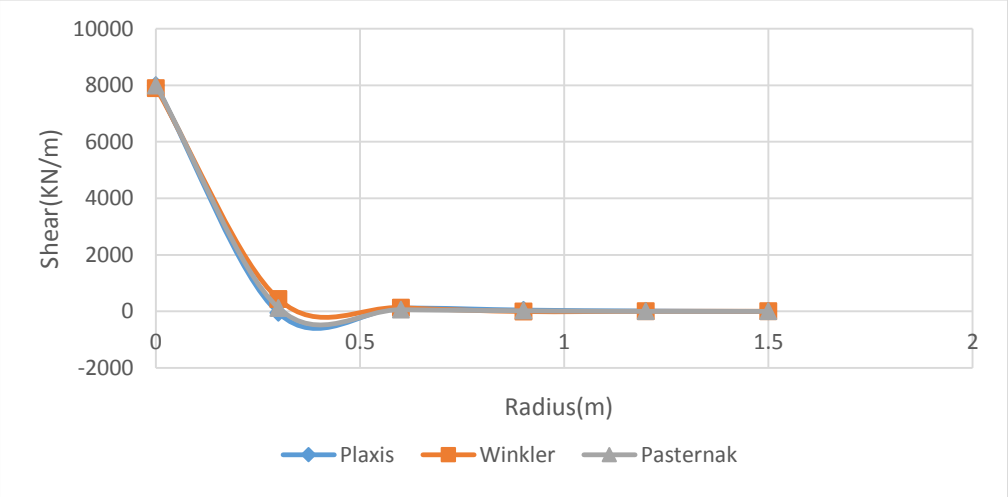

Figure 4.31 Response of a small circular plate on medium dense sand subjected to central concentrated load

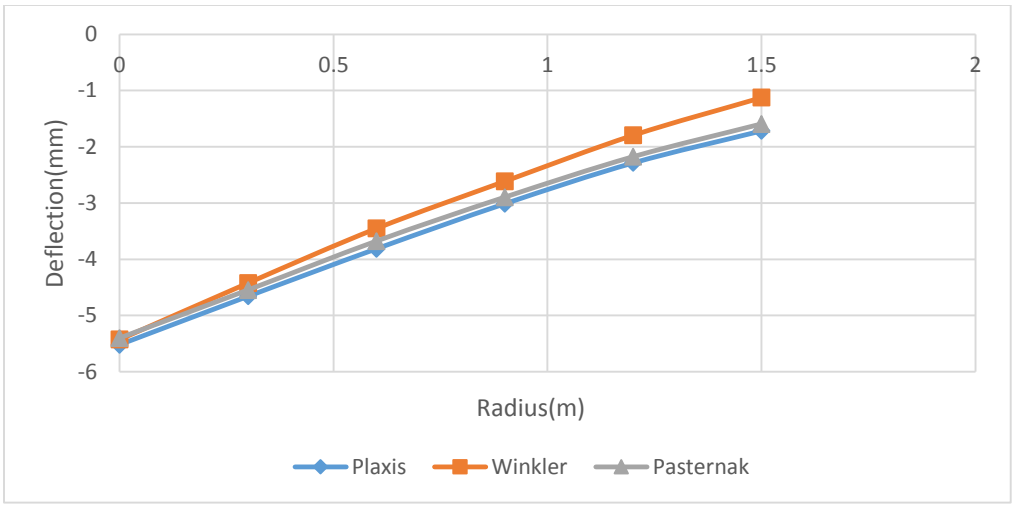

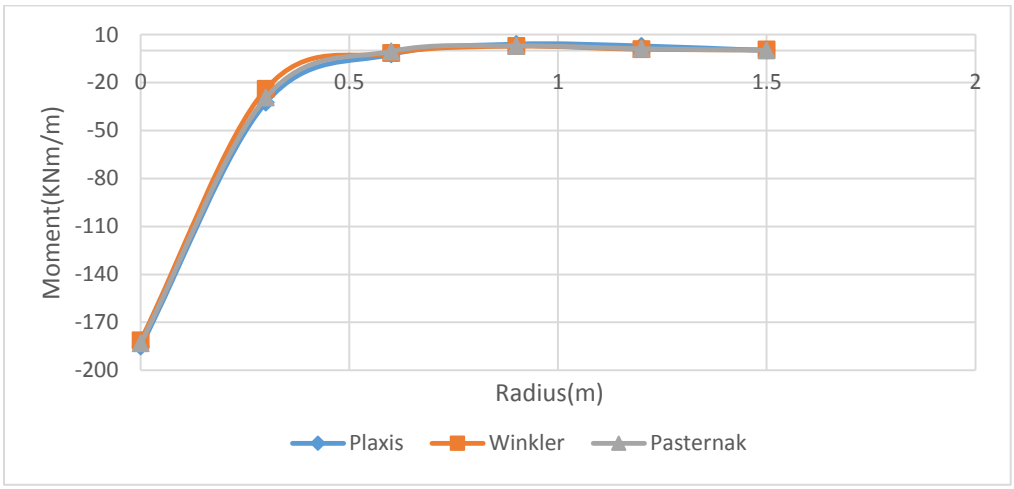

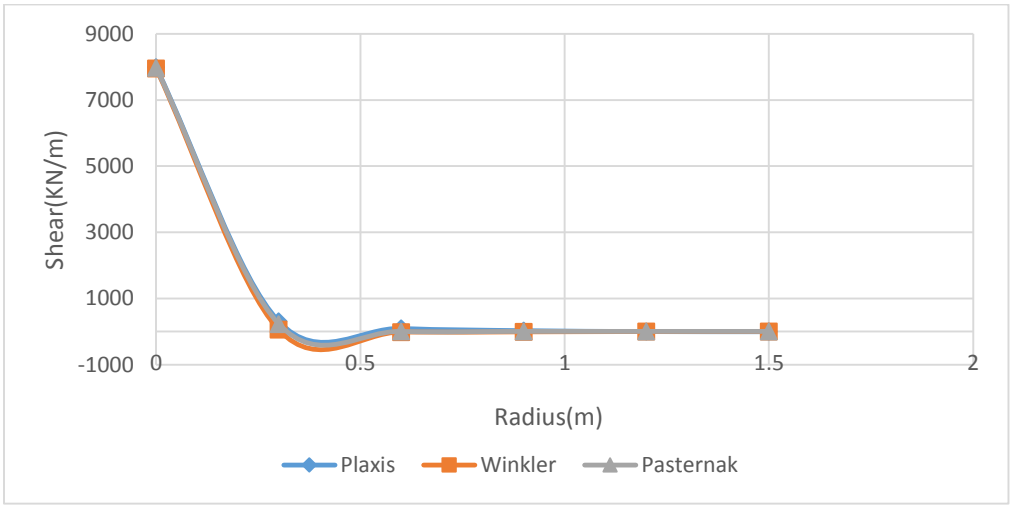

Figure 4.32 Response of a small circular plate on dense sand subjected to central concentrated load

4.5.2.2 Concentrated Edge Load

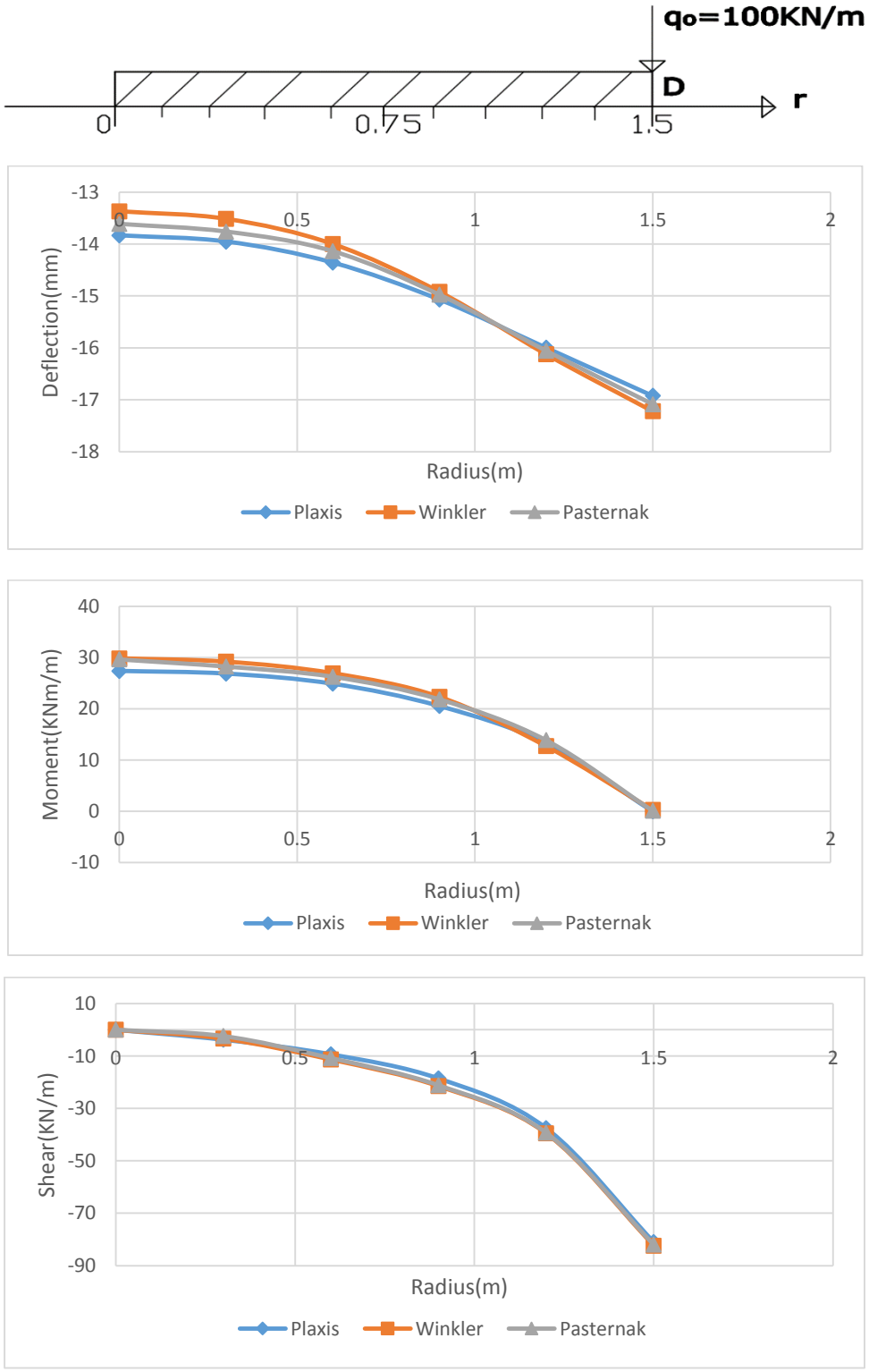

Figure 4.33 Response of a small circular plate on soft clay subjected to concentrated edge load

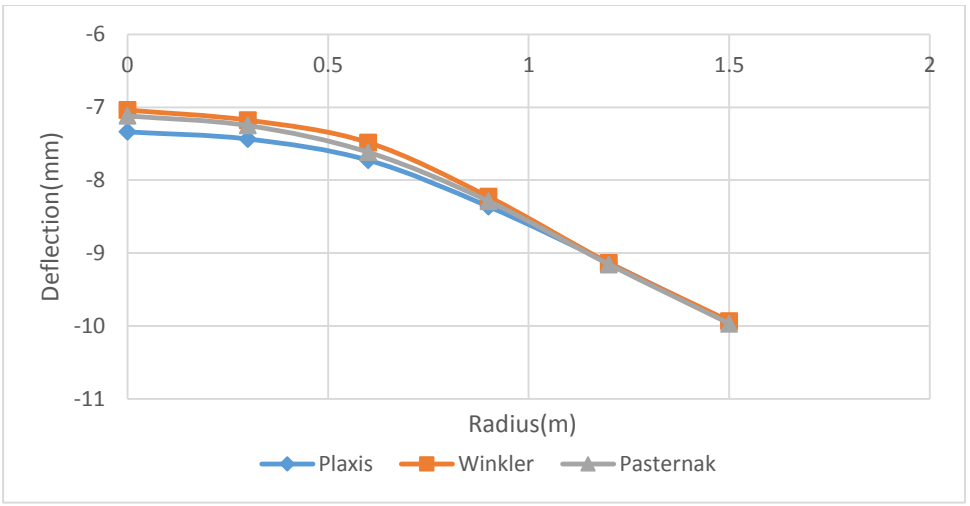

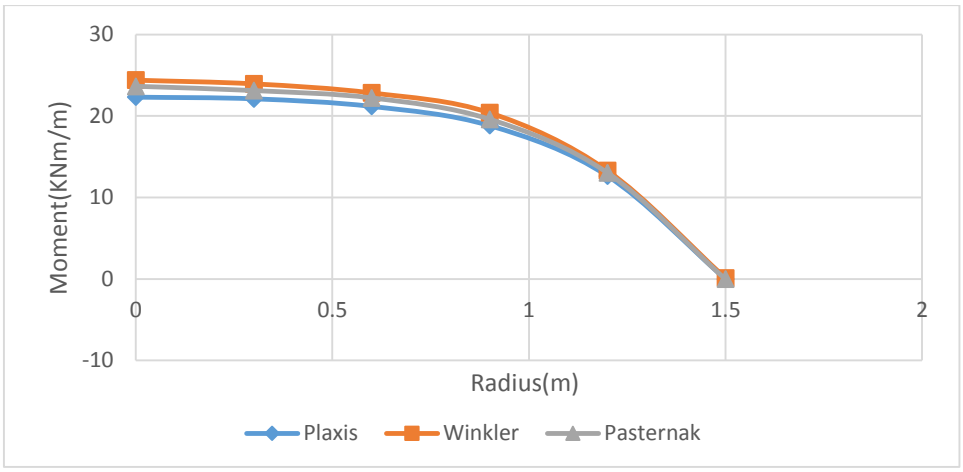

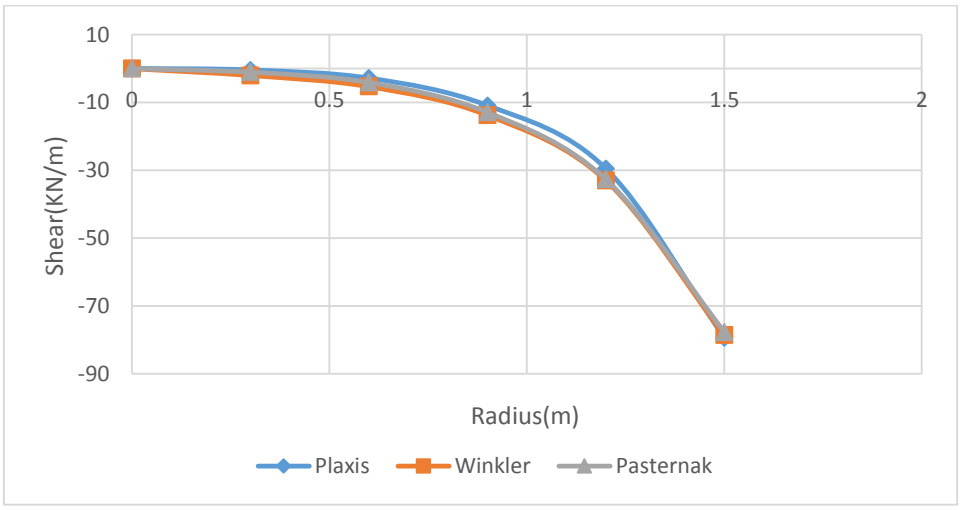

Figure 4.34 Response of a small circular plate on medium stiff clay subjected to concentrated edge load

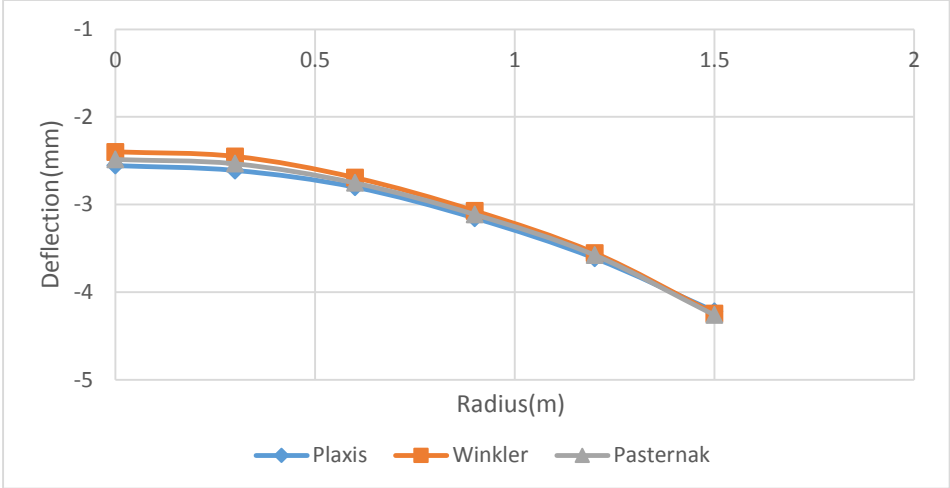

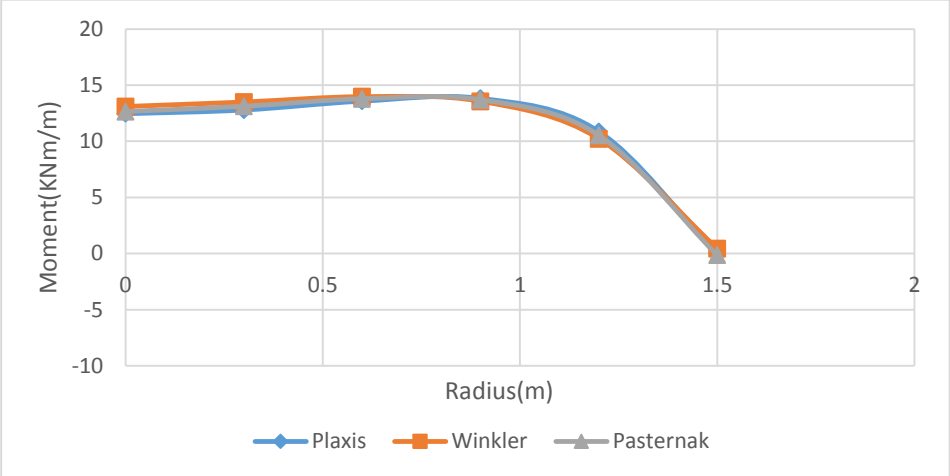

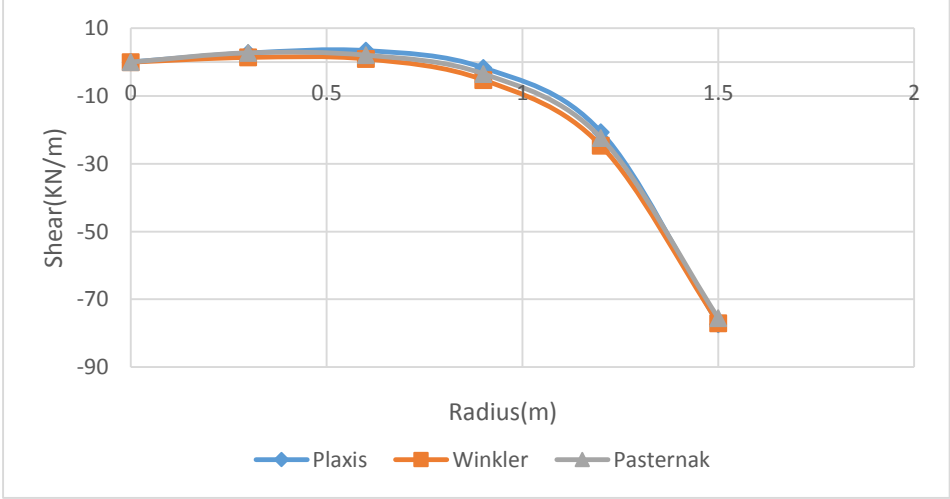

Figure 4.35 Response of a small circular plate on stiff clay subjected to concentrated edge load

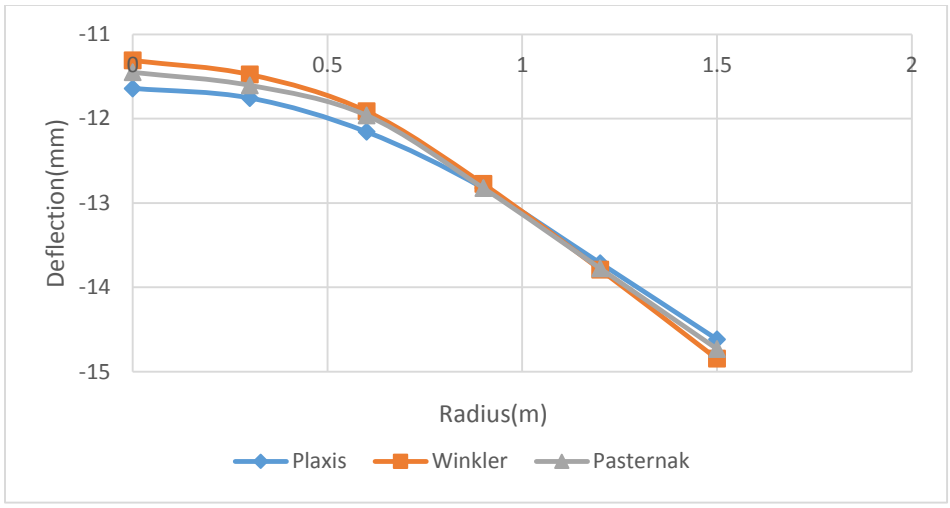

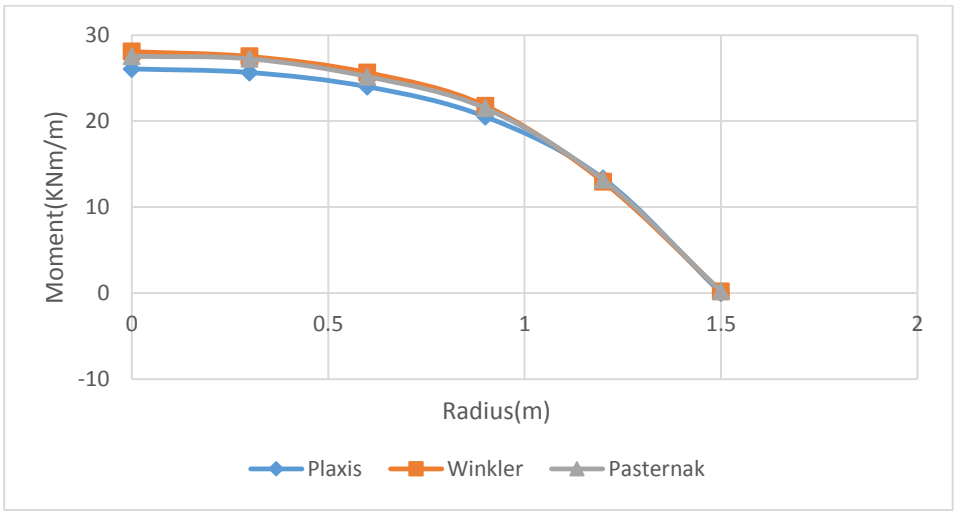

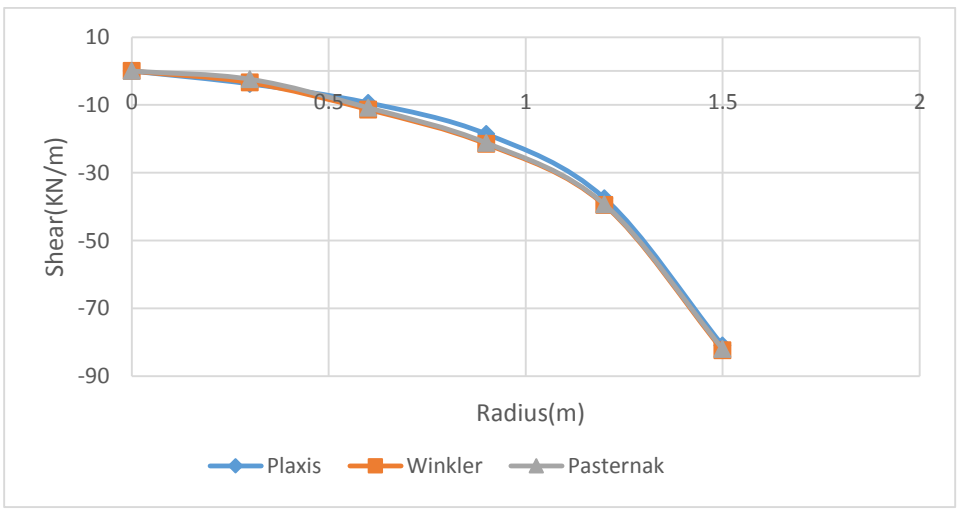

Figure 4.36 Response of a small circular plate on loose sand subjected to concentrated edge load

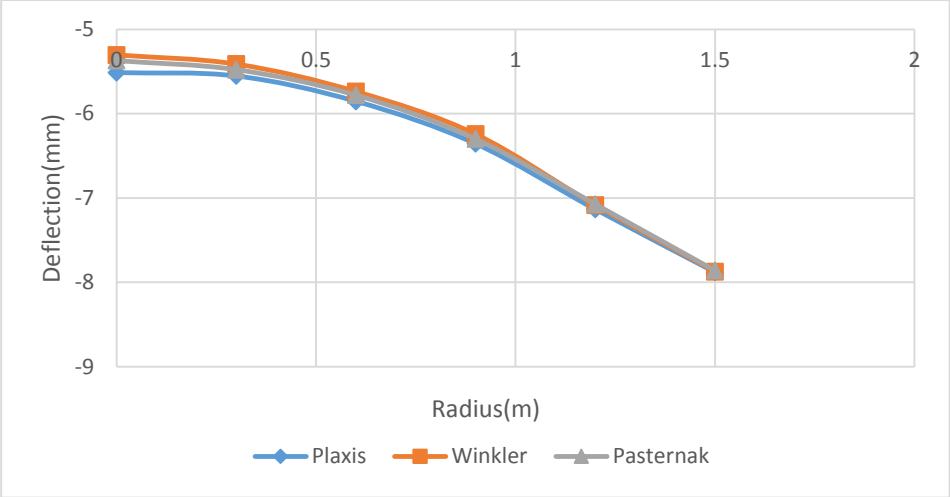

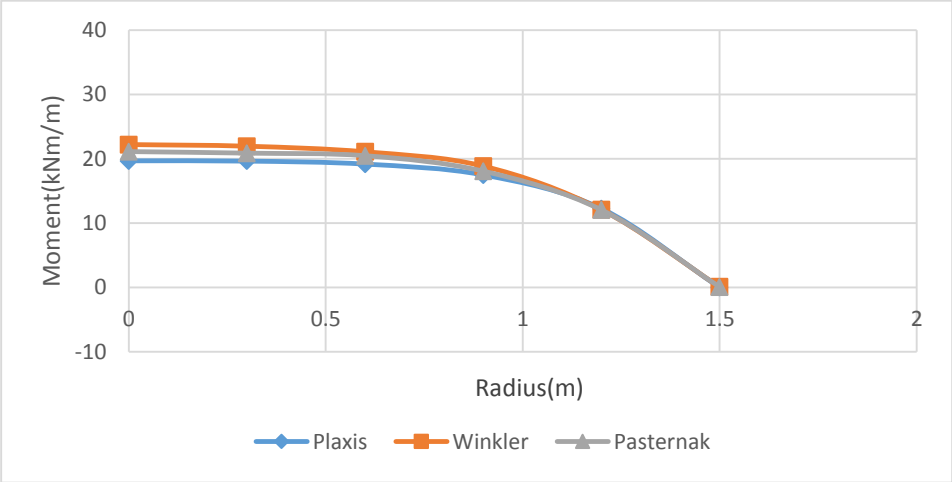

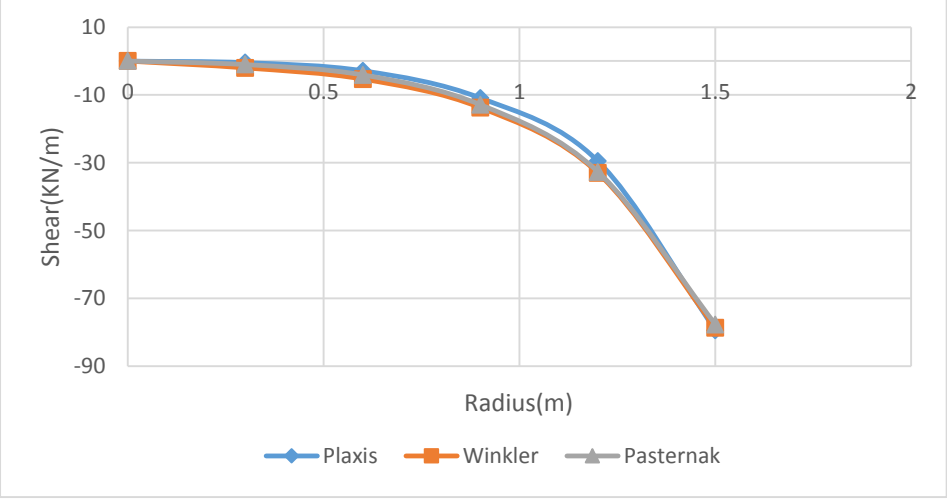

Figure 4.37 Response of a small circular plate on medium dense sand subjected to concentrated edge load

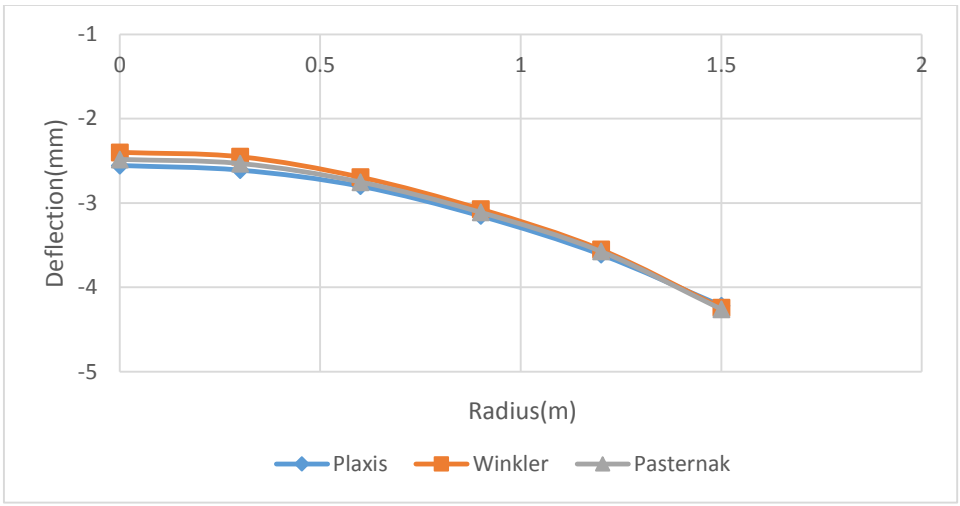

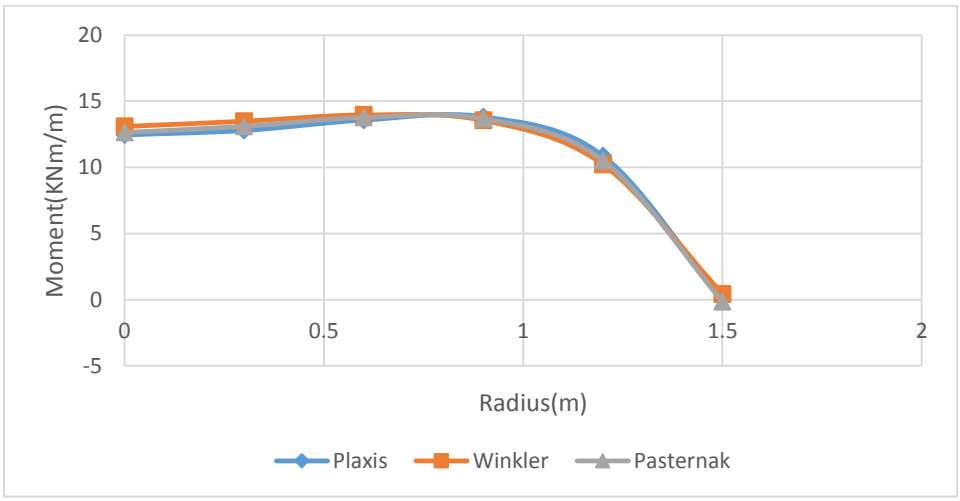

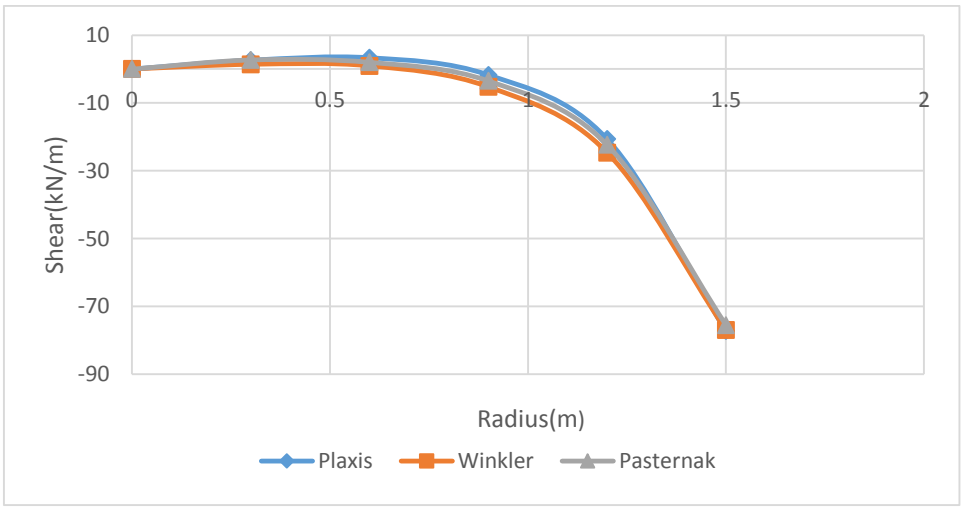

Figure 4.38 Response of a small circular plate on dense sand subjected to concentrated edge load

As far as the maximum deflection is concerned, excellent agreements of both models with the PLAXIS 2D are observed. For the case of weak soils, however, the maximum deflections are once again underestimated in both models for the concentrated central loading. And the divergence for this soil type may aggregate to 4.4% and 2.5% for Winkler's and Pasternak's model respectively as compared to the PLAXIS result. In addition, a similar trend in the variation of the deflections is observed for both models as the case of large plates.

Considering the maximum bending moments of both models, the differences are almost negligible than those of the maximum deflections. And the shear forces are practically the same for both models and the FE outputs.

For the case of concentrated edge loading, unlike the previous loading conditions, the maximum deflection for weaker soils is slightly overestimated by both models. The deviation for Winkler's model is up to 2.4% whereas for Pasternak's model is nearly 1.2%.

Regarding the internal actions, the deviations are almost negligible for the bending moments and the shear force values are in good agreement with the FE results for both models.

Chapter Five: CONCLUSIONS AND RECOMMENDATIONS

5.1 Conclusions

Application of the generalized continuum foundation models developed by Worku in the analysis of large and small circular plates has been studied and presented in this research. The results obtained after calibration are compared with FE-based PLAXIS 2D results. From the foregoing analyses, the following conclusions may be drawn:

- Among the different solution cases that ascended in the derivation of a closed form solution on a two parameter subgrade model, case III (.i.e. $T > 1$) is of practical significance for almost all problems.
- In almost all cases, Pasternak's model gives consistently close results with the PLAXIS 2D outputs than Winkler's model. Nevertheless, in the case of weaker soils, the deflections computed by Pasternak's model shows close convergence with that of Winkler's model. And the maximum deflections are underestimated by both models.
- For both large and small plates, the discrepancies in deflection pronounced in Winkler's model are increased with distance from the center. These differences are attributed to the end conditions and the assumption made in developing the model. Furthermore, to the calibration factor, which is obtained based on only the maximum deflection.
- Considering the internal actions of both large and small plates, the divergences in the moment are small for both models. And the shear forces are practically equal with the FE outputs. This implies that shear force is little affected by the model used.
- Treating a small plate with a different loading condition (i.e. concentrated edge load) using the respective calibration factor, has shown similar trend of the results with the large plates subjected to the other loading conditions.
- Because of the excellent results obtained when Pasternak's subgrade model is used, the incorporation of this model into FE based structural software is encouraged.

This will eliminate the complications in developing the analytical solutions for different loading types.

- The calibrated value of the stratum thickness for Winkler's model has shown that the depth of influence for circular plates is large unlike the usually assumed one in 2D problems such as beams.

Finally, it should be noted that Winkler's model may not provide as reliable estimates of the response of the foundation-soil system as Pasternak's model. This is a result of the missing shear interaction in the soil attributed to the use of a single parameter (i.e. soil spring constant).

The calibrated Pasternak model better represents the real physical problem than the calibrated Winkler model because it directly accounts for shear interaction from the outset. And this study shows that the New Kerr-Equivalent Pasternak model is attractive and more appropriate for the analysis of circular plates.

5.2 Recommendations

Since this study is limited to the analysis of thin solid circular plates modeled as an axisymmetric problem (i.e. with rotationally symmetric loads and edge conditions resting on a homogeneous stratigraphy), the following can be suggested for future works.

- This work can be used as a good basis to analyze axisymmetric circular plates on a three parameter subgrade model.
- Analysis of circular plates on elastic foundation could be better extended to other types of boundary conditions and loads to see the different effects in the soil structure interaction.
- Different cases of studies can be made by treating the plate as thick, annular, resting on non-homogeneous soil and extending the problem to a three-dimensional one.
- Moreover, conducting numerical illustrations for the loading condition (i.e. concentrated edge moment) using the solutions developed in this study is recommended since it has not been covered.

REFERENCES

Boas, M.L., "Mathematical Methods in the Physical Sciences," *Department of Physics,* New York 1966.

Braja M.D., "Principles of Foundation Engineering," *Sixth Edition,* U.S.A 2007.

Cauwelaert, F.V., "Pavement Design and Evaluation," *The Required Mathematics and its Applications,* Brussels 2003.

Debnath, L. and Bhatta, D., "Integral Transforms and Their Applications," *Second Edition,* New York 2007.

Degu, Y., "Analysis of Beams on Elastic Foundation Using Generalized Continuum–Based Subgrade Models," *Thesis presented to the Addis Ababa Institute of Technology,* Addis Ababa-Ethiopia 2008.

Hetenyi, M., "Beams on Elastic Foundation," *Theory with Applications in the Fields of Civil and Mechanical Engineering,* United States of America 1979.

Hildebrand, B., "Advanced Calculus for Applications," *Hindley Public Library*, New Jersey 1962.

Horvath, J.S., "Soil-Structure Interaction Research Project - Basic SSI Concepts and Applications Overview," *Report No*. CGT-2002-2, *Manhattan College, School of Engineering, Bronx,* New York, U.S.A.

Horvath, J.S., "Modulus of Subgrade Reaction: New Perspective," *Journal of Geotechnical Engineering,* Vol. 109, No. 12, December, 1983.

Horvath, J.S., "New Subgrade Model Applied to Mat Foundations," *Journal of Geotechnical Engineering,* Vol. 109, No. 12, December, 1983.

Horvath, J.S., "A Study of Analytical Methods for Determining the Response of Mat Foundations to Static Loads," *Thesis presented to the Poly-technic Institute of New York at Brooklyn,* New York, in 1979.

Horvath, J.S., "Subgrade Models for Soil-Structure Interaction Analysis," *Foundation Engineering proceeding*, June1983.

Bowles J. E., "Foundation Analysis and Design," *Fifth Edition*, New York 1997.

Kelly, R., "Plate Theory," *Solid Mechanics Part II*, Canada 2007.

Kerr, A. D., "Elastic and Viscoelastic Foundation Models," *Journal of Applied Mechanics*, Vol. 31, 1964.

Ministry of Works &, Urban Development., "EBCS-2; Ethiopian Building Code Standard," *Structural Use of Concrete*, Ethiopia 1995.

Piessens, R., "The Hankel Transform," *The Transforms and Applications Handbook: Second Edition*, New York 2000.

Rajapakse, R. K. N. D. and Selvadurai, A. P. S., "Response of Circular Footings and Anchor Plates in Non-Homogeneous Elastic Soils," *International Journal for Numerical and Analytical Methods in Geomechanics*, Vol. 15, Canada 1991.

Reddy, J. N., "Theory and Analysis of Elastic Plates and Shells," *Second Edition*, London New York 2007.

Reissner, E., "A Note on Deflection of Plates on Viscoelastic Foundation," *Journal of Applied Mechanics*, 1958.

Selvadurai, A.P.S., "Elastic Analysis of Soil-Foundation Interaction," *Department of Civil Engineering*, New York 1979.

Spiegel. G., "Advanced Mathematics for Engineers and Scientists," *Schaum's Outline Series. McGraw Hill Book Company*, New York 1971.

Steele, C.R. and Balch, C.D., "Introduction to the Theory of Plates," *Department of Mechanical Engineering*, Stanford University, 2003.

Szilard, R., "Theories and Applications of Plate Analysis," *Classical, Numerical and Engineering Methods*, Canada 2004.

Timoshenko, S. and Goodier, J.N., "Theory of Elasticity," *Engineering Societies library*, New york 1951.

Worku, A., "Part I: A Generalized Formulation of Continuum Models for Elastic Foundations," *Advances in Analysis, Modeling & Design*, GeoFlorida 2010.

Worku, A. and Degu, Y., "PART II: Application of Newly Derived and Calibrated Continuum Subgrade Models in the Analysis of Beams on Elastic Foundations," *Journal of Eng. Mechanics*, ASCE, GeoFlorida, 2010.

Worku, A., "Calibrated Analytical Formulas for Foundation Model Parameters," *International Journal of Geomechanics*, Vol. 13, No. 4, August 1 2013.

Worku, A., "Development of a Calibrated Pasternak Foundation Model for Practical Use," *International Journal of Geotechnical Engineering*, Vol. 8, No. 1, 2014.

Appendix A

Gamma Functions and Properties of Bessel Functions

I. Gamma Functions (Helpful relations)

$$\Gamma(P+1) = p\Gamma(p) \tag{A-1}$$

$$\Gamma(n+1) = n! \tag{A-2}$$

$$\Gamma(n+p+1) = (n+p)! \tag{A-3}$$

$$\frac{\Gamma'(n+1)}{\Gamma(n+1)} = -\gamma + \frac{1}{1} + \frac{1}{2} + \frac{1}{3} + \ldots + \frac{1}{n} \tag{A-4}$$

$$\gamma = \lim_{n\to\infty}\left(1 + \frac{1}{2} + \frac{1}{3} + \ldots \frac{1}{n} - \log n\right) = 0.5772157 \tag{A-5}$$

II. General Bessel functions

Consider the differential Bessel equation

$$x^2 y'' + xy' + \left(x^2 - p^2\right) y = 0$$

The Complete solution for $x = r$ is given by

$$w = aJ_o(r) + bN_o(r)$$

a) Bessel functions of first kind in terms of infinite series

$$J_p(r) = \sum_{n=0}^{\infty} \frac{(-1)^n \left(\frac{r}{2}\right)^{2n+p}}{n!\Gamma(n+p+1)} \tag{A-6}$$

$$J_{-p}(r) = \sum_{n=0}^{\infty} \frac{(-1)^n \left(\frac{r}{2}\right)^{2n-p}}{n!\Gamma(n-p+1)} \tag{A-7}$$

Special case

$$J_o(r) = \sum_{n=0}^{\infty} \frac{(-1)^n \left(\frac{r}{2}\right)^{2n}}{n!^2} \tag{A-8}$$

In particular,

$$J_o(r) = 1 - \frac{r^2}{2^2} + \frac{r^4}{2^4(2!)^2} - \frac{r^6}{2^6(3!)^2} + \ldots \quad \text{(A-9)}$$

b) Bessel functions of second kind in terms of infinite series

$$N_p(r) = Y_p(r) = \frac{J_p(r)\cos(\pi p) - J_{-p}(r)}{\sin(\pi p)}, \text{ for p not an integer} \quad \text{(A-10)}$$

$$N_p(r) = \lim_{p \to 0} \frac{J_p(r)\cos(\pi p) - J_{-p}(r)}{\sin(\pi p)}, \text{ p is an integer} \quad \text{(A-11)}$$

Special case

$$N_0(r) = \frac{1}{\pi}\left[\frac{\partial J_p(r)}{\partial p} - \frac{\partial J_{-p}(r)}{\partial p}\right] \quad \text{(A-12)}$$

In particular,

$$N_o(r) = \frac{2}{\pi}\left\{\left(\log\left(\frac{r}{2}\right) + \gamma\right)J_o(r) + \frac{\left(\frac{r}{2}\right)^2}{1!1!} - \frac{\left(\frac{r}{2}\right)^4}{2!2!}\left(1 + \frac{1}{2}\right) + \frac{\left(\frac{r}{2}\right)^6}{3!3!}\left(1 + \frac{1}{2} + \frac{1}{3}\right)\ldots\right\} \quad \text{(A-13)}$$

c) Bessel functions of third kind in terms of infinite series

$$H_p^{(1)}(r) = J_p(r) + iN_p(r) \quad \text{(A-14)}$$

$$H_p^{(2)}(r) = J_p(r) - iN_p(r) \quad \text{(A-15)}$$

Asymptotic values

$$H_p^{(1)} \cong \sqrt{\frac{2}{\pi r}}\, e^{i\left(r - \frac{\pi}{4} - \frac{p\pi}{2}\right)} \quad \text{(A-16)}$$

$$H_p^{(2)} \cong \sqrt{\frac{2}{\pi r}}\, e^{-i\left(r - \frac{\pi}{4} - \frac{p\pi}{2}\right)} \quad \text{(A-17)}$$

III. Modified Bessel functions

Consider the differential Bessel equation

$$x^2 y'' + xy' - \left(x^2 + p^2\right)y = 0$$

The Complete solution for $x = r$is given by

$$w = cI_p(r) + dK_p(r)$$

a) Modified Bessel functions of first kind in terms of infinite series

$$I_p(r) = i^{-p} J_p(ir) = \sum_{n=0}^{\infty} \frac{\left(\frac{r}{2}\right)^{2n+p}}{n!\Gamma(n+p)!} \tag{A-18}$$

Special case

$$I_o(r) = \sum_{n=0}^{\infty} \frac{\left(\frac{r}{2}\right)^{2n}}{n!^2} \tag{A-19}$$

b) Modified Bessel functions of second kind in terms of infinite series

$$K_p(r) = \frac{\pi}{2} i^{p+1} \left[J_p(ir) + iN_p(ir) \right] \tag{A-20}$$

IV. *Ber* and *Bei* functions

$$ber(r) = \sum_{n=0}^{\infty} \frac{(-1)^n \left(\frac{r}{2}\right)^{4n}}{(2n)!^2} = 1 - \frac{\left(\frac{r}{2}\right)^4}{2!2!} + \frac{\left(\frac{r}{2}\right)^8}{4!4!} - \frac{\left(\frac{r}{2}\right)^{12}}{6!6!} + \ldots \tag{A-21}$$

$$bei(r) = \sum_{n=0}^{\infty} \frac{(-1)^n \left(\frac{r}{2}\right)^{4n+2}}{\left[(2n+1)!\right]^2} = \frac{\left(\frac{r}{2}\right)^2}{1!1!} - \frac{\left(\frac{r}{2}\right)^6}{3!3!} + \frac{\left(\frac{r}{2}\right)^{10}}{5!5!} - \ldots \tag{A-22}$$

Asymptotic values of *ber* and *bei*

- For high values of the argument

$$ber(r) \cong \frac{J_o\left(r\sqrt{i}\right) + J_o\left(r\sqrt{-i}\right)}{2} = \frac{e^{\frac{r}{\sqrt{2}}}}{\sqrt{2\pi r}} \cos\left(\frac{r}{\sqrt{2}} - \frac{\pi}{8}\right) \tag{A-23}$$

$$bei(r) \cong \frac{J_o\left(r\sqrt{-i}\right) - J_o\left(r\sqrt{i}\right)}{2i} = \frac{e^{\frac{r}{\sqrt{2}}}}{\sqrt{2\pi r}} \sin\left(\frac{r}{\sqrt{2}} - \frac{\pi}{8}\right) \tag{A-24}$$

V. *Ker* and *Kei* functions

$$\ker\left(\lambda r\right)=\left[\frac{k_o\left(\lambda r\sqrt{i}\right)+k_o\left(\lambda r\sqrt{-i}\right)}{2}\right] \tag{A-25}$$

$$kei\left(\lambda r\right)=\left[\frac{k_o\left(\lambda r\sqrt{i}\right)-k_o\left(\lambda r\sqrt{-i}\right)}{2i}\right] \tag{A-26}$$

Where

$$k_o\left(r\sqrt{i}\right)=\left[ber\left(r\right)+ibei\left(r\right)\right]\left[\log\frac{r}{2}+\gamma+i\frac{\pi}{4}\right]+i\frac{\left(\frac{r}{2}\right)^2}{1!1!}-\frac{\left(\frac{r}{2}\right)^4}{2!2!}\left(1+\frac{1}{2}\right)$$

$$-i\frac{\left(\frac{r}{2}\right)^6}{3!3!}\left(1+\frac{1}{2}+\frac{1}{3}\right)+... \tag{A-27}$$

$$k_o\left(r\sqrt{-i}\right)=-\left[ber\left(r\right)-ibei\left(r\right)\right]\left[\log\frac{r}{2}+\gamma-i\frac{\pi}{4}\right]-i\frac{\left(\frac{r}{2}\right)^2}{1!1!}-\frac{\left(\frac{r}{2}\right)^4}{2!2!}\left(1+\frac{1}{2}\right)$$

$$+i\frac{\left(\frac{r}{2}\right)^6}{3!3!}\left(1+\frac{1}{2}+\frac{1}{3}\right)+... \tag{A-28}$$

Asymptotic values for *ker* and *kei*

- For high values of the argument

$$\ker\left(\lambda r\right)\cong\sqrt{\frac{\pi}{2\lambda r}}e^{-\lambda r/\sqrt{2}}\cos\left(\frac{\lambda r}{\sqrt{2}}+\frac{\pi}{8}\right) \tag{A-29}$$

$$kei\left(\lambda r\right)\cong-\sqrt{\frac{\pi}{2\lambda r}}e^{-\lambda r/\sqrt{2}}\sin\left(\frac{\lambda r}{\sqrt{2}}+\frac{\pi}{8}\right) \tag{A-30}$$

VI. Recurrence relations

$$\frac{\partial J_p\left(r\right)}{\partial p}=\sum_{n=0}^{\infty}\left(-1\right)^n\frac{\left(\frac{r}{2}\right)^{2n}}{n!\Gamma\left(n+1\right)}\left[\log\left(\frac{r}{2}\right)-\frac{\Gamma'\left(n+1\right)}{\Gamma\left(n+1\right)}\right] \tag{A-31}$$

$$\frac{\partial J_{-p}\left(r\right)}{\partial p}=\sum_{n=0}^{\infty}\left(-1\right)^n\frac{\left(\frac{r}{2}\right)^{2n}}{n!\Gamma\left(n+1\right)}\left[-\log\left(\frac{r}{2}\right)+\frac{\Gamma'\left(n+1\right)}{\Gamma\left(n+1\right)}\right] \tag{A-32}$$

$$\frac{d}{dr}Y_o(\alpha r)=\begin{Bmatrix}-\alpha Y_1(\alpha r),\left(y=J,\mathrm{N},\mathrm{k},H^{(1)},H^{(2)}\right)\\ \alpha Y_1(\alpha r),(y=I)\end{Bmatrix} \tag{A-33}$$

$$\int J_o(rt)\,dr=\frac{J_1(rt)}{t},\ \text{n-even} \tag{A-34}$$

$$\frac{d}{dr}J_p(rt)=tJ_{p-1}(rt)-\frac{p}{r}J_p(rt) \tag{A-35}$$

Appendix B

General Solution of Plates on Winkler's Subgrade Model

The governing homogeneous differential equation for the deflection of a circular plate is given by

$$\left(\frac{d^2}{dr^2}+\frac{1}{r}\frac{d}{dr}\right)\left(\frac{d^2w_o}{dr^2}+\frac{1}{r}\frac{dw_o}{dr}\right)+\frac{k_w w_o}{D}=0 \qquad \text{(B-1)}$$

Letting $\lambda = \sqrt[4]{\frac{k_w}{D}}$, this equation reduces to

$$\Delta_r{}^2 w_o + \lambda^4 w_o = 0 \qquad \text{(B-2)}$$

Putting $\lambda r = \sqrt[4]{-1}\,r$, Eq. (B-2) can be transformed into the following to have the form of modified Bessel equation.

$$\Delta_r{}^2 w_o - w_o = 0 \qquad \text{(B-3)}$$

Note: By property of linear operators $Lw_o = L_1L_2w_o$ and if $L_1L_2w_o = L_2L_1w_o$, the two operators L_1 and L_2 are commutative (Boas, 1966).

$$\Delta_r{}^2 w_o - w_o = 0$$
$$= (\Delta_r{}^2 - 1)w_o = 0$$
$$= (\Delta_r - 1)(\Delta_r + 1)w_o = 0$$

Let $(\Delta_r - 1) = L_1$ and $(\Delta_r + 1) = L_2$ and any $L = L_1L_2w_o = 0$ can be taken as the resolved component. So, Eq. (3) can in turn be resolved as

i. $(\Delta_r - 1)(\Delta_r w_o + w_o) = 0$ or $\Delta_r(\Delta_r w_o + w_o) - (\Delta_r w_o + w_o) = 0$

ii. $(\Delta_r + 1)(\Delta_r w_o - w_o) = 0$ or $\Delta_r(\Delta_r w_o - w_o) + (\Delta_r w_o - w_o) = 0$

The solution for Eq. (B-2) is the sum of; $\Delta_r w_o + w_o = 0$ and $\Delta_r w_o - w_o = 0$.

Hence the solution for $\Delta_r w_o + w_o = 0$ is given by the solution of Bessel equation:

$$\Delta_r w_o + w_o = \frac{d^2w_o}{dr^2}+\frac{1}{r}\frac{dw_o}{dr}+w_o = 0$$

Multiplying this equation by r^2 we get,

$$r^2 w_o'' + r w_o' + r^2 w_o = 0 \qquad \text{(B-4)}$$

This equation has the form of Bessel function; $x^2 y'' + xy' + \left(x^2 - p^2\right) y = 0$.

Such type of DE is solved by assuming a series of the form according to Boas (1966) and Hildebrand (1962**)**:

$$y = w_o = \sum_{n=0}^{\infty} a_n x^{n+s} \text{ , Method of Frobenius}$$

We have,

$$y = w_o = a_o x^{s+1} + a_2 x^{s+2} + \ldots = \sum_{n=0}^{\infty} a_n x^{n+s} \qquad \text{(B-5a)}$$

$$w_o' = s a_o r^{s-1} + (s+1) a_1 r^s + (s+2) a_2 r^s + \ldots = \sum_{n=0}^{\infty} (n+s) a_n x^{n+s-1} \qquad \text{(B-5b)}$$

$$w_o'' = s(s-1) a_o r^{s-2} + (s+1) a_1 r^{s-1} + (s+2)(s+1) a_2 r^s + \ldots = \sum_{n=0}^{\infty} (n+s)(n+s-1) a_n r^{n+s-2} \qquad \text{(B-5c)}$$

Substituting Eq. (B-5a-c) into Eq. (B-4) and tabulating the coefficients of powers of '*r*' for the Legendre equation,

	r^s	r^{s+1}	r^{s+2} ……	r^{n+s}
$r^2 w''$	$s(s-1) a_o$	$s(s+1) a_1$	$(s+2)(s+1) a_2$ …..	$(n+s)(n+s-1) a_n$
rw'	$s a_o$	$(s+1) a_1$	$(s+2) a_2$ …..	$(n+s) a_n$
$r^2 w$			a_o ……..	a_{n-2}

The total coefficient of each power of r must be zero. From the coefficient of r^s we get $\left(s^2 - s + s\right) a_o = 0$, since $a_o \neq 0$ by hypothesis, $s^2 = 0$. Hence, $s = 0 = p$.

For $s = 0$, coefficient of r^{s+1}in the table gives, $a_1 = 0$.

We can use the general formula given by the last column because the first two columns in the table do not contain the a_{n-2} term.

$$(n+s)(n+s-1)a_n+(n+s)a_n+a_{n-2}=0$$

For $s = 0$, $n(n-1)a_n+na_n=-a_{n-2}$, we find that

$$a_n=-\frac{a_{n-2}}{n^2}\ \text{for}\ n\geq 2$$

Since $a_1=0$, this gives all odd a's equal to zero. For even a's it is convenient to replace *n* by *2n*;

$$a_{2n}=-\frac{a_{2n-2}}{(2n)^2}$$

$$a_2=-\frac{a_o}{4}, a_4=-\frac{a_2}{16}=\frac{a_o}{4(2)^4},\ a_6=-\frac{a_4}{36}=-\frac{a_o}{36(2)^6}\ \cdots$$

The series solution applying Eq. (B-5a-c) (for *s*=0) is

$$w_o=a_o r^0-\frac{a_o r^2}{4}+\frac{a_o}{4(2)^4}-\frac{a_o}{36(2)^6}$$

$$=a_o r^0\left[1-\left(\frac{r}{2}\right)^2+\frac{1}{4}\left(\frac{r}{2}\right)^4-\frac{1}{36}\left(\frac{r}{2}\right)^6+\ldots\right] \qquad \text{(B-6)}$$

Choose arbitrary value for a_o .i.e. a_o =1,

Then *w* is called Bessel function for first kind and zero order, and written $J_p(r)$ as previously defined in Appendix A, eq. (A-6).

The general solution is expressed as

$$w_o(r)=2^p\Gamma(1+p)J_p(r) \qquad \text{(B-7)}$$

Though for *p* = 0, using (B-7) from Appendix A,

$$w_o(r)=J_o(r) \qquad \text{(B-8)}$$

In order to find the second linearly independent solution of Bessel's equation, we use Neumann's function (Weber's function) defined in Appendix A, Eq. (A-10).

But for our case since p is an integer, $J_p(r)$ and $J_{-p}(r)$ are linearly independent (Van Cauwelaert, 2003). So, the second solution is as defined previously in Appendix A, Eq. (A-11).

Applying de L'Hospital rule

$$N_0(r) = \frac{\frac{\partial J_p(r)}{\partial p}\cos(\pi p) - J_p(r)\pi\sin(\pi p) - \frac{\partial J_{-p}(r)}{\partial p}}{\pi\cos(\pi p)} \tag{B-9}$$

Then we can use Eq. (A-12) from Appendix A.

Computing the derivatives of $J_p(r)$ and $J_{-p}(r)$, from Recursion relation, Appendix A, the second solution can be rewritten in the following form since J_{-p} is the same as J_p for $p = 0$. (Hildebrand, 1962).

$$N_0(r) = \frac{2}{\pi}\left[\left(\log\left(\frac{r}{2}\right)+\gamma\right)J_o(r) + \sum_{n=0}^{\infty}(-1)^{n+1}\varphi(n)\frac{\left(\frac{r}{2}\right)^{2n}}{n!^2}\right] \tag{B-10}$$

Where; $\varphi(n) = \sum_{m=1}^{n}\frac{1}{m} = 1+\frac{1}{2}+\ldots+\frac{1}{n}, (n \geq 1)$

Thus,

$$N_o(r) = \frac{2}{\pi}\left\{\left(\log\left(\frac{r}{2}\right)+\gamma\right)J_o(r) + \frac{\left(\frac{r}{2}\right)^2}{1!1!} - \frac{\left(\frac{r}{2}\right)^4}{2!2!}\left(1+\frac{1}{2}\right) + \frac{\left(\frac{r}{2}\right)^6}{3!3!}\left(1+\frac{1}{2}+\frac{1}{3}\right)\ldots\right\} \tag{B-11}$$

Where γ is as defined in Appendix A, Eq. (A-5).

Therefore, the complete solution of $\Delta_r w_o + w_o = 0$ is

$$w_o = aJ_o(r) + bN_o(r) \tag{B-12}$$

Similarly, the solution for $\Delta_r w_o - w_o = 0 = \frac{d^2 w_o}{dr^2} + \frac{1}{r}\frac{dw_o}{dr} - w_o = 0$,

is derived multiplying by r^2;

$$r^2 \frac{d^2 w_o}{dr^2} + r\frac{dw_o}{dr} - r^2 w_o = 0 \tag{B-13}$$

Eq. (B-13) differs from Bessel's equation only in the sign of r^2 in the coefficient of w, is thus transformed into modified form of Bessel's equation by substituting $ir = t$ to the equation (Hildebrand, 1962).

$$t^2 \frac{d^2 w_o}{dr^2} + t\frac{dw_o}{dr} + t^2 w_o = 0, \text{ Bessel's equation form} \tag{B-14}$$

Hence, the general solution is of the form $w_o = Z_p(t)$ or in terms of the original variable r,

$$w_o = Z_p(ir)$$

$$w_o = cJ_p(ir) + dN_p(ir) \tag{B-15}$$

As previously done, $p = 0$ (i.e. both the first and second kind Bessel functions are zero order).

$$w_o = cJ_0(ir) + dN_0(ir) \tag{B-16}$$

Alternatively,

$$w_o = cI_p(r) + dK_p(r) \tag{B-17}$$

Where, $I_p(r)$ and $K_p(r)$ are as defined in Appendix A, Eq. (A-18 and A-20)

Note: I_p and J_p are of similar terms but I_p's are all positive.

For p=0,

$$w_o = cI_o(r) + dK_o(r) \tag{B-18}$$

Therefore, the complete solution will be the sum of Eq. (B-12) and (B-16) with original variable,

$$w_o = aJ_o\left(\pm\lambda r\sqrt{+i}\right) + bN_o\left(\pm\lambda r\sqrt{+i}\right) + cI_o\left(\pm\lambda r\sqrt{-i}\right) + dN_o\left(\pm\lambda r\sqrt{-i}\right) \tag{B-19}$$

Where *a*, *b*, *c* and *d* are open constants.

By introducing the following functions, the solution can be expressed in real function of argument λr.

$$z_1(\lambda r) = \frac{J_o\left(\lambda r\sqrt{+i}\right) + J_o\left(\lambda r\sqrt{-i}\right)}{2}$$

$$z_2(\lambda r) = \frac{J_o\left(\lambda r\sqrt{-i}\right) - J_o\left(\lambda r\sqrt{+i}\right)}{2i}$$

$$z_3(\lambda r) = z_1(\lambda r) + \frac{i\left[N_o\left(\lambda r\sqrt{+i}\right) - N_o\left(\lambda r\sqrt{-i}\right)\right]}{2} \tag{B-20a-d}$$

$$z_4(\lambda r) = z_2(\lambda r) + \frac{N_o\left(\lambda r\sqrt{+i}\right) + N_o\left(\lambda r\sqrt{-i}\right)}{2}$$

If the argument is denoted by *r* and applying Eq. (A-9) of Appendix A,

$$z_1(r) = 1 - \frac{\left(\frac{r}{2}\right)^4}{2!^2} + \frac{\left(\frac{r}{2}\right)^8}{4!^2} - \frac{\left(\frac{r}{2}\right)^{10}}{6!^2} + \ldots$$

$$z_2(r) = -\frac{\left(\frac{r}{2}\right)^2}{1!^2} + \frac{\left(\frac{r}{2}\right)^6}{3!^2} - \frac{\left(\frac{r}{2}\right)^{10}}{5!^2} + \ldots$$

$$z_3(r) = \frac{z_1(r)}{2} - \frac{2}{\pi}\left[R_1 + \log\frac{\gamma r}{2} z_1(r)\right], R_1 = \left(\frac{r}{2}\right)^2 - \frac{\varphi(3)}{3!^2}\left(\frac{r}{2}\right)^6 + \frac{\varphi(5)}{5!^2}\left(\frac{r}{2}\right)^{10} \ldots \tag{B-21a-d}$$

$$z_4(r) = \frac{z_2(r)}{2} + \frac{2}{\pi}\left[R_2 + \log\frac{\gamma r}{2} z_1(r)\right], R_2 = \frac{\varphi(2)}{2!^2}\left(\frac{r}{2}\right)^4 - \frac{\varphi(4)}{4!^2}\left(\frac{r}{2}\right)^8 + \frac{\varphi(6)}{6!^2}\left(\frac{r}{2}\right)^{12} \ldots$$

Then the general solution will be

$$w_o = A_1 z_1(\lambda r) + A_2 z_2(\lambda r) + A_3 z_3(\lambda r) + A_4 z_4(\lambda r) \tag{B-22}$$

Where A_1 to A_4 are open constants and, $z_1(\lambda r)$, $z_2(\lambda r)$, $z_3(\lambda r)$ and $z_4(\lambda r)$ are four independent solutions of the governing equation for an argument λr applying Eq. (A-21, A-22, A-25, A-26, A-27 and A-28) from Appendix A.

Note:

$$z_1(\lambda r) = ber(\lambda r)$$

$$z_2(\lambda r) = -bei(\lambda r)$$

$$z_3(\lambda r) = z_1(\lambda r) + \frac{i\left[N_o\left(\lambda r\sqrt{i}\right) - N_o\left(\lambda r\sqrt{-i}\right)\right]}{2} = -\frac{2}{\pi} kei(\lambda r)$$

$$z_4(\lambda r) = z_2(\lambda r) + \frac{N_o\left(\lambda r\sqrt{i}\right) + N_o\left(\lambda r\sqrt{-i}\right)}{2} = -\frac{2}{\pi} \ker(\lambda r) \qquad \text{(B-23a-d)}$$

With these notations, the above general solution Eq. (B-22) can be expressed as:

$$w_o = aber(\lambda r) + bbei(\lambda r) + c\ker(\lambda r) + dkei(\lambda r) \qquad \text{(B-24)}$$

Appendix C

General Solution of Plates on Pasternak's Subgrade Model

The governing homogeneous differential equation for the deflection of a circular plate is given by

$$\left(\frac{d^2}{dr^2}+\frac{1}{r}\frac{d}{dr}\right)\left(\frac{d^2w_o}{dr^2}+\frac{1}{r}\frac{dw_o}{dr}\right)-\frac{G_p}{D}\left[\frac{d^2w_o}{dr^2}+\frac{1}{r}\frac{dw_o}{dr}\right]+\frac{k_p}{D}w_o=0 \qquad \text{(C-1)}$$

This equation with the use of a differential operator, Δ_r, can be expressed as

$$\Delta_r{}^4 w_o(r)-\frac{G_p}{D}\Delta_r{}^2 w_o(r)+\frac{k_p}{D}w_o(r)=0 \qquad \text{(C-2)}$$

In reference to Boas (1966), the differential operator can be split into a product of two operators of second order as

$$(\Delta_r{}^2-d_1)(\Delta_r{}^2-d_2)\,\mathrm{w}_o(r)=0 \qquad \text{(C-3)}$$

According to Spiegel (1971), resolution of Eq. (C-3) by means of characteristic equation

$$\left[a_oD^n+a_1D^{n-1}+\ldots+a_{n-1}D^n+a_n\right]\Phi=0,\Phi=e^{mx}\text{, m-constant}$$

One can then obtain

$$a_om^n+a_1m^{n-1}+\ldots+a_n=0\ \ldots\ \text{Characteristic equation}$$

Factoring this equation, as $a_o(\mathrm{m}-\mathrm{m}_1)(\mathrm{m}-\mathrm{m}_2)\ldots(\mathrm{m}-\mathrm{m}_n)=0$, we get the roots as m_1, m_2.

Consequently, for a homogeneous linear DE of order 4, the characteristic equation writes:

$$m^4+2m^2+1=0$$

Following this, the roots of equation (C-2) will give the argument of the modified Bessel functions.

$$d^4-\frac{G_p}{D}d^2+\frac{k_p}{D}=0 \qquad \text{(C-4)}$$

Solving for this equation,

Let,

$$d^2 = n$$

$$n^2 - \frac{G_p}{D} n + \frac{k_p}{D} = 0$$

The roots of this quadratic equation are given by

$$n_{1,2} = \frac{1}{2}\left[\frac{G_p}{D} \pm \sqrt{\left(\frac{G_p}{D} \right)^2 - \frac{4k_p}{D}} \right]$$

Thus, the roots are given as

$$d_{1,2,3,4} = \pm \sqrt{\frac{1}{2}\left[\frac{G_p}{D} \pm \sqrt{\left(\frac{G_p}{D} \right)^2 - \frac{4k_p}{D}} \right]} \qquad \text{(C-5)}$$

There are three possible cases of the general solution of equation (C-4) depending on whether $G_p{}^2 < 4k_pD,\ G_p{}^2 = 4k_pD$ or $G_p{}^2 > 4k_pD$.

Previously on the Winkler's subgrade model we have

$$\lambda = \sqrt[4]{\frac{k_p}{D}} = \frac{1}{l}$$

Now let

$$\frac{k_p}{D} = \frac{1}{l^4}$$

Eq. (C-1) becomes

$$\left(\frac{d^2}{dr^2} + \frac{1}{r}\frac{d}{dr} \right)\left(\frac{d^2 w_o}{dr^2} + \frac{1}{r}\frac{dw_o}{dr} \right) - \frac{G_p}{D}\left[\frac{d^2 w_o}{dr^2} + \frac{1}{r}\frac{dw_o}{dr} \right] + \frac{w_o}{l^4} = 0 \qquad \text{(C-6)}$$

Then the three cases;

Case I

i. $G_p{}^2 < 4k_pD$

The term $\sqrt{\left(\frac{G_p}{D}\right)^2 - \frac{4k_p}{D}}$ is a complex number, so Eq. (C-5) can be re-written as

$$d_{1,2,3,4} = \pm\sqrt{\frac{1}{2}\left(\frac{G_p}{D} \pm i\left(\frac{4k_p}{D} - \left(\frac{G_p}{D}\right)^2\right)\right)} \qquad \text{(C-7)}$$

Introducing the algebraic relationship from the algebra of complex numbers,

$$\sqrt{y+iz} = \pm\left[\sqrt{\frac{1}{2}(r+y)} + sign(\mathrm{z})\,\mathrm{i}\sqrt{\frac{1}{2}(r-y)}\right]$$
$$r = \sqrt{y^2+z^2}$$

Eq. (C-7) will have the form,

$$d_{1,2,3,4} = \pm\left(\sqrt{\frac{\frac{4k_p}{D} + \left(\frac{G_p}{D}\right)^2}{2}} \pm i\sqrt{\frac{\frac{4k_p}{D} - \left(\frac{G_p}{D}\right)^2}{2}}\right) \qquad \text{(C-8)}$$

Hence, the complementary solution is

$$w_o(r) = \mathrm{B}_1 u_o(r/l) + \mathrm{B}_2 v_o(r/l) + B_3 f_o(r/l) + B_4 g_o(r/l) \qquad \text{(C-9)}$$

Where

$$
\begin{aligned}
u_o(r/l) &= \mathrm{Re}\, J_o\left(\sqrt{d}r/l\right) = \frac{1}{2}\left[J_o\left(\sqrt{d}r/l\right) + J_o\left(\sqrt{\bar{d}}r/l\right)\right] \\
v_o(r/l) &= \mathrm{Im}\, J_o\left(\sqrt{\bar{d}}r/l\right) = \frac{1}{2i}\left[J_o\left(\sqrt{d}r/l\right) - J_o\left(\sqrt{\bar{d}}r/l\right)\right] \\
f_o(r/l) &= \mathrm{Re}\, H_o^{(1)}\left(\sqrt{d}r/l\right) = \frac{1}{2}\left[H_o^{(1)}\left(\sqrt{d}r/l\right) + H_o^{(2)}\left(\sqrt{\bar{d}}r/l\right)\right] \\
g_o(r/l) &= \mathrm{Im}\, H_o^{(2)}\left(\sqrt{\bar{d}}r/l\right) = \frac{1}{2i}\left[H_o^{(1)}\left(\sqrt{d}r/l\right) - H_o^{(2)}\left(\sqrt{\bar{d}}r/l\right)\right]
\end{aligned}
\qquad \text{(C-10 a-d)}
$$

Bessel functions of first kind and third kind of zero order are selected because $J_o\left(\sqrt{d}r/l\right)$ & $J_o\left(\sqrt{\bar{d}}r/l\right)$ remain finite as $r \to 0$ and tend to infinity as $r \to \infty$ from the functions $e^{r/l}\cos(r/l)\, and e^{r/l}\sin(r/l)$ which have a resemblance to behaviour of u_o and v_o.

$H_o^{(1)}\left(\sqrt{d}r/l\right)$ & $H_o^{(2)}\left(\sqrt{\bar{d}}r/l\right)$ have a resemblance to the functions $e^{-r/l}\cos(r/l)$ and $e^{-r/l}\sin(r/l)$ indicating that they tend to zero as $r \to \infty$, thus $f_o(r/l)$ and $g_o(r/l)$. $f_o(r/l)$ has a singularity of the type $(r/l)^2\log(r/l)$ as $r \to 0$ and $g_o(r/l)$ tend to zero as $r \to \infty$.

Note: *d* and $\bar{d}$ are introduced constants for the root expressed as

$$
d = \frac{l^2}{2}\left[-\frac{G_p}{D} + \sqrt{\left(\frac{G_p}{D}\right)^2 - \frac{4k_p}{D}}\right]
$$

$$
\bar{d} = \frac{l^2}{2}\left[-\frac{G_p}{D} - \sqrt{\left(\frac{G_p}{D}\right)^2 - \frac{4k_p}{D}}\right]
$$

And $H_o^{(1)}$ and $H_o^{(2)}$ are conjugate complex functions of Hankel's functions as defined previously in Appendix A, Eq. (A-14, A-15, A-16 and A-17) for zero order.

Case II

ii. $G_p^{\,2} = 4k_pD$

Substituting $G_p^{\,2} = 4k_pD$ in the homogeneous form of Eq. (C-6)

$$d_{1,2,3,4} = 1 \tag{C-11}$$

Then the complementary solution is given by

$$w_o(r) = \mathrm{A}_1 J_o(r/l) + A_2 H_o^{(1)}(r/l) + A_3 J_o(r/l) + A_4 H_o^{(2)}(r/l) \tag{C-12}$$

Case III

i. $G_p^{\,2} > 4k_pD$

Since $G_p^{\,2} > 4k_pD$, all the roots are real. Applying the algebra of complex numbers the roots are,

$$d_{1,2,3,4} = \pm\sqrt{\frac{1}{2}\left[\frac{G_p}{D} \pm \sqrt{\left(\frac{G_p}{D}\right)^2 - \frac{4k_p}{D}}\right]} \tag{C-13}$$

Hence, the complementary solution for the homogeneous equation is

$$w_o(r) = \mathrm{A}_1 J_o\left(\sqrt{d}r/l\right) + A_2 H_o^{(1)}\left(\sqrt{d}r/l\right) + A_3 J_o\left(\sqrt{\bar{d}}r/l\right) + A_4 H_o^{(2)}\left(\sqrt{\bar{d}}r/l\right) \tag{C-14}$$

Note: $\bar{d}$ and d are as defined in case one.

An alternative way to find the roots of Eq. (C-2)

Substituting $\frac{G_p}{D}$ by $\frac{2T}{l^2}$ and $\frac{k_p}{D}$ by $\frac{1}{l^4}$, we have

$$d^4 - 2\frac{T}{l^2}d^2 + \frac{1}{l^4} = 0 \tag{C-15}$$

Where T and l are simply symbols chosen to represent the ratio of shear modulous to the characteristic size of the soil-plate system.

The explicit solution depends on the value of T.

Solving for this equation,

Let,

$$d^2 = n$$
$$n^2 - \frac{2T}{l^2} n + \frac{1}{l^4} = 0$$

The roots of this quadratic equation are given by

$$n_{1,2} = \frac{1}{l^2}\left[T \pm \sqrt{T^2 - 1} \right]$$

Thus, the roots are given as

$$d_{1,2,3,4} = \pm \frac{1}{l} \sqrt{T \pm \sqrt{T^2 - 1}} \qquad \text{(C-16)}$$

There are three possible cases of the general solution of equation (C-15) depending on whether $T > 1$, $T = 1$ or $T < 1$.

Then the three cases;

<u>Case I</u>

i. $T < 1$

The term $\sqrt{T^2 - 1}$ is a complex number, so Eq. (C-5) can be re-written as

$$d_{1,2,3,4} = \pm \frac{1}{l} \sqrt{T \pm i\left(1 - T^2\right)}$$

Introducing the algebraic relationship from the algebra of complex numbers;

$$d_{1,2,3,4} = \pm\left(\sqrt{\frac{1+T}{2}} \pm i\sqrt{\frac{1-T}{2}}\right) \tag{C-17}$$

Hence,

$$\begin{aligned} d_1 &= \sqrt{\frac{1+T}{2}} + i\sqrt{\frac{1-T}{2}} \\ d_2 &= \sqrt{\frac{1+T}{2}} - i\sqrt{\frac{1-T}{2}} \end{aligned} \tag{C-18}$$

Case II

ii. $T = 1$

Substituting $T = 1$ in the homogeneous form of Eq. (C-6)

$$d_{1,2,3,4} = 1 \tag{C-19}$$

Case III

i. $T > 1$

Since $T > 1$, all the roots are real. Applying the algebra of complex numbers the roots are,

$$d_{1,2,3,4} = \pm\sqrt{T \pm \sqrt{T^2 - 1}} \tag{C-20}$$

And then

$$\begin{aligned} d_1 &= \sqrt{T + \sqrt{T^2 - 1}} \\ d_2 &= \sqrt{T - \sqrt{T^2 - 1}} \end{aligned} \tag{C-21}$$

The solution, the deflection, for these representation of the three cases is the same as alternative one. Note that this alternative is added for simplicity of the representation of the cases.